
# Sorbonne Université

École Doctorale Cerveau-Cognition-Comportement (ED3C)
Paris-Saclay Institute of Neuroscience (NeuroPSI)


## Doctoral Thesis

# Causal manipulations of auditory perception andlearning strategies in the mouse auditory cortex


Sebastian Arturo Ceballo Charpentier

**Supervisor**:

Dr. Brice Bathellier

**Thesis committee members**:

Dr. Maria Neimark Geffen. *Examiner*

University of Pennsylvania. Philadelphia. United States of America

Dr. Kerry Walker. *Examiner*

University of Oxford. Oxford. United Kingdom

Dr. Philippe Faure. *President of the committee*

Institut de Biologie Paris-Seine (IBPS). Paris. France

Dr. Brice Bathellier. *Thesis director*

Paris-Saclay Institute of Neuroscience (NeuroPSI). Gif sur Yvette, France

**External invited expert**:

Dr. Jean-François Leger

Institut de biologie d l'Ecole Normale Superior (IBENS-ENS). Paris. France

'You have to *die* a few times
before you can really *live*'
Charles Bukowski

# Abstract

Through our senses, the brain receives an enormous amount of information. This information needs to be filtered and refined in order to extract the most salient features that will help us to guide our behavior. In this process, the brain encodes the environment into an internal 'perceptual world' in correspondence with our changing needs. An important advantage also is the ability to create new associations about external cues and their behaviorally relevant outcomes. This gives the possibility to generate predictions and respond precisely to various events in a challenging and always changing environment. Thus, previous experiences will shape our sensation and determine the responses to perceptual-based decisions.

The study of sensory perception is complicated as we cannot have direct access to well-isolated internal sensory representations. These representations need to be inferred from animal behavior in response to well characterized sensory stimuli. In this context, the study of animal learning and its contingencies are key elements for the study of sensory representations, as different learning strategies or learning rules can lead to different behavioral outcomes. How the brain actually extracts and generates these different perceptual features and wires them to behavior remains the two major questions in modern neuroscience. To answer these questions, novel neural engineering approaches are now employed to map, model and finally generate, artificial sensory perception with its learned or innate associated behavioral outcome.

In this work, we have used a combination of different modern technologies together with computational modeling to give important hints about the type of computations that auditory cortex performs under simple and more complex sound discrimination tasks. We have also explored the learning strategies that mice can adopt under a sound-basedperceptual discrimination task. More concretely, using a Go/noGo discrimination task combined with optogeneticsto silence auditory cortex during ongoing behavior in mice, we have established the dispensable role of auditory cortex for simple frequency discriminations,butalso its necessary role to solve a more challenging task. Specifically, we showed that for mice trained to discriminate between a frequency-modulated sound and a pure tone withboth startingat the same frequency,auditory cortex wasnecessary as discrimination was fully impaired during

the optogenetic manipulations. By the combination of different mapping techniques and light-sculpted optogenetics to activate precisely defined tonotopic fields in auditory cortex, we couldelucidate the strategy that mice use to solve the task, revealing a delayed frequency discrimination mechanism.In parallel, observations about learning speed and sound-triggered activity in auditory cortex led us to study their interactions and causally test the role of cortical recruitment in associative learning. Using modern optogenetics, we reproduced a well-known cue interaction phenomenon that has been observed in different learning paradigms, the overshadowing effect. These precise cortical manipulations demonstratedthat neuronal recruitment can be thoughtof as the neurophysiological correlate of saliency. The description of this relationship confirms implicit assumptions of mainstream associative learning theories. Altogether these results push forward our comprehension of the learning rules governing sensory-based associations in the brain.Finally and more broadly, this work provides insight into the integrationof modern optical techniques into sensory rehabilitation approaches in order to improve sensory feature mapping and sensory discrimination e.g. hearing-impaired patients.

# List of content

# List of figures

# List of tables



# List of equations

# List of abbreviations

2AFC: Two alternative forced choice

AAF: Anterior auditory field

AC: Auditory cortex

AChE: Acetylcholinesterase

AI: Primary auditory cortex

ChR: Channelrhodopsin

CN: Cochlear nucleus

CNIC: Central nucleus of the inferior culliculus

CO: Cytocrome oxidase

CS: Conditioned Stimulus

DCIC: Dorsal cortex of the inferior culliculus

IC: Inferior colliculus

ILDs: Interaural level differences

ITDs: Interaural time differences

LCIC: Lateral cortex of the inferior culliculus

LSO: Lateral superior olive

MGB: Medial geniculate nucleus

MGd: dorsal nucleus of medial geniculate body

MGm: medial nucleus of medial geniculate body

MGv: ventral nucleus of medial geniculate body

MSO: Medial superior olive

nBIC: Branchium of the inferior culliculus

NS: Neutral Stimulus

PV: Parvalbumin

S1: Primary somatosensory cortex

SC: Superior culliculus

SOC: Superior olivary complex 10

UCR: Unconditionned Response

UCS: Unconditioned Stimulus

V1: Primary Visual Cortex

# 1. General introduction

## 1.1. The cerebral cortex

The link between the brain, and sensory perception becomes most dramatically evident in cases of loss or disturbance of perceptual functions after some form of brain damage (Sacks, 1985). From the periphery, the information finally arrives to the cerebral cortex into hierarchically organized sensory areas, where it is processed and sent to different 'higher' areas in the brain. In mammals, the cerebral cortex has a central role indifferent cognitive processes, analysis, integration and sensory perception, as also in planning of goal directed behavior, learning and memory retrieval. Composed of the allocortex (containing the archicortex or the hippocampal region and the paleocortex or olfactory cortex) and the iso or neocortex, this structure is considered the evolutionarily youngest brain region (Gao et al., 2013). Structural as well as functional principles within cortical circuits, especially in primary sensory areas, display a high degree of conservation across different species, even in the lissencephalic rodent brain. These conserved characteristics allow experimental studies in the laboratory using different animal models and the post-hoc extension to understand the general organization and principles of the human brain (Schreiner et al., 2000).

### 1.1.1. Columnar organization

Early observations of the sensory systems in the brain by Santiago Ramón y Cajal and one of his disciples Rafael Lorente de Nó, noted the presence of vertically arranged and highly connected cells (de Castro and Merchán, 2017; Larriva-Sahd, 2014). Years later Vernon Mountcastle, using electrophysiological recordings in the somatosensory and motor cortex of cats and monkeys, described how these columnar structures responded to the same type of mechanical stimulus (Mountcastle, 1957; Mountcastle and Powell, 1959). The preceding efforts of Hubel and Wiesel in the 1960s, studying the primary visual cortex of cats, led to the discovery of 'orientation columns' and 'ocular dominance columns', corroborating previous observations and theories about the functional columnar organization of the principal sensory systems in the neocortex (Hubel and Wiesel, 1959; Hubel and Wiesel, 1962), which have been later

validated by many different techniques (Ohki et al., 2006). From these foundational studies, similar structural principles were observed studying other sensory modalities as for example, the frequency tuning in auditory cortex of different species including humans (Goldstein et al., 1970; Winer, 2011). Following with this idea, it has been largely observed and described that in each sensory domain, neurons tend to be preferentially clustered in groups that share similar input features and response properties (Andermann and Moore, 2006; Schubert et al., 2007; Ko et al., 2011; Issa et al., 2014 ; Deneux et al., 2016 ; Issa et al., 2017; Bimbard et al., 2018). Recently proposed, this characteristic of neocortical circuitswould emerge during development, where cells that belong to the same progenitor are preferentially connected creating local connectivity patterns(Kandler et al., 2009). Later, through sensory experience, these circuits would be refined by Hebbian plasticity mechanisms (Peinado et al., 1993; Gao et al., 2013) and different connectivity rules at macro and micro-scales (Barkat et al., 2011; Vasquez-Lopez et al., 2017; Hayashi et al., 2018; Nishiyama et al., 2019).

### 1.1.2. Senses and their organization in the cortex

An important characteristic of the previously described neocortical columnar organization, is that often reflects some of the corresponding sensory topographic representation in the periphery (Douglas and Martin, 2007; Larriva-Sahd, 2014; de Castro and Merchán, 2017). Neurons in the peripheral nervous system are fundamental units of information processing, capturing and translating changes in our environment into a readable code for the brain. The five most commonly described senses, olfaction, vision, gustation, touch and hearing, emerge from specialized sensory receptors neurons that can be classified on the basis of their structure, position and functionality in relation to the stimuli they sense. Regarding structural characteristics they are clustered in three groups; neurons with free nerve endings sensing directly the stimuli, neurons with encapsulated ending of connective tissue and specialized receptor neurons with special components that translate the stimuli into electrical signals (Purves, 2004). Classified also by their position, they can be grouped as an exteroreceptor; if it is located near the stimulus in the environment, interoreceptor; if it senses internal organs or internal variables as blood pressure, or propioreceptor; located near a muscle or an area in the body that receives motion signals (Purves, 2004). Classified by their functionality, sensory receptors can be chemoreceptors that translate chemical sensation, osmoreceptors that respond to solute concentrations, nociceptor that detect the presence of certain molecules, mechanoreceptors that are in charge of physical stimuli such as variations

in pressure and thermoreceptors which are sensitive to temperature (Purves, 2004). Each sensory modality is then equipped with one or more of these different types of receptors,in order to transduce different type of signals. From the periphery, the information flows through the axons of interconnected neurons to finally reach the brain (Hackett, 2011). Besides the important number of relay and processing stations from periphery to primary sensory areas in the neocortex(Krubitzer, 1995), important sensory features can be foundin the cortical surface in form of representational maps. In the following sections, before a complete description of the auditory system, I will briefly describe some of these sensory representations in the cortex. Sensory representations those are accessible using different type of techniques but which precise role for sensory perception has not been yet fully addressed.

## Somatosensation

The somatosensory system is composed of two major components: one in charge of the detection of mechanical stimuli and another for the detection of pain and temperature. Somatosensation is in this way related to several sub-modalities such as light touch, vibration and pressure that via a diverse set of neural receptors, mainly mechanoreceptors located in the skin and hair follicles, convey the information in a topographic manner through several ascending pathways to the spinal cord, brainstem, and ventral posterior complex in the thalamus to finally reach the primary somatosensory cortex (S1). In humans, S1 is located in the postcentral gyrus of the parietal lobe (Brodmann's areas 3a, 3b, 1 and 2) and each of these zones contains an entire somatotopic representation of the body (Figure 1-1A). In each of these parallel somatotopic maps, neurons encode specific to certain features of skin stimulation such as texture, shape or movement direction(Purves, 2004). In rodents, the body representation is largely biased towards the topographical representation of the whisker pad, containing the classic 'barrels', where each of them is composed of neurons responding to principally one specific whisker of the whisker pad (Benison et al., 2007) (Figure 1-1B-C). Also recent observations in rodent S1 have described that neurons within a single barrel column appear to be spatially clustered forming a map of orientation selectivity within single barrel columns(Andermann and Moore, 2006; Kremer et al., 2011).

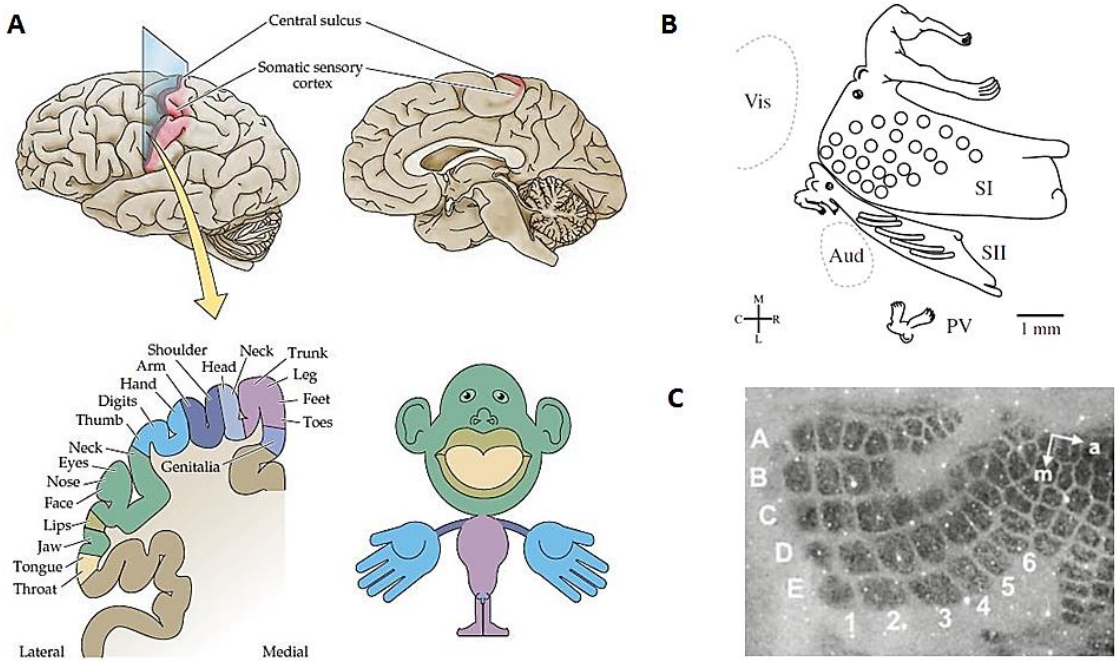


**Figure 1-1. Human and rodent body representations in the primary somatosensory cortex.**

(A) Diagram showing the location of the human primary somatosensory cortex (S1) in the brain and schematic of the body representation in a coronal view of S1. Also a classic representational quantification of the area dedicated to each part of the body (*homunculus*) made in the 1930s but still generally valid. *Adapted from Purves (2004).* (B) Same representation as A but for a rat. The *Rattunculus*shows graphically the area dedicated to each part of the rat's body in S1 and S2 in the brain. *From Benison and colleagues (2007)* (C) Barrel cortex in a mouse stained with cytochrome oxidase to reveal the 'barrels' in dark grey in S1. Each barrel is labeled with the stander nomenclature representing each whisker on the mouse snout. *From Schubert and colleagues (2007).*

## Vision

The visual system begins with one of the most advanced sensory organs, the eye. The eye, along with its lens and muscles, focuses and modulates the amount of light that is received at back part of the *globus ocularis,* where the retina is found. In the retina, there are specialized receptor neurons that contain a light-sensitive photo pigment, called photoreceptors. These neurons are dedicated then to the detection of photons and their transformation into electrical signals. The extremely well organized architecture of the retina, transforms already the information at this stage, emphasizing some aspects of the visual field, that will be sent through the optic nerve and optic track to several brain structures such as the

pretectum (involved in pupillary light reflex), the suprachiasmatic nucleus of the hypothalamus (involved in the day/night cycle), the superior colliculus (involved in the coordination of head and eye movements) and the thalamus (Purves, 2004). Visual information arrives firstto the dorsal lateral geniculate nucleus (LGN) in the thalamus, from where is sent mainly to the primary visual cortex (V1). The spatial organization of the photoreceptors in the retina is maintained through the whole visual pathways, creating organized visual representations of the space or retinotopy. Most of the neurons in the visual pathway receive information from both eyes but as a general rule, the left half of the visual field is represented in the right half of the brain, and vice versa (Purves, 2004). In humans, V1 is located in the calcarine fissure in the occipital lobe (Brodmann's area 17), where V1 neurons are mainly responsive to the orientation of edges in a simple or in a more complex way, where approximately all edge orientations are equally represented in the form of orientation columns (Hubel and Wiesel, 1962;Ohki et al., 2006) (Figure 1-2). The description of visual cortical neuron receptive fields and their organization is an enormous field of active research, which have showed that basic spatial organization principles are relatively well conserved across species (Krubitzer, 1995). However, recent observations in rodents mitigate this idea whereas contrary to cats and monkeys, visual stimulus orientation in the rodent primary visual cortex would be represented in a 'salt and pepper' organization, showing substantial heterogeneity in the tuning properties of neighboring neurons (Bachatene et al., 2016).

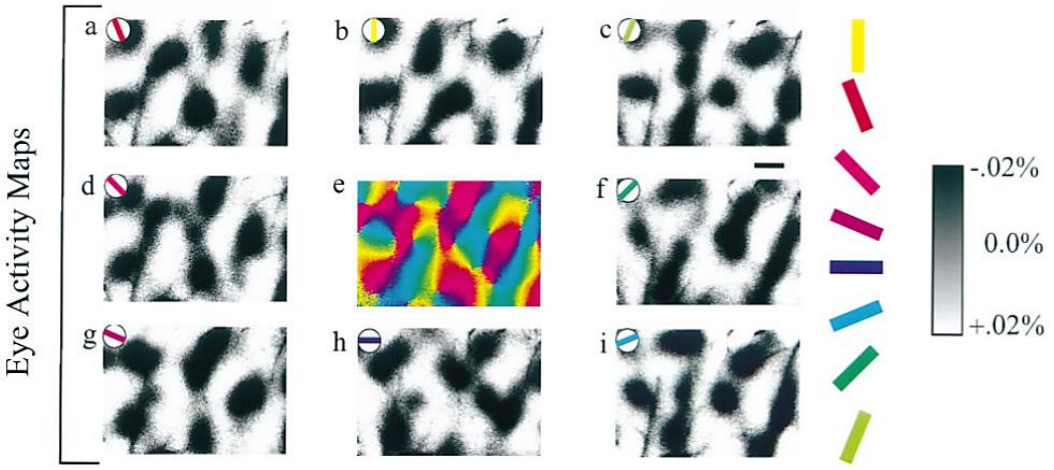


**Figure 1-2. Orientation maps from the visual cortex of the cat.**
Orientation preference maps obtained with optical imaging of intrinsic signals from the visual cortex of an anesthetized cat. Dark areas correspond to regions in the cortex that are active during the monocular presentation of a grating at the orientation indicated in the upper left

part of each image (all panels but e). In the center, the summed imaged of all orientation preference map color coded to each direction. Scale bar: 500 mm. *Adapted from Crair and colleagues (1997).*

## Gustation

Gustation is one of the chemical senses and is in charge of the detection of taste. Gustatory receptor neurons in the taste buds or papillae, mainly located on the tongue and upper digestive track, detect chemicals (sweet, bitter and umami) and ions (salty and sour). Taste cells are then innervated by branches of the facial (VII), glossopharyngeal (IX) and vagal (X) nerves which contact the gustatory nucleus of the solitary tract in the medulla (Purves, 2004). The rostral part of this nucleus sends projections to the ventral posterior medial nucleus in the thalamus, which in turn sends projections to the anterior insula in temporal lobe, the operculum of the frontal lobe and also to a second group of neurons in the caudolateral orbitofrontal cortex, where neurons are involved in satiety and motivation to eat (Pritchard et al., 2008). Neurons along the taste pathway are particularly responsive for one taste and the information flows in a sort of topographic map to the brain, creating separate taste representations in the cortex (Chen et al., 2011; Prinster et al., 2017).

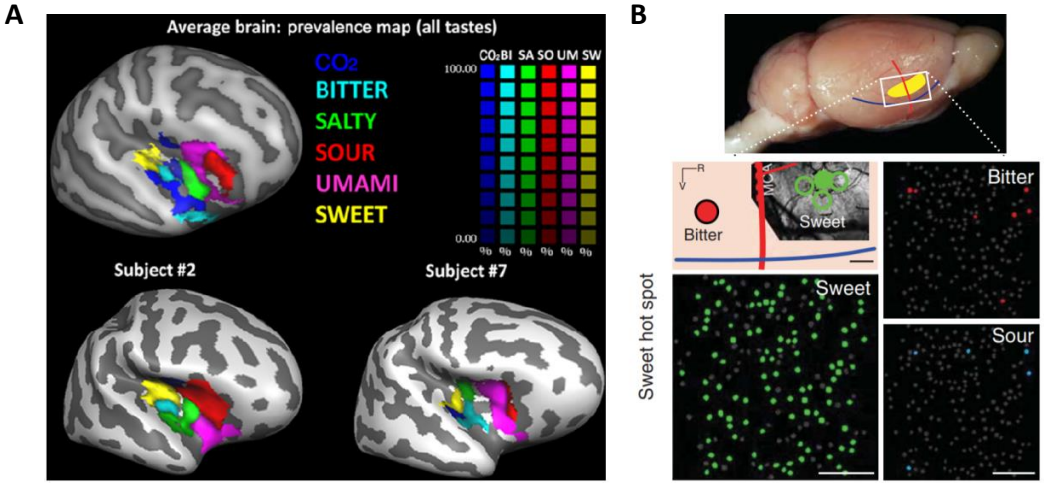


**Figure 1-3. Taste representations in the cortex of humans and mice.**
(A) Functional magnetic resonance imaging (fMRI) responses to the standardized five basic tastes together with a cortical surface representation of the human right insular cortex in two different subjects and average image in a pilot study. *Adapted from Prinster et al., (2017).* (B) Two photon calcium imaging in the mouse insular cortex. On top image of the brain with the approximate location of the recording site in the primary taste cortex (yellow). On bottom,

neurons are represented with small circles and high neuronal responses to different tastants in a single trial color coded for the same recording site, depending on the stimulus applied to the animal's tongue. *Adapted from Chen and colleagues (2011).*

## Olfaction

Olfaction, the other chemical sense, is in charge of the detection of small molecules called odorants. Olfactory receptors neurons are located on a relatively small portion of tissue in the nose. In close contact with the different odorants dissolved in the mucus, receptor cells detect and transduce these signals through the olfactory tract. The precise information arrives to a single glomerulus, where then is split to different sensory areas of the brain(Johnson and Leon, 2000; Rubin and Katz, 1999; Stewart et al., 1979). Afferent projections from the olfactory bulb mainly reach the piriform cortex, in humans located in the temporal lobe. This sensory system is really unique as it is the only one not containing a thalamic relay.Also, the main area dedicated to it in the cortex is not six-layered, but only thee-layered cortex. Another difference of this system is the poor feature representation in the olfactory bulb and pyriform cortex, as no map of odorant features has been described yet (Purves, 2004; Choi et al., 2011). Despite the lack of fine representations, large-scale odor responses in the olfactory bulb glomeruli can be used to predict the identity of odors in rats (Linster et al., 2001) (Figure 1-4A-B). Olfactory receptor neurons vary greatly in the diversity of G-coupled protein receptors at their cell surface (more than 400 in human and close to 1200 in rodents) (Purves, 2004). These particularities make odor perception vary a lot depending on the molecular structure, concentration and timing of exposition of the different odorants in the air, as also the fact that the constitution of the most common odor's perception is in fact the result of a complex mixture of odorant molecules.

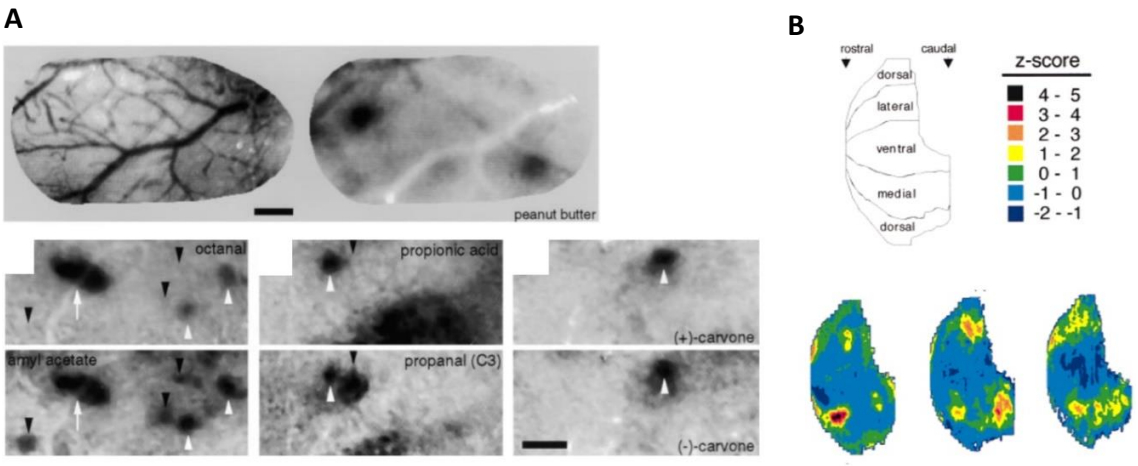


**Figure 1-4. Single odor representations in the olfactory bulb.**
(A) Surface of the olfactory bulb and optical imaging of intrinsic signals in response to different odorants in the rat olfactory bulb. Dark areas represent neuronal activations in presence of each odor presentation in the same area. Scale bar 250 µm. *Adapted from Rubin and Katz (1999)*. (B) Contour of the different areas in the olfactory bulb of a rat and average deoxyglucose charts showing the spatial distribution of [$^{14}$C]2-deoxyglucose uptake evoked by different odorant enantiomers. *Adapted from Johnson and Leon (2000).*

### 1.1.3 Perspective

The columnar organization of sensory features in the mammalian neocortex revised here corresponds to a fundamental principle observed in almost all species studied. Yet one of the major goals of sensory neuroscience is try to link these cortical representations with the precise sensory percepts and their role in for example, learning and memory recall. Modern neurophysiological techniques make possible today formulate and test these type of causal hypothesis. After a comprehensive description of the auditory system and associative learning theory, several attempts on this venue willbe described, as they constitute the background and supportof the work presented here.

# 1.2. The auditory system

## 1.2.1. Overview

Most hearing research today focuses on the study of both, normal and pathological aspects of hearing comprehending different animal models. Comparative hearing research has been able to determine some of the fundamental principles shared across species for the main structures of the auditory system, their physiological functions and their role for different hearing abilities, often with a successful translation to the human auditory system. This system depends on highly evolved and complex structures as well as external physiological processes. The ear, first auditory relay station, is responsible for the detection and decomposition of sounds. Sound is the oscillation of air molecules in the form of three dimensional waves. As any wave, sound waves contain three major features; phase, amplitude or loudness and frequency or pitch. Most natural sounds are composed of complex waveforms of sinusoidal waves varying in amplitude, frequency and phase. The hearing bandwidth (the audible range) has been tested in more than 60 mammalian species. Varying only in some extreme cases, it shares some important similarities and generalizations, such as the minimum sound detection thresholds (Schreiner et al., 2000; Vater and Kössl, 2011). These conserved fundamental hearing capabilities reflect the coevolved adaptations of the middle and inner ear across most mammalian species (Basch et al., 2016). In general, all mammals analyze and decompose the sound into its constituent frequency components with different degrees of resolution (Mann and Kelley, 2011). The ear then is a highly specialized biological Fourier analyzer of sound waves, followed by an extremely well organized hierarchical routing system that allows the transformation and segregation of sound into a precise neural code.

## 1.2.2. Lower auditory structures

The first stage of sound transformation occurs in the external and middle ear, where air vibrations are amplified and transmitted to the cochlea in the inner ear. There, frequency, amplitude and phase are transduced by hair cells and then transmitted to the central nervous system by the auditory nerve. One key feature of the auditory system is the topographic organization or tonotopy of its projections from the cochlea to the auditory cortex (AC) in the brain, in what is called the lemniscal pathway. From the

cochlear nucleus (CN), the auditory information flows in parallel tonotopic streams, that reach first the superior olivary complex (SOC), where the information of the two ears first interacts allowing the localization of sound in space. Following the pathway, the next stage is the inferior colliculus (IC) in the midbrain, where auditory information is integrated and interacts with the motor system (Casseday and Covey, 1996; Xiong et al., 2015). The IC projects to the medial geniculate nucleus (MGB) in the thalamus, which in turn projects to the primary auditory cortex (AI) (Figure 1-5). Here the information is routed to different secondary auditory areas in the brain and feedback to the thalamus and the IC in a dynamic manner. The auditory pathway is very complex as it counts on many feedforward and feedback projections and only an overview of the main processing stations and their connections is provided.

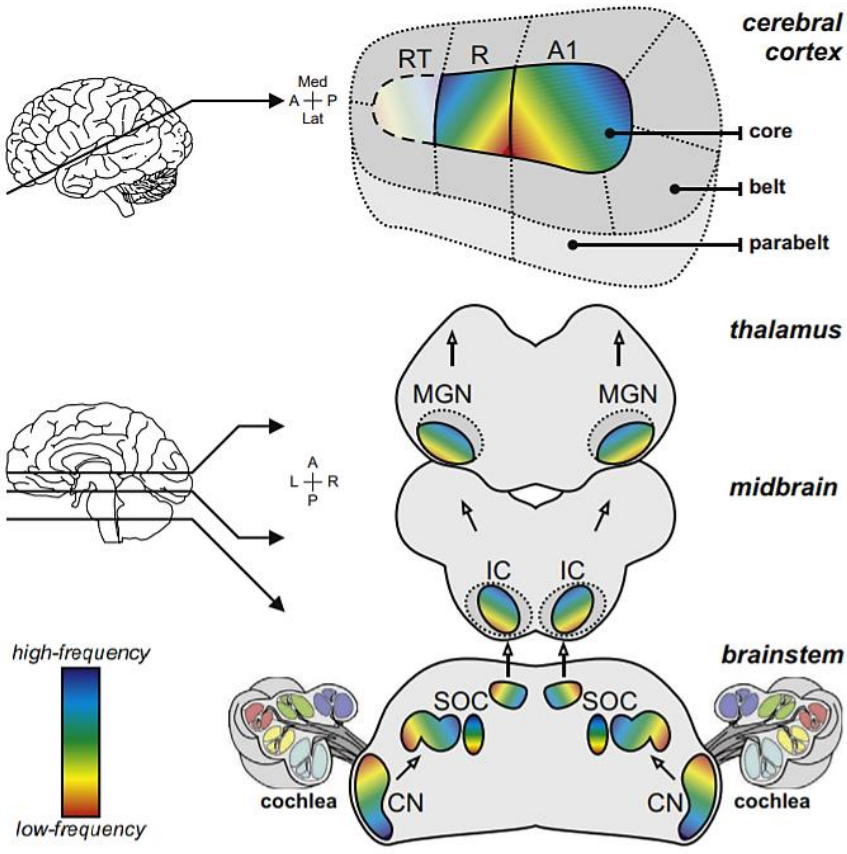


**Figure 1-5. Schematic view of the auditory system.**
All nuclei of the lemniscal auditory pathway are tonotopically organized. Cochlear nucleus (CN), superior olivary complex (SOC), inferior colliculus (IC), and medial geniculate nucleus (MGN).Primary (belt), secondary (belt) and tertiary (parabelt) auditory cortex in the human brain are located in the superior part of the temporal lobe. *From Saenz and Langers (2014).*

# Periphery

## External Ear

The external ear corresponds to the visible part of the auditory system and comprises the pinna, concha, ear canal and eardrum or tympanic membrane. Sound waves are captured in the pinna, then enter the ear canal and push the tympanic membrane which will vibrate according to the sound waves, transmitting them to the middle ear. In humans, this region particularly enhances the detection of sound around frequencies close to human speech, as this perceptual system is thoughtto have evolved to encode environmental stimuli in the most efficient way (Gervain and Geffen, 2019).

## Middle Ear

The function of the middle ear is to act as interface between the mechanical boundaries between the air-filled spaces of the external ear with the liquid-filled spaces of the cochlea. This structure is composed of three small bones (*ossicles*) called the *malleus*, *incus* and *stapes*. These bones form a sort of chain that match the distinct resistances encountered from the air to an aqueous fluid – perilymph and endolymph – in the inner ear. In simple terms, a wave traveling through the air is too weak to cross this air-water boundary and produce the same oscillations, so the energy or pressure of the sound wave needs to be concentrated in a small area. This transformation occurs thanks to the close contact of the *malleus* with the tympanic membrane, its anchorage with the *incus* which in turn moves the *stapes*, the final part of the chain that is in contact with the cochlear surface through the oval window. The correct sound transmission and transformation is also regulated by two muscles in the middle ear, regulating the stapedius reflex (also called the acoustic reflex), which is triggered by loud noises or self-generated vocalizations to reduce the amount of energy transmitted to the cochlea.

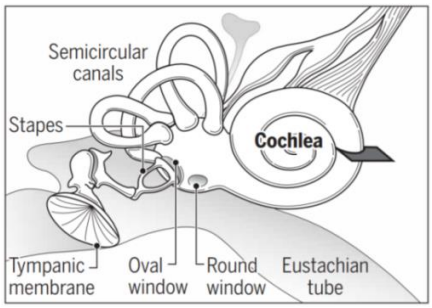


**Figure 1-6. Structures of the middle ear.**

In the middle ear are located the auditory ossicles. These three small bones are in charge of the transformation of sound air waveforms, which impact the tympanic membrane, into oscillations in a liquid media inside the cochlea, through extremely precise movements of the oval window. Also are shown the cochlea and the vestibular system. *From Nyberg and colleagues(2019)*.

## Inner ear

Apart from the cochlea, in the inner ear is also located the vestibular system, responsible for the sense of balance by the continuous gathering of information concerning direction and acceleration of the head in the space. The cochlea is the most critical and important structure in the auditory system, which with its coiled architecture, is where the pressure waves are amplified, decomposed and transformed into electrical pulses. This structure is divided into three fluid-filled chambers (the *scale vestibule, scala media*and *the scale tympani*) separated by two membranes, the Reissner's membrane or tectorial and the basilar membrane. The basilar membrane is the most important for audition, as it lies over the Organ of Corti (*see later*), and covers the entire length of the cochlea, changing its thickness from narrow and stiff in the basal end (near the oval and round windows) to wider and more flexible in the apical end. The movement applied on the oval window, propagates through this membrane and also through the cochlear fluids from the base to the apex, depending on its frequency. Low frequencies will cause vibrations mostly at the apex of the basilar membrane and increasing frequencies will shift the maximal vibration toward the basal end. This means that each location of the basilar membrane will have a 'best' frequency, precisely translated to the Organ of Corti. This last structure contains the inner hair cells and outer hair cells, the mechanoreceptor neurons of the auditory system. The movement generated on the basilar membrane moves the cilia on inner hair cells, opening cation-selective channels near the tip, which leads to the entry of $K^+$ ions into the hair cell. The increase in intracellular $K^+$ results in the depolarization of the cell and, due to the entry of $Ca^{2+}$ through voltage-gated $Ca^{2+}$ channels in the soma, the release of neurotransmitters to the synaptic contacts with spiral ganglion neurons. Together, the axons of these neurons form the auditory branch of the vestibulocochlear or VIIIth cranial nerve. This process is non-linearly amplified, in a poorly understood manner, by outer hair cells depending on the frequency range of stimulation. In this way, each cycle of the sound wave is reflected by a sinusoidal change in the membrane voltage, which is extremely precise for the low frequency sounds (phase locked) but less precise or sensitive for high frequency ones, due to the continuous depolarization of the cell whose magnitude reflects then the amplitude of the stimulus (Cheatham, 1993). Extracellular

recordings of an auditory nerve fiber stimulated at different frequencies, have shown that spikes tend to occur near the crest of the sine wave (when the deflection of the stereocilia of the hair cells is maximal) but not with clockwork precision (Schnupp et al., 2011). This is due to nerve fibers changing their firing rates from roughly Poisson distributed intervals to a lessregular phase-locked mode. This effect depends on the frequency of stimulation, as they can skip some cycles or spikes can occur not on the crest of the wave (Schnupp et al., 2011). In summary, as single hair cells respond to a specific narrow frequency band, the collection of hair cell response features creates the tonotopy observed along the whole auditory pathway present in almost all mammals studied (Schnupp et al., 2011).

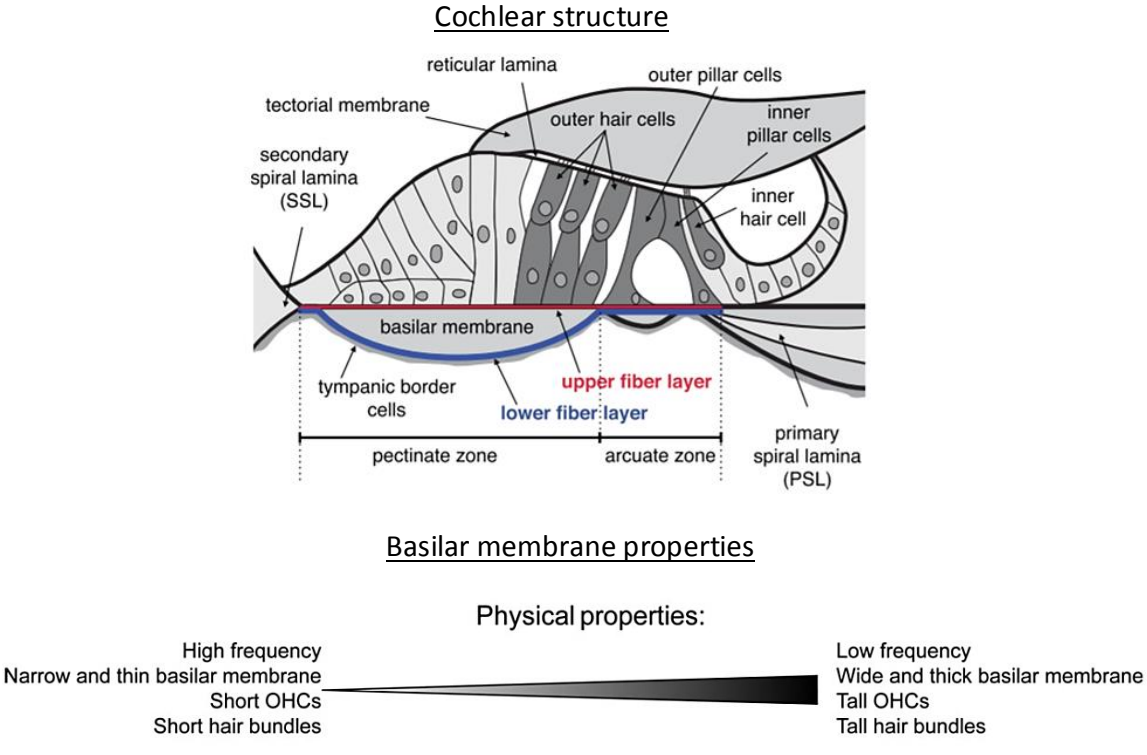


**Figure 1-7. The cochlea and the basilar membrane.**

(A) Schematic structure of the cochlea that shows the basilar and tectorial membrane, as well as the location and organization of the different cell types that generate the mechanostransduction of oscillations into electrical activity by the inner hair cells. *From Kapuria and colleagues (2017)*(B) Summary of the most important physical properties of thebasal-to-apical basilar membrane,as frequency tuning, thickness, cell type and their basic morphological characteristics.*Adapted from Basch and col (2016).*

## Auditory nuclei

### Cochlear nucleus

The auditory nerve fibers join the VIIIth cranial nerve after leaving the cochlea and project to the first relay station of the auditory system, the CN. As described before, each nerve fiber receives inputs from only one inner hair cell projecting to the ipsilateral CN in the brainstem, which is divided into two parts: the ventral part and the dorsal part. At this stage, terminals of the auditory nerve axons differ in density and type, innervating different populations of CN neurons with different properties. Neurons of the CN differ in their anatomical location, morphology and spectro-temporal response profiles but importantly the connections maintain thecochlear tonotopic organization. Neurons of the ventral part of the CN project ipsilaterally and contralaterally to the SOC and neurons from the dorsal part bypass the SOC and project directly to the nuclei of the lateral lemniscus on the contralateral side to then arrive at the IC, the first processing station of the midbrain.

### Olivary complex

In this structure, the spatial position of the sound is encoded using either Interaural Time Differences (ITDs) for low frequencies (< 3 kHz) in the medial superior olive (MSO) or Interaural sound Intesity Differences (ILDs) for high frequency sounds (> 2 kHz) in the lateral superior olive (LSO) (Kandler et al., 2009) (Figure 1-8). Later, ascending fibers reach the contralateral nucleus of the lateral leminiscus which in turn projects toward the IC.

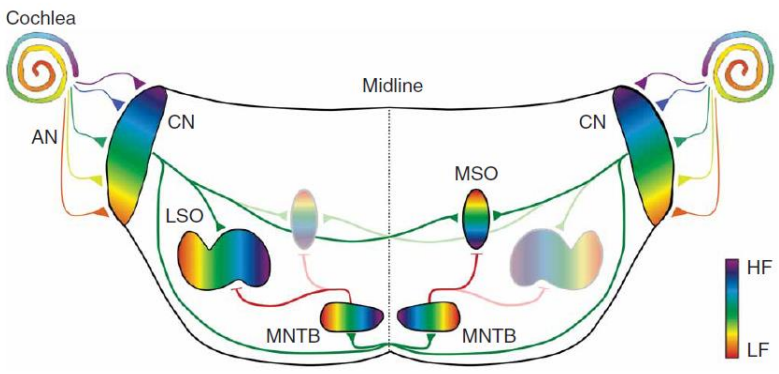


**Figure 1-8. Brainstem auditory sound localization circuits.**

Tonotopic distribution of cochlear outputprojections that innervate the cochlear nucleus (CN). From the CN excitatory (green) and inhibitory (red) connections are detail with the lateral superior olive (LSO) and medial superior olive (MSO). Together these circuits make possible sound localization in space based on spike time differences. HF; High frequency sounds, LF; Low frequency sounds.*Adapted from Kandler and colleagues(2009).*

## Inferior colliculus

Inputs from the brainstem nuclei converge along a fiber bundle known as the lateral lemniscus, which arrives in the IC together with commissural connections between left and right ICs. The IC is subdivided into several sub-regionscontaining one or severalsub-nuclei(C. Chen et al., 2018). Generally the IC is subdivided in core (ICc) and shelter (ICx) regions. ICc is compose of the central nucleus (CNIC) which receive most input from the lemniscal pathway arriving from the brainstem. The CNIC is then surrounded by the ICx, which is composed of the dorsal cortex at the top (DCIC), the external or lateral cortex (LCIC) and the nucleus of the branchium (nBIC) (Chen et al., 2018) (Figure 1-9). Together to the ascending projections from lower auditory stations that innervate the IC, there are an important amount of cortifugal projections arriving to ICx (Bajo et al., 2007; Winer et al., 1998), maybe participating in fine sound localization but their functions are not yet well stablish (Bajo et al., 2010) (Figure 1-9). The complicated pattern of innervations as the combination of binaural information in this structure generates complex neuronal responses, finding for example neurons responding to sound frequency, intensity, duration, as well as neurons able to encode sound localization due to ITD (Grothe et al., 2010; King et al., 1998). Other more refined features can also be found as for example, neurons in the IC of the barn owl, were they are not only tuned to specific horizontal regions in the physical spaces but also to preferred elevations (Grothe, 2018). Comparable maps have not yet been described in mammals, but other features can be found already at this stage such as frequency-modulation responsive neurons (Clopton and Winfield, 1974; Felsheim and Ostwald, 1996; Hage and Ehret, 2003; Rees and Møller, 1983). The CNIC is the structure tonotopically arranged, where neurons responding best to low frequencies are located near the dorsal surface and neurons responding progressively towards higher frequencies are located more ventrally (Barnstedt et al., 2015; Schnupp et al., 2011). ICx neurons send projections to the superior colliculus (SC) where auditory information interacts with head and reflexive eye movements to orientate them to unexpected sound sources(King et al., 1998). Most of the projections from the CNIC and DCIC arrive to the biggest processing and relay auditory nucleus in the thalamus, the MGB or as is simply known, the auditory thalamus(Figure 1-9).

## Auditory thalamus

The MGB receives its inputs mainly from the IC but also direct projections from lower auditory nuclei. In general the MGB is described as an obligatory relay station for all of the ascending auditory projections. The MGB, as the IC, is subdivided into several sub-nuclei, most notably the ventral (MGv), dorsal (MGd) and medial nuclei (MGm) (Figure 1-9). The MGv is part of the lemniscal system,where neurons respond best to one particular frequency, and therefore the tonotopic organization is extremely well conserved. This area corresponds to the major thalamo-cortical relaywith approximately 85% of boutons arriving and clustered in layers III and IV in the cortex (Polley et al., 2007) (Figure 1-9). In parallel to this, the MGd is part of the non-lemniscal system as it receives less tonotopically organized projections from the CNIC (Lee, 2015). This area also sends projections to the granular layer of the cortex but with much more dispersion than MGv. MGm is also not well tonotopically organized receiving its inputs from all nuclei of the IC but also from other lower structures (Hackett, 2011). Neurons in the MGB are tuned not only to frequency, but to other complex features because of the convergence of spectrally and temporally separate auditory pathways (Malmierca et al., 2015). For example, neurons responding best to combinations of frequencies are first observed at this stage (Syka, 1997). Outputs from the MGB are many including dorsal striatum (Chen et al., 2019) and limbic structures such as the amygdala (Antunes and Moita, 2010), but in the vast majority of thalamic projections arrive to the primary and secondary auditory cortical areas (Hackett, 2011; Lee, 2015). Recent experiments indicate that the different subdivisions of the MGB in fact project to non-overlapping areas of the AC, where MGv projects to the core or primary auditory areas whereas theMGd sends its projections the belt or secondary and parabelt or terciary AC regions (Smith and Populin 2001) (Figure 1-9). Consequently, it is thought that in secondary and associative areas of the AC, the main input to layer IV would be projections from primary auditory cortical areas (Hackett, 2011). Mention that the MGB is only a relay station of auditory information to upcoming structures is mostly for schematics and representational reasons as it is well-known that corticofugal feedback projections from AC to the MGB outnumber largely the feedforward cortical projections of the MGB. Primary as well as secondary auditory areas project to all nuclei of the MGB meaning that information that is routed from the MGB to AC, is under constant transformation and strict control of these numerous corticothalamic feedback connections (Kimura et al., 2005; Winer et al., 2001; Winer and Lee, 2007).

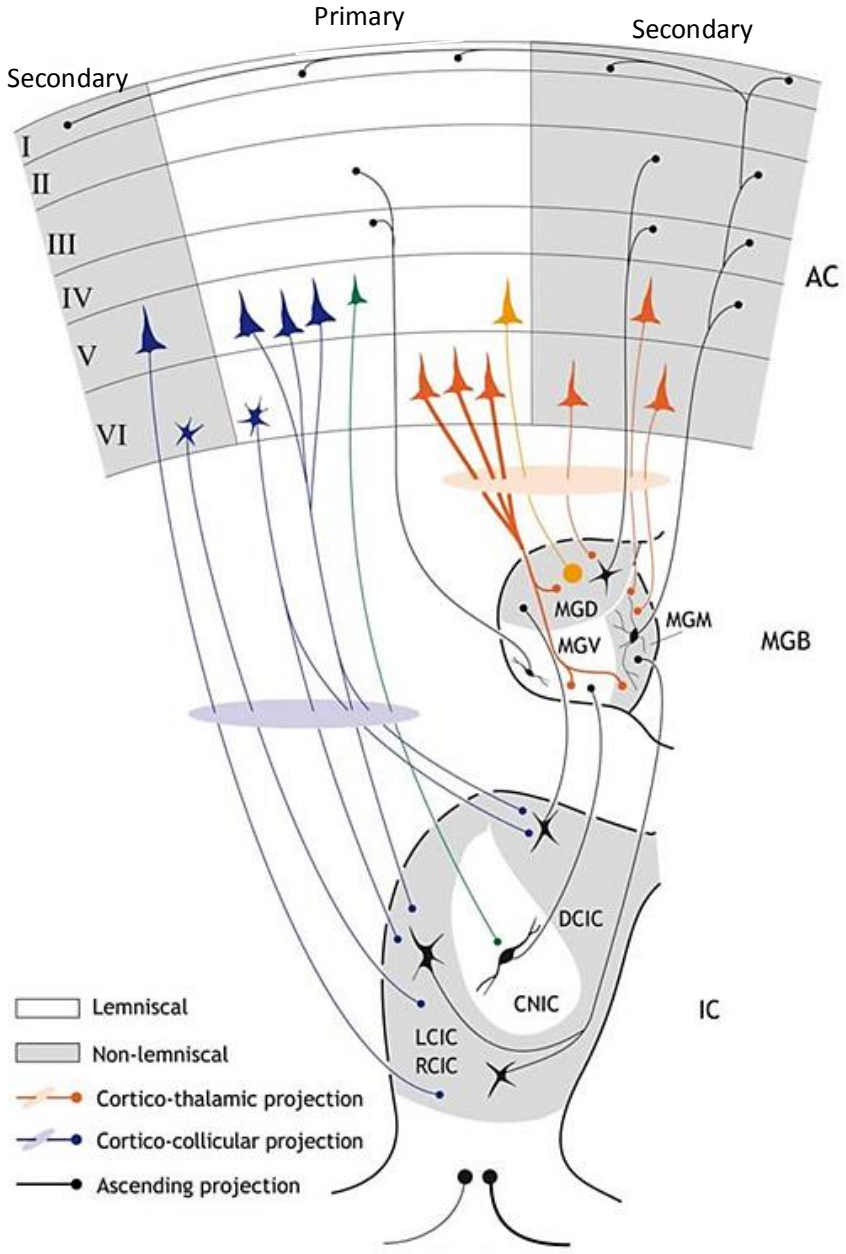


**Figure 1-9. Schematic representation of auditory thalamus projections to AC.**

Feedforwardprojections from MGB to AC arrive to different auditory areas accordingly to the nuclei from they emerged. The ventral nucleus of the MGB projects mainly to AI whereas the dorsal and medialnucleus project towards secondary and tertiary auditory areas. Corticofugal projections reach all nuclei of MGB. Indicated with roman numbers are the neocortical layers from where connections arrive and exit the cortex.Black connections indicate ascending projections and red descending projections.Non-lemniscal areas arehighlighted in grey.*From*Malmierca and colleagues (2015).

### 1.2.3. The auditory cortex

The first evidence about the existence of a brain area dedicated specifically for the processing of sounds, came from the early experiments performed by David Ferrier in the 1870s ("Ferrier on the Functions of the Brain," 1877). First, by direct galvanic stimulations and profound ablations of different areas of the brain in monkeys, he localized and described in much better detail, the motor cortex than his predecessors. Using similar techniques, he realized that precise stimulations in the superior temporal gyrus of monkeys generates a startle response and lesions in the temporal lobe generate severe deafness in the subjects without other apparent motor or cognitive deficiencies. After several decades of research, it is now known that only humans and macaques show some degree of hearing loss after removal or ablation of the AC, unlike smaller mammals such as ferrets, cats and dogs (Warren, 2005). Using diverse techniques, the AC has been precisely located and recognized as the last step in a long chain of hierarchically arranged stages of sound processing (Hackett, 2011). In humans and primates the AC, is located in the temporal lobe and is comprised of the superior temporal gyrus and Heschl's gyrus. In ferrets, cats and dogs,it is located in the sylvian gyrus. Thanks to an extensive amount of research, the AC has been subdivided in a great number of sub-areas, where some of them show a clear and well organized tonotopy (Figure 1-10). Generally, there is evidence to suggest that in primates, there are at least three hierarchically arranged sub-areas within the AC, primary or 'core', secondary or 'belt' and associative or 'parabelt' (Winer, 2011). These different sub-areas, are delineated by their anatomical connectivity patterns, cytoarchitectonic characteristics, physiological criteria and different cell-biological markers (Hackett et al., 2001; Wallace et al., 1991). Primary areas are considered to be the main targets of the ascending lemniscal pathway and they are delimited by the extensive accumulation of granular-like neurons (mainly located in layer IV), short response latencies, strong expression of cytochrome oxidase (CO), acetylcholinesterase (AChE) and parvalbumin (PV), together with a strong myelination pattern. In contrast, secondary and more associative areas present large pyramidal neurons with longer response latencies, and a fractured tonotopic organization with diffuse myelination patterns and less metabolic activity (Polley et al., 2007; Kuśmierek and Rauschecker, 2009; Guo et al., 2012; Joachimsthaler et al., 2014).

In general, the core or primary auditory areas present two or three subdivisions, extensively characterized by tracer injections and extracellular recordings studies. In non-human primates these

subdivisions are the primary auditory cortex (AI), rostral area (R) and rostrotemporal area (RT), arranged from caudal to rostral (Figure 1-10). In other mammals, they are mainly defined as AI and anterior auditory field (AAF) (Hackett, 2011) (Figure 1-10). The homology of brain regions across species, particularly for these areas, is difficult as it shows an incredible specialization regarding the specific animal needs. For example in echolocating bats, there is a considerable number of areas specialized for the processing of echo delays and Doppler shifts, which obviously does not have a counterpart in the human or non-human primate brains (Grothe et al., 2010; Schnupp et al., 2011).

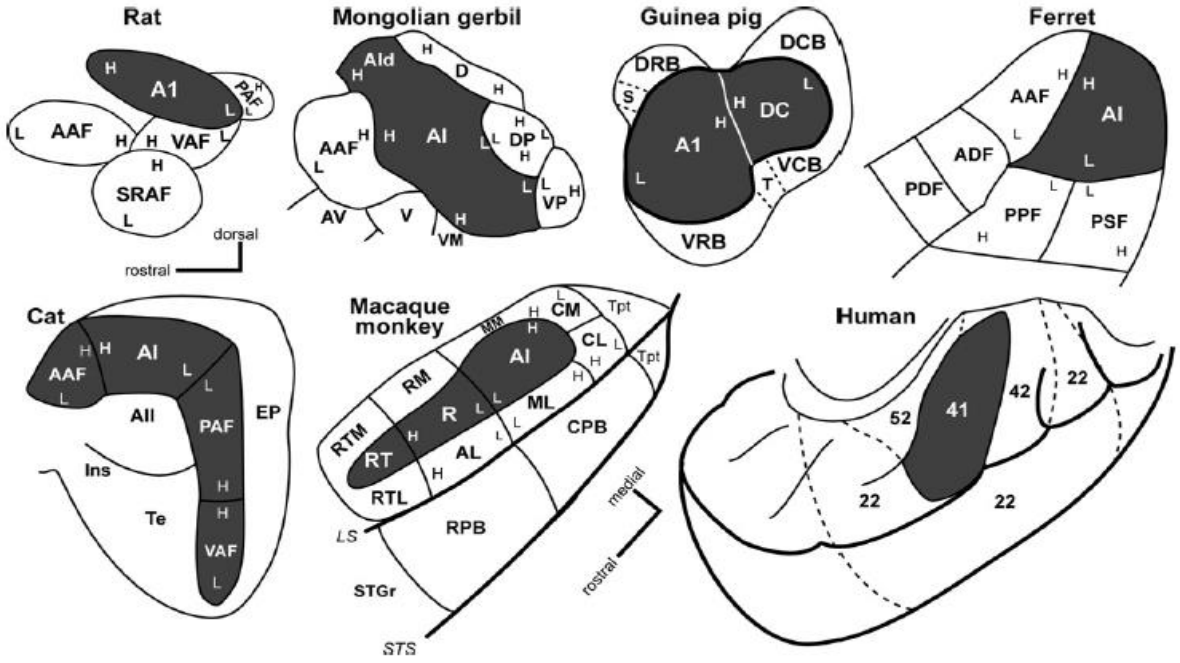


**Figure 1-10. Schematic representation of AC in some of the most studied mammals.**

Primary auditory areas are in darker color. Most of the secondary and tertiary areas described so far are also indicated. Low (L) and High (H) tonotopic fields are indicated in each panel. *From Hackett and colleagues (2011).*

The connectivity pattern in between the different sub-areas of the AC varies between species. While in carnivores, it is usually described that AI and AAF present comparable amounts of thalamic inputs, cortico-cortical connections and similar neurophysiological properties, the secondary auditory area or belt present very distinct connectivity patters (Figure 1-9). In non-human primates as well as in cats, it has been described that AI send direct projections to the secondary areas which in turn, send projections

back to AI and to the posterior ectosylvian region (comparable in some degree to the parabelt region in primates) (Fay and Popper, 1994).

## Tonotopic organization

The first demonstrations of tonotopy were provided by recordings of evoked potentials in the exposed ectosylvian cortex of the cat, while stimulating isolated auditory nerve fibers from different regions of the cochlea (Woolsey and Walzl, 1942; Rose and Woolsey, 1949b). This structural organization was seriously doubted years later by several different groups arguing that responses from isolated units in AC were sparse (Davies et al., 1956; Evans and Whitfield, 1964; Gerstein and Kiang, 1964; Evans et al., 1965; Abeles and Goldstein, 1970) and highly modulated by several factors such as attention and anesthesia (Evans and Whitfield, 1964; Katsuki et al., 1959). Although some of these works argued in favor of the columnar organization of the AC, as they observed a clear macroscopic tonotopic organization after averaging the best or characteristic frequency from nearby isolated neurons, this started a long lasting dispute in the field (Goldstein and Abeles, 1975). The emergence of new technologies to precisely locate and record the activity of thousands of neurons at the same time and at different spatial resolutions (Denk et al., 1990; Grinvald et al., 1986), resurfaced the question about how good the tonotopic organization was maintained across neighboring neurons in the AC, especially in superficial layers. In humans there is evidence from MEG studies, recordings with implanted electrodes or functional imaging (fMRI) of at least one tonotopic gradient in the core region (Howard et al., 1996; Lütkenhöner and Steinsträter, 1998; Talavage et al., 2000). A mirror second tonotopic map has been described recently through high power fMRI, homologous to AI and R areas in the monkey's brain (Formisano et al., 2003). For other mammals, large-scale tonotopic organization has been observed in great detail, using several low resolution optical techniques in the marmoset (Zeng et al., 2019), cat (Langner et al., 2009 ; Spitzer et al., 2001), ferrets (Nelken et al., 2004; Versnel et al., 2002), chinchilla (Harel et al., 2000; Harrison et al., 1998), gerbils (Schulze et al., 2002), rats (Bakin et al., 1996 ; Kalatsky et al., 2005) and mouse (Bathellier et al., 2012; Deneux et al., 2016; Horie et al., 2013; Issa et al., 2014; Issa et al., 2017; Kato et al., 2015; Kubota et al., 2008; Moczulska et al., 2013; Sawatari et al., 2011; Stiebler et al., 1997; Takahashi et al., 2006; Tsukano et al., 2015; Tsukano et al., 2016). Using microelectrode arrays/single electrodes or wide-field two photon calcium imaging recent studies have found the same macroscopic structural organization reported by low resolution optical techniques in the cat (Atencio and Schreiner,

2010), rat (Polley et al., 2007) and with high detail in the mouse cortex (Bao et al., 2001; Barkat et al., 2011; Guo et al., 2012; Hackett et al., 2011; Issa et al., 2014; Issa et al., 2017; Joachimsthaler et al., 2014; Stiebler, 1987; Yang et al., 2014; Zhang et al., 2005). Together these works removed all doubt about the large-scale tonotopic organization of the AC, underlining five subdivisions: two highly tonotopically organized comprising the primary auditory cortex (AI) and the anterior auditory field (AAF), and three non-tonotopic subdivisions, the secondary auditory field (A2), ultrasonic field (UF) and dorsoposterior field (DP) (Figure 1-11A). The segregated UF is often described as a particular feature of the AC in the mouse, as neurons with responses to ultrasonic vocalizations and best frequencies over 40 kHz are mostly observed here (Holy and Guo, 2005; Asaba et al., 2014). Recent findings, based mostly on retrograde tracing studies (Tsukano et al., 2016), have introduced new insights about the number and name of the subdivisions of primary and secondary areas in the AC of mice, discribing at least six subdivisions with four being tonotopically arranged (AI, AII, AAF and dorsomedial field or DM) and two non tonotopically arranged (dorsoanterior field or DA and DP) (Tsukano et al., 2017a) (Figure 1-11B).

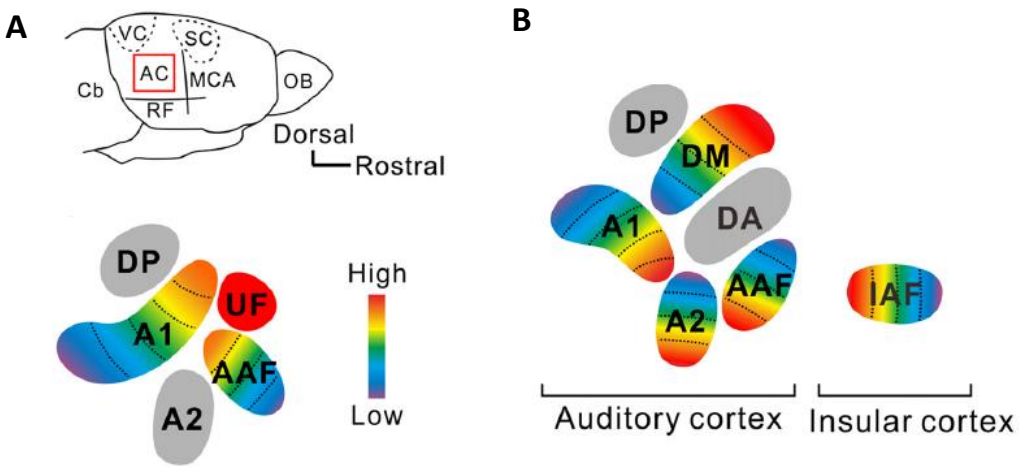


**Figure 1-11. Schematic representation of the mouse AC.**
(A) Drawing of the mouse brain and approximate location of the AC (top) and first detailed tonotopic representation of the main sub-divisions present in the mouse AC (*based on* Stiebler et al., 1997) (B) New proposal for the sub-divisions of the AC in the mouse based on recent findings of tracer experiments of connections from MGB to AC. Abbreviations correspond to; AI: primary auditory field; A2: secondary auditory field; AAF: anterior auditory field; UF: ultrasonic field; DP: dorsoposterior field, DM: dorsomedial field and DA; dorsoanterior field. *Adapted from Tsukano and colleagues (2017).*

Low resolution optical imaging techniques average neuronal responses over several thousands of micrometers or even millimeters of neuronal tissue and can show in great detail the macro architecture of the main tonotopically arranged subdivisions of the AC, but this technique has several drawbacks. Similar to microelectrode studies, where the signal or activity registered can be largely biased towards highly active areas or areas with neurons sharing some similar properties, these methods can hide fine detailed structural features (Kanold et al., 2014). Again different scenarios have been reported using single cell resolution techniques such as the loading or expression of $Ca^{+2}$ indicators combined with two photon microscopy (Svoboda et al., 1997; Tian et al., 2009; Ohki et al., 2005). Independent of the calcium tracer used, either Oregon Green Bapta-1 (OGB-1), Fluo-4 or the different versions of the genetically encoded calcium tracer GCamP (GCamP3, GCamP6m or GCamP6s), a series of recent publications has not reliably observed a fine or smooth transition from the global to the local tonotopy (Bandyopadhyay et al., 2010; Rothschild et al., 2010; Winkowski and Kanold, 2013). Generally, looking at the best frequency or characteristic frequency responses of neurons in superficial layers in the anesthetized mice, a poor tonotopic organization can be observed over spatial scales of <200 µm (Bandyopadhyay et al., 2010; Rothschild et al., 2010) (Figure 1-12). However, the high noise correlations observed between nearby neurons and the presence of the expected average global tonotopic organization by looking across multiple fields of view (>200 µm), indicates a high connectivity and a robust columnar organization (Bandyopadhyay et al., 2010; Rothschild et al., 2010) (Figure 1-12). This has also been recently confirmed by recordings using multichannel silicon probes (See et al., 2018). Only few years later, using the same approach but now in awake mice, an impressive smooth and detailed tonotopic organization was reported (Issa et al., 2014), as also found recently in the marmoset (Zeng et al., 2019). Apparently, differences in the structural properties of the AC can arise from the different methodologies and differences in the cortical state of the animals at the moment of the recording (Guo et al., 2012; Issa et al., 2014; Kanold et al., 2014; Pachitariu et al., 2015).

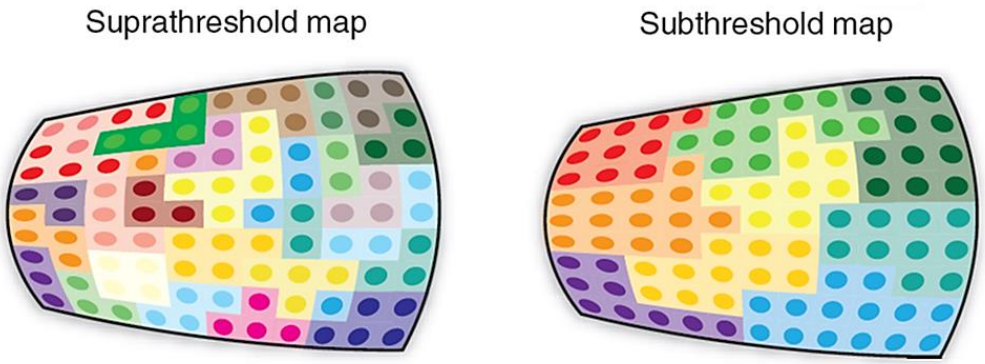


**Figure 1-12. Schematic tonotopy of superficial layers in the mouse AI.**
Tonotopic organization derived from two photon calcium recordings in anesthetized mice. Differences in suprathreshold and subthreshold activity account for a model of interconnected subnetworks with a fractured tonotopic organization based on best frequency tuning characteristics. *Adapted from Castro and Kandler (2010).*

## Other stimulus representations in auditory cortex

Cortical maps are efficient for reducing complexity and redundancy, and enhancing coding power by coordinated parallel processing of the incoming sensory information (Chklovskii and Koulakov, 2004). Different sensory features are thought to be transformed in overlaid maps of sensory processing subnetworks that work together in order to generate single sensory percepts. Apart from the tonotopic organization previously described, there is evidence that other sensory features are mapped through the auditory system of birds, such as source location in the owl (Knudsen, 1984) and object distance in the bat (O'Neill et al., 1989). In the mammalian brain there have been reports of response maps of latency (Mendelson et al., 1997), sound intensity (Heil et al., 1994), amplitude and frequency modulations in a large variety of species (*e.g.*Clarey et al., 1994; Eggermont, 1998; Godey et al., 2005; Issa et al., 2017; Mendelson et al., 1993; Zhang et al., 2003) and binaural interactions in almost all of the species that haven been studied (Schreiner and Winer, 2007), including mice (Panniello et al., 2018). How these cortical maps interact is a matter of debate and active research (King et al., 2018), even though some theories have been presented such as the observations that neurons tuned to low frequencies would prefer sweeps going from low to high frequencies and the contrary, that neurons tuned to high frequencies would respond more often to sweeps in the opposite direction (Godey et al., 2005; Zhang et al., 2003). Technical limitations in conjunction with changing cortical states, due to different attentional states of the animals, during the course of long mapping experiments (Fritz et al., 2003) or task-specific

modulations(Bartlett and Wang, 2005; Scheich et al., 2007) have been largely detrimental for the correct mapping of auditory features and their interpretation. It has been observed that even looking at the same neuron, it can show in a short period of time a high ambiguity in its response profile (Schreiner and Winer, 2007).

## Laminar organization

Looking in more detail, besides the columnar organization of the neocortex, there is a hierarchically laminar organization parallel to the pial surface which is the result of radial waves of migration of post-mitotic neurons during development. During early stages of development, neuroepithelial cells lining in the ventricles transform into radial glial progenitors (RGP), the main neuronal progenitor cell type responsible for the production of other progenitors and eventually for the final neuronal output (Purves, 2004; Uzquiano et al., 2018). At early stages, radial glial cells self-amplify in order to increase the progenitor pool. Progressively they produce other type of progenitor cells, namely basal progenitors. Humans brains are characterized by abundant basal radial glial progenitors, which are highly proliferative and thought to be important for neocortical expansion and evolution. In rodents, basal progenitors are mainly constituted by intermediate progenitors, dividing symmetrically and producing post-mitotic neurons (Douglas and Martin, 2007; Uzquiano et al., 2018). This last mentioned cell type, residing in the ventricular zone (VZ) of the dorsal telencephalon, enters into numerous rounds of symmetric division, generating different types of newborn neurons which in turn, migrate radially and differentiate producing the final columnar organization of the neocortex (Kornack, 2000).

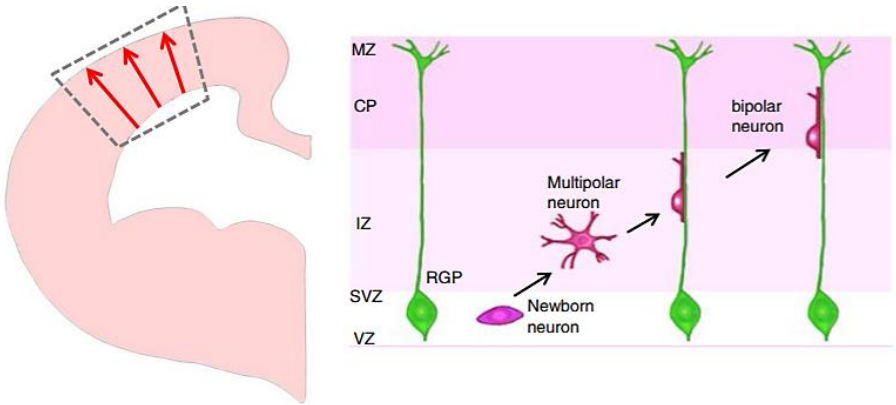


**Figure 1-13. Radial neuronal migration in the developing brain.**

Radial migration is observed during early development when new born neurons, from radial glial progenitors at the ventricular zone, migrate to the cortical plate and proliferate forming the layers of the cortex in an 'inside-out' manner. *Adapted from* ***Moffat and colleagues(2015)****.*

The different layers are grouped into three parts: (1) supragranular layers containing layers from I to III, (2) internal granular layer comprising only the layer IV, (3) andinfragranular layers covering the layers V and VI. Although there is intricate connectivity between layers in a feedforward and feedback manner, the amount and type of cellular populations allows us to determine in part the functional role of each of these layers. In general terms in primary auditory areas, the information arrives mainly into layer IV, from which is broadcast to other cortical layers. Recordings of sound onset latencies in the different layers can account for this as smaller latencies are usually observed in layer IV with gradual increases towards the upper layers (Mendelson et al., 1997) (Figure 1-14). Layers II and III serve with intra-cortical and cortico-cortical projections whereas layers V and VI correspond to the main output layers to subcortical and other cortical structures. Although the functional impact and fine architectural features of all cortical layers has not yet been completely defined, there are some common rules that have been found in most mammals (Hackett et al., 2011).

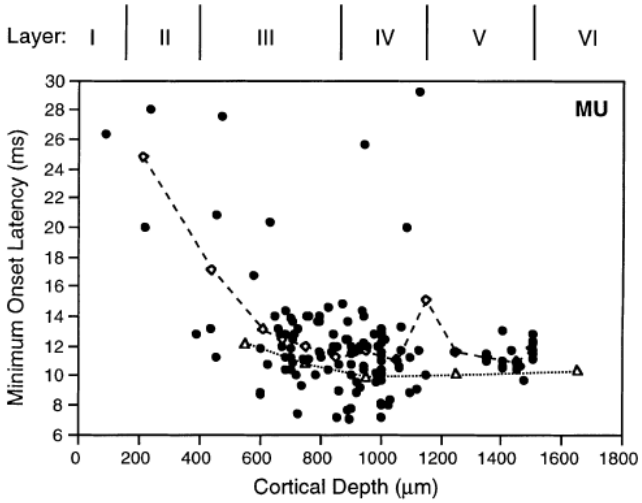


**Figure 1-14. Sound onset latency and recording depth for multi-units in AI.**
The minimum sound onset latency for multi-units (MU) recorded across all layers of AI in the AC of cats plotted against cortical depth. The averaged approximate location of the cortical laminae is indicated with Roman numerals. Dashed line corresponds to averages of locally minimum onset latencies whereas the dotted line corresponds to the average onset latency

for five depths in nine electrode penetrations. *Adapted from Mendelson and colleagues(1997)*

### Layer I

Layer I contains a small number of neurons where almost of all them are GABAergic VIP interneurons. These neurons are heavily innervated by lower layers and high-order cortical areas, making of this layer the main input of top-down modulations (Fu et al., 2014; Letzkus et al., 2011; Muralidhar et al., 2013).

### Layers II-III

Even though these layers are usually described together, there is a growing interest to separate them based on their structural and functional differences. These layers receive inputs principally from layer IV and a small fraction directly from the thalamus, together with strong lateral inhibitory inputs (Meyer et al., 2011). This is translated into low spontaneous and evoked firing rates with high stimulus selectivity, particularly in awake animals (Haider et al., 2013; Lefort et al., 2009). Similar results were obtained during whole-cell recordings of neurons in awake head-fixed mice, where high variations in subthreshold activity were observed but only few spontaneous spikes probably because of the presence of large inhibitory inputs (Poulet and Crochet, 2018; Petersen et al., 2003). Recently, in AI, it has been shown that layer II neurons respond significantly stronger to pure tones and they tend to be more tuned in an intensity-dependent manner than the neurons layer III (Oviedo et al., 2010). Also these layers differ in their inputs and long-range projections, layer II receives mainly intra-columnar inputs from layer IV, whereas layer III can receive it from out-of-columun layer VI and auditory thalamus (Winer, 2011). More striking is the difference in their output targets, where layer II sends projections to lower sub-areas of the AC and layer III neurons showed clear and strong projections to the contralateral AC (Oviedo et al., 2010). Thus, in addition to their morphological differences,layer II and III not only present different sound-evoked responses *in vivo*and also different circuitry suggesting a clear segregation in sound processing and global function (Oviedo et al., 2010).

### Layer IV

This layer corresponds to the main point of arrival of the lemniscal pathway as it receives strong tonotopically organizedfeedforward connections from the auditory thalamus (Hackett et al., 2011), although other properties such as temporal and spectral features are less concisely aligned between the two stations (Lee and Winer, 2008).The morphology of the neurons in this layer is unique in that most of

them are non-pyramidal spiny stellate cells (Winer, 2011). Neurons in this layer send projections to upper layers, mainly layer II and III of the corresponding column (Hackett, 2011).

### Layer V

This layer corresponds to the thickest layer in primary auditory areas and integrates information from almost all cortical layers thanks to long apical dendrites. In return, this layer sends long-range axonal projections to other cortical and subcortical brain regions. The neurons in this region, contrary to layer I, are mainly excitatory with the second smallest quantity of inhibitory cells (Tremblay et al., 2016).

### Layer IV

This layer contains a large number of cell types, whit a few of them having the most elaborate axonal projections connecting neighboring cortical columns (Narayanan et al., 2015). Because of these varied neuronal morphologies, this layer receives information from a broad range of stimuli coming from thalamic and different intra-cortical connections together with weak inhibitory inputs, as it is the layer with the least inhibitory cells in the AC and a sustained high firing rate(Radnikow and Feldmeyer, 2018; Tremblay et al., 2016). Excitatory neurons in this layer send projections to other intra-cortical areas, but mainly supply feedback projections to the auditory thalamus (Winer, 2011).

## Principal cortical cell types

The earliest detailed descriptions of the different types of neurons in the cortex are the observations of Santiago Ramón y Cajal in the last decade of the 19$^{th}$ century (Gil et al., 2014) (Figure 1-15). Studying the axonal structure, somatic morphology and dendritic profiles, he described a great amount of different cell types and proposed several theories about neuronal circuits, most of which were validated using modern fluorescent and electrophysiological techniques (Markram et al., 2015). Currently, neocortical neurons are classified in two main classes: glutamatergic projection neurons, principally pyramidal shape neurons, that correspond to approximately the 80% of cortical neurons, and GABA (ϒ-aminobutyric acid) –ergic interneurons, that correspond to roughly 20% of cortical neurons (Markram et al., 2004). In general, the interneurons receive local excitatory as well as inhibitory inputs and their classification depends on many different morphological, anatomical, genetic and physiological properties (Chen et al., 2015; Purves, 2004). In general, cortical inhibitory neurons can shape tuning specificity, stimuli response

strength and robustness, as well as the shapeof the correlations between intra and extra-cortical domains (Aizenberg et al., 2015; Briguglio et al., 2018). Recently, it has been observed that attentional and state-dependent cortical dynamics in primary sensory areas can be largely modulated by higher order inputs in a top-down manner involving different neuromodulators, such as cholinergic inputs which arrives mainly to superficial layers. These can have an important impact in attentional engagement, mainly thought local inhibitory circuits (Kuchibhotla et al., 2017). Even though, cortical neurons process complex and non-linear features that differ between sensory modalities, there are some neuronal connectivity rules shared among different sensory areas that tell us more about how the sensory information is treated than the features that are encoded and extracted. In this sense, the connectivity patterns and functionality of the most abundant and generally mentioned cell types, is quickly described;


**Figure 1-15. Drawing by Santiago Ramón y Cajal of the cerebral cortex.**
This drawing ofa Golgi staining byCajal conveyed some of his findings reported for small mammals. Different type of cell morphologies are appreciated and their approximate localization in the laminar organization of the neocortex. *Adapted from Gil and colleagues (2014).*

## Excitatory cells

Excitatory neurons or principal cells are named like this because of their quantitative superiority in the cortex. They are generally divided into two main groups, spiny stellate cells and pyramidal cells, with both groups differentially located in the cortical layers (Simons and Woolsey, 1984) (Figure 1-16A). Besides the morphological differences in excitatory neurons, their local organization also can be distinguished by their electrophysiological properties. According to their spiking profile, there are also two main groups, regular-spiking (RS) and burst-spiking (BS) neurons (McCormick et al., 1985) (Figure 1-16B). More recent and complex classifications have been made regarding their biophysical properties, such as their axon conduction velocities, together with enzymes, neurotransmitters and more detailedimmune-histochemical profiles, which greatly exceeds the scope of this manuscript.

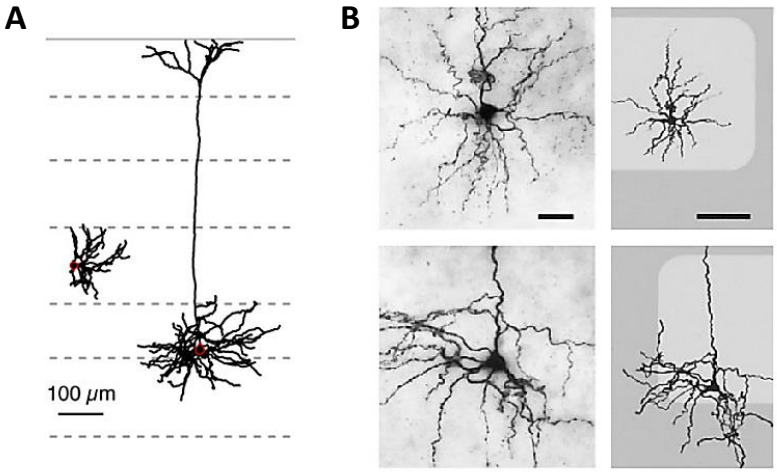


**Figure 1-16. Principal excitatory neurons in layer IV of the neocortex.**
(A) Reconstruction of two of the most classic and well-described cell types found in the neocortex (mouse C2 barrel), spiny stellate and pyramidal cells in order. Differences in their dendritic and axonal arborizations are evident as well as their differential localization. *Adapted from Schubert and colleagues (2003)* (B) Photomicrographs of one spiny stellate neuron (top, scale bar 25 µm and 100 µm) and one pyramidal neuron (bottom) stained with biocytin found in the mouse neocortex. Adapted from Lefort and col (2009).

## Inhibitory cells

Inhibitory cells in the neocortical circuits have the most diverse morphological and functional properties of any other cell type in the cortex. Generally they are thought of as the main source of spike timing control in the cortical circuitry as in awake animals they control the output signal of presumably every

neuron in the brain (Haider et al., 2013). Despite their great heterogeneity, there are three genetically defined sub-classes that are the most studied interneurons so far.

### *Parvalbumin-expressing (PV) interneurons*

This class of interneurons consist of two main subgroups; basket cells which make up almost 50% of interneurons and target mostly the soma and proximal dendrites of pyramidal cells, and chandelier cells targeting the axon initial segment (Markram et al., 2004) (Figure 1-17A). Both types of interneuron receive strong inputs from thalamus, inputs from other types of interneurons, as well as from different areas of the cortex, together with the strong inputs of the pyramidal cells in their vicinity (Markram et al., 2004). This pattern of connectivity suggests that this class of interneurons produces a strong and fast inhibitory conductance decreasing quickly and precisely the excitability in their local vicinity, as dysfunctions in their properties can leads to epileptic activity in cortical neural circuits (Casanova et al., 2003). At the same time, this connectivity feature has been used in a number of recent publications, where acute and strong activations of this genetically targeted neuronal population,are used to heavily modulate or even inactivate large cortical domains (Briguglio et al., 2018; Hong et al., 2018). PV interneurons have also been shown to tbe causally involved in the generation and maintenance of gamma oscillations (30-80 Hz) in the brain, which are believed to enhance information transmission and processing (Kim et al., 2016; Sohal et al., 2009). Generally in the AC, these type of interneurons are described with wide tuning properties (Maor et al., 2016), and controlling more the balance or gain of excitatory activity rather than specific features (Li et al., 2015) (Figure 1-17B). Light modification of their firing rate can sharpen the tuning profile of principal cells in the AC with a consequent increase in behavioral acuity during frequency discrimination (Aizenberg et al., 2015). Also, this particular type of interneurons has been linked to the active suppression in cortical circuits observed by self-generated movement and sounds (Angeloni and Geffen, 2018).

### *Somatostatin-expressing (SOM) interneurons*

This second class of interneurons consists mainly of Martinotti cells targeting the tuft dendrites of pyramidal cells and other types of interneurons such as $PV^+$ interneurons (Figure 1-17A). Also broadly tuned but less so than PV interneurons (Li et al., 2015) (Figure 1-17B), these types of interneurons are globally modulated by behavior-dependent activity patterns. They control the main output of pyramidal cells by sharpening their responses profiles as well as generating strong lateral inhibition (Kato et al., 2015; Wilson et al., 2012). Recently, these types of interneurons have been suggested as the main source

of inhibition caused by habituation in primary sensory systems (Natan et al., 2017) and play a necessary role for learning in mice (Chen et al., 2015).

*5HT3A-receptor-expressing interneurons*

The last major class of interneurons consists largely of vasoactive intestinal peptide (VIP) interneurons, which are located almost entirely in upper cortical layers. By their location they receive inputs from high-order cortical areas being involved in learning dependent changes and behavioral neuromodulation. Also, it has been observed in primary visual and auditory cortices that the firing rate of this type of interneuron is largely modulated by locomotion or foot-shocks through cholinergic inputs (Fu et al., 2014).

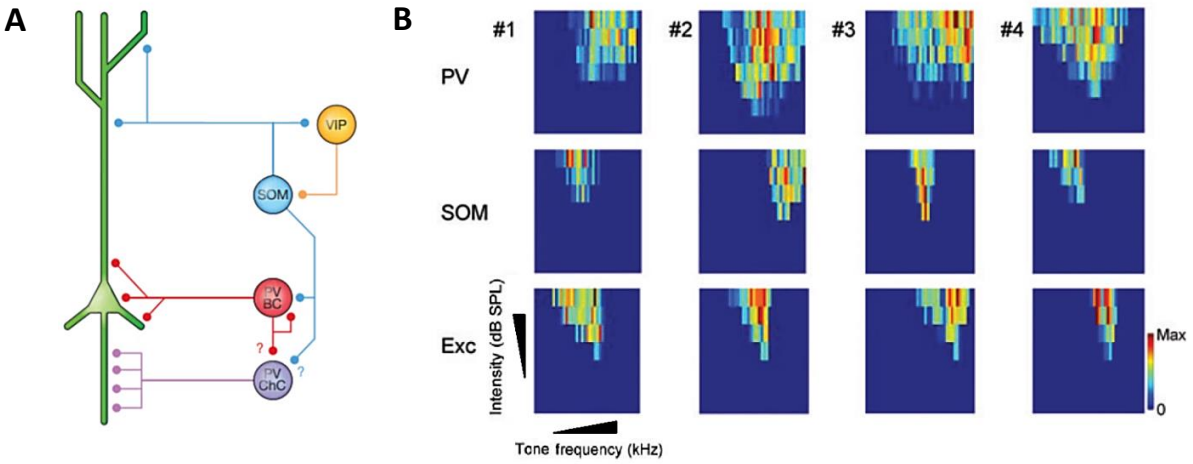


**Figure 1-17. Schematic representation of neocortical circuits and their responses to sounds.**

(A) Sketch of the connections for pyramidal cells (green), Basket cells (red) and Chandelier cells (Purple) from the parvalbumin expressing group of interneurons, somatostatin expressing interneurons (Light blue) and vasoactive intestinal peptide cells from the 5HT3A-receptor-expressing group of interneurons. (B) Tonal receptive field of spikes at a particular frequency and intensity combination from genetically identified different class of neurons. *Adapted from Li and colleagues (2015).*

## 1.2.4. Sensory perception and behavior

The auditory system is well-known to be strictly organized by the decomposition of sound frequencies made in the inner ear and maintained through the whole auditory pathway until it reaches the auditory

cortex. Contrary to these observations, an important review of the early literature in sensory systems by Whitfield in 1979, pointed out experiments where some level of sensory detection and discrimination can be achieved in trained animals after ablation of sensory cortical regions. The goal now, is to be able to describe what are the features encoded and retrieved at each step of the sensory processing pathway and what are the transformations that occur in cortical circuits. Together with the minimal components that allow animals to achieve simple and more difficult sensory-based decisions. The link between sensory perception and behavioral actions is established through experience and learning. It Is for this reason that for the proper study of cortical circuits and their role in perception, we need a good understanding of how these associations or connections are built and reinforced in the brain. Fundamental theories of associative learning described how the brain predicts future outcomes based on previouslearned associations, how saliency can define the rate of learning or how attention can select certain stimulus features. In the next section, a brief historical and descriptive introduction is made to understand these basic learning rules as also how learningis most commonly modeled. Learning models have been useful totestgeneral assumptions about cue interactions observed during animal learning and today are an important tool to unravel learning and its mechanisms.

# 1.3. Learning and modeling animal behavior

## 1.3.1. Classical and operant conditioning

Learning through experience and sensation, allows us to precisely adapt our behavior. From infancy, we interact with our environment via exploratory sensorimotor commands and we adapt our sensation in response to our changing environment (Berg and Sternberg, 1985; Dehaene-Lambertz and Spelke, 2015). Through the evolutionary process, different animals have acquired impressive sets of skills to sense their environment and survive in challenging conditions. For example, bats use sound, instead of vision, to move through space at night (Schnitzler et al., 1987) or bees that are able to detect UV light which helps to choose flowers depending on their reflectance (Chittka et al., 1994). The adult brain together with its specialized perceptual systems is responsible for solving these challenging situations with its enormous capacity to link environmental cues with surprising outcomes and to adapt behavior in order to meetinnate or immediate needs. In the laboratory we can study this capacity and train animals to linkbasic behaviors, such as seeking for reward/pleasant events or avoidance of harmful/unpleasant ones, with different stimuli in order to explore the basic rules of associative learning. To start unraveling perception and sensory based decisions, we need to have precise control of the input or sensory stimulus and a good understanding of the behavioral task and the structure that the animals will follow to learn a new association. Therefore, it is necessary to minimize the external contingencies and variables that can affect the behavior with the ultimate goal of obtaining the most stereotyped behavior in a population of animals whit a similar overall level of performance. In this direction, the simplest learning paradigm is “classical conditioning”, introduced by Pavlov in 1902, wherean unconditioned stimulus (UCS) and an unconditioned response (UCR) are used to create a new association with a neutral stimulus (NS). In simple terms, an environmental cue or stimulus (food-UCS) that naturally produces an unlearned/innate behavior (salivation-UCR) is linked to another stimulus which previously has no effect on the subject (sound-NS). During conditioning, for every trial the NS becomes more associated with the UCS because oftheir consecutive presentations (Figure 1-18A). By doing this, the NS rapidly become a signal or cue that predicts the presence of the UCS. After this association is made, the NS is now called, conditioned stimulus (CS) because now can trigger theconditioned response (CR, before UCR). In this classic experiment, the presence of the sound will produce salivation before the presentation of the

food.Indeed, Pavlov's principle is able to explain the emergence of this type of conditioned response but it was unable to account for the appearance of repeated/stereotyped behaviors, as for example an animal pressing a lever to obtain food after a sound cue. From those observations it can be predicted that, at the moment that the animal is pressing the lever, it salivates because of the association between lever and food, but Pavlovian principlescannot explain why the animal decided to press the lever in the first place.

Around the same time as Pavlov, Thorndike in 1898 implemented a set of experiments that were gave important clues to understand animal motivation, behavior and learning. He made several observations of animals creating new associations in complex settings. In a typical experiment, he would place a cat in a puzzle box and measure the time or number of trials that the animals needed to escape or get a bowl of food by pulling the correct lever inside the box (Figure 1-18B). By studying their learning curves, he observed that the learning was gradual and continuous, displaying a step by step slow increase due to trial and error (Figure 1-18C). This idea, described in more detailin his theory of 'law of effect' (Nevin, 1999), is the foundation of what B.F. Skinner later developed as "operant conditioning" (Skinner, 1932). In this context, a stimulus-action that is followed by rewarding events will be repeated and the opposite, if the same stimulus-action is followed by non-rewarded/unpleasant events it will be avoided or less likely to be repeated. In this regard, the CS can be appetitive and predict reward or it can be aversive and predict punishment. An important feature also pointed out at this time was the restricted temporal contiguity needed between a stimulus and a response to promote successful conditioning (e.g.Smith and Roll, 1967; Mahoney and Ayres, 1976).

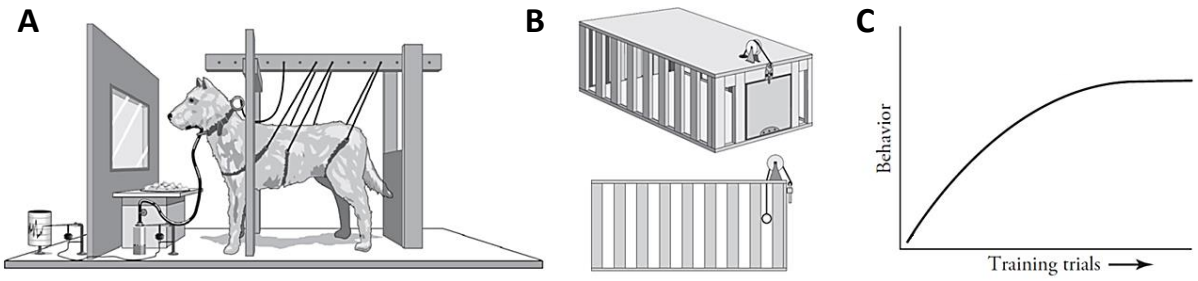


**Figure 1-18.Pavlov's conditioning and Thorndike's puzzle box experiments.**
(A) Schema of the Pavlovian salivary conditioning for dogs. A cannula collects the saliva while different devices control the presentation of the sensory stimuli. (B) Thondike's puzzle box for cat where pulling of the loop inside the box triggers the opening of the door (C)

Theoretical learning curveobserved in such type of experiments. *Adapted from Domjan and Grau (2015).*

From these foundational experiments, it was stablish thestudy of animalsin the laboratory during learning of casual relationships (Dickinson, 1981). Later different settings and training paradigms helped to formalize themost common concepts of conditioning and reinforcementlearning in animal behavior.

### 1.3.2. Discrimination and generalization

Even though classical/Pavlovian conditioning, which allows anticipation of biologically important events, and operant/instrumental conditioning, which gives control to the occurrence of these events, aretreated separately, both forms of conditioning are necessary to generate internal predictions andrespond accordingly to the cues in the environment (Domjan and Grau, 2015). Using a combination of these two methods in the laboratory, we can study perceptual decisions in behaving animals. Via classical conditioning, we can train animals to create basic associations and then through instrumental conditioning, refine the previous acquired behavior regarding some salient stimulus features. One type of such protocols, are Go/NoGo discriminations and normally consist in 4 training phases. In the first phase, animals are habituated to be head-fixed until theydo not show signs of evident stress. In the second phase, for several trials, a sound (CS+) is paired with a water/food reward, independent of the behavior of the animal. In the third phase, the animal needs to lick right after the presentation of the sound in order to get the reward. In the last phase, when the animals are generally highly conditioned to respond to the sound (CS+), a new sound is introduce but not followed by any reward (CS-). During CS- presentations, behavioral responses can be punished with a time out or a soft air puff or mild foot shock. At the beginning of this stage, the animals generalize and respond for both CS+ and CS- in the same way. Only after several trials do the animals start to decrease their behavioral response to the CS- and respond only to the CS+ (Figure 1-19).

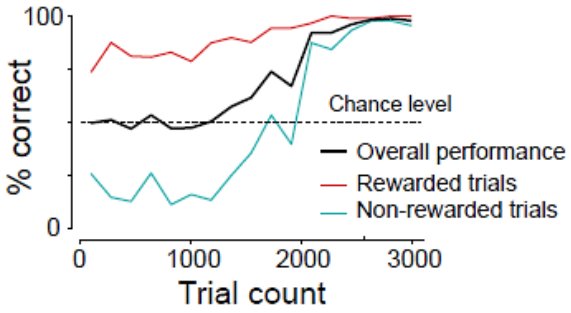


**Figure 1-19. Performance of one animal in a sound discrimination task.**
Individual learning curvesof the last phase of a simple discrimination conditioning (when the CS- is introduced)from one representative mouse. Note that at the beginning the animals generalize and respond to both stimuli (red and blue), until it stops responding for the non-rewarded stimulus and discrimination improve. In black overall performance corresponding to the average of the two curves. *Adapted from Bathellier and colleagues(2013)*

In the last decades, it has been shown that almost all animals, even very simple organisms as unicellular ciliatesfrom the genus *Paramecium* (Hennessey et al., 1979), are ablewith training to discriminate between a rewarding (CS+) and a neutral or unpleasant (CS-) stimulus. It is hard to account for all types of classical/operant conditioning that have been tested so far, but it is worth pointing out a few examples where the capacity of certain animals to associateand categorize eventswith a relevant outcome is just remarkable. In an experiment performed byHernstein and colleagues (1976), pigeons were trained to peck a response key after the presentation of very complex visual stimuli or ordinary landscape snapshots (Figure 1-20A). Only responses to one set of randomly assignedimages delivered food (CS+) and another set had no behaviorally relevant outcome (CS-). As it was previously described,at the beginning of the training subjects responded in a similar way to both set of pictures, but only after several pairings, they started to peck more rapidly to the CS+ and slowly or not to the CS-set. Later a high level of discrimination is observed, novel or non-trained images can be tested and study how animals categorize them into one of the two trained groups (CS+ or CS-). This phenomenon, where two stimuli can be highly discriminable but at the same time sufficiently similar to be considered or 'judgde' in the same category, is called generalization. In this regard, it is generally thought that discrimination is limited by peripheral sensory factors while generalization can be influenced by context and task requirements. To probe this ability in birds, Hernstein and colleagues (1976) trained pigeons to discriminate between images of scenes or landscapes containing a tree and others than don't (Figure 1-20A). In several test sessions, novel/non-trained images were presented to the animals and remarkably, they could use the

categorical information (presence of a tree or not) to discriminate and respond correctly, as no decrease in performance was observed when the new images were presented randomly between regular trained ones (Figure 1-20B) (Hernstein et al., 1976). This experiment has been replicated using different objects to create this categorical classification, as water or people, showing the remarkable ability of animals to extract certain information and generalize (Figure 1-20B) (Vaughan and Greene, 1984).

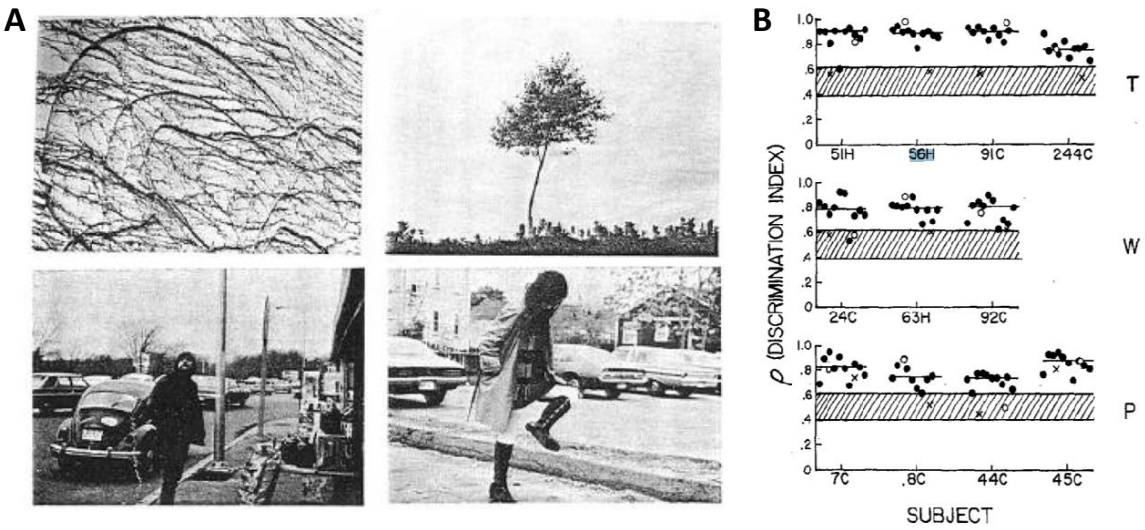


**Figure 1-20. Pictures used to trained different groups of pigeons and generalization results.**

(A) On top images used to test generalization and classification for trees (T) and on bottom for people (P), images of water (W) not shown. (B) Generalization results where the discrimination index is plotted for each animal trained. These plots are showing that the probabilitiesofuntrained novel images corresponding to the same trained category are highly categorized. Horizontal lines show the medians. *Adapted from Hernstein and colleagues (1976).*

This type of stimuli generalization is not only restricted to visual stimuli it can also be studiedusing sounds (Wright and Zhang, 2009). Interestingly, it has been observed in Mongolian gerbilstrained to discriminate between symmetric pairs of frequency-modulated tones or chirps (linearly ascending and descending), their capacity to create sound feature categories and transfer they learned behavior to novel/non-trained sounds (Wetzel et al., 1998). Using a shuttle box and a Go/no-Go avoidance task, animals were trained with an ascending chirp (CS+) to cross the hurdle of the box or stay in the same side during the presentation of a descending chirp (CS-). If the proper behavior was not done, at the end

of the sound animals were punished with a mild foot shook. Once the animals had reached stable performance, in order to create a categorical classification of chirp direction, a new pair of frequency modulated tones was introduced and the animals were re-trained.The generalization and categorization were later tested by presenting randomly a novel/untrained chirp to a well-trained animal, and observing if the transfer of the 'concept or the category' was achieved. All animals tested responded to the vast majority of the novel chirps used as good as for the trained sounds, proving the ability of the animals to form categories with artificial behaviorally non relevant sounds (Wetzel et al., 1998).

Different theories aim to explain how the process of generalization is implemented in the brain but for the purpose of this work, *feature theory*will be discussed in more detail as is the most relevant for this work. In simple terms, the comparison of two different stimuli can be made in different ways. One possible approximation (*prototype theory*) is to compare each stimulus to an inborn or learned 'model or prototype' but it is difficult to understand and explain how this prototype is primarily formed. A more straightforward approximation is to compare different stimuli by their decomposition into simple or basic features. Then, during training of a novel stimulus, a new association will be formed with a sub-set of features creating a 'concrete representation' where only a fraction of the information is stored. Generalization then occurs because every new input or entry will be compared and categorized by the sum of its common features. The more elements two stimuli have in common; bigger will be the probability to generalize between them. Cerella in 1980 trained pigeons to peck for food in response to only drawings of Charlie Brown and not for other characters or similar shapes. To test generalization, he presented different slides containing scrambled or clipped versions of Charlie Brown cartoons, but that contained several of its characteristic original features (Figure 1-21A,*Top*). Surprisingly, pigeons responded almost as well to these untrained novel images similar as they did for the trained images (Figure 1-21A, *Bottom*). Similar observations can be extracted froma more recent study by Bathellier and colleagues (2012), where they trained mice to lick in order to get a water reward after hearing a complex sound (Figure 1-21B). After reaching a good level of detection for the CS+, they introduced a novel non-rewarded complex sound (CS-). As discussed before, animals at the beginning respond similarly to both sounds, but after several training sessions, mice learned to keep licking for the CS+ and refrain or stop licking for the CS- sound. In well-trained mice, they presented randomly a novel untrained set of sounds that formed a continuous transformation from sound CS+ into CS-(Figure 1-21B, *Bottom*). Mice categorize these sounds in anon-linear/discrete manner showing an abrupt change of categorization

from CS+ to CS- sound (Figure 1-21B, *Top*) (Bathellier et al., 2012). These results can be easily explained using the feature theory framework, where more difficult discriminations will redefined the sub-set of features learned or recognized in order to achieve the correct outcome and maximize rewards, creating an abrupt change in categorization. We can conclude from these experiments that simple features embedded in complex stimuli can'call' one or another totally different stimulus representation. Then, we can make the assumption that by the activation of a subset of neurons that encode one of these features we could trigger artificially any stimulus representation in the brain. This is one of the major subjects of this work and it will be treated in depth in the following sections.

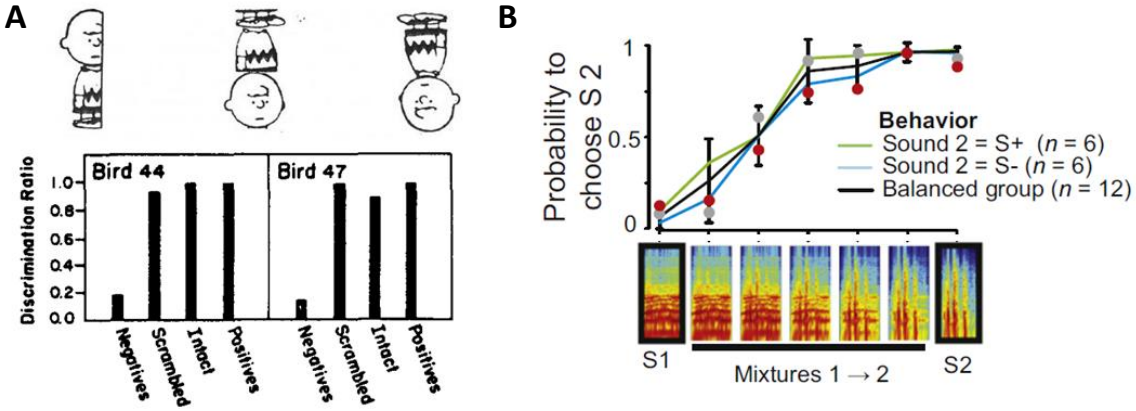


**Figure 1-21. Generalization experiments using images or sounds.**

(A) Modified and scramble images of Charlie Brown(top) and discrimination ratio showing that pigeons generalized over the different images (bottom).*Adapted from Cerella (1980).*(B) Different group of mice trained either with S1 (blue curve) or S2 (green curve) as CS+. Plotted is the probability to choose S2 sound showing the generalization for each group to novel mixed sounds (Top) and spectrograms for each sound tested (Bottom).*Adapted from Bathellier and colleagues (2012)*

### 1.3.3. Learning from predictions

The first theories and models of learning came from the observations that animals preferentially learn from cues that are good predictors of biologically important outcomes (Domjan and Grau, 2015; Garcia and Koelling, 1966; Hollis et al., 1997). A prime example of this is a bird trying to catch a fish under the water. Sudden ripples on the surface have a great saliency for the animal as they are good predictors of a fish getting close to the surface. Associative learning then is related to the formation of connections between environmental cues andactions with their respective outcomes. Internal signals will then translate this relationship cue-action into motivationally significant events (Dickinson, 1981). At every pairing, the cue that preceded the behavior becomes relevant because it acquires a predictive value of behaviorally pleasant or unpleasant events. From this, it was inferred that the learning process depends on the unpredictability of primary appetitive/aversive events, because only unpredicted events are effective for conditioning as no learning occurs when the reward/punishment becomes fully predictable (Kamin, 1967). In other words, the rate of learning or acquisition will depend on how big is the difference between the prediction and the expected outcome (Rescorla and Wagner, 1972).

Predictions are essential for survival because making inferences about future events leads us to prepare better behavioral actions, decrease reaction times and avoid previously experienced adverse conditions. Consequently, when the predictions are accurate and important outcomes can be anticipated, it is thought that no change will occur to this representation and no internal resources will be expended, as information processing and memory storage are energetically costly (Johnston, 1982; Mery and Kawecki, 2003).One of the first observations of this paradigm was made in experiments done by Kamin in 1967, where the acquisition of a new association was closely related to the novelty or the predictive power of the stimulus. In a group of animals (Group A) trained with a light + noise (NS) follow by a mild foot shook (UCS), after very few sets of trials the presence of the light + noise (now CS) produced freezing (CR). If another group of animals (group B) is first pre-trained with only the noise paired with the mild foot shock, and then with light + noise as was done for Group A, in a final test only using light, only animals of group A will show the CR (*see*Table 1). In this case, the results are often explained by assuming that for group B, the noise-shock association was learned first and then blocked any consecutive learning as the noise already predicted fully the presence of the shock.

**Table 1. Summary of a simple training strategyof blocking.**

| | Pre-Training | Training | Test Light Only |
|---|---|---|---|
| **Group A** | | Noise + Light → Shock | Strong CR |
| **Group B** | Noise → Shock | Noise + Light → Shock | Weak or non CR |

In another and more complex experiment, now using two sets of compound stimulus, If a group of animals is trained with two stimuli A and B, but only one followed by a reward (A → CS+, B → CS-). In a second stage, if A is presented together with a novel stimulus X (AX) and paired again with the reward, when X is tested alone, it won't have any behavioral outcome due to the blocking effect (Schultz and Dickinson, 2000). Interestingly is that, if B is presented together with a novel stimulus Y (BY) but now followed by a reward, when Y is presented alone, it will be a much better predictor of the reward than X, even if both were paired with the reward the same amount of times (Table 2).

**Table 2. Summary of a training experimentofblocking using a discrimination paradigm**

| | First training | | Second training | Test X alone | Third training | Test Y alone |
|---|---|---|---|---|---|---|
| **Stimuls** | CS+ | CS- | CS+ | | CS+ | |
| | A | B | AX | No CR | BY | Moderate CR |

This key aspect of learning is also present in human experiments. In a study, using a conditioned suppression learning paradigm, blocking was achieved in human subjects trained on an operant discrimination task based on a video game(Arcediano et al., 1997). Thought clear evidence of blocking in human experiments, these types of results are not free of controversy as several others, have failed to induce this phenomenon (Davey, 1988; Shanks and Lopez, 1996). This failed has been mainly attributed to the fact that we integrate differently the stages of training, perceiving every phase as an independent experiment (Tonneau and González, 2004). However these limitations, blocking experiments that have succeeded have used modified experimental conditions, where single-phase designed protocols appears to be a valid approach (Hinchy et al., 1995; Arcediano et al., 1997). In general, these kinds of experiments have proven that for successful associative learning to occur, the close pairing of the stimulus and

thereward is of course necessary, but the predictive power of the cue at the moment of the pairing also plays an integral role. These observations have been translated into several formal theories and have become the basis of different models of learning (Bathellier et al., 2013; Bush and Mosteller, 1951; Gluck and Bower, 1988; Mackintosh, 1975; Rescorla and Wagner, 1972; Pearce and Hall, 1980). The most influential framework so far, is the one proposed by Rescorla and Wagner in 1972 (from now R-W) as it has become the background and starting point of almost all following models, with profound implications not only in traditional learning theory but also in others areas of research (Miller et al., 1995). A short introduction of this theory is provided in the following section to understand the basis and concepts treated by this model.

### 1.3.4. Rescorla-Wagner Model

One convention was very important in the formulation of this model and it comes from the empirical finding that repeated pairing of CS-US does not produce an unlimited linear increment of the CS-US association strength. On the contrary, the effect of pairing decreases during the course of the conditioning producinga gradual deceleration of learning (Rescorla and Wagner, 1972). As mentioned above, it is assumed that the connection between the stimulus representation and the US representation gets gradually strengthened in a trial-by-trial base, reaching in some point an asymptote (λ). This has been interpreted as the amount of learning increases, also does the expectancy of the US on the basis of CS presence. The following equation summarizes this assumption:

$$\Delta V_{CS} = \alpha\beta(\lambda_{US} - V_{CS})$$

**Equation 1. R-W's model of associative learning**

where α and β are constants and do not change over the course of conditioning. The constant α is related to the associability of the CS regarding its relative saliency andβ is related to the associability of the US also regarding its saliency. $\lambda_{US}$ represents the magnitude of the US association reflecting the maximum strength that the CS-US association can achieve(from 0 to 1) and $V_{CS}$ represents the strength of the CS-US association at that particular moment or trial.$\Delta V_{CS}$ is the change in the CS-US association strength after one trial, which is limited by the actual value of $V_{CS}$ and its distance to the value of $\lambda_{US}$. When the first CS-US encounter occurs, $V_{CS}$ is equal to 0 and $\Delta V_{CS}$then will only depend on the value of α

and β. After every pairing, learning occurs as the value of $V_{CS}$ increases accordingly to the difference between its actual value and the maximum possible for that association ($\lambda - V_{CS}$). Asit can be inferred, the value of ($\lambda - V_{CS}$) referred also as the 'error term', represents the extent to which the US is predicted by the stimulus ,getting smaller with further training and having less and less of an impacton the connection between the two representations, until learning stops when $V_{CS}$ reaches the value of λ. Following this equation, we can model the experimental observation of learning occurring fast at the beginning and slowly plateaus as the error term or 'surprise' tends to 0 and the US becomes 'fully predictable'. An important parameter so far unexplored is α, If is modified, it changes the speed or rate of learning but not the final scope of the association. Now if we consider that one trial can be more than one stimulus at the time, early versions of this type of model (e.g. Bush and Mosteller, 1951) implemented this, as considering independent error terms for each of the cues present in the trial. In view of the results by Kamin in 1967 (see Table 1), the idea of cue independence is challenged, as learning previously about one cue can influence learning of another one. In this way the idea of competition was implemented in the R-W's model into Equation 1 and now by looking at equation 2, it is possible to understand how blocking occurs;

$$\Delta V_L = \breve{U}_L \beta_{US} (\lambda - V_{CS})$$

$$\Delta V_L = \breve{U}_L \beta_{US} (\lambda - [V_L + V_N])$$

$$L = Light; N = Noise$$

**Equation 2. Blocking results explained using R-W's terms**

During the first trials of conditioning for group A with light and noise, the noise was already associated with the shock, so the prediction of the animal is the difference of the magnitude of the shock (λ) and of the sum of strengths of predictive values of light and noise combined. As $V_N$ can already fully predict the shock, no change in the association of light --> shock occurs. As we can notice in this equation, the predictive strength of the CS (V) is actually the sum of all associative strengths for each stimulus on the compound ($\Sigma V = V_A + V_B + V_C$, *etc.*). This is an important feature of this model, making easy the implementation of compound stimuli. From this model then, we can derive that two stimuli in a compound, compete and *perse* acquire different association strengths. This prediction has been extensively tested experimentally and has its origins in observations that can be tracked down as early as experiments made by Pavlov in 1927. In summary, animals that are trained with compound stimulus will

tend to respond strongly to the most salient part, even if the parts separately can achieve similar levels of conditioning (Kamin, 1967;Mackintosh, 1975). This phenomenon called 'overshadowing effect', has been widely observed in different animals species (*e.g.* Mackintosh, 1971; Matzel et al., 1985; Perez et al., 2015) as also in human experiments (*e.g.* Siegel and Allan, 1985; Baetu and Baker, 2010; Vandorpe and De Houwer, 2005).

### 1.3.5. Attention based models

The overshadowing effect, resides on the relative intensity difference of the two stimuliin a compound stimulus, as little or no overshadowing occur when the stimuli have similar intensities (Pearce and Bouton, 2001). Underthe R-W's model framework, this effect is explained because of the increment in associative strength of every part in a compound stimulus, is restricted to the level of the current response strength of the entire compound. In this way little or non-conditioning occurs with the less salient part because the more salient one reaches an asymptote for every possible associative strength in the compound. Another important strength of the R-W's model is its ability to account for another phenomenon called latent or conditioned inhibition (Lubow and Moore, 1959; Lubow, 1989). This effect is observed when in an initial stage, animals are trained with a stimulus (A) paired with ashock (US) until a reliable CR is reached. Subsequently, regular A-US trials are intermixed with a non-reinforced compound stimulus (AB). At the end of this training protocol, where A certainly predicts the US but at the same time, B signals its absence, it can be observed that A does not decreased its power to produce the CR. Conditioned inhibition is related to the results obtained when B, is later used alone to trained the animals in a subsequent learning stage. In this case, the association B-US will progress much slower than the A-US association. This can be explained, as that during the second stage of training (A+ and AB- stimuli), $\lambda$ is equal to 0 and $\Sigma V$ is positive, making B acquire a negative associative strength. Even though, conditioned inhibition provided another good demonstration for the power of the R-W's model to account for the interactions of cues during the learning process, another set of experiments around that time, showed several hints that challenged the validity of this proposal as for example, a phenomenon called 'unblocking' (Dickinson et al., 1976). Unblocking consists in the failure of pre-training animals with a salient stimulus A, to overshadow the learning about B in a consecutive stage. The R-W model can predict in part the results observed but only when the US is of a bigger magnitude. In this case, $\lambda$ will acquired a bigger value, letting the AB stimulus gain some associative strength. On the contrary, when

the US is of a reduce magnitude, W-R's model fails to account for this experimental observation. Another variety of experimental findings has been difficult to explain using W-R's model (Miller et al., 1995) and from here, theories of learning started to deviate and explain these discrepancies using different terms and principles.

One important difference in later models of learning is that R-W's model takes the difference between the expected and the outcome (prediction-error) to determine the 'effectiveness' of learning, whereas others models have also considered it in this way, but in parallel the 'ability or associability' of a CS to generate an effective conditioning. Associability has been defined in the following models by the parameter α, with the ability to change during the course of learning. In early deviant theories applying this concept, it was described that animals cannot learn from several stimuli at the same time. Instead, the saliency of the CS and its relevance for the subject, due to previous experiences with it, can modify the extent of the animal's ability to learn (Kosten et al., 2012). In this context, it was defined that stimulus processing is mainly done by different 'analyzers' holding different acquired strengths through the evolutionary process (Garcia and Koelling, 1966; Gemberling and Domjan, 1982; Shapiro et al., 1980). Following this approach, then each analyzer will respond to a single stimulus dimension (color, texture, sound, etc). Different connections with the behavioral responses would be created and strengthened, when the response is reinforced and weakened when is not. A summary of these and updated previous concepts of learning are in the 'theory of selective attention' proposed by Mackintosh in 1975. In his theory, he specifies that these connections are created with each specific stimulus feature and not with entire stimulus dimensions (Mackintosh, 1975).

Mackintosh's theory (1975) explained the results of unblocking described before, by proposing that associability is tightly related to predictability, changing its value as a result of experience. Animals then can be able to 'turn off' a stimulus that had no significant outcome (conditioned inhibition), but its unexpected change can 'turn back' attentional mechanisms, letting now the animal re-learn or modify an old association. Further support to his theory, were the results from experiments using stimuli that contains several dimensions. For example, animals can be trained with four stimuli composed by 2 colors and 2 types of lines (red vertical lines, red horizontal lines, green vertical lines and green horizontal lines) where only one feature is rewarded (for example, the color red)(Figure 1-22A-B). In a later discrimination stage, associability for one feature's dimension can be tested by changing the stimuli's color and

orientation, and at the same time, the relevant feature that signals the reward. The measure of learning speed of these new compound stimuli trained in two parallel different groups can give important clues about attention mechanism. For example, in the first group the same relevant dimension indicates the reward (intra-dimension or IDS, as color) and a second group the previous irrelevant dimension indicates it (extra-dimension or EDS, as orientation of the bars) (Figure 1-22C). Animals learned faster if there was an intra-dimensional shift than an extra-dimensional one, according with the principle previously described by Mackintosh's model and suggesting that associability could be generalized from one stimulus to another as a function of their similarity (Mackintosh and Little, 1969; Dias et al., 1996; George and Pearce, 1999; Redhead et al., 2001; Trobalon et al., 2003; George and Pearce, 2003). In front of this kind of scenario, the R-W's model fails to solve this discrimination as it proposes that the change of associative strength for one stimulus or feature compete with all the other parts in the compound for the same maximal value of associative strength. In this case, where two compounds contains the same amounts of features, the model should react in the same way making the discrimination impossible to solve (George et al., 2001).


**Figure 1-22. Patterns used in an Intra-Extra dimensional binding experiment**
(A) All patterns used to train animals in a classic pattern recognition task. (B) Discrimination of one feature in this case; color. (C) Second stage of learning were different patterns of stimuli are presented and is tested if an intra dimensional shift produces a faster learning speed. *Adapted from George and Pearce(2003).*

In summary, Mackintosh's model propose that an association will be learned faster if the compound stimulus contains a feature that can be a good predictor of the possible outcome. This principle can be described inthe following equation;

$$\Delta V_A = \breve{U}_A \beta (\lambda - V_A)$$

**Equation 3. Mackintosh's model of associative learning**

where the change in the association ($\Delta V_A$) between a stimulus (A) and the US is influenced by its associability ($\alpha_A$) and the learning rate constant β. As described before ($\lambda - V_A$) correspond the 'error term' that represents the discrepancy between the asymptote of learning of the (US) or the maximal value expected by that CS and the current strength of the A-US association. Finally, the associability value according to this modelcan be defined according to the following rule;

$$\Delta \check{U}_A > 0 \; if \; \beta \partial - V_A \beta < \beta \partial - V_X \beta$$

and,

$$\Delta \check{U}_A < 0 \; if \; \beta \partial - V_A \beta \geq \beta \partial - V_X \beta$$

where $\alpha_A$ will have a positive value when A on that trial, is a good predictor. This because the discrepancy between its current associative strength and the expected outcome is less than the discrepancy between the sums of all associative strengths of all stimuli that participates in the compound apart of A in that trial. Conversely, $\alpha_A$ will decrease if the outcome can be predicted by other stimulus or as well as it can be done by A. Thanks to these modifications, first in the error term; where now the change in associative strength is due to the difference $\lambda - V_{CS}$ and second in the specific changes of $\alpha_{CS}$ during learning; which now can account for the learning history of the CS, this model was able to account for all experimental results exposed before.

After only few years of the proposal of Mackintosh's theory (Mackintosh, 1975), another framework appeared to better explain the relationship between attention/associability and learning (Holland and Schiffino, 2016). Pearce and Hall (1980) after several observations that the associability of a cue will be greater when it does not predict entirely a reinforcement (stimulus A not paired with a US in all trials), than when it does it precisely (A paired with US in all trials). They stipulated that the associability of a stimulus in a particular trial, is proportional to the sum of the aggregate prediction errors until that trial (Pearce and Hall, 1980). Using this principle, they argued that reliable predictors should not receive a lot of attention, as they should not be able to change animal's behavior. On the contrary, stimuli whose predictive value is poor, would attract more attention as constant learning is required to predict the real likelihood of their outcomes. Following with this idea, if an animal is trained with CS-US and suddenly the

expected US is absent, in the following trial the prediction-error should be high. Using these terms, they proposed that associability of a stimulus is determined by the following equation;

$$\check{U}_A^{\,n} = \left| \partial^{n} - V_{Total}^{\,n-1} \right|^{\,n-1}$$

**Equation 4.Calculation of associative power according to Pearce and Hall's model**

where *n* correspond to the current trial. $\alpha_A$ will be equal to the current absolute discrepancy of the previous trial between λ and $V_{Total}$. $V_{Total}$ is calculated in the same way that in the R-W's model, where its value corresponds to the sum ofthe all stimuli associative strengths present at that trial or in other words, the extent to which the US was predicted by all stimuli presented on that trial. The value of $\alpha_A$ then will be high, when a stimulus it has been followed by a US that was unexpected and it will continue high in front of an unexpected absence (as the difference of $|\lambda - V_{Total}|$ will also be high). The final expression of this formulation is the following;

$$\Delta V = \check{U} S \partial$$

**Equation 5. Pearce and Hall's model of associative learning**

where at every trial, the change in associative strength (ΔV) will be determined by the adjustments in associability or attention on α as it was defined above, the saliency of that particular stimulus (S) and the asymptote of learning for that particular US (λ) .In simple terms, this model proposes that an animal will pay more attention to a new stimulus or that its associability will be high long enough the stimulus does not fully predict the US (Pearce and Hall, 1980). This is somewhat is a counterintuitive claim, as better the stimulus predict the US, its associability decrease and no further attention is directed to that stimulus. Using this formulation, it was possible to explain the experiments were certain level of uncertainty accompanies the US (Holland and Schiffino, 2016) and more recent paradigms as reversal conditioning (Jarvers et al., 2016).

In a parallel stream, according to the connectionist approach previously proposed by Mackintosh (Mackintosh, 1975), it has been suggested that when a compound stimulusis used for conditioning, indeed an association is form with each stimulus in the compound even with the less salient one, but

they claim that the later retrieval of the less salient cue-US association is some way fails. Following this framework, several post-learning protocols have shown the possibility to 'restore' in some extent the overshadowing effect (Kaufman and Bolles, 1981; Matzel et al., 1985; Sissons et al., 2009). Some of these results can also be explained by Pierce and Hall's model, as when the pairing of a cue with a low associability can be restored presenting the cue without the expected outcome. Again the experiments of Honey and Hall in 1991, are also in accordance with this connectionist proposal. In this experiment, rats were exposed in separate occasions to two different flavors (A and B). Both flavors then were rendered similar by the addition of a third flavor (X) to each of them. After training the animals with an aversion protocol with A followed by an US, it was observed in a final test, using each compound separately, that flavor B could also evoke the conditioned CR (Honey and Hall, 1991). Separate CS associations, linked to the same US, could activate part of its representations as in this case, the presentation of B could activate the representation of X-US. These ideas have found recent support, where old fear memories apparently can be 'retrieved' by the direct activation of the neurons encoding that fear representation (Guskjolen et al., 2018) or by direct activations of specific CS-US representations in the hippocampus (Liu et al., 2012; Ramirez et al., 2015).

In general, all theories previously described share some common assumptions. For example, the fact that learning increase gradually and that only the best predictor of an outcome, gets strengthened its association with the reinforcer, even though some associations can still be formed between the other parts of the stimulus. Taken together, even if this in some sense seems contradictory, it appears that predictiveness as much as uncertainty can lead to high levels of associability. Regarding the R-W and Mackintosh' models, high predictability of an US and a cue generates high associability, but for P-H's model the same conditions leads to a decrease associability, as the aggregate prediction error approximates to zero. In the literature, there is support and evidence for all of these models, where each of them can explain certain results and othersdon't or with some constrains. This led to the appearance of hybrid models with the assumption that both central types of models are right but by their own they cannot fully account for the influence of the 'associative history' or previous training on subsequent learning stages. Varying in the detail, hybrid models (*e.g*. Le Pelley, 2004) incorporate a dual associability change. For one side, one component of the cue's associability is computed for stimulus selection according to principles taken from R-W and Mackintosh's models and in another one, a second associability component is computed for learning using the equation provided by P-H's model (Le Pelley,

2004). The product of these two components then determines the learning properties of each stimulus. To some extent this approach can be very problematic, even though if this kind of models can explain a wide variety of results, they can lead to the search of distinct neural mechanisms to the same central process.

### 1.3.6. Adaptive network models

The amount of empirical findings in non-human animal behavior that share aspects with human learning and cognition, have generated a lot of attention from different areas of research, such as cognitive psychology and computer science. The merging of these fields generated that models of cognitive processes, known as parallel distributed processing or connectionist networks (*e.g.* Rumelhart et al., 1986), bind with current associative learning theories to study more in detail the commonalities between complex human abilities and associative rules studied in simple organisms. The connectionist networks, where neuron-like computing elements are massively interconnected by weighted unidirectional links, typically are organized with a layer of sensory units, an intermediate or association unit layers and one last layer of response units (Figure 1-23A). All this structure work together under a framework of total error reduction (TER) that simply means, that they will try to reduce as maximum the total error in a desire input-output matching loop (Gluck and Bower, 1988; Witnauer et al., 2014).

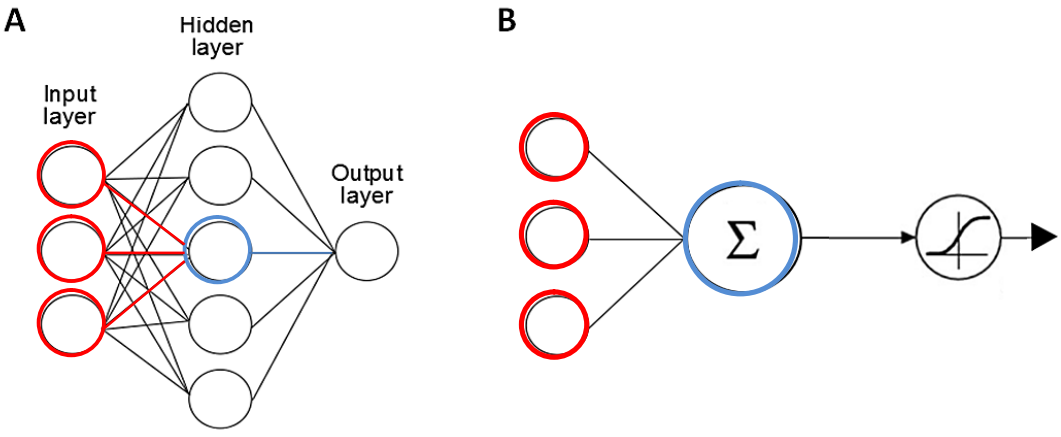


**Figure 1-23. Diagram of a classic adaptive network model.**
(A) Multilayered neural network containing one input layer, one hidden layer and one output layer. Each layer is constituted by units or neurons which can backpropagate learning gradients. (B) Schematic showing units labels on A and how its response is generated. At each

itineration, the sum of all weighted inputs passes through a non-linear function to get the output of the unit. Different equations are the used to calculate the error of each unit in the hidden layers with the target value. In this way the weights are re-calculated until the network reaches the target value.

In their essence, the presentation of one stimulus, activate the sensory units in the first layer which in turn, generate an activity pattern directly in the second/hidden layer or response unit (Figure 1-23A). In more complex networks (as found in backpropagation models) intermediate layers are interconnected and the activation of their units is accordingly to the sum of all its weighted inputs togheter with a linear or non-linear threshold that will (or not) trigger the following unit (Figure 1-23B). In this way, the input and output of one unit can be expressed in the following equation:

$$X_j = \sum_i y_i w_{ji}$$

**Equation 6. Output function of a classic unit in simple layered network model.**

where the total input $X_j$ of unit j, is the sum of all the previous outputs ($\sum_i y_i$) multiplied by its weighted connections $w_{ij}$. Eventually the propagation of activity will terminate in an output element, which in turn will update the weights of the interconnected units in the previous layers. This weighting is in agreement with an additive or multiplicative rule to reach the desire or correct final output by repeated cycles of input-output matching. As it can be inferred from classical learning theory, these weights can be though as the associative strengths between a stimulus and a desired conditioned behavioral action. Also the threshold or ruleby which the weightsare updated corresponds to the learning rule such as the one used in the R-W's model(Witnauer et al., 2014). In general this type of models has been used, merged with classical associative learning theory, to train different machine learning algorithms in pattern recognition as other more complicated classifications and categorizations task achieving outstanding results (LeCun et al., 2015).

### 1.3.7. Variability

Learning considered as the acquisition of knowledge through experience depends on a multitude of neural and cognitive processes which most of them are not accessible experimentally and constitute the basis of the high intrinsic variability between individuals(Evans, 2003). In order to representlearning,

performance (i.e. probability of correct responses, computed as the proportion of correct trials among *n* number of trials) is one of the most recurrent outputs measured and quantified over the curse of any learning paradigm. Consequently, learning models are derived from experimental observations which generallyare based on group-average performances and/oraveraged learning curves. To probe the accuracy of any of such type of models, typically model's predictions are compared with learning curves obtained from averaged data using some smoothing techniques, as trial-by-trial moving windows or across block of trials even sometimes whole learning sessions comprising hundreds of trials per subject. Then variability can be heavily masked depending on the number of trials taken to compute each bin of the individual learning curves (Bathellier et al., 2013; Brown and Heathcote, 2003; Deliano et al., 2016). Models are often compared to grouped learning curves averaging many individual's learning curves. This is in practice misleading or misrepresentative due to the extent of individual's variability seen in real experiments. In this way, averaged learning curves, where the cumulative progress or performance is plotted against time or number of trials, can show a gradual increase of performance butin reality for some subjects, learning ca occurs incredible fast (Bathellier et al., 2013) (Figure 1-24). Only observing averaged learning curves, important dynamics can disappear, as slope steepness, fast learning-related changes, differences in the asymptotic level of performance and latency of acquisition taken as the number of trials before an abrupt change in the learning curve's slope occurs (Gallistel et al., 2004) (Figure 1-24). This abrupt change in learning curve's slope, from the initial response level ('pre-resolution period') until the asymptote, usually span over few trials, in part contradicting the most common theoretical assumption; which assumesthat learning of a simple behavior is the slow and gradual strengthening of connections between one or more sensory representations. From the last, It can be extrapolated the existence of a certain behavioral threshold that needs to be crossed, through the successive extraction of information and successful storage in either recent or long term memory, to let a certain behavior to be expressed.

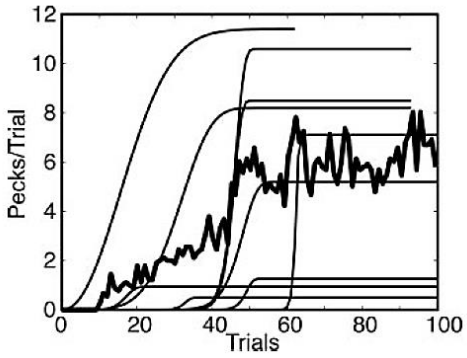


**Figure 1-24. Learning curves of pigeons trained in a classicalpavlovian conditioningtask.**

Best fitting for number of pecks versus trials (light black) for single animals and average learning curve for all animals (strong black). *Adapted from Gallistel and colleagues (2004).*

From the previous, it is obvious that modeling and the study of animal's behavior needs to account for this high variability, greatly observed in animal conditioning and Bathellier and colleagues (2013) did a steep forward on this matter. They developed a reinforcement learning model whichwas built using the type of architecture of adaptive network models (*e.g.* Gluck and Bower, 1988) combined with a multiplicative learning rule and a prediction-error term as the one used in most associative learning models (*e.g.* Rescorla and Wagner, 1972). In detail, this model is contained of three sensory units, where one represents the 'context' and trial initiation, and two other units corresponding to the CS+ and CS- (Port, S+ and S- unit in Figure 1-25). All this modules are then connected to a decision circuit and an inhibitory unit which in turn is also connected to the decision unit (Figure 1-25). In presence of an input or stimulus, the decision circuit will then sums linearly the sensory inputs from the three sensory modules and the inhibitory one, to give an all-or-none output that represents the decision to Go or not to Go for that particular stimulus, where S+ represents the rewarded stimulus and S- is the non-rewarded one (Figure 1-25).

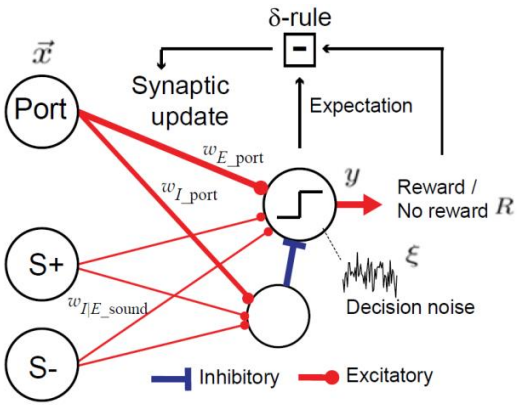


**Figure 1-25. Sketch of the multiplicative reinforcement model for associative learning.**

This model is composed of three different sensory units projecting towards a decision unit and an inhibitory unit. The decision unit linearly sums the sensory inputs together with the feed-forward inhibition from the inhibitory unit to respond in all-or-none fashion. Synaptic weights are updated through a learning rule trial-wise according to stimulus, response and presence or not of a reward. *Adapted from Bathellier and colleagues (2003).*

A correct response then is rewarded and the model learns by updating the weights in a trial-by-trial base using the multiplicative rule, weighting more positive expectation errors. This means that anunpredicted reward (at beginning of the conditioning)will produce a stronger effect than an unpredicted omission, making the model able to account for the differential learning speeds of CS+ and CS- and further reversal learning for individual learning curves (Figure 1-26A) as also for the average population (Figure 1-26B). Altogether, this model is able to explain the pre-resolution period and account for inter-individual variability during normal and reversal learning, by exposing the unconsidered intrinsic variability of initial connections between the representation of the relevant stimuli and the action at the beginning of the training (Bathellier et al., 2013). Importantly this model also account for important biological processes generally ignored by early theoreticians of associative learning, as the asymmetric response to rewards and absence of expected rewards which appears in the activity of dopaminergic neurons of the basal ganglia encoding prediction-error rewards (Schultz et al., 1997; Schultz, 2007; Cohen et al., 2012).

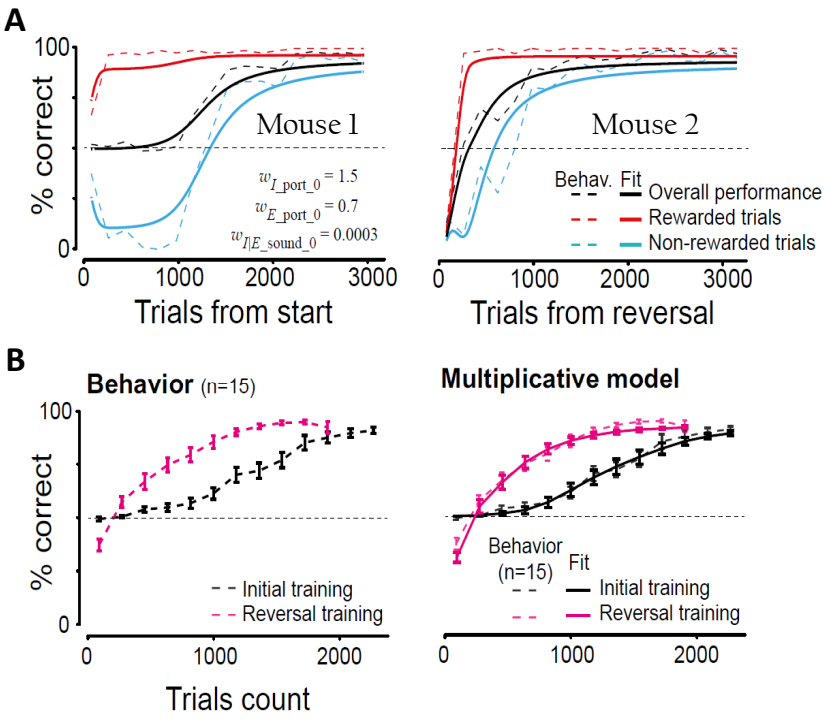


**Figure 1-26. Individual and averaged learning curves for an associative learning task in mice.**

(A) Behavioral data and fit obtained from single animals learning curves discriminating two different complex sounds. (B) Behavioral averaged population learning curves and fit from the reinforcement learning model. *Adapted from Bathellier and colleagues (2013).*

## 1.3.8. Neuronal basis of associative learning

Associative learning, as previously described, is based on the unpredictability of rewarded outcomes. In this way, associative learning models as well as connectionist and adaptive network models are based on this assumption that have found a physiological correlate only at the end of the 20$^{th}$ century (Schultz et al., 1997; Schultz and Dickinson, 2000). The search for biological underpins of associative learning theories converged in a neurotransmitter called Dopamine (DA), historically associated with motor functions from early observations of Parkinsonian patients (Burns et al., 1983), nowadays it has been proven its role as a key element in the acquisition of predictable value and motivational importance to otherwise neutral stimulus and reward-seeking behavior (Schultz and Dickinson, 2000). DA is produced by midbrain neurons in the ventral tegmental area (VTA) and the substantia nigra pars compacta (SNc), from where they project to different regions of the brain in three different streams: nigrostriatal system,

mesolimbic system and mesocortical system. Damage of specific fibers in the nigrostriatal system can alter feeding and drinking behaviors, whereas damage in the mesolimbic system can produce a several problems in locomotion and reward-seeking behavior (Schultz, 1998). In several species, including humans, it has been shown that activity of midbrain DA neurons reflects a prediction-error signal (Schultz et al., 1997). Dopaminergic neurons increase their firing rate when an unpredictedreward is received, which peak is largely modulated by continuous encounters until there is not, when the reward is fully predictable (Patriarchi et al., 2018) (Figure 1-27A). Furthermore, as animals use external cues to learn and predict the probability of rewarded events, when an association occurs due to several pairings as in a classical conditioning paradigm, DA neurons now start to respond progressively to the apparition of the cue instead of the delivery of the reward, and more interestingly is that their activity is largely suppressed when a cue-predicted reward is omitted (Figure 1-27B).

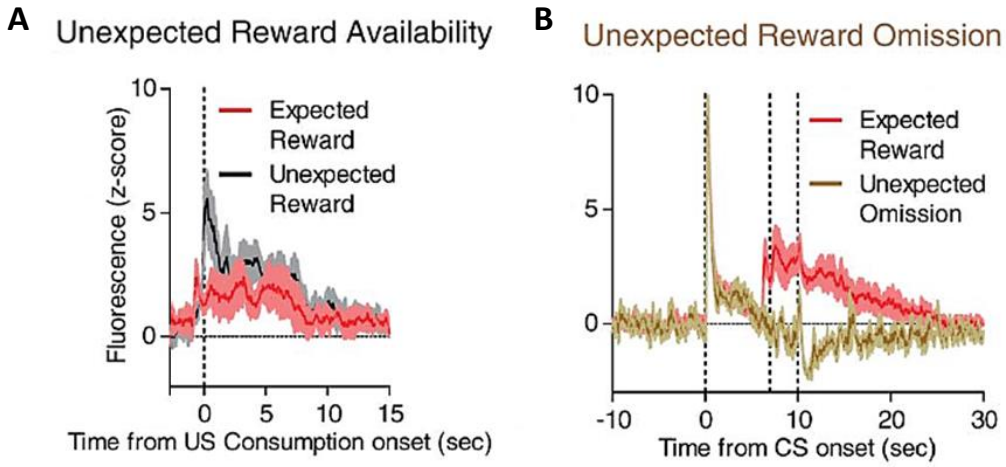


**Figure 1-27. Dopamine dynamics of DA neurons during a conditioning task.**
(A) Averaged fluorescence responses of a genetically encoded dopamine sensor, expressed in DA neurons of the NAc, during the expected (red) and unexpected (black) delivered of reward in four mice trained in a classic appetitive Pavlovian conditioning schedule.Conditioning consisted of the presence of a light and sound (CS) paired with a drop of water with sucrose (US). (B) Same as A, when the same animals were already conditioned and they expect the reward (red) and when in some random trials, the expected reward was omitted (brown). *Adapted from Patriarchi and colleagues (2018).*

These observations indicate that the activity DA neurons serve as a signal of any prediction-error mismatch. In general, presence/absence of unexpected/expected reward respectively, will generate an error in between the predicted outcome and the actual outcome, leading to the acquisition or

modification of the behavior until the outcome can be again reliably anticipated. These observations had a profound significance for the associative learning theory as it could probe that many years of models and predictions could finally have a biological traceable counterpart observable in many different species including humans.

# 1.4. To record, decode and manipulate neuronal representations

## 1.4.1. Linking two disciplines

Associative learning has become the main experimental framework to study the link between a certain region and sensory perception. Different learning paradigms such as go/no discrimination or two alternative forced choice tasks (2AFC) are the most used entry point to unravel sensory perception and learning induced chances in sensory as well as other brain circuits. With the development of new technologies that can record and manipulate cortical circuits during behavior, the field has moved fast in elucidating causal functions for certain brain circuits in perception and their functional limits (Houweling and Brecht, 2008; Salzman et al., 1990; Yang et al., 2008; Yang and Zador, 2012). These techniques have led to definitions in which neuronal populations can be instructive, permissive or without any perceptual role for a certain behavior. In this endeavor, the experiments in macaques, where the role of the middle temporal area (MT) has been studied in great detail in the visual cortex for motion perception, have a crucial importance. As it was described in previous chapters, some stimulus features are encoded by cortical neurons in a columnar manner, such as the MT area of the macaque's brain which is highly organized regarding direction selectivity flow and its firing rate has a statistical relationship with animal's choice in visual motion discrimination (Newsome et al., 1989; Britten et al., 1996). Lesions in this area generate a total 'blindness' for the judgment of motion direction with little effect on other perceptual judgments (Newsome et al., 1986) proving the necessary role of MT neurons in motion perception. On the other hand, direct electrical stimulation in a particular MT direction selectivity column, activates neurons coding for a specific motion direction which can have a profound repercussion in perceptual decisions of motion direction in behaving monkeys (Salzman et al., 1990; Salzman et al., 1992; Salzman and Newsome, 1994). Following these fundamental observations, the direct manipulation of neuronal activity in the cortex is the most powerful approach to study an area's role in motor or sensory perception but first is necessary to know if the information in a certain brain region can have enough predictive power of the perceptual stimulus sensation to then manipulate it specifically.

The study of sensory neuronal representations and their decoding to elicit behavioral choicesare two research directionsthat have come together only recently (Figure 1-28). A small number of recent articles have shown that it is possible to predict behavioral discriminations from neural representations (Panzeri et al., 2017). As described in a previous section, odors are represented in the olfactory bulb as single odorant receptors project to only to one glomerulus. By studying the similarity of odors representations in the glomerular layer of the olfactory bulb inrats, large-scale odors representations that failed to be significantly different also failed to be discriminable for the subjects in a behavioral task (Linster et al., 2001). In early stations of the auditory system, such as the inferior colliculus, it is possible to decode the identity of several complex natural sounds using the activity of only a few neurons (Lyzwa et al., 2015). Going further, neural representations of complex sounds in AC can also be used to predict the identity of the sounds (Carruthers et al., 2015) and even more importantly, behavioral discrimination and generalization in ferrets (Town et al., 2018), rats (Centanni et al., 2014; Engineer et al., 2008; Engineer et al., 2013; Orduña et al., 2005; Shetake et al., 2011) and mice (Bathellier et al., 2012; Runyan et al., 2017). It is known that certain stimulus features are encoded in local ensembles of cortical neurons and from those experiments, we know that behavioral choices can be predicted accurately from coarse neuronal activity in primary sensory areas but it is still unclear if theses representations are enough to trigger sensory perception or if they are enough to generate a sensory based behavioral decision.

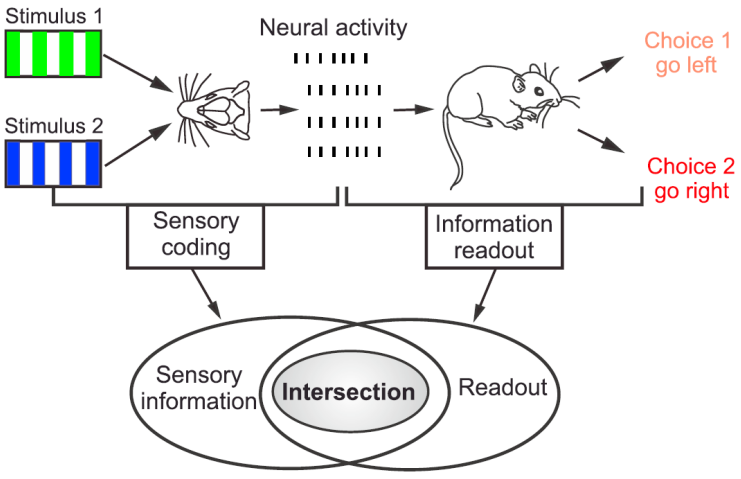


**Figure 1-28. Intersection between sensory coding and behavioral readouts**
Features encoded in neuronal population activity (sensory information) can be used to readout the perceptual behavioral choices of animals engaged in a sensory discrimination task. Going further, from knowing the particular features encoded in the circuit, it can be

possible to manipulate the information and bias the perceptual decision of the subject. *Adapted from Panzeri and colleagues (2017).*

### 1.4.2. Role of auditory cortex in the discriminations of sounds

The link between certain brain regions and the control of certain specificlearnedbehaviors is doubtless. For example, lesions in the Broca or Wernicke's areas will give rise to non-overlapping deficits in speech (Damasio and Geschwind, 1984). On the contrary, many others brain areas have no clear or a not yet defined role in motor control or sensory perception. The role of the AC for sound perception and discrimination has been largely debated due to several contradictory observations. An extensive amount of work has been done with the aim to test the necessity of AC in different species under different contexts, such as for simple frequency discriminations, sound localization, pattern recognition, fear conditioning, detections of changes in continuous sound sequences, and others simple and more complicated features (Warren, 2005). The first ablation experiments of the AC date from the end of the 19$^{th}$ century where lesions in monkeys and dogs had profound behavioral deficits for sound detection and frequency discrimination (Winer, 2011). Years later, similar kinds of experiments in the cat, showed some contradictory results (*e.g.*Butler et al., 1957). In much better controlled AC lesions experiments, it was observed that intensity thresholds were unchanged after surgery (Raab and Ades, 1946), and AC was not necessary for the detection of frequency changes (Butler et al., 1957) and pure tone frequency discrimination (Thompson, 1959; Goldberg and Neff, 1961; Diamond et al., 1962; Dewson, 1964) as long as the inferior colliculus remained intact (Neff et al., 1975). The discrepancies with earlier experiments were attributed at that time, to the possibility that not all species had the same cortical dependence, possible differences in the methodologies applied and/or in the real extent of the cortical lesions, as similar results were obtained some years later (Abeles et al., 1975). It is Important to note are the experiments of Meyer and Woolsey in 1952, where they trained cats to discriminate between two trains of pulses that differed only in the frequency of the last pulse. Using this protocol, animals with large bilateral ablations of AC responded similarly to both sounds, result that was understood as that animals without the AC, had lost the ability to inhibit their response to non-target or neutral stimulus (Meyer and Woolsey, 1952; Thompson, 1960). Similar observations have been made in more complex sound discriminations where the discrimination is also impaired due to high rates of false alarms, as for example discriminations of auditory patterns in cats (Butler et al., 1957) and the direction of frequency

modulated sounds observed also in cats (Kelly and Whitfield, 1971) and gerbils (Wetzel et al., 1998; Ohl et al., 1999). Another interesting example of note, is the experiments in macaques where they had to distinguish and discriminate a group of their 'coo' calls (Petersen et al., 1978). In this case, bilateral and only left unilateral lesions resulted in small but significant deficits to discriminate between these complex sounds, where calls are similar to raising frequency modulated sounds at different bandwidths and intensities (Petersen et al., 1978; Harrington et al., 2001), demonstrating the selective nature and the kind of sound processing that the AC could be involvedin mammals, as the same results were obtained recently in rats (Kudoh et al., 2006; Rybalko et al., 2006; Cooke et al., 2007; Jaramillo and Zador, 2011; Porter et al., 2011).

In parallel, lesion experiments have tested the role of the AC in the processing of other sound features, convincingly showing that proper sound localization and the association of sounds with a certain location in the space needed the entire auditory pathway, including the AC, for humans (Mendez and Geehan, 1988), monkeys (Heffner, 1978; Heffner and Heffner, 1990), cats (Diamond et al., 1956; Strominger, 1969; Jenkins and Masterton, 1982; Jenkins and Merzenich, 1984), ferrets (Kavanagh and Kelly, 1987) and gerbils (Smith et al., 2004). Although different results were obtained using the same paradigm in rats (Kelly and Glazier, 1978; Kelly, 1980), suggesting some species disparities. These important observations attracted a lot of attention as little was really known about the perceptual functions of the AC in rodents, contrary to the detailed progress in the anatomical categorization of their AC subfields(Stiebler et al., 1997). Recent studies in this area, have used more transient inactivation protocols to test the role of AC, due to the failure of some lesions studies to report a clear role of AC in simple frequency discrimination protocols (*e.g*. Pai et al., 2011). Differences again could be attributed to the real lesion size (Pai et al., 2011), post-lesion recovery (Yamasaki and Wurtz, 1991) and/or the potential brain reorganization after ablation (Otchy et al., 2015; Robertson and Irvine, 1989; Scharlock et al., 1963; Wakita, 1996). For example, Talwar and colleagues (2001), trained rats to detect and to discriminate simple pure tones after the application of the Ɣ-aminobutyric acid $(GABA)_A$ receptor agonist, muscimol. The application of this compound to the surface of the AC leads to a strong cortical silencing, leaving the thalamic activity unaffected(Intskirveli et al., 2016). After approximately 30 minutes, rats showed a "profound but reversible" effect on discrimination performance (Talwar et al., 2001). Similar results were obtained under a similar cortical inactivation procedure for pure tone localization in space in gerbils (Smith et al., 2004) and in a pure tone discrimination task in mice (Kuchibhotla et al., 2017), challenging previous

observations from several lesion studies also in rats, where AC was showed not to be necessary for pure tone discriminations (Kudoh et al., 2006, Rybalko et al., 2006).

In summary, lesion experiments typically examine behavior after several days or weeks after surgery, observing behavioral effects linked to task complexity, animal model, biological relevance of stimuli and sometimes nonspecific negative consequences after surgery. These variables may have hindered the study of AC functions due to the ability of the mammalian brain to reorganize its functions or to the animals changing behavioral strategies rapidly. Acute manipulations have contested well-known previous beliefs challenging the field to revisit and reconsider the role of AC in perceptual decisions.

### 1.4.3. Acute manipulations of cortical representations

Local ensembles of neurons transfer information in form of spikes. It often is considered that there are two possible strategies to 'encode' the information. A "sparse code" is related to the spiking of small sets of silent but highly selective neurons, converting the information into a precise temporal sequence of action potentials (temporal-based). The opposite can be thought as well, where a "dense code" can decipher the information as the variation of a high firing rate of active but not really selective neurons, transforming in this case the information into a number of action potentials fired in a certain period of time (rate-based). A large list of publications can account and support with evidence that both types of strategies are implemented in the brain, as temporal-base transfer can be found in phase locked systems where spikes are correlated to stimulus onset or certain phase of brain oscillations (*e.g.* Cardin et al., 2009; Colgin et al., 2009; Kim et al., 2016 ; Kühn and Helias, 2017) and rate-base transfer in the correlation between firing rate and stimulus intensity in several sensory systems (*e.g.* Shadlen and Newsome, 1994; Harvey et al., 2013). Other more recent theories, have also noticed that the enormous spiking variability in the brain, often considered as 'noise', can also encode information in the interspike-interval between 2 subsequent spikes, but more support is needed to validate these kind of approaches (Li et al., 2018). Although those concepts are useful to summarize in some way the vast amount of observable findings, it can miss the real strategy that the brain uses to decode the incoming information. The rate-based coding accuracy to predict a behavioral output is in some way constrained to the relationship between the external stimuli and the timescale of the observation.For example, classifiers discriminate and predict better behavioral discriminations of speech sounds when they are trained with

1 ms time bins of single and multiunit neuronal recordings in AI of rats, than when they are trained with 40 ms time bins averages (Engineer et al., 2008). Similar observations were made before in ferrets but indicating a time scale from 10 to 50 ms to ensure an efficient decoding (Schnupp et al., 2006). Spikes trains evolve in a continuous dynamical space where setting a certain arbitrary time window for one neuron, or a population will reduce the complexity of a spike-based or temporal-based code into a rate-based code (Brette, 2015; Panzeri et al., 2017). Following this, it can be a more precise question, if from a condensed point of view (rate information) of a highly variable and stochastic system (temporal information) it can be inferred certain causality in the system with the unfortunate loss of precise stimulus information (Reich et al., 2001). Timing of single spikes can contain important information about an external stimulus but maybe a rate-based system can be more efficiently used to generate behavioral choices due to the high redundancy of spike information from single neurons in the brain (Salzman and Newsome, 1994; O'Connor et al., 2010;O'Connor et al., 2013; Peng et al., 2015).

## Optogenetics

The ability to manipulate individual components or spikes in the brain was envisioned a long time ago by Francis Crick (Crick, 1979). After several decades of efforts, it is possible and it is called 'optogenetics'. This term comprises any specific genetic targeting of cells or proteins combined with optical technology for either observing or controlling the target within intact, living circuits (Deisseroth et al., 2006). Specifically in neuroscience, optogenetics is used to control the firing rate of specific neuronal populations by the expression of a natural light-sensitive ion-transporting membrane protein (Fenno et al., 2011). Channelrhodopsins (ChRs), first characterized *ex vivo* (Nagel et al., 2002) and later improved and introduced in mammalian cells (Boyden et al., 2005), are the family of the most commonly used light-sensitive channels. These channels originally found in the algae *Chlamydomonas reinhardtii* are fundamental for their phototaxis (Sineshchekov et al., 2002), as in presence of blue light (~470 nm) they allow the entry of sodium ($Na^+$) into the cells, leading to excitatory currents and the generation of action potentials (Figure 1-29). Several rounds chimeragenesis and mutagenesis have increased light sensitivity and millisecond time scale kinetics of these channels, such as channelrhodopsin-2 with H134R mutation (ChR2/H134R) (Nagel et al., 2005) and the E123T mutation (ChETA) (Gunaydin et al., 2010). Subsequent modifications supported by modern bioinformatics have led to red-shifted versions as VChR1 (Lin et al., 2013). In parallel, the search of other types of light-sensitivity channels resulted in the discovery of light-

sensitive chloride ($Cl^-$) pumps (eNpHR) to hyperpolarize the cell membrane and achieve a specific neuronal silencing in the presence of yellow light (~590 nm) (Gradinaru et al., 2008) (Figure 1-29). The optogenetic toolbox increases rapidly and several options are now available with different origins, kinetic properties, wavelength sensitivity andionic conductance (Fenno et al., 2011; Wietek and Prigge, 2016). In the last years, optogenetic manipulations combined with transgenic animal lines or viral delivery systems, have overtaken the field and now constitute the standard protocol to modulate the firing rate of specific population of neurons (Deisseroth, 2015; Kim et al., 2017). From the fascinating experiments were it was possible to control motor neuron and mechanosensory neuron's activity in transgenic intact live nematodes (*Caenorhabditis elegans*) with a direct testable behavioral readout, a new paradigm has been settled in neuroscience to study the causal role of neuronal activity in ongoing behavior (Nagel et al., 2005; Zhang et al., 2007).

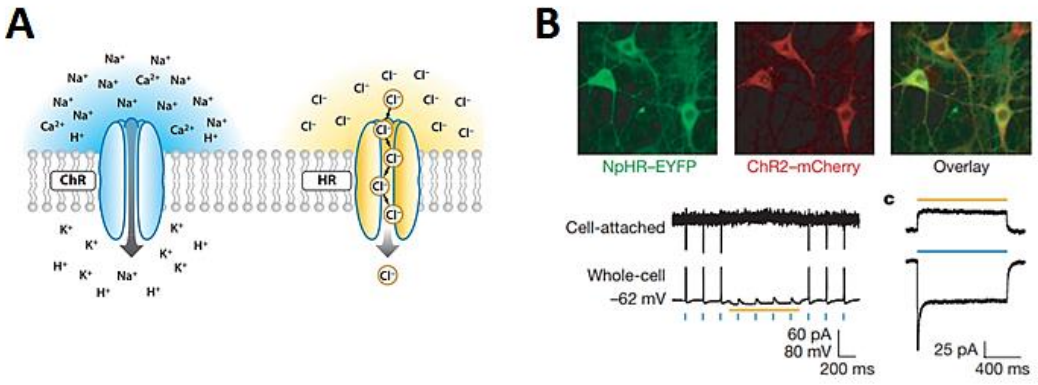


**Figure 1-29. Different opsins allow the bidirectional control of neuronal activity.**

(A) Channelrhodopsin (ChR) in presence of blue light allow the entry of sodium ions, at the other side, halorhodopsins in presence of yellow light allow the entry of chloride anions, generating depolarization and hyperpolarization in neuronal membranes, respectively. *Adapted from Fenno and colleagues (2011).* (B) Cell-attached and whole-cell recordings of cell-cultured neurons expressing an excitatory (ChR2) and an inhibitory (NpHR) opsin allowing the bidirectional control of neuronal activity. *Adapted from (Zhang et al., 2007).*

The delivery of ChRs into cells can be done in several ways, most commonly via viral expression systems and/or transgenesis in order to create a stable expression in a mouse line (Arenkiel et al., 2007; Madisen et al., 2012). Adeno-associated (AAV) and lenti virus expression systems are versatile and allow a robust expression of the protein of interest in a specific animal cell type (Kim et al., 2017) or subcellular

compartment (Rost et al., 2017) via well-known specific promoters (Zhang et al., 2010). Transgenic mouse lines permit the direct expression of any gene in a more stable using the Cre-LoxP system (Sjulson et al., 2016). Together, these biotechnological tools allowed for the first time a direct testing of causal hypotheses concerning neuronal activity in specific neuronal populations and their impact on perceptual systems.

### Photo-inhibition in genetically identified interneurons

Silencing the activity of a specific cell population in the cortex (Figure 1-30) can help to elucidate in detail its functions (Kato et al., 2015; Letzkus et al., 2015) or the role of an entire particular area of the brain (Hong et al., 2018), in a more acute manner than any pharmacological silencing (*e.g.* Hikosaka and Wurtz, 1985; Smith et al., 2004), cooling (Long and Fee, 2008) and beyond doubt, lesion experiments (*see page* 60: Role of auditory cortex in the discriminations of sounds). The expression of ChR2 in parvalbumin-expressing (PV+) interneurons has resulted in a good strategy to intersect the real contribution of a specific cortical area during ongoing behavior without perturbing other cognitive neither motor functions. This methodology has allowed testing and probing the necessity of V1 in mice to perform a threshold detection task for either contrast or orientation stimuli (Glickfeld et al., 2013), as also virtual navigation in a visually guided behavioral task designed to study learning dependent changes in neuronal representations (Poort et al., 2015). Also recently and more dramatically, the expression of an inhibitory opsin (Halo) directly into excitatory neurons helped to elucidate the dispensable role of S1 in mice for the acquisition and execution of a single whisker detection task (Hong et al., 2018), contrary to previous results using similar techniques (Sachidhanandam et al., 2013; Guo et al., 2014).

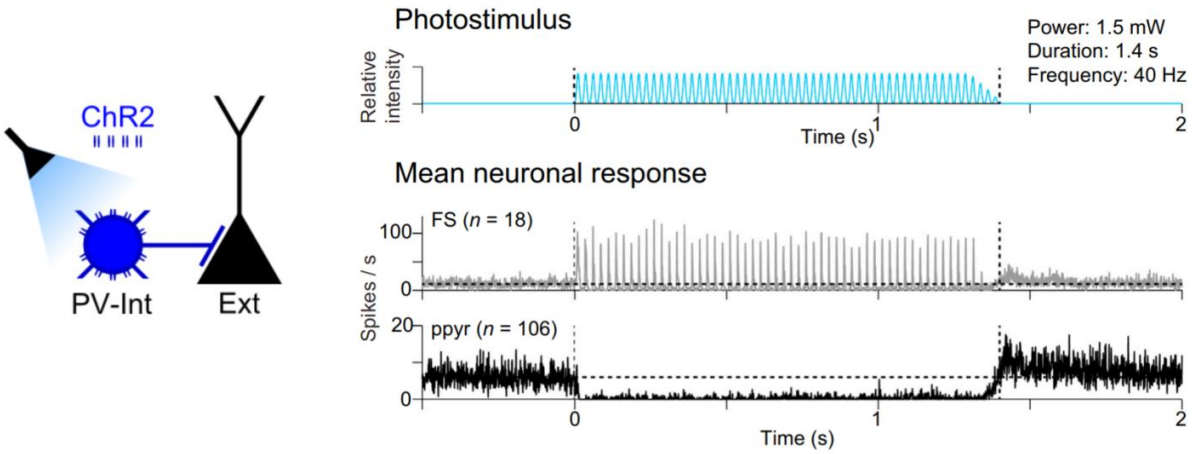


**Figure 1-30. Focal silencing strategy in awake animals.**
The expression of an excitatory opsin (ChR2) in genetically identified PV-interneurons can lead to the almost entire inactivation of anextensive cortical area (left). On top photo stimulation regime and in bottom mean peristimulus time histogram (PSTH) of 1 ms time bin for fast spiking interneurons and pyramidal cells classified in terms of their response to the optogenetic stimulation. *Adapted from Guo and colleagues (2014).*

## Directed photo-activations

Neuronal activations in the cortex using optogenetics has proven to be incredibly specific and drive behavior with millisecond precision. Animals can be trained to report an optogenetics stimulations directly in the cortex(Choi et al., 2011; Huber et al., 2008; Nomura et al., 2015; Musall et al., 2014) as it was shown that mice can report only a few spikes triggered by ChR2 in a small subset of superficial cortical layers (Huber et al., 2008) (Figure 1-31). Another similar experiment showed that different small ensembles of neurons in the piriform cortex of mice can be used to train distinct behaviors in the first type of optogenetic-induced discrimination protocol (Choi et al., 2011). Optogenetics in this way can be combined with behavioral experiments and this was pushed forward by O' Connor and colleagues in 2013. In their experiment combining behavior, electrophysiology, whisker detection and genetic targeting to deliver ChR2 specifically into layer IV neurons of the mouse primary somatosensory cortex, they showed that mice during behavior, trained to detect with a single whisker the position of a pole, can confound precisely triggered artificial activity in the barrel cortex ('virtual touch') with the activity elicited by the real touch of the whisker with the pole (O'Connor et al., 2013). A similar experiment showed that in the primary gustatory cortex of mice, where taste neuronal ensembles are non-overlapping and well organized, ChR2-based specific activations elicited behavioral responses as

expected in a mouse trained to discriminate between two different flavors, 'bitter' or 'sweet' (Peng et al., 2015).

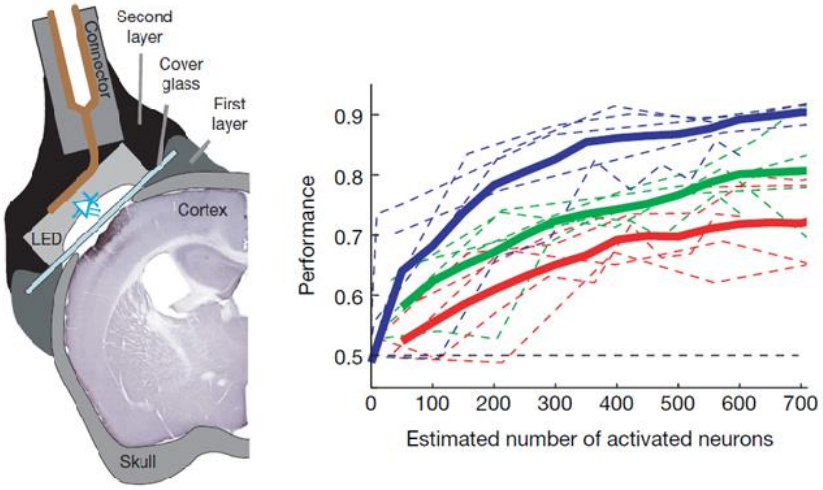


**Figure 1-31. Cortical activation of superficial layers in S1 of freely moving mice and cell quantification.**

Schematic of the photo-stimulation setup to optogenetically activate superficial pyramidal cells in S1 in *in utero* electroporated freely moving mice (left) and performance of photo-stimulation detection in function of estimated number of activated cells for different number of light pulses at 20 Hz; five light pulses (blue lines), two light pulses (green lines) and one single light pulse (red). Thick lines mean performance across five animals and dotted lines mean of individual animals across five sessions of 200 to 1000 trials (right). *Adapted from Huber and colleagues (2008).*

In the AC, although thereare well-organized tonotopic fields, their functional and causal implications for sound processing remain to be tested. Only few reports have shown targeted activations of AC based on the frequency properties of the neurons. Znamenskiy and Zador (2013) performed this type of manipulations where they trained rats to discriminate low and high frequency of a 'cloud of pure tones' in a two-alternative forced choice task (Figure 1-32A). During the task, short non-overlapping pure tones where presented and the rats had to judge the 'average' frequency of the complex sound and choose between the left or right port depending if it was low (5 – 10 kHz) or high (20 – 40 kHz) frequency, respectively (Figure 1-32A). By measuring psychometric curves, they tested if an optogenetic manipulation of an inserted probe at different areas of the tonotopic map had an effect on pitch perception and if it could bias the response of the subjects towards the main tonotopic frequency stimulated. In their hands, using a broad expression of ChR2 in the AC by injections of an AAV virus, they

indeed could perturb the task but the direction of the bias was not correlated or predicted by the tuning of the cortical area activated (Figure 1-32B). Going further, they succeeded and managed to bias correctly the choice of the animals but by only targeting corticostriatal neurons using a combination of a CRE dependent retrograde virus (HSV-1) in the striatum and injections of Cre-dependent ChR2 with an AAV virus in the AC. In this way the expression of ChR2 was mainly in layer V neurons of the AC projecting to striatum and their activation during the task could bias the choice towards the main frequency of the stimulated region (Figure 1-32C).

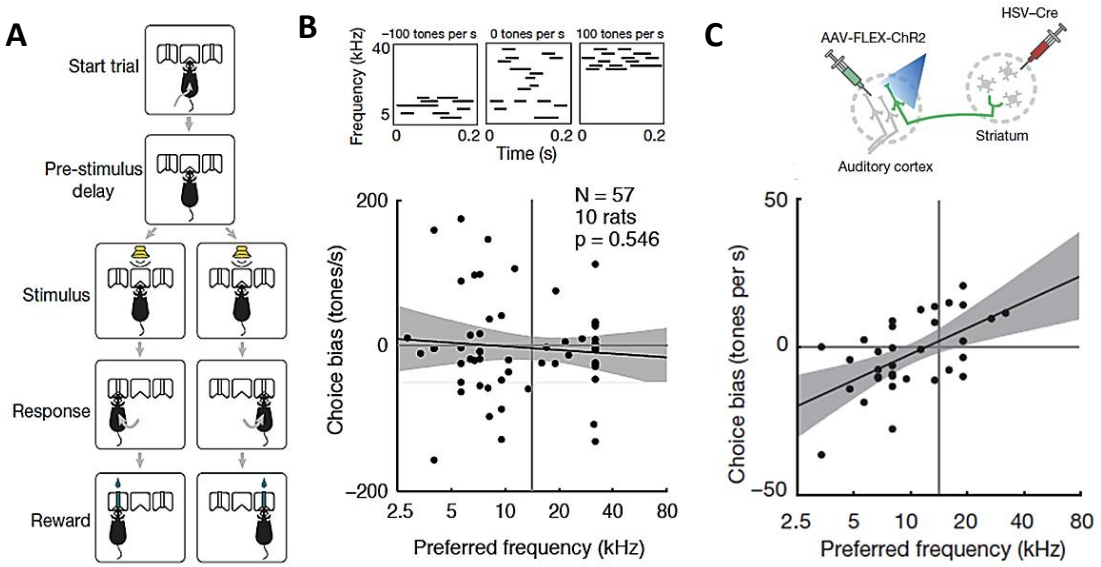


**Figure 1-32. 2AFC task in rats and frequency detection bias.**

(A) Diagram of the behavioral task. Rats initiate the trial by a nose poke in the middle area. After hearing the cloud of tones they had to judge the average frequency and indicate by moving towards the correct side in order to collect a water reward. (B) Schema of the cloud of tones used in the task (top) and perturbation experiment in rats widely expressing ChR2 in AC (bottom). Bias did not correspond with the preferred frequency of neurons recorded and stimulated using an tetrode combined with an optic fiber in freely moving rats performing the task. (C) Retrograde targeting strategy of corticostriatal projecting neurons in the AC using a combination of HSV-Cre and AAV-FLEX-ChR2 (top) and bias experiment in 2 rats (33 penetration sites) showed a biasing predicted by the frequency of the stimulated corticostriatal projecting neurons. *Adapted from (Znamenskiy and Zador (2013).*

Directed photo-activations, but now in parvalbumin-positive (PV+) interneurons, have shown to also modify the perceptual frequency detected in mice. More in detail, using two types of conditioned behaviors, the expression and activation of ChR2 or Arch in genetically identified PV+ interneurons

generated opposite changes in frequency discrimination acuity and specificity of auditory conditioning (Aizenberg et al., 2015). These experiments have probed the power of optogenetic perturbations, both directly into excitatory or indirectly into inhibitory interneurons, to study the contribution of AC in associative learning and frequency discrimination behaviors in mice.

Also importantly, is to mention a more recent experiment (Tsunada et al., 2016),using a similar perceptual decision task but now in monkeys (Figure 1-33A) butwhere instead of using an optogenetic stimulation, they used classic micro-stimulations protocols. Tsunada and colleagues (2016) observed similar results to the work ofZnamenskiy and Zador (2013). In they work, micro-stimulationsin certain locations of one of the main targets of AI, the belt region AL (Figure 1-33B), can actually bias the perceptual pitch-judged decision accordingto the tonotopic region and therefore the preferred frequency of neurons in the stimulated cortical area of monkeys (Figure 1-33C).

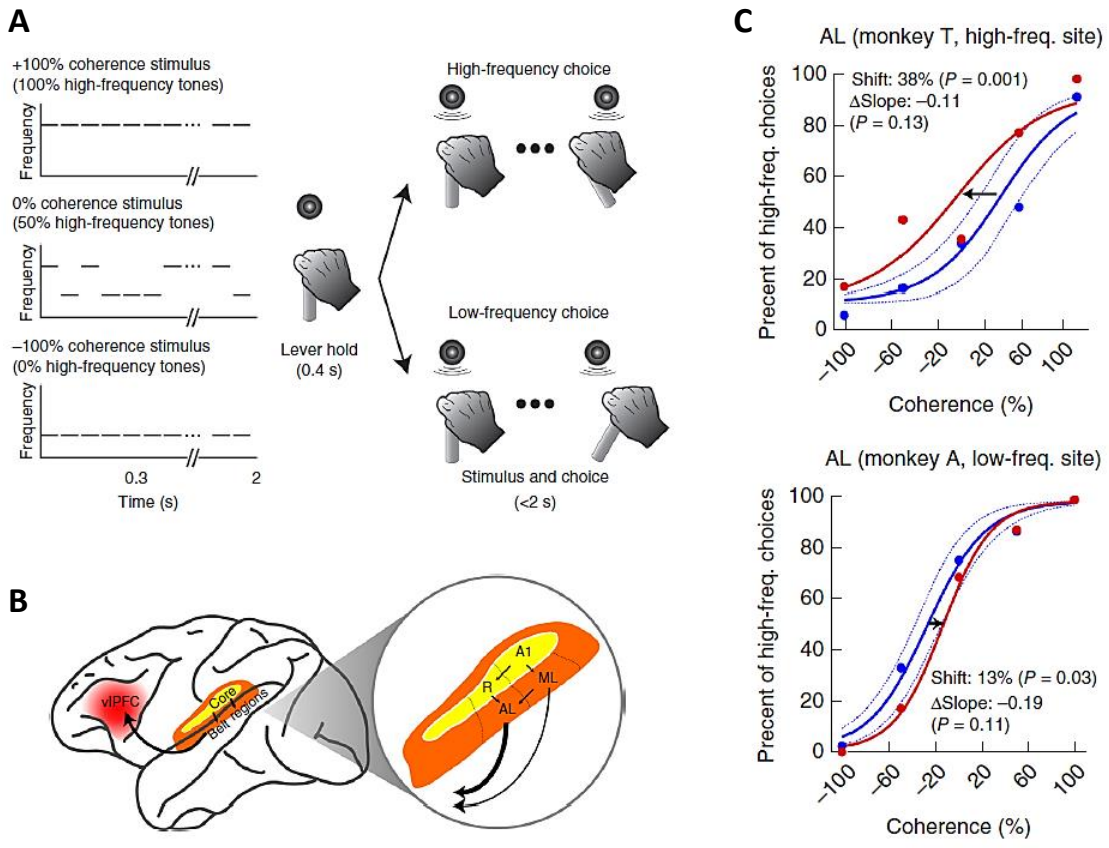


**Figure 1-33. Perceptual decision bias in monkeys by micro-stimulation in AL.**

(A) Stimuli and perceptual task in monkeys. A temporal sequence of tone bursts with different coherence was presented at every trial where monkeys had to judge the frequency and move a joystick depending if it was high frequency towards the left and low frequency towards the right. (B) Micro-stimulations in AL area of the belt of AC but not AI could bias perceptual decisions. (C) Single site micro-stimulation effect on behavioral performance and frequency judge plotted as psychrometric functions. Red and blue dots correspond to data with and without perturbation observing a shift towards the frequency of the tonotopic area stimulated in AL for two monkeys (high frequency on top and low frequency on bottom). *Adapted from Tsunada and colleagues (2016)*.

Several questions remained to be answered regarding the direct role of primary AC processing in the perception of sounds and sound-guided behavioral decisions, such as its role in frequency decomposition, frequency resolution and temporal integration for simple and more complex sound discriminations.

# 2. Results: Section I

In most animals, the auditory system allows the detection, identification and classification of sounds and their precise sources. In conjunction, these capabilities give animals the possibility to detect biologically significant sounds, orient with good precision towards the source and quickly respond with the proper behavioral output. Importantly, in humans, hearing loss and sensitivity deficits are the third-most common condition in older adults that, in addition to the obvious disabilities, have important consequences for social interactions and thus life quality, often leading to more profound emotional deficits than the loss of any other sensory modality (Leverton, 2019; Li et al., 2014). Several approaches have been used to restore normal hearing thresholds in deaf people, where electric cochlear implants are the most successful between all the different existing neuroprostheses (Jeschke and Moser, 2015). However, cochlear implant users struggle with speech comprehension in noisy environments as well as for the appreciation of music due to abnormal pitch perception (Kohlberg et al., 2014; Zeng et al., 2014). Trauma and damage directly to the auditory nerve, together with the existence of several hearing anomalies, which are based on transduction problems from lower auditory centers, requires us to seek alternative strategies to improve pitch and general sound perception in hearing impaired humans. While the cochlea is certainly required for normal auditory perception, little is known about the causal relationship between primary auditory cortical computations and perception. To further explore this relationship, in this work we used different neuronal mapping approaches, combined with inactivationand targeted optogeneticperturbations of the AC during behavior to show that auditory cortex is not always involved in auditory discriminations. On the other hand, when it is required for solving a more complex task, even coarse targeted perturbations at this stage can bias an animal's behavioral choices. This proved AC causal involvement in sensory-guided behavioral discriminations depending on the strategy and learning rules used to solve the task. This result lays the groundwork for future research aiming at sensory rehabilitation based on direct auditory cortical stimulation, pointing towards the usefulness of strategies to eventually harness the role of parallel pathways while auditory cortical perception is manipulated.

# Targeted cortical manipulation of auditory perception

**Sebastian Ceballo**[1], Zuzanna Piwkowska[1,2], Jacques Bourg[1], Aurélie Daret[1] and Brice Bathellier[1,*]

[1]Paris-Saclay Institute of Neuroscience (NeuroPSI)

Department for Integrative and Computational Neuroscience (ICN)

UMR9197 CNRS/University Paris Sud, CNRS Bldg. 32/33

1 Av. de la Terrasse, 91190 Gif-sur-Yvette, France

[2] Present address: Institute Pasteur.Dynamic Neuronal Imaging Unit. Paris, France.

* Corresponding author: brice.bathellier@unic.cnrs-gif.fr, phone: +33(0)169823408

*Submitted and currently under review*

## 2.1. Abstract

Driving perception by direct activation of neural ensembles in cortex is a necessary step for achieving a causal understanding of the perceptual code and developing central sensory rehabilitation methods. Here, using optogenetic manipulations during an auditory discrimination task in mice, we show that auditory cortex can be short-circuited by coarser pathways for simple sound identification. Yet, when the sensory decision becomes more complex, involving temporal integration of information, auditory cortex activity is required for sound discrimination and targeted activation of specific cortical ensembles changes perceptual decisions as predicted by our readout of the cortical code. Hence, auditory cortex representations contribute to sound discriminations by refining decisions from parallel routes.

## 2.2. Introduction

The role of primary sensory cortical areas in perceptual decisions is complex. Primary sensory areas are often viewed as necessary links between peripheral sensory information and decision centers, but multiple observations challenge this simplified model. For example, human subjects with primary visual cortex lesions display residual visual abilities, a phenomenon termed 'blindsight' (Sanders et al., 1974; Schmid et al., 2010). In animals, classical associative conditioning (Bruce, 2001; LeDoux et al., 1984) or some operant behaviors (Hong et al., 2018) based on sensory stimuli can be performed in the absence of primary sensory cortex. However, several studies also report sensory-based behaviors that are abolished or severely impaired by primary sensory cortex silencing (Letzkus et al., 2011; O'Connor et al., 2010; Poort et al., 2015; Sachidhanandam et al., 2013). In addition, cortical stimulation experiments show that primary cortex for all sensory modalities can perturb perceptual decisions or initiate sensory-driven behaviors, suggesting a role in perception (Choi et al., 2011; Houweling and Brecht, 2008; Huber et al., 2008; Musall et al., 2014; O'Connor et al., 2013; Peng et al., 2015; Salzman et al., 1990; Yang et al., 2008; Znamenskiy and Zador, 2013). This apparent contradiction is particularly evident in hearing, for which involvement of auditory cortex (AC) is controversial even for discrimination of two distinct sounds. Indeed, lesions or reversible silencing of AC lead to deficits or have little effect depending on task conditions, silencing methods and animal models (Gimenez et al., 2015; Jaramillo and Zador, 2011; Kuchibhotla et al., 2017; Ohl et al., 1999; Pai et al., 2011; Rybalko et al., 2006; Talwar and Gerstein, 2001). Thus, AC does not seem to be always necessary for sound discrimination.

Moreover, requirement of AC in particular task settings points towards two alternative mechanistic implications. One alternative is that AC requirement reflects a permissive role for the task (Otchy et al., 2015), for example by providing some global gating signals to other areas, which is not informative about the decision to be taken, but without which the behavioral decision process is impaired. The second alternative 59 is that AC actually provides for each stimulus distinct pieces of information which contribute to drive the discriminative choices. Optogenetic manipulations of AC activity can modulate auditory discrimination performance (Aizenberg et al., 2015), which could be both explained by a permissive or a driving role of AC in the task. Targeted manipulation of AC outputs in the striatum can bias sound frequency discrimination towards the sound frequency corresponding to the preferred

frequency of the manipulated neurons (Znamenskiy and Zador, 2013). This indicates that AC output can be sufficient to drive discrimination, but as necessity was not shown in this task, it remains possible that this manipulation does not reflect the natural drive occurring in the unperturbed behavior. In support of this, targeted manipulation of generic AC neurons failed to drive consistent biases in this task (Znamenskiy and Zador, 2013). Thus, necessity and sufficiency of precise AC activity patterns in a sound discrimination behavior remain to be established.

Here we combine optogenetic silencing and patterned activation techniques in head-fixed mice to show that AC is not required in a simple frequency discrimination task but is necessary for a difficult discrimination involving more complex sounds with frequency overlaps. We also show based on a discrimination of distinct optogenetically driven AC activity patterns that specific AC information is sufficient for driving a discrimination, and decisions in this case also take longer than choices made in the simple task. Last, we show that focal stimulation of AC in the mouse is able to modify the animal's choice in the difficult task but not in the simple one. We also show that the AC region most sensitive to focal stimulation contains AC encodes auditory features used by the mouse to discriminate the two trained sounds. These results indicate that AC provides necessary and sufficient information to drive decisions in difficult sound discriminations, while other pathways bypass it in simple discriminations.

## 2.3. Results

### 2.3.1. Requirement of auditory cortex depends on sound discrimination complexity.

Lesion studies in rats and gerbils (Ohl et al., 1999; Rybalko et al., 2006), suggest that the involvement of AC in sound discrimination could be related to the sound features that have to be discriminated, and thus potentially to the difficulty of the discrimination. To test this idea in mice, we trained one group of head-fixed mice to discriminate only frequency features (a 4 kHz against a 16 kHz pure tone, PTvsPT task) while a second group had to integrate frequency variations over time to discriminate a linearly rising frequency modulated sound (4-12 kHz) against a pure tone (4 kHz, FMvsPT task), (Figure 2-1A). While the PTvsPT task was rapidly learned, the FMvsPT task was more challenging as it required much longer

training (67 ± 13 trials, n = 30 mice for the PTvsPT, against 415 ± 53 trials, n = 29 mice, for FMvsPT task to reach 80% performance; Wilcoxon rank-sum test, $p = 6.8\times10^{-8}$,Figure 2-1B-C).

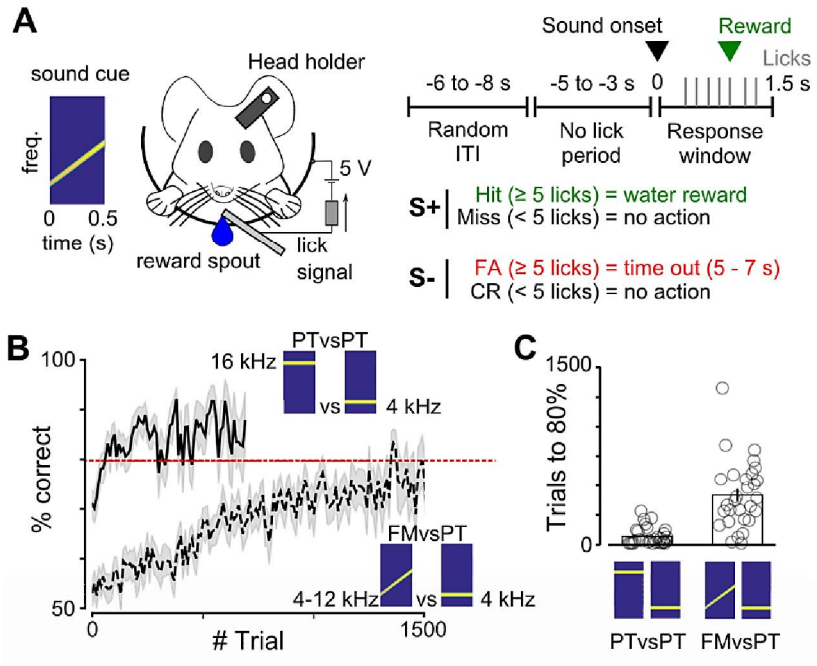


**Figure 2-1. Discriminating a FMs from a PT is harderthan two PTs.**

(A) Sketch of the head-fixed Go/NoGodiscrimination task. (B) Learning curves for all mice performing each task. (C) Number of trials needed to reach 80% discrimination performance for PTvsPT and FMvsPT discrimination task (PTvsPT, n = 30. FMvsPT, n = 29. Wilcoxon rank-sum test, P < 0.001). Open circlescorrespond to single mice. Bar plots show the mean and SEM.

We thus wondered whether this difference in task difficulty could relate to differential involvement of AC. To investigate, we decided to silence AC by activating parvalbumin-positive interneurons (PV) expressing channelrhodopsin (hChR2-tdTomato). Electrophysiological calibration in awake, passive mice (Figure 2-2A and Figure 2-8) showed that this manipulation strongly disrupted cortical activity (Figure 2-2B), decreasing population firing rates to target sounds by ~70%, with about 50% of putative PV-negative neurons displaying a complete suppression of their response (Figure 2-2C and Figure 2-8). To evaluate the effect of PV-activation on task performance, we trained a linear Support Vector Machine (SVM) classifier to discriminate the two target sounds based on the population activity of putative PV-negative neurons (n=125, in 2 mice). We then measured the performance of the classifier with AC

responses to the same sounds during PV-activation. For the pure tones, the SVM performance dropped from almost perfect classification to less than 70% and for the FM sounds, SVM performance dropped to chance levels (Figure 2-2D).

When bilaterally applying this PV-activation protocol through cranial windows in behaving mice, we indeed observed a drop of performance down to chance level (50%) in the FMvsPTtask, while mice lacking Chr2 expression performed normally (Figure 2-2E). However, the samemanipulation during the PTvsPT task yielded less than a 10% performance drop (Figure 2-2E).Because the same inactivation strategy applied to the inferior colliculus, an earlier stageof the auditory system, fully abolished PTvsPT performance (Figure 2-2F), we suspected that the continued performance of the PTvsPT task after AC perturbation was not due to incompleteness of the silencing (Figure 2-2C andFigure 2-8), but rather to the absence of AC involvement. We thusperformed bilateral lesions of the entire AC and observed no impact on behavioral performance for the PTvsPT task, even on the day following lesion (Figure 2-2G andFigure 2-9). In summary,AC is dispensable for a simple pure tone discrimination task while it is necessary for the more difficult FMvsPT task.

### 2.3.2. Information from auditory cortex can drive slow discriminative choices

Necessity alone does not prove that AC activity patterns causally drive decisions in the FMvsPT task (Hong et al., 2018; Otchy et al., 2015). Seeking to establish a proof of sufficiency for AC activity in this task, we first tested if two distinct activity patterns in AC can provide enough information to drive a discrimination task, as so far, cortical stimulation studies haveonly demonstrated detection of a single cortical stimulation (Houweling and Brecht, 2008; Huber et al., 2008; Musall et al., 2014; O'Connor et al., 2013; Peng et al., 2015; Salzman et al., 1990; Znamenskiy and Zador, 2013). To this end, we used a micro-mirror device(Dhawale et al., 2010;Zhu et al., 2012) to apply two-dimensional light patterns onto the AC surface through a cranial window in Emx1-Cre x Ai27 mice expressing channelrhodopsin in pyramidal cells (Figure 2-3**A**).

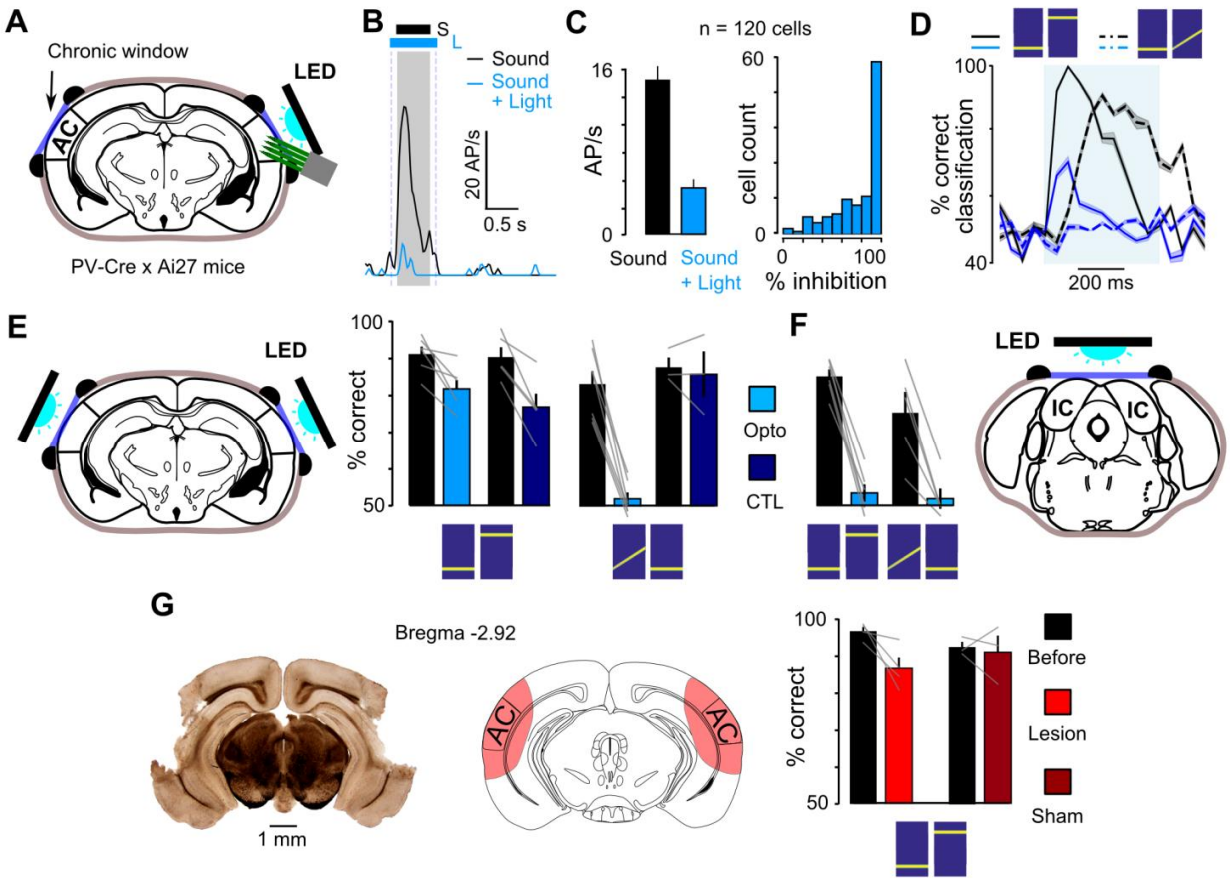


**Figure 2-2. Cortical requirement for sound discrimination depends on discrimination complexity.**

(A) Sketch of the optogenetic inactivation strategy through a cranial window covering the primary and secondary auditory cortex. For calibration, silicon probes were inserted beneath the window. (B) Sound response PSTH of a sample PV-negative cell with and without light-driven PV-neuron activation. (C) Mean population response to sounds with and without optogenetic activation of parvalbumin cells (15 ± 1.4 Hz vs 4.7 ± 0.9 Hz; n = 125, p = 6.2×10-18, Wilcoxon rank-sum test) and distribution of sound response reduction during light-ON trials for putative PV-negative neurons. (D) S+ versus S- discrimination performance for a linear SVM classifier trained on a sample of normal population responses (5 repetitions) and tested on either normal population responses or on population responses recorded during optogenetic inactivation (5 independent repetitions) (n=125 cells, from 2 mice).(E) Discrimination performance without (black) and with (blue) optogenetic inactivation of AC during PTvsPT (left, 91 ± 2.4% vs 82 ± 2%, n = 6, 574 p =0.025, Wilcoxon rank-sum test) andFMvsPT (right, 83 ± 1.7% vs 52 ± 3.5%, n = 7, p =, 0.002, Wilcoxon rank-sum test) tasks in mice expressing ChR2 in PV interneurons. The same measurements are shown for control mice without ChR2 expression (dark blue). (F) Discrimination performance without (black) and with (blue) optogenetic inactivation of inferior colliculus during PTvsPT (left, 85 ± 2.3% vs 54 ± 1.9%, n = 6, p = 0.004, Wilcoxon rank-sum test) and FMvsPT (right, 75 ± 2.7% vs 52 ±

5.6%, n = 5, p = 0.016, Wilcoxon rank-sum test) tasks. (G) Left; Example histological section showing the extent of bilateral AC lesions. Right; Mean discrimination performance during PTvsPT before and after AC lesion (97 ± 1.1% vs 87 ± 2.9%, n = 4, p = 0.043, Wilcoxon rank-sum test) or sham surgery (93 ± 1.4% vs 91 ± 4.5%, n = 4, p = 0.8, Wilcoxon rank-sum test).

We chose to trigger the two discriminated activity 133 patterns with light disks of 0.4 mm diameter at two distinct positions. To make sure that optogenetic patterns were qualitatively similar to sound-evoked activity, we calibrated them in awake mice by recording isolated single units with multi-electrode silicon probes while targeting the light disks to many locations within the cranial window (Figure 2-3A). In this procedure we observed that recorded single units tended to respond only to a subset of the tested locations (e.g. Figure 2-3B). Pooling together the activity of all recorded neurons, we observed that optogenetically and sound-triggered responses had similar latencies and time courses above a 50 ms time scale (Figure 2-3C, note that optogenetic responses followed the 20Hz modulation of the light stimulus below the 50 ms time scale). Moreover, response amplitudes were similar in particular for the lowest light intensity tested (12mW, Figure 2-3C), reflected by a high correlation of response amplitudes to the preferred sound and the optogenetic pattern (Figure 2-3D). Last, the spatial extent of optogenetic responses (600-800 µm diameter, depending on light intensity, Figure 2-3E) matched the extent of pure tone responses in primary auditory cortex (e.g. Figure 2-10).

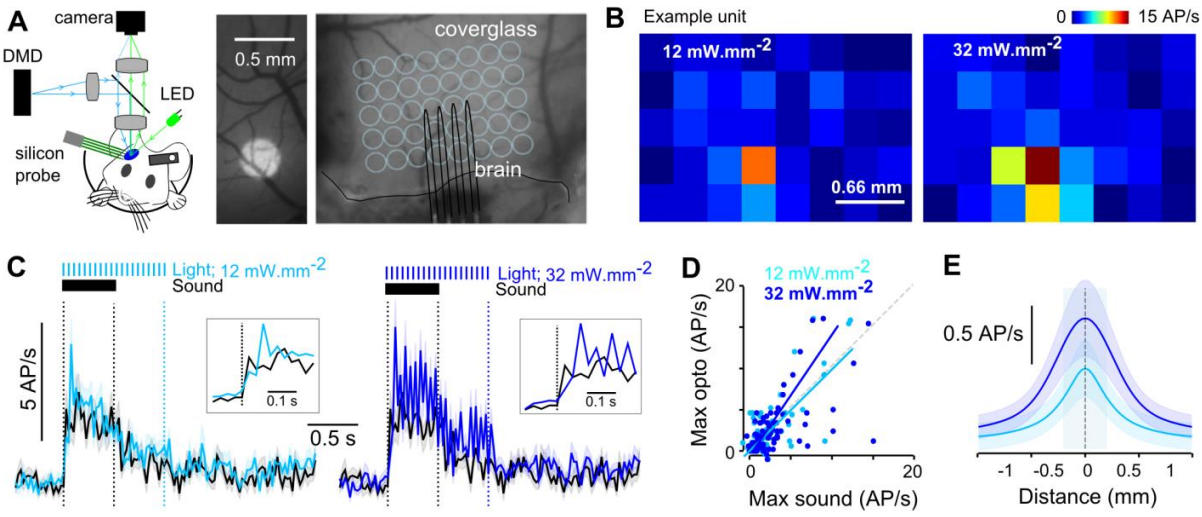


**Figure 2-3. 2D-light pattern triggers focal activity in auditory cortex.**
(A) Left, Photostimulation setup and optogenetic calibration protocol. Right, example image of a ~400 µm disk projected onto the cranial window. (B) Left, image of the AC cranial window with a sketch of the silicon probe insertion site and grid locations where light was

projected (light blue). Middle & right, 2D maps of an example single unit for two light intensities, representing the mean firing rate over 10 repetitions during photo-stimulation of the different locations on the grid. (C) Time course of mean firing rate (50ms time bin) in response to a single pure tone of 500 ms at 70 dB (black line) or in response to 12 mW.mm-2 (left) or 32 mW.mm-2 (right) focal optogenetic stimulations (light blue line, disk diameter 400 µm) for n = 84 single units (shadings represent SEM). Insets: magnification at stimulus onset. (D) Best photo-stimulation response plotted against best sound response. For 12 mW.mm-2 the slope of the regression line was 1.01 and the correlation coefficient 0.74, p = 2.4×10-16, n = 84 single units recorded between 300 and 900 µm in depth. (E) Mean of Gaussian models that were fitted to the lateral distribution profile of photo-stimulation responses for single units with significant spatial modulation. Half-width diameter: 560±147 µm at 12mW.mm-2 and 800±235 µm at 32mW.mm-2 (n = 15 single units).

Together, these measurements indicated that the chosen cortical stimulation patterns yielded response characteristics within the range of natural sound responses. Using the same behavioral protocol as for the sound discrimination tasks, we trained mice to discriminate between unilateral cortical stimulations (32 mW mm-2) in low versus high frequency tonotopic areas of the primary auditory field of AC (Figure 2-4A-C). The locations of these areas with respect to blood vessel patterns were identified using intrinsic imaging (Figure 2-4C andFigure 2-10) as previously established (Bathellier et al., 2012; Deneux et al., 2016; Kalatsky et al., 2005; Nelken et al., 2004). Blood vessels were then used as landmarks to robustly target the same regions across days. We observed that mice could learn to discriminate these artificial AC patterns within hundreds of trials (Figure 2-4D), showing AC activity can drive a discrimination task.Strikingly however, discrimination of cortical patterns was executed about four times slower than the cortex-independent discrimination of real pure tones (~400 ms vs ~100 ms, Figure 2-4E-F), as measured by determining the first time point after stimulus onset at which licking behavior significantly differed for S+ and S- stimuli (Figure 2-11). In addition, ~400ms reaction times were observed for the detection of optogenetic activation in AC, independent of pattern size and intensity (Figure 2-11), showing that the long decision latencies for AC-driven discrimination are not due to insufficient drive from the artificial cortical patterns, but rather to a rate-limiting process in the pathway downstream of AC that triggers the animal's decisions. Interestingly, in the cortex-dependent auditory task (FMvsPT), discrimination times were also ~400 ms (Figure 2-4E-F), but contrary to direct cortical stimulation, discrimination was preceded by an early non-discriminative response whose onset timing was similar to the discriminative lick response in the PTvsPT task (Figure 2-4F, arrowhead). These observations suggest that sound discrimination activates two pathways. (i) An AC-independent pathway producing an early response which can distinguish very distinct sounds but fails to discriminate more complex differences.

(ii) An AC-dependent, slower pathway which can provide specific information to improve the responses initiated by the AC independent pathway, in case these fail to discriminate the proposed sounds.

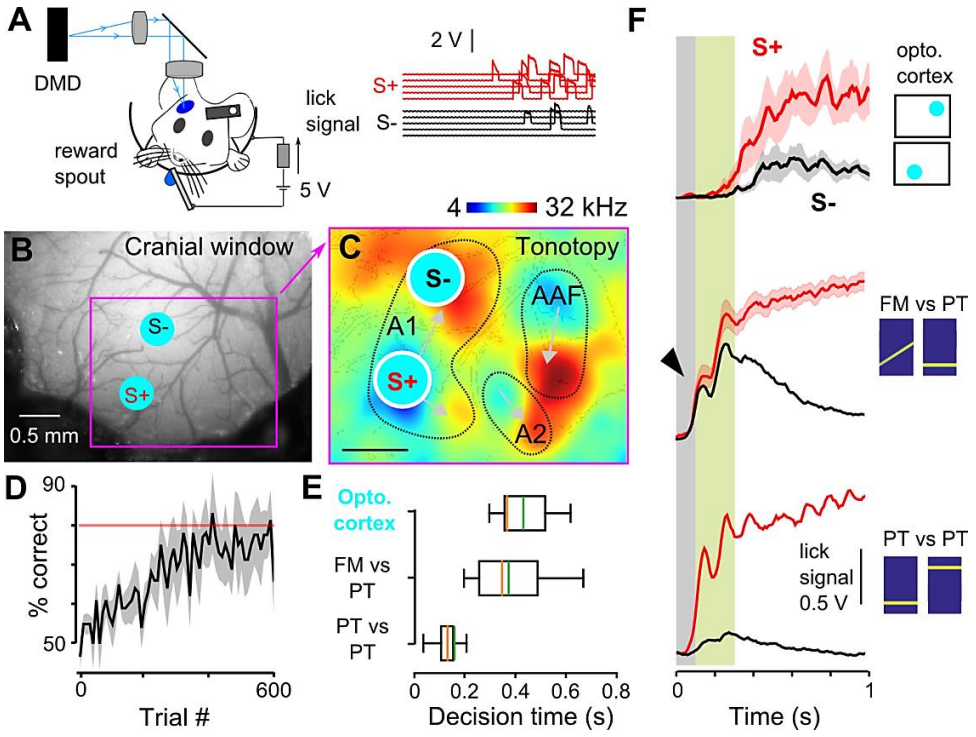


**Figure 2-4. Mice can discriminate two artificial activity patterns in AC.**
(A) Sketch of the Go/NoGo discrimination task for optogenetic stimuli with sample trials showing licking signals for each stimulus. (B) Sample cranial window superimposed with thelocation of two optogenetic stimuli in AC. (C) Localization of the two optogenetic stimuli in theAC tonotopic map obtained from intrinsic imaging. Same mouse as in B. (D) Population learningcurve for discrimination of two optogenetic stimulations (340±105 trials to reach 80% correctperformance, n = 5). (E) Mean decision times for the three different discrimination tasks (optogenetic 424 ± 58 ms, n= 5; FMvsPT, 366 ± 25 ms, n= 29; PTvsPT, 153 ± 22 ms, n= 30mice). PTvsPT was significantly different from the two other groups (p = 7.3×10-9 for FMvsPTand p = 1.1×10-3 for optogenetic, Wilcoxon rank-sum test) which were not different from eachother (p=0.2, Wilcoxon rank-sum test). (F) Mean licking traces for S+ and S- stimuli duringoptogenetic (top), FMvsPT (middle) and PTvsPT (bottom) discrimination. Arrowhead: unspecific initial licks.

### 2.3.3. Focal auditory cortex stimulations bias decisions in the complex discrimination

If indeed AC provides specific information to drive the correct decision exclusively in the difficult task, then specific activation of neural ensembles in AC should influence behavioral decisions in the FMvsPT task but not in the PTvsPT task. To test this hypothesis, we trained two groups of Emx1-Cre x Ai27 to perform these tasks. For both groups, the non-rewarded stimulus (S-) was the 4 kHz pure tone. The rewarded stimulus was the 16kHz pure tone for one group and the 4-12 kHz FM sweep for the other group. After task acquisition, the right AC of each mouse was functionally mapped 182 using intrinsic imaging to determine its tonotopic organization (Figure 2-5A). Then a grid of optogenetic stimulus locations (400µm disks) was aligned to this map. Each location was stimulated during behavioral performance as occasional non-rewarded catch trials (10% occurrence) together with the non-rewarded 4 kHz pure tone (Figure 2-5B). The purpose of this design was for the 4 kHz tone to drive the rapid non-specific response and test if additional specific cortical drive mimics, at least partially, the perception of the rewarded stimulus instead of the presented S-, thereby changing the late discriminative response. To mimic sound-induced activation as closely as possible with our method, we used the lower of our two calibrated light intensities (12 mW.mm-2, Figure 2-5C-D). Unlike previous studies (O'Connor et al., 2013; Znamenskiy and Zador, 2013), these catch trials were not rewarded to measure a spontaneous interpretation of optogenetic perturbations by the brain and rule out reward-associated responses potentially generated by fast learning processes. Each of the 17 locations in the grid was tested across five catch trials and the average lick count elicited was compared to the mean expected lick count distribution in five regular S- trials to assess statistical significance (e.g. Figure 2-5C, $p<0.05$). We accounted for multiple testing across the 17 locations using the Benjamini-Hochberg correction. This conservative analysis showed that specific locations (e.g. Figure 2-5D) significantly increased lick counts above random fluctuations and brought the behavioral response close to the normal rewarded stimulus (S+) response for the FMvsPT task (Figure 2-5E). Moreover, the fraction of locations perturbing behavior was significantly above the false positive rate across all animals tested (Figure 2-5F). This was not the case for the easier PTvsPT task (Figure 2-5F), in which no stimulus location could raise the lick count close to S+ level (Figure 2-5E). Together, this experiment showed that targeted, physiologically realistic AC stimulation is sufficient to change the decisions of mice in the difficult auditory task but not in the simple task, corroborating the idea that AC is not involved in the former but contributes decisive information in

the latter. This idea was also reinforced by the observation that locations significantly 207 perturbing behavior clustered around a specific area of AC when mapped across all animals in the FMvsPT task but not in PTvsPT task (Figure 2-5G,H). This area spanned the mid-frequency range of the primary auditory field (AI) and to a lesser extent the central region of AC (Figure 2-5H) as defined from intrinsic imaging maps (Figure 2-5A and Figure 2-6A).

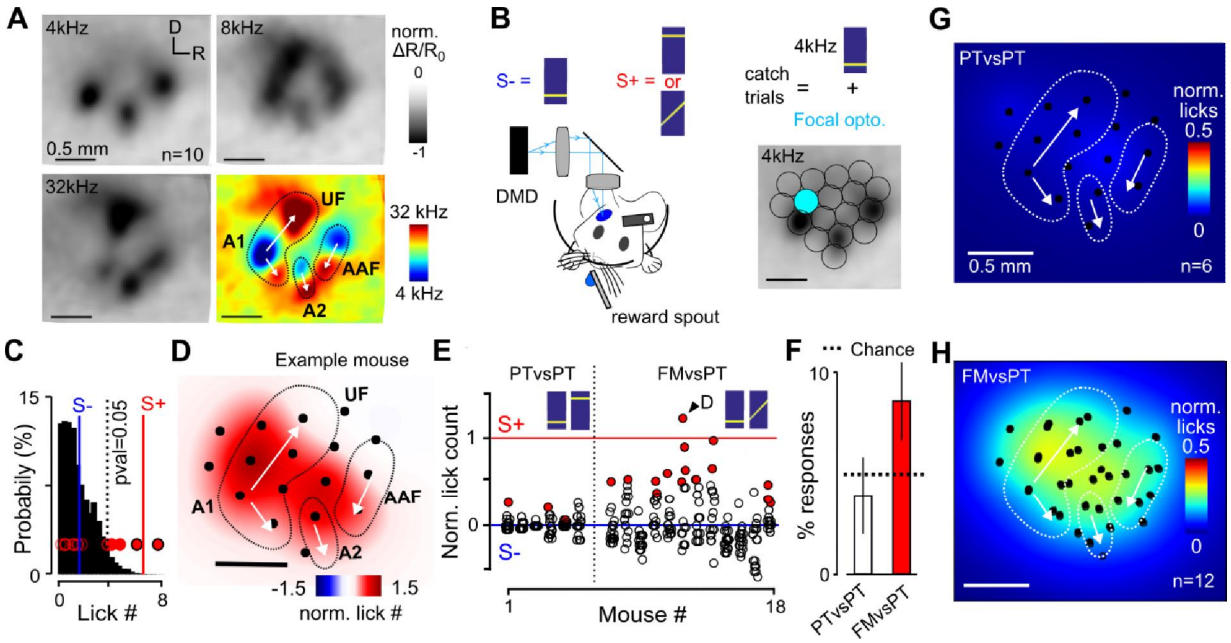


**Figure 2-5. Focal optogenetic AC activation can bias behavioral decisions.**

(A) Intrinsic imaging response maps for three pure tones, aligned and averaged across 10 mice. Bottom right, map of tonotopic gradients obtained by subtracting the 4 and 32 kHz response maps. The approximate contours and direction of the main tonotopic gradients (primary auditory field AI, anterior auditory field AAF, secondary auditory field A2) are superimposed. (B) Schematic of the focal AC perturbation experiment: optogenetic stimuli at different locationswere superimposed in occasional trials with the S- sound (4 kHz). (C) Probability distribution of S- lick counts averaged over three random trials in one sample mouse. The superimposed red circles represent the mean lick counts over three trials for each optogenetic stimulus location. Open circles: non-significant responses. Filled circles: lick count is larger than 95% of S- lick counts. Filled circles with black contours: significant locations after Benjamini-Hochberg correction for multiple testing ($P<0.05$). (D) Map of normalized lick counts for optogenetic perturbations obtained by summing the estimated 2D neuronal population response profile for one light disk, multiplied by observed lick count and positioned at all optogenetic locations with a significant response. (E) Mean lick counts for all optogenetic stimulus locations and all mice involved in the PTvsPT or FMvsPT tasks. Red filled circles correspond to significant locations ($P < 0.05$, corrected for multiple testing). (F) Percentage 635 of significant locations found in the PTvsPT and FMvsPT tasks across all mice.

Dashed line: expected false discovery rate. (G) Maps of normalized lick counts for significant optogenetic locations averaged across all mice performing the PTvsPT task. Black circles: centers of optogenetic stimuli. (H) Same as (G) but for the FMvsPT task.

### 2.3.4. Tonotopic location of effective focal stimulations matches frequency cues used for discrimination

The central, non-tonotopic region of AC, potentially part of secondary auditory areas (A2), was recently suggested to contain neurons specific for vocalizations and FM sweeps(Honma et al., 2013; Issa et al., 2014; Issa et al., 2017). This is in line with its contribution to the decisions in the FMvsPT task. We thus wondered if the mid-frequency area of AI is also involved in coding the 4-12 kHz FM sweep. First, we observed that strong intrinsic imaging responses to the FM sweep occur in AI, particularly in the mid–frequency area (Figure 2-6A). To better quantify the information contained in this area, we performed two-photon calcium imaging in layer 2/3 of AC in awake, passively listening mice who had been injected with pAAV1.Syn.GCaMP6s virus. All imaged fields were aligned to intrinsic imaging maps using blood vessel patterns (Figure 2-6B) allowing a comparison of micro- and mesoscale maps. Color coding cell locations with respect to their best frequency, we qualitatively observed a good match between tonotopic maps derived from the intrinsic and calcium imaging (Figure 2-6C, Figure 2-12), even if a certain level of disorganization could be seen in the high resolution map as reported previously (Bandyopadhyay et al., 2010; Rothschild et al., 2010). For example, the mid-frequency area identified with intrinsic imaging mostly contained cells with best frequencies at 8 or 16kHz when imaged at high resolution (e.g. Figure 2-6C, Figure 2-12). Based on these data, we calculated the similarity (correlation coefficient) between population responses to FM sweeps and to different pure tones and found, both at coarse and high spatial resolution, that the response to the FM sweeps is most similar to the 232 responses to pure tones around 8 kHz (Figure 2-6D). We reasoned that cells coding for this frequency range in AI could be particularly important for discriminating the FM sweep from the 4 kHz tone. To quantify this idea with our two-photon calcium imaging measurements, we calculated the fraction of neurons responding to different pure tones within the population that responds to the FM sweep but not to the 4 kHz pure tone (discriminative FM sweep neurons). This showed that neurons which discriminatively respond to the FM sweep indeed have a preference for frequencies around 8kHz (Figure 2-6E), a result in line with the localization of the most disruptive optogenetic perturbations in the mid240 frequency region of AI, at least if AC representations are similar in passive and active mice. To

evaluate if context-dependent changes (Francis et al., 2018; Kuchibhotla et al., 2017), could impact our conclusions, we also performed calcium imaging in mice engaged in the FMvsPT task. We found as previously reported positive and negative modulations (Kuchibhotla et al., 2017) for a fraction of neural responses during engagement, which averaged to a net decrease of population responsiveness (Figure 2-13). However, AC population activity classifiers trained in the passive state maintained good performance in discriminating the sounds when tested in the active state (Figure 2-13), confirming the overall similarity of active and passive sound representations in AC.

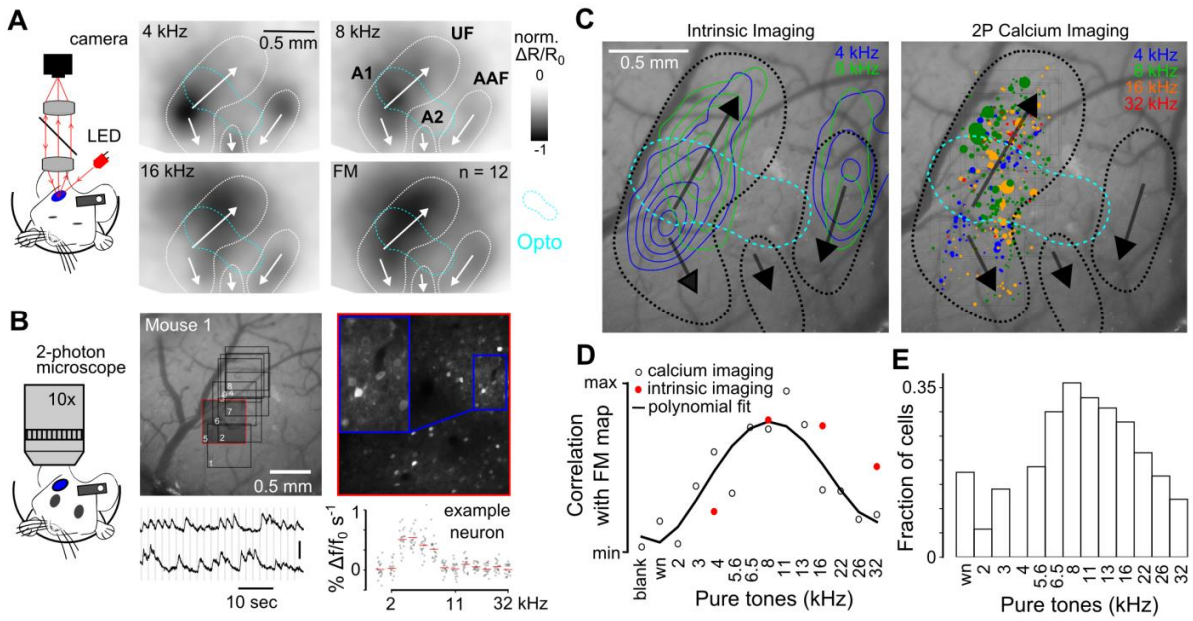


**Figure 2-6.AC neurons coding for intermediate frequencies distinguish sounds from the difficult task.**

(A) Sketch of intrinsic imaging setup and averaged re-aligned intrinsic imaging maps sampled over 12 mice for 4, 8 and 16 kHz pure tones and FM sweeps. White lines and arrows indicate the main tonotopic fields as in Fig 5A. (B) Sketch of 2-photon setup and picture of the AC surface with the localization of calcium imaging fields-of-view (FoV) for a sample mouse. A magnification of FoV 5 is shown on the right. Raw calcium traces (scale bar: 50 %Δf/f0) and a pure tone tuning curve (70 dB SPL) for a sample neuron are shown on the bottom. The calcium imaging setup is sketched on the left. (C) Magnification of cranial window shown in (B) with the contours of intrinsic imaging responses to 4 and 8 kHz pure tones (left) and the locations of all significantly responding neurons which do not respond to both 4 kHz and 4-12 kHz (discriminative neurons see methods) 652 recorded with 2 photon calcium imaging (non-discriminative neurons removed). Color-code corresponds to their preferred frequency over the same sounds used during intrinsic imaging experiments. Circle diameters are proportional to the mean deconvolved calcium response for the best frequency sound over 20 repetitions

(right). The dashed line indicates the position of the main tonotopic fields. (D) Red dots: Correlation of the pooled intrinsic response maps of the FM sweeps with pooled maps of four different pure tones (n=12 mice for the aligned maps). Black dots: correlation between the population vector responses of the FM sweeps and of various pure tones (time bin 0 to 1s after sound onset, from 5157 significantly responding neurons over 30 sessions in 5 mice). Intrinsic: max=1; min 0.75. Calcium imaging: max = 0.25; min=0. (E) Fraction of neurons that respond significantly to pure tones and FM sweeps (n=520 neurons, Wilcoxon rank sum test, $\alpha = 0.01$) from the pool of significantly responding neurons (discriminative neurons, n= 4692 neurons).

Thus together, our optogenetic and imaging experiments suggest that AC contributes to the discrimination of the 4-12 kHz sweep vs 4 kHz pure tone by engaging spatially segregated neurons that preferentially code for intermediate frequencies around 8 kHz. A prediction of this model is that mice engaged in the FMvsPT discrimination should strongly associate the 4-12 kHz sweep with pure tones in the 8 kHz frequency range. To test this prediction, we presented pure tones in occasional non-rewarded catch trials during the task and measured the lickingresponses of the mouse (Figure 2-7A). We observed that mice responded to 5.6 kHz and 8 kHznon-rewarded pure tones with a number of licks similar to the lick count observed after therewarded 4-12 kHz sweep (Figure 2-7B), revealing the 257 expected association of these frequencies with the FM sound. We thus wondered if this categorization behavior crucially depends on neurons sensitive to frequencies in the 8 kHz region. We trained a linear classifier (SVM) to discriminate the 4-12 kHz sweep and the 4 kHz pure tone based on the responses of neurons imaged in passive mice and significantly activated by only one of the two sounds (discriminative neurons). When testing this classifier with the single trial population responses elicited by pure tones, we could qualitatively reproduce the categorization curves observed during behavior (Figure 2-7B). This indicates a match between the structure of the coding space in AC and of the perceptual space as probed in the FMvsPT behavioral task. However, when the classifier was trained without the neurons that significantly respond to the 8 kHz pure tone, then no match is observed between behavioral and cortical categorization curves, although the remaining neurons still discriminate the FM sweep from the 4 kHz pure tone (Figure 2-7B). This result corroborates the idea that activation of neurons responding in the 8 kHz frequency range critically contributes to the identification of the FM sweep against the 4 kHz tone, in line with the observation that focal optogenetic stimulation in the region most sensitive to the mid-frequency ranges promotes licking responses associated with the FM sweep (Figure 2-5H).

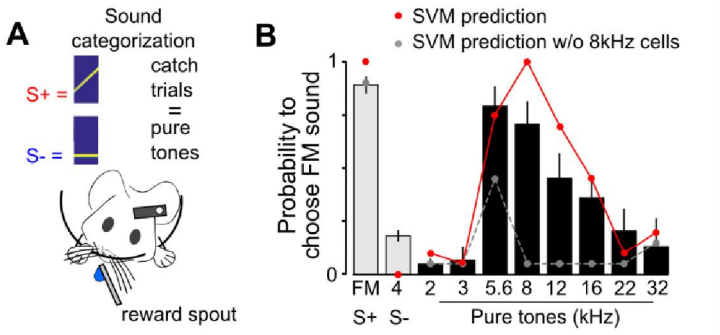


**Figure 2-7.Mice use intermediate frequencies as a cue to discriminate between FM sound and low frequency PT.**

(A) Sketch of the auditory categorization assay. (B) Mean response probabilities in response to unrewarded pure tones occasionally replacing trained stimuli in the FMvsPT discrimination task (mean ± SEM, n=6 mice). Circles in red are the probabilities of an SVM classifier, trained to discriminate between FM sweeps and 4 kHz pure tones, to classify different pure tones as an FM sweep. Population vectors used to train the classifier correspond to the 672 mean deconvolved calcium responses of 4692 significantly responding and discriminative neurons in a [220 ms ; 448 ms] time bin with 20 repetitions for each sound). Circles in grey correspond to the same analysis but after exclusion of neurons that respond significantly to an 8 kHz pure tone.

## 2.4. Discussion

Together, our results demonstrate that, while AC is dispensable for a simple pure tone discrimination task, specific activity patterns in AC provide necessary and sufficient information for discrimination of a more complex sound pair (FMvsPT task). Here the more complex task involves two sounds which overlap in frequency at their onset but then diverge due to upward frequency modulation for one of them. The two sounds are thus theoretically distinguishable thanks to both spectral (mid- and high-frequencies of the FM sound) and temporal (continuous frequency variations) cues. It is striking that despite the large spectral differences between the two sounds of the FMsPT task, this discrimination was much harder for mice to learn than the pure tone discrimination task. The challenge might come from the frequency overlap at the beginning of the two sounds. This spectral overlap implies that both sounds activate a large group of identical neurons throughout the auditory pathway, as we observe in the AC (the FM sweep also activates the 4 kHz region, Figure 2-6A, Figure 2-12). Activation of the set of neurons coding for the overlapping frequency is a strong and early predictor of rewards in S+ trials. Therefore, a simple reinforcement learning rule might associate activity of these neurons to the licking response, which makes it difficult for the animal to refrain from licking in S- trials, in which the same neurons are active. The challenge for the brain might be to use information from the non-overlapping parts of the sound representations to counteract such generalization. Analysis of the licking profiles in the FMvsPT task indicates that mice do not fully resolve this problem. Indeed, their initial response both to S- and S+ is to lick shortly after sound onset. It is only after this initial impulse that modulation of licking leads to the discriminative response (Figure 4F). The role of AC might be to solve this initial confound, while alternative pathways are able to learn the correct associations when discriminated stimuli are encoded with little overlap as expected for the distant pure tones of the PTvsPT task. Interestingly, a similar phenomenon is observed in a Pavlovian discriminative fear condition protocol, in which conditioning to a specific direction of frequency ramps cannot be achieved without AC, while AC is dispensable for fear conditioning to a specific pure tone (Letzkus et al., 2011). Thus, the requirement of auditory cortical areas for distinguishing temporal variations in frequency overlapping stimuli might be a generic principle independent of the sound association protocol used to uncover it. Our study does not identify the alternative pathways which provide auditory information to motor centers in the absence of AC in the simple PTvsPT task. Connectivity studies suggest multiple connections between the auditory system and motor related centers (Pai et al., 2011). Primary auditory thalamus is known to project to striatum

(LeDoux et al., 1991) a brain region necessary for appetitive sound discrimination tasks (Guo et al., 2018). Thalamo-striatal projections could possibly implement the main sensory-motor association in the easy task (Gimenez et al., 2015;Guo et al., 2017). Sensory-motor associations are also possible at the mid-brain level, where inferior colliculus contacts superior colliculus which projects to several motor centers (Stein and Stanford, 2008). The strong impact of optogenetic silencing of the inferior colliculus on the PTvsPT discrimination suggests that the sensory-motor association does not occur at brainstem level before information reaches colliculus (Figure 2A), although further investigation would be necessary to verify that our colliculus silencing experiment does not uncover a permissive effect of colliculus in the task (Otchy et al., 2015). Likewise, thalamic silencing was shown to strongly impact frequency discrimination (Gimenez et al., 2015), suggesting that the sensory-motor association in our PTvsPT task does not occur before auditory information reaches thalamus. Finally, another possibility is that decisions in the PTvsPT task are driven by alternative cortical routes excluding AC but receiving auditory information from primary or secondary thalamus. Such direct pathways, for example to more associative areas have been proposed to support "blindsight" abilities in patients lacking primary visual cortex (Cowey, 2010). In line with this possibility, recent results indicate that fear conditioning to simple sounds does not require AC but requires the neighboring temporal association area (Dalmay et al.). Also, recordings in prefrontal cortex during an auditory discrimination task show the presence of fast responses to sounds (Fritz et al., 2010), compatible with a direct pathway. Similarly, in our task, bypass pathways to temporal or prefrontal associative areas could eventually be sufficient to make simple auditory decisions, even in absence of AC, Independent of the identity of the alternative pathway involved in the PTvsPT, our results suggest that it provides a faster route to generate motor responses than the route which involves AC. This idea derives from the long discrimination times (~400 ms) observed when mice discriminate two optogenetically-driven cortical activity patterns as compared to the short discrimination times (~150ms) observed for the PTvsPT task (Figure 2-4E-F). This long discrimination time is unlikely to result from difficulties in differentiating the two optogenetic stimuli, as detection of one stimulus required also ~400ms independent of stimulus strength and size (Figure 2-11), consistent with previous measurements in another optogenetic stimulus detection task (Huber et al., 2008). Calibration of our optogenetic stimuli also showed that the two chosen stimulus locations can be efficiently discriminated based on triggered cortical activity within 50 to a 100ms (Figure 2-11). However, although population firing rate and spatial extent parameters of optogenetic stimuli were similar to sound responses in AC (Figure 2-3), we cannot fully rule out that some non-controlled parameters of the

artificial stimulations lead to extended reaction times. It is also possible that absence of subcortical drive in the optogenetic task leads to threshold effects that slow down the behavioral response. Yet, in support of a slowsensory cortical pathway, discrimination times observed in cortex-dependent sensory discrimination tasks in head-fixed mice using visual or tactile cues are typically above 400ms (O'Connor et al., 2010; Poort et al., 2015; Sachidhanandam et al., 2013). In the cortex dependent auditory task presented in our study (FMvsPT), discrimination times are also long (~350ms, Figure 2-4E-F). We measured that AC activity starts to be discriminative for the FM sweep and 4kHz pure tone only about 100 to 150ms after sound onset while two pure tones arediscriminated by AC activity already 50ms after onset (Figure 2-2D). This leaves a supplementary delay between information arrival and decision of at least 100ms in the cortex dependent FMvsPT task as compared to the cortex independent PTvsPT task. This delay could be due to complex multisynaptic pathways downstream to AC (e.g. including associativecortical areas) or to downstream temporal integration processes. Timing differences could alsoplay a role in the absence of AC engagement in simple tasks. Indeed, while AC rapidly receives auditory information (Figure 2-2D), its slow impact on behavior could allow alternative pathwayswhich provide faster responses to short-circuit information coming from AC. This might explain the absence of strong perturbations of the easy PTvsPT task when we applied non-rewarded focal stimulations of AC, calibrated to typical sound response levels, despite specific targeting to the tonotopic fields relevant for the discrimination. We do not exclude that rewarding licking responses to the occasional focal stimulations could rapidly lead,after some learning, to a reinforced participation of stimulated cortical areas in behavioral decisions. In the case of the harder FMvsPT task, focal stimulations had a significant effect on behavior despite the absence of rewards in our protocol. This indicates that, despite the coarseness of the stimulation approach which globally targets heterogeneous cell ensembles enriched with particular spectral information due to tonotopic organization (Figure 2-6, Figure 2-12), some optogenetically-driven ensembles activate large enough parts of the stimulus representations to change behavioral decisions. Thus, our results demonstrate that manipulation of AC representations impact perception, at least, if the behavioral task for perceptual read out is appropriately chosen. This opens interesting possibilities for central auditory rehabilitation techniques. In the FMvsPT task, we took advantage of the fact that spectral cues can be used to distinguish the two auditory stimuli, such that neural ensembles relevant for discrimination in AC tend to be clustered in space and can be activated with broad light patterns, while minimizing activation of cell types carrying confounding information. However the spatial organization in the mouse AC, is not absolutely strict(Bandyopadhyay et al., 2010;

Rothschild et al., 2010), especially for more complex features, as for example temporal modulations (Deneux et al., 2016; Kuchibhotla and Bathellier, 2018). Thus, fine scale stimulation methods (Packer et al., 2015)implemented at a sufficiently large scale 380 would be necessary to precisely interfere at AC level with the discrimination of sounds that only differ based on complex, non-spectral features, and thereby eventually construct more precise artificial auditory perceptions. The fact that the AC pathway is dispensable for simple discriminations suggests that auditory judgements, and potentially perception, result from the interplay between a coarse description of sensory inputs and a time-integrated, more elaborate description that involves AC. As we showed by attempting to drive auditory judgments directly at the cortical level (Figure 2-5), the coexistence of these pathways is a critical issue to manipulate auditory perception. It might thus be advantageous to combine stimulations of cortical and sub-cortical (Guo et al., 2015) levels in order to improve the quality of artificially generated perception in the central auditory system.

# 2.5. Material and methods

## 2.5.1. Experimental model and subject details

We used the following mouse lines: PV-Cre (Jax # 008069) x Ai27 (flex-CAG-hChR2-tdTomato; Jax # 012567), for optogenetic inactivation, Emx1-IRES-Cre (Jax #005628) x Ai27 (Jax # 012567) for optogenetic activation, and C57Bl6J for lesion experiments. In all experiments, young adult females and males between 8 to 16 weeks old were used. Animals were housed 1–4 animals per cage, in normal light/dark cycle (12 h/12 h). All procedures were in accordance with protocols approved by the French Ethical Committee (authorization 691 00275.01).

## 2.5.2. Behavioral experiments

Behavior was monitored and controlled using an homemade software (Elphy, G. Sadoc, UNIC, France) coupled to a National Instruments card (PCIe-6351). Sounds were amplified (SAI Stereo power amp, Tucker-Davis Technologies) and delivered through high frequency loudspeakers (MF1-S, Tucker-Davis Technologies) in a pseudo-random sequence. Water delivery (5–6 µl) was controlled with a solenoid valve (LVM10R1-6B-1-Q, SMC). A voltage of 5V was applied through an electric circuit joining the lick tube and aluminum foil on which the mouse was sitting, so that lick events could be monitored by measuring voltage through a series resistor in this circuit. Before starting the training procedure, mice were water restricted for two consecutive days. The first day of training consisted of a habituation period for head fixation and 703 to reliably receive water by licking the lick port without any sound. After this period, S+ training was conducted for 2 or 3 days where S+ trials were presented with 80-90% probability, while the remaining trials were blank trials (no stimulus). A trial consisted of a random inter-trial interval (ITI) between 6 and 8 seconds to avoid prediction of stimulus appearance, a random 'no lick' period between 3 and 5 seconds and a fixed response window of 1.5 seconds. Licking during the response window on an S+ trial above lick threshold (3-5 consecutive licks) was scored as a 'hit' and triggered immediate water delivery. No licks was scored as a 'miss' and the next trial immediately followed. Each behavioral session contained ~150 rewarded trials allowing mice to obtain their daily water supply of ~800 µl. At the beginning of each session, ~20 trials with 'free rewards' were given

independent of licking to motivate the mice. When animals reached more than 80% 'hits' for the S+ stimulus, the second sound (S-) was introduced, and the lick count threshold was set to 5 licks (in a few PTvsPT experiments, only 3 licks). During presentation of the S+ sound, licking below threshold was considered as a 'correct rejection' (CR) and the next trial immediately followed, licking above threshold on S- trials was considered as a 'false alarm' (FA), no water reward was given, and the animal was punished with a random time out period between 5 and 7 seconds. Each session then contained 300 trials with 50% probability for each trial type. Sounds of 0.2 seconds at 60 dB were used for the PT vs PT task and sounds of 0.5 seconds at 70 dB for the FM vs PT task. During the entire behavioral training period, food was available ad libitum and animal weight was monitored daily. Water restriction was interleaved with a 12h ad libitum supply overnight every Friday.

### 2.5.3. Behavior analysis.

Learning curves were obtained by calculating the fraction of correct responses over blocks of 10 trials. Discrimination performance over one session was calculated as (hits + correct rejections)/total trials. Discrimination time was calculated on collections of10 trial blocks in which the discrimination performance 728 was greater than or equal to 80%, containing a total of at least 100 trials. The licking signal for each stimulus was binned in 10 ms bins, and for every time bin, we used the non-parametric Wilcoxon rank sum test to obtain the p-value for the null hypothesis that the licking signal was coming from the same distribution for S+ and S-. The discrimination time was determined as the first time bin above a p-value threshold of 0.01 while applying the Benjamini-Hochberg correction for multiple testing over all time bins.

### 2.5.4. Cranial window implantation.

To allow chronic unilateral access to AC (for 2-photon calcium imaging or electrophysiology), a cranial window was incorporated into the skull and a metal post for head fixation was implanted on the contralateral side of the craniotomy. Surgery was performed in 4 to 6 week old mice placed on a thermal blanket under anesthesia using a mix of ketamine (Ketasol) and medetomidine (Domitor) (antagonized with atipamezole - Antisedan, Orion pharma at the end of the surgery). The eyes were covered using Ocry gel (TVM Lab) and Xylocaine 20mg/ml (Aspen Pharma) was injected locally at the site where the

incision was made. The right masseter was partially removed and a large craniotomy (~5 mm diameter) was performed above the AC using bone sutures of the skull as a landmark. For 2P calcium imaging, we did 3 to 5 injections (~300 µm separation) of 200nL (35 nl/min) using pulled glass pipettes of rAAV1.syn.GCamP6s.WPRE virus diluted 10 times (Vector Core, Philadelphia, PA, USA). After this, the craniotomy was immediately sealed with a 5 mm circular cover slip using cyanolite glue and dental cement (Ortho-Jet, Lang). For AC inactivation experiments with optogenetics, the same procedure was repeated on both brain hemispheres in a single surgery. For inferior colliculus inactivation experiments, the 5mm cranial window was placed on the midline such that it covered the dorsal part of both hemispheres of the inferior colliculus. In all cases, mice 752 were subsequently housed for at least one week without any manipulation.

### 2.5.5. Optogenetics inactivation of AC during behavior.

For optogenetic inactivation experiments, mice were first trained to respond to the S+ stimulus alone (see Behavior), then when the S- stimulus was introduced for discrimination training, a pair of blue LEDs (1.1W, PowerStar OSLON Square 1+, ILS, wavelength 455nm) was placed 2 cm above their head, facing each other at 1 cm distance, and were flashed 1 over 5 trials for visual habituation of the animal to light flashes (initially inhibiting licking). When discrimination performance was above 80% and similar both with and without light flashes, one to three test sessions were performed in which the LEDs were either placed on the bilateral AC cranial windows, or on the inferior colliculus window (1 LED only). Stimulus presentation was pseudo-randomized over blocks of 100 trials and light flashes appeared in 1 out of 5 trials for each stimulus with the same reward or punishment conditions as regular trials. Blue light delivery followed a square wave (20Hz) time course and started 100ms before onset lasting for 700ms (sound duration was no longer than 500ms). Light intensity at the brain surface was measured to be 36 mW/mm2. Discrimination performance was computed as the number of hits and correct rejections over the total number of trials, separating trials in which the LED was turned ON or OFF.

### 2.5.6. Patterned optogenetics during ongoing behavior.

For patterned optogenetic activation in the mouse AC, we used a LED-based video projector (DLP LightCrafter, Texas Instruments) tuned at 460 nm. To project a two-dimensional image onto the

ACsurface (Figure 2-2 and Figure 2-4), theimage of the micromirror chip was collimated through a 150 mm cylindrical lens (Thorlabs,diameter: 2 inches) and focused through a 50 mm objective (NIKKOR, Nikon). Light collectedby the objective passes through a dichroic beam splitter (long pass, >640nm, FF640-FDi01,Semrock) and is collected by a CCD camera 777 (GC651MP, Smartek Vision) equipped with a 50 mm objective (Fujinon, HF50HA-1B, Fujifilm). For discrimination of artificial AC patterns, two disks of 400 µm were placed at two different locations in AC. The first disk was defined as the S+ stimulus and systematically located at the center of the low frequency domain in AI.The second disk, defined as the S- stimulus was placed at the center of the high frequency domain in the UF obtained with intrinsic imaging (Figure 2-11, see Intrinsic Imaging below).Alignment of optogenetic stimulus locations across days was done using blood vessel patterns at the surface of the brain with a custom made GUI in Matlab. In short, a reference blood vessel image was taken at the beginning of the experiment. In subsequent days, a new blood vessel image was taken and aligned to the reference image by optimizing the image cross-correlation to obtain the appropriate rotation and translation matrix. Behavioral training with optogenetic stimuli was done with the same protocol as for sounds.For focal AC activation during sound discriminations, a grid of 15 to 17 locations was constructed using disks of ~400 µm distributed in 5 rows. The grid was aligned to AC for each animal using the three regions of maximal responses in the intrinsic imaging response map to a 4 kHz pure tone (see Intrinsic Imaging) as a reference for horizontal position and orientation. Each grid was constructed to maximize the coverage of the different frequency domains and tonotopic subfields seen in intrinsic imaging (seeFigure 2-4). To probe responses to optogenetic perturbation during discrimination behavior we performed test sessions of 300 pseudo-randomized trials in which 45 to 54 trials were non-rewarded catch trials with stimulation of a grid location together with the S- sound. Sound (4 kHz, 500 ms at 70dB) and light (12 mW/mm2, 1 s duration, square wave intensity profile at 20 Hz) started at the same time. In two animals, we performed test sessions in which 50% of the catch trials were rewarded if the animals licked above lick count threshold (5 licks). These two animals had also a non-reversible lesion of the contralateral AC, but we noticed in another set of experiments (notshown) that contralateral lesions did not significantly 802 increase response probability to AC perturbations. Responses to focal optogenetic perturbations were computed over 3 catch trial repetitions. The significance of these responses was assessed by computing the distribution of lick count responses over 10,000 random triplets of responses to S- alone. The p-value of the response to a particular optogenetic stimulation location was taken as the percentile of this distribution corresponding to the trial-averaged lick count for the optogenetic stimulation. Based on the pvalues computed for all

grid locations, we performed a Benjamini-Hochberg correction for multiple testing to identify the locations with a significant response at a false positive rate of 0.05. For display, lick count responses L to optogenetic perturbations were normalized for each mouse as (L-s-)/(s+ - s-), where s+ and s- are the mean lick counts observed for S+ and S- stimuli. Maps of response to optogenetic perturbation were aligned across different mice, by matching the grid locations placed on the 4kHz landmarks, calculating the best rotation and translation matrix as for alignment of the intrinsic imaging maps (see Intrinsic Imaging). To account for the actual spread of the optogenetic stimulus in the AC network, the response at each location was represented by a two-dimensional spatial profile identical to the estimated profile shown in Figure 2A for 12 mW/mm2 focal stimuli. Profiles of all significant locations were summed to construct the maps (Figure 2-4F).

### 2.5.7. In vivo electrophysiology.

Recordings for calibration of optogenetics were done in mice implanted already with a cranial window above AC for at least 2 or 3 weeks. On the day of the recording, the mouse was briefly anesthetized (~30 min, ~1% isoflurane delivered with SomnoSuite, Kent Scientific) to remove some of the cement seal and a piece of the cover slip of the cranial window was cut using a diamond drill bit. The dura was resected ventral to AC as previously delimited using intrinsic imaging (see methods below). The area was covered with Kwik-CastTM silicon (World precision 827 instruments) and the animal was placed in his home cage to recover from anesthesia for at least 1 hour before head-fixation in the recording setup (same as used for behavior). All recordings were performed using four shank Buzsaki32 silicon probes (Neuronexus). Before each recording, the tips of the probe were covered with DiI (Sigma). The silicon was gently removed and the area cleaned using warm Ringer's buffer. The probe was inserted at a ~30° angle with respect to brain surface with a micromanipulator (MP-225, Butter Instrument) at 1-2 µm per second, with pauses of 1-2 minutes every 50 µm. Each recording session time, including probe insertion and removal, lasted no more than 3 hours. After the experiment, the animal was deeply anesthetized (isoflurane) and euthanized by cervical dislocation. Brains were fixed overnight by 4% paraformaldehyde (PFA) in 0.1 M phosphate buffer (PB). Coronal brain slides of 80 µm were prepared and imaged (Nikon eclipse90i, Intensilight, Nikon) to identify the electrode track tagged with DiI and determine recordingdepth. For calibration of optogenetic inactivation experiments, sounds played during the recordings included a blank, 4, 4.5, 4.7, 5, 6, 8, 16 kHz pure tones of 200 ms duration at 60 dB, 4 kHz 500

ms pure tone at 70 dB, 4 to 12 kHz 500 ms frequency modulated sound at 70 dB and white noise ramps of 1000 ms from 60 to 85 dB and 85 to 60 dB. The same blue directional LED (24° light cone) as used for inactivation during behavior was placed above the cranial window, however at a slightly higher distance (about 0.75 cm) of the window to leave space for the electrode. Light was delivered for 700 ms, starting 100 ms before sound onset. Silicon probe voltage traces were recorded at 20 kHz and stored using RHD2000 USB interface board (Intan Technologies). Raw voltage traces were filtered using a Butterworth high-pass filter with a 100 Hz cutoff (Python). Electro-magnetic artefacts from the LED driving current were removed by subtracting a template calculated across all LED ON trials. For calibration of focal optogenetic activations, we used a grid of contiguous 8x5 400 µm circles. Each location was played randomly and repeated 10 times. Also, a 4 kHz pure tone of 500 ms at 70 dB, 4-12 kHz FM sound of 500 ms at 70 dB and white noise ramps 852 of 1000 ms from 60 to 85 dB and 85 to 60 dB were played to compare later with optogenetic responses.

### 2.5.8. Analysis of electrophysiology.

Spikes were detected and sorted using the KlustaKwik spike sorting algorithm (Harris et al., 2000) (Klusta, https://github.com/kwikteam/klusta) with a strong and weak threshold of 6 and 3 respectively. Each shank was sorted separately where putative single units were visualized and sorted manually using KlustaViewa. Data analysis was done using custom Python scripts. Spikes were binned in 25 ms bins. Firing rates during stimulation periods were calculated by averaging across trials. For AC inactivation, significant responses to at least one sound were identified using the Kruskal-Wallis H-test for independent samples and the Benjamini-Hochberg procedure was applied to correct for multiple testing across units ($p < 0.05$). Percentage of inhibition was calculated as follows: $100 – (L * 100/ S)$, where S corresponds to best sound response and L to the response to the same sound during optogenetic activation of PV interneurons. To estimate the robustness of sound representations in our recordings, we trained a linear Support Vector Machine classifier to discriminate two sounds based on single unit responses binned in 50 ms bins. Only units that were inhibited by light (putative PV-negative cells) were used to train the classifier. To evaluate classification performance without optogenetics, the classifier was trained over 5 trials for each pair of sounds and tested with other 5 trials. To test the effect of light on sound responses, the classifier was trained with 10 unperturbed sound delivery trials and tested with 10 sounds and light delivery trials. For focal optogenetic activations, we calculated for each single unit

the trial-averaged firing rate change with respect to baseline over the 1s optogenetic stimulation for all locations, yielding two-dimensional spatial response maps. Using the centers of each location, a 2D map was created for each unit and fitted with two-dimensional Gaussian model.

### 2.5.9. Auditory cortex lesions and immunohistochemistry.

Mice after learning a PT vs PT discrimination task were anesthetized (~1.5% isoflurane delivered with SomnoSuite, Kent Scientific) and placed on a thermal blanket. Craniotomies were performed as described above and focused thermo-coagulation lesions were done bilaterally. The area was then covered using Kwik-Cast silicon (World precision instruments) and closed with dental cement (Ortho-Jet, Lang). After a period of recovery on a heating pad with accessible food pellets, mice were taken back to their home cage and a nonsteroidal anti-inflammatory agent (Metacam®, Boehringer Ingelheim) was injected intramuscularly. To test if mice could still perform the discrimination task, they were placed on the behavioral setup the next day after surgery. If a mouse presented signs of pain, liquid meloxicam was given in drinking water or via subcutaneous injection. Discrimination was tested in a normal session and performance calculated as previously described. After the experiment, mice were transcardially perfused with saline followed by 4% paraformaldehyde (PFA) in 0.1 M phosphate buffer (PB) and then brains post-fixed overnight at 4 °C. After washing with phosphate-buffered saline (PBS), brains were cut in 80 µm coronal slides and immuno-histochemical reactions were performed on free-floating brain slices as follows. Slides were blocked for 2 h using PBS + 10% goat serum and 1% Triton-X 100 at room temperature. After washing in PBS (10min×3), the sections were incubated 2h at room temperature with a dilution 1:100 of mouse anti-NeuN conjugated with Alexa Fluor® 488 (MAB377X, Merck). Slides were washed and mounted for imaging using a Nikon eclipse 90i microscope (Intensilight, Nikon).

### 2.5.10. Intrinsic imaging and alignment of tonotopic maps across animals.

Intrinsic imaging was performed to localize AC in mice under light isoflurane anesthesia (~1% delivered with SomnoSuite, Kent Scientific) on a thermal blanket. Images were acquired using a 50 mm objective (1.2 NA, NIKKOR, Nikon) with a CCD camera (GC651MP, Smartek Vision) equipped with a 50 mm objective (Fujinon, HF50HA-903 1B, Fujifilm) through a cranial window implanted 1-2 weeks before the experiment (4-pixel binning, field of view between 3.7 x 2.8 mm or 164 × 124 binned pixels, 5.58-µm

pixel size, 20 fps). Signals were obtained under 780 nm LED illumination (M780D2, Thorlabs). Images of the vasculature over the same field of view were taken under 480 nm LED illumination (NSPG310B, Conrad). Two second sequences of short pure tones at 80 dB were repeated every 30 seconds with a maximum of 10 trials per sound. Acquisition was triggered and synchronized using a custom made GUI in Matlab. For each sound, we computed baseline and response images, 3 seconds before and 3 seconds after sound onset, respectively. The change in light reflectance $\Delta R/R_o$ was calculated over repetitions for each sound frequency (4, 8, 16, 32 kHz, white noise). Response images were smoothed applying a 2D Gaussian filter ($\sigma$ = 3 pixels). The different subdomains of AC corresponding to the tonotopic areas appeared as regions with reduced light reflectance. To align intrinsic imaging responses from different animals, the 4 kHz response was used as a functional landmark. The spatial locations of maximal amplitude responses in the 4 kHz response map for the AI, A2 and AAF (three points) was extracted for each mouse and a Euclideantransformation matrix was calculated by minimizing the sum of squared deviations (RMSD) for the distance between the three landmarks across mice. This procedure yielded a matrix of rotation and translation for each mouse that was applied to compute intrinsic imaging responses averaged across a population of mice.

### 2.5.11. Two-photon calcium imaging.

Two-photon imaging during behavior was performed using a two-photon microscope equipped with an 8 kHz resonant scanner (Femtonics, Budapest, Hungary) coupled to a pulsed Ti:Sapphire laser system (MaiTai DS, Spectra Physics, Santa Clara, CA). The laser was tuned at 900 nm during recordings and light was collected through a 20x (XLUMPLFLN-W) or 10x (XLPLN10XSVMP) Olympus objective. Images were acquired at 31.5 Hz. For each behavioral trial, imaging duration 928 was 7s with a pause of 5s in between trials. Sound delivery was randomized during the trial to prevent mice from starting licking with the onset of the sound (45 dB SPL) emitted by the microscope scanners at the beginning of each trial. All sounds were delivered at 192 kHz with a National Instruments card (NI-PCI-6221) driven by homemade software (Elphy, G. Sadoc, UNIC, France), through an amplifier (SAI Stereo power amp, Tucker-Davis Technologies) and high frequency loudspeakers (SAIand MF1-S, Tucker-Davis Technologies, Alachua, FL). During the active context mice performed the discrimination task, a regular session consisted in ~250 trials, followed immediately after by a passive context session with ~150 trials (lick tube was withdrawn). Data analysis was performed using Matlab and Python scripts. Motion artifacts were first corrected

frame by frame, using a rigid body registration algorithm. Regions of interest (ROIs) corresponding to the neurons were selected using Autocell a semi-automated hierarchical clustering algorithm based on pixel covariance over time (Roland et al., 2017). Neuropil contamination was subtracted (Kerlin et al., 2010) by apply the following equation: Fcorrected (t)= Fmeasured (t) – 0.7 Fneuropil (t), where Fneuropil (t) is estimated from the immediate surroundings (Gaussian smoothing kernel, excluding the ROIs (Deneux et al., 2016), □ = 170µm). Then the change in fluorescence (ΔF/F0) was calculated as (Fcorrected (t) - F0) / F0, where F0 is estimated as the 3rd percentile of the low-pass filtered fluorescence over ~40 s time windows period. To estimate the time-course of the firing rate, the calcium signal was temporally deconvolved using the following formula: r(t) = f'(t) + f(t) / τ in which f' is the first time derivative of f and τ the decay constant set to 2 seconds for GCaMP6s. In total 7605 neurons were recorded across active and 11 passive sessions in 3 mice. We kept for analysis only 1008 neurons significantly responding to the S+ or S- stimuli with respect to baseline activity (Wilcoxon rank-sum test, p = 0.01 and Bonferroni correction for multiple testing). The deconvolved signals where smoothed with a Gaussian kernel (α = 33ms). To estimate the discriminability of two sounds based on cortical popul 953 ation responses, linear Support Vector Machine classifiers were trained independently on each time point to discriminate population activity vectors obtained from halfof the presentations of each sound and context (training set), and were tested on activity vectors obtained on the remaining presentations of the same sounds and context or on all presentationsof sounds in the non-trained context (test sets). To estimate behavioral categorization of sounds based on population activity in AC, we trained linear SVM classifier to discriminate AC responses to single presentations of the trained target sounds, and tested the classifiers with AC responses in single presentations of the non-trained sounds. Classification results were averaged across presentations to generate the categorization probability.

### 2.5.12. Quantification and statistical analysis

All quantification and statistical analysis were performed with custom Matlab or Python scripts.Statistical assessment was based on non-parametric tests reported in figure legends together with the mean and SEM values of the measurements, the number of samples used for the test and the nature of the sample (number of neurons, recording sessions or mice). A custom bootstrap test (see Methods) was used for identification of optogenetic stimulation locations producing a behavioral effect. Unless otherwise mentioned, false positive rates below 0.05 were considered significant and the Benjamini-Hochberg

correction for multiple testing was applied for repeated measurements in the experiments. In all analyses, all subjects who underwent a particular protocol in the study were included. For small groups, a minimum of 4samples in each compared group was used to allow significance detection by standard non-parametric tests (*e.g.* Wilcoxon ranksum test).

### 2.5.13. Data and software availability

All data and analysis code are available from the corresponding author upon reasonable request.

## 2.6. Acknowledgements

We thank A. Chédotal, D. DiGregorio, Y. Frégnac, J. Letzkus and E. Harrell for comments onthe manuscript, G. Hucher for histology and the GENIE Project, Janelia Farm Research Campus, Howard Hughes Medical Institute, for GCAMP6s constructs. This work was supported by the Agence Nationale pour la Recherche (ANR "SENSEMAKER"), the Fyssen foundation, the Human Brain Project (WP 3.5.2), the DIM "Region Ile de France", the Marie Curie Program (CIG 334581), the International Human Frontier Science Program Organization (CDA-0064-2015), the Fondation pour l'Audition (Laboratory grant), the European Research Council (ERC CoG DEEPEN), the DIM Cerveau et Pensée and Ecole des Neurosciences de Paris Ile-de-France (ENP, support to SC).

## 2.7. Author contributions

BB, ZP and **SC** designed the study. BB, AD and **SC** performed behavioral experiments. BB andJB performed inferior colliculus surgeries. **SC** and ZP performed cortical activation experiments. **SC** and BB analyzed the data and wrote the manuscript with comments from all authors.

## 2.8. Supplementary figures

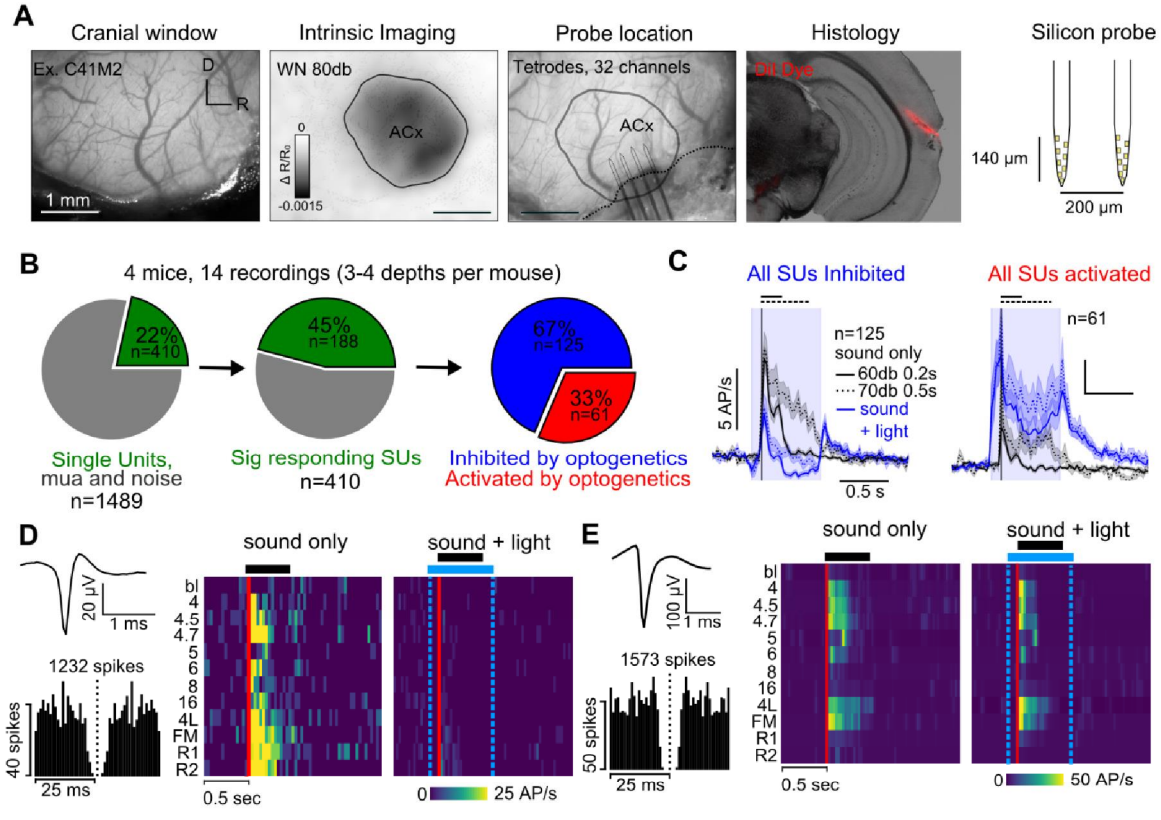


**Figure 2-8. PV interneuron activation strongly perturbs AC responsesto sounds.**

(A) To localize AC during calibration experiments, the white noise intrinsic imaging responsemap (middle left), was used to target probe insertion. The cover slip of the window wasslightly broken and removed, allowing the insertion of the probe into the exposed brain(middle right, see dashed line indicating glass border). At the end of the recording, the animalwas perfused, and histology was done to track probe location and depth using fluorescent dyeDiI. (B) Left, Fraction of single units identified as spike clusters obtained using theKlustaKwik spike sorting algorithm which displays a clear refractory period in their spike train autocorrelogram (example in D). Middle, Fraction of single units that significantlyrespond to sounds (see Methods). Right, Fraction of sound-responsive cells that are activated(red) or inhibited (blue) by light-gated PV activation. (C). Time course of mean firing rateacross all single units in response to PTs of 0.2s at 60db (black line) and to the 0.5s long 4kHz and 4-12kHz chirp at 70dB (black dashed line). In blue are shown the responses to the samesound groups but during PV interneuron activation. (D) Example of a single unit for whichsound responses were inhibited by light. Left, Mean spike waveform (electrode site withlargest amplitude) and spike train autocorrelogram for this unit. Right, Heat map of

meanfiring rate in response to sounds (average over 10 trials for each sound) during sound andsound + light trials. The solid red line corresponds to sound onset. Dashed blue linescorrespond to light onset and offset. E. Same as D but for a cell which is not inhibited byoptogenetic activation of PV neurons.

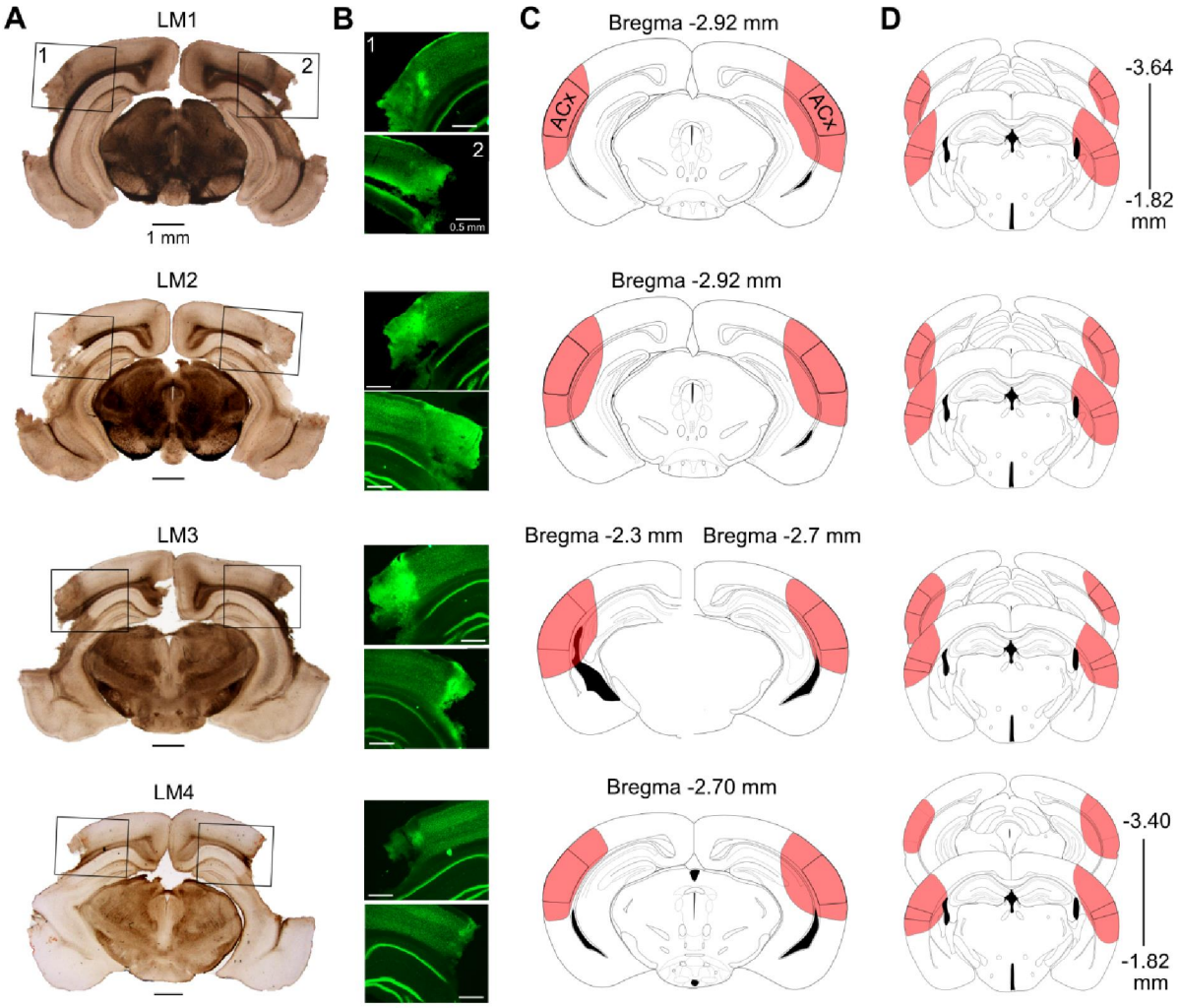


**Figure 2-9. Irreversible lesions covered the full extent of auditory cortex.**
(A). Bright-field images of coronal brain slices showing the extent of bilateral lesions for the four animals shown in Figure 2G. (B). Epifluorescence images of identified cortical neurons (NeuN staining) for the two areas delimited by the black squares in A. Punctate NeuN staining indicates intact cell bodies outside of the lesion. The absence of a punctate pattern on the tissue bordering the lesion indicates that the cortical network was damaged in this zone, which was thus included into the lesioned area in our quantification. (C) Coronal slide reconstruction modified from the mouse brain atlas (Paxinos and Franklin, 2004) showing the location and extent of the lesion (red shading) with respect to AC (more intense black

contour) at the anteroposterior location corresponding to the center of AC along this axis. The anteroposterior coordinates from bregma and AC location are indicated for each section. (D) Same as C but for the anteroposterior locations corresponding to anterior and posterior limits of AC. Overall our reconstructions show that primary and secondary auditory cortex were fully lesioned for all four animals.

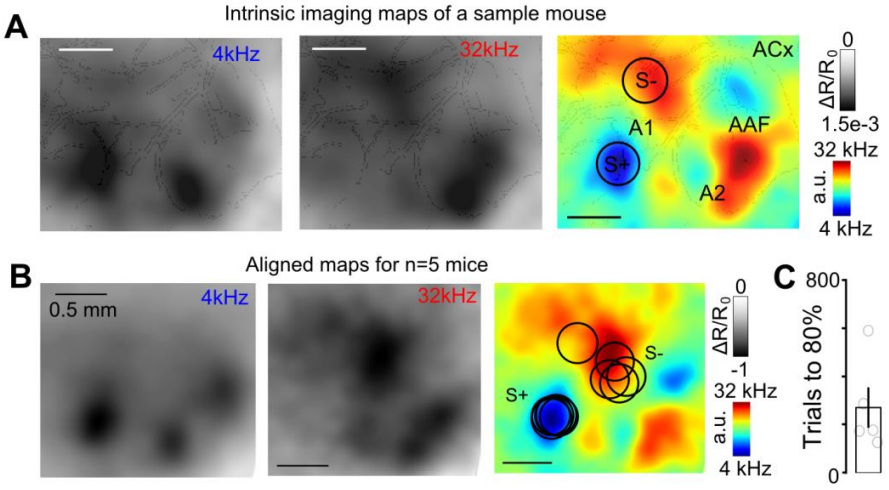


**Figure 2-10. Discriminated artificial optogenetic stimuli were located insimilar tonotopic locations across mice.**

(A) Intrinsic imaging response maps to 4 kHz and 32 kHz pure tones, on the right the maintonotopic fields are revealed by plotting the difference of 4 kHz and 32 kHz response maps.AI; primary auditory cortex, A2; secondary auditory cortex, AAF; anterior auditory field. UF;ultrasonic field. Circles correspond to the optogenetic stimulus locations shown used to driveartificial discrimination behavior in this mouse. (B) Aligned intrinsic imaging responses to 4kHz and 32 kHz pure tones averaged across five mice. The resulting difference map is shown on the right. The optogenetic stimulus locations for the same five animals are superimposed asblack circles. (C) Mean number of trials to reach 80% performance. Empty circles correspondto single animals and the bars to mean and SEM.

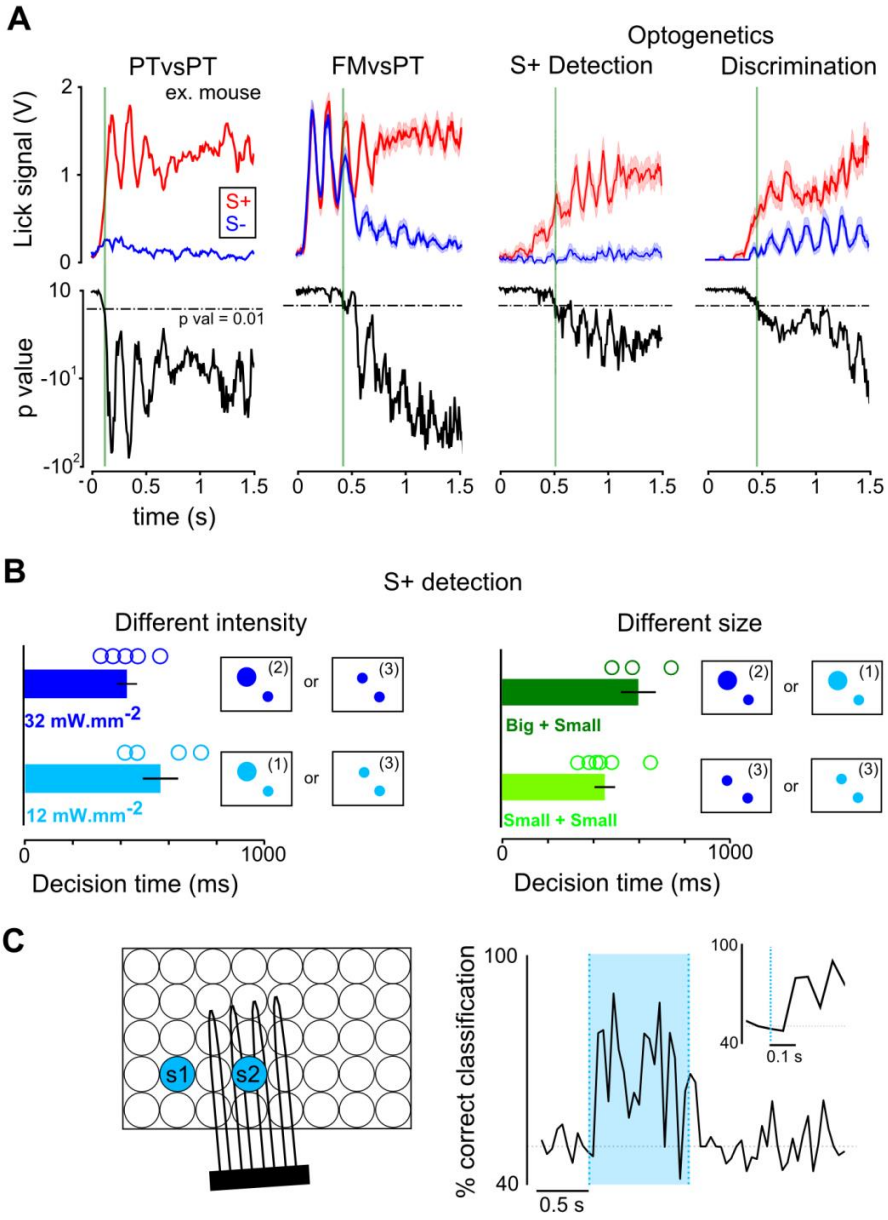


**Figure 2-11. Reaction time for detection of a single focal cortical stimulus is similar to discrimination time for choosing between two focal cortical stimuli.**

(A) Top, Time course of averaged lick traces for each stimulus in one example mouse for the two sound discrimination tasks and for detection and discrimination of optogenetic stimuli. Bottom, p-values for the null hypothesis that S+ and S- lick signals come from the same distribution obtained for every time point (Wilcoxon rank-sum test). Green lines indicate the first significant time point corresponding to discrimination time. (B) Reaction times of 8 mice for the detection of an optogenetic stimulus of different intensities (left, 12 vs 32 mW.mm-2) or of different sizes (right, two small disk vs one small disk + one large disk of doubled

diameter). Dark blue: 32 mW.mm-2 (n= 4 mice). Light blue: 12 mW.mm-2 (n= 4 mice). Dark green: larger stimulus (n= 3 mice). Light green: smaller stimulus (n= 5 mice). (C) Left, Sketch of the silicon probe location and grid indicating the two spots used to train an SVM classifier.Right, Performance of an SVM classifier trained for each time bin of 50 ms to discriminatebetween single unit population responses (n=8 neurons showing significant spatiallymodulated optogenetic activation for light intensity 12mW/mm-2) of two optogeneticstimulations separated by approximately same distance as optogenetics stimuli used to train 5 mice during the discrimination task (~800 µm; stimuli used are the location of peak response for each neuron and another ~800 µm distant location). The classifier was trained with asubset of 5 trials and tested on 5 different trials. Inset shows a magnification around stimulusonset indicating that discrimination is achieved between 50 and 100 ms from stimulus onset.

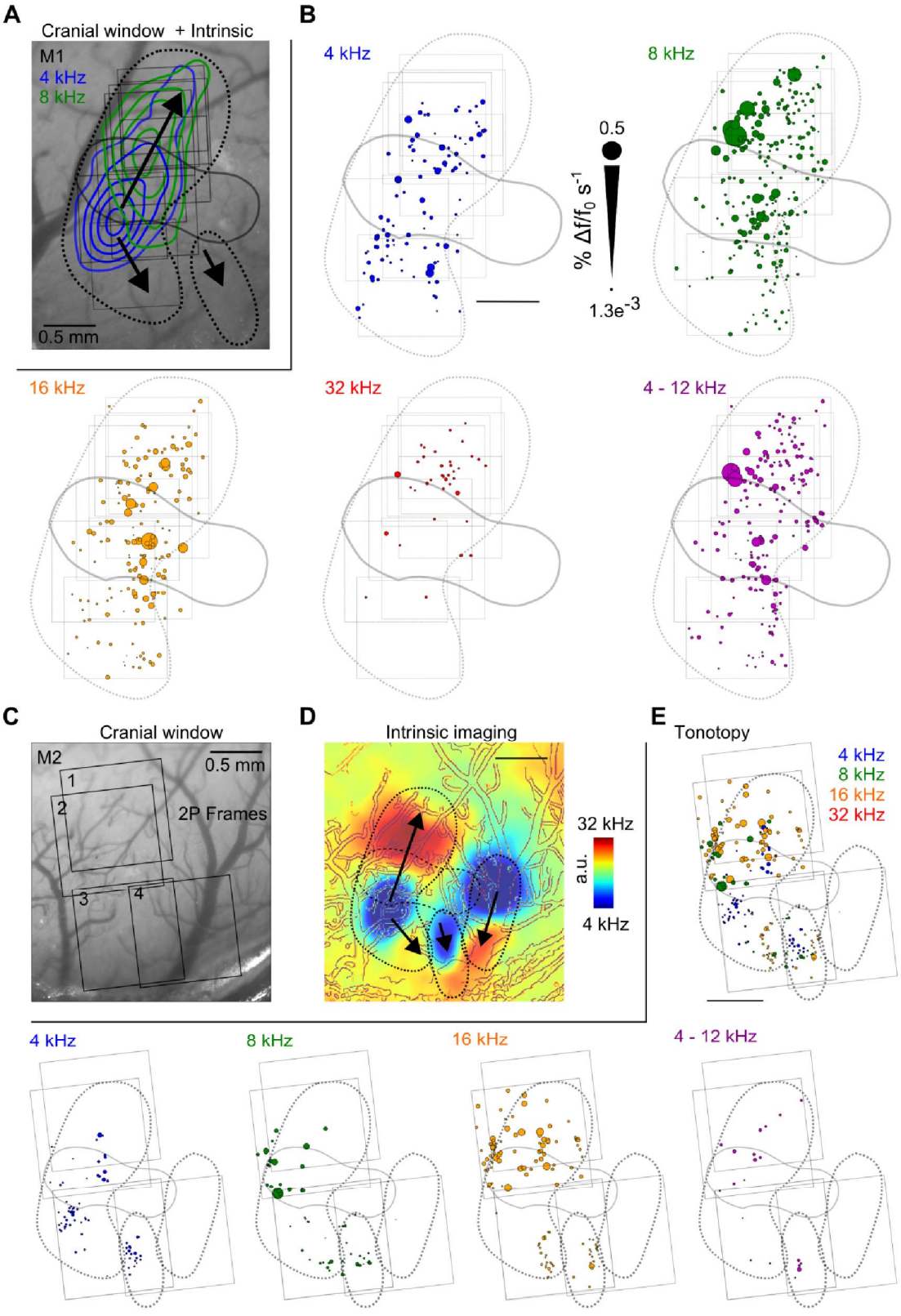
A
Cranial window + Intrinsic
M1
4 kHz
8 kHz
0.5 mm
B
4 kHz
8 kHz
0.5
% Δf/f0 s-1
1.3e-3
16 kHz
32 kHz
4 - 12 kHz
C
Cranial window
M2
0.5 mm
1
2
3
4
2P Frames
D
Intrinsic imaging
32 kHz
a.u.
4 kHz
E
Tonotopy
4 kHz
8 kHz
16 kHz
32 kHz
4 kHz
8 kHz
16 kHz
4 - 12 kHz

**Figure 2-12. Tonotopic maps from intrinsic and two-photon calcium imaging are similar.**

(A) Auditory cortex surface and localization of 2P calcium imaging field-of-view (light grey). Contour of intrinsic imaging responses to pure tones (4 kHz in blue and 8 kHz in green) and approximate tonotopics gradients (AI and A2) obtained from-- mean intrinsic imaging responses of 12 mice showed in Figure 2-6A (dashed black lines). Area of optogenetic stimulation that elicited behavioral responses showed in Figure 2-5H (black line). (B) 2P calcium imaging responses in same animal presented in A. Neurons displayed presented significant responses (Wilcoxon rank sums pval <0.01) to pure tones. Circles diameters are proportional to the mean deconvolved calcium response over 20 repetitions. (C) Auditory cortex surface and localization of 2P calcium imaging field-of-view of another example mouse (light grey). (D) Tonotopic gradients obtained by subtraction of the 4 and 32 kHz intrinsic response maps. (E) Top, 2P calcium imaging responses of field-of-views in C. Circles correspond to the localization of all significantly responding neurons. Color-code correspond to their preferred frequency over the same sounds used during intrinsic imaging experiments and size proportional to the mean deconvolved calcium response over 20 repetitions. Bottom, Same representation of 2P calcium imaging responses as B.

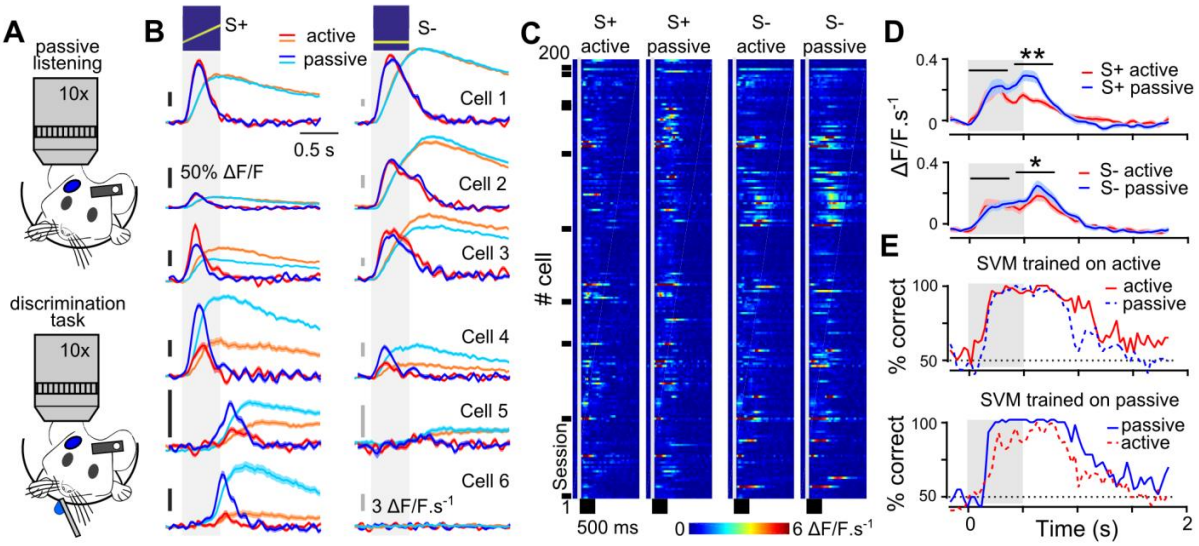


**Figure 2-13. Stability of AC sound representations despite context dependent modulations.**

(A) Sketch of 2-photon imaging during passive listening and discrimination behavior. (B) Traces of mean raw (light blue and orange) and deconvolved (blue and red) calcium signals for six example neurons. Cells 1 and 2 had similar responses in the active and passive states while cells 3 and 4 had boosted early responses in the active state and cells 5 and 6 diminished late responses during the active state (discrimination task). (C) Heatmap showing mean deconvolved calcium signal to S+ and S- during the two different contexts for the 200 most responsive neurons (11 imaging sessions, 3 mice) for either sound and context (ranked by their p-value for the Wilcoxon signed rank test, n = 63 trials). (D) Mean deconvolved signal for 1008 imaged neurons in response to S+ (top) and S- stimuli (bottom) during active and passive contexts. (E) Discrimination performance of an SVM classifier trained with neuronal population activity (1008 neurons) during active (top) and passive context (bottom) and tested with both contexts.

# 3. Results: Section II

In the last decades, learning theories have constantly evolved going far beyond the intuitive thinking of early models. Complexity comes with redundancy and increased reliability, but at the expense of parsimonious computer simulations (Witnauer et al., 2017). Early associative models of learning helped to explain a small category of cue-competition learning effects, but failed to account for more complex interactions such as latent inhibition or overshadowing recovery with CS-US association extinction. Revised versions of early models (*e.g.* Le Pelley, 2004), such as new theories based on attentional effects, have been important to address human and more complex animal learning observations. In parallel, adaptive network models and their more recent versions (deep neuronal networks) have evolved incredibly fast, being able to outperform humans in some tasks such as pattern recognition (Assael et al., 2016). The acceptance or rejection of models depends on how well they fit the available data and, at present, it is difficult to find one model that can fully integrate all the important principles of associative learning,such as similarity or generalization (Niv et al., 2015), reversal learning (*e.g.* Jarvers et al., 2016) and subject variability (*e.g.* Brown and Heathcote, 2003; Matzel et al., 2003). Although these models are useful to describe the establishment of associations between internal stimuli representations and reinforcement, it is also important to find the biological correlates and causal events that give rise to these associations and cue interactions. The following work followed the classical associative learning framework, in particular reinforcement learning, and investigated one of the most widely used but at the same time poorly understood parameter of most associative learning models, saliency.To probe the strong correlation of cortical recruitment with the saliency parameter, we used targeted cortical manipulations using modern optogenetics. Here we showed causally that differences in cortical recruitment for stimuli with similar detectability can largely affect learning strategy. Also, well-controlled cortically implanted stimuli were able to reproduce the well-known overshadowing effect, explaining how this cue interaction can emerge due to differences in neuronal recruitment for different trained stimuli.

# Cortical recruitment determines learning dynamics and strategy

**Sebastian Ceballo**[1], Jacques Bourg[1], Alexandre Kempf[1], Zuzanna Piwkowska[1,2], Aurélie Daret[1], Pierre Pinson[1], Thomas Deneux[1], Simon Rumpel[2] and Brice Bathellier[1,5]

[1] Paris-Saclay Institute of Neuroscience (NeuroPSI)

Department for Integrative and Computational Neuroscience (ICN)

Gif-sur-Yvette, France

[2] Present address: Institute Pasteur. Dynamic Neuronal Imaging Unit. Paris, France.

[3] Institute of Physiology, University Medical Center, Johannes Gutenberg University, Mainz, Germany.

* Corresponding author: brice.bathellier@unic.cnrs-gif.fr, phone: +33(0)169823408

*Published online the 1st Apr 2019 on Nature Communications*

doi: 10.1038/s41467-019-09450-0

## 3.1. Abstract

Salience is a broad and widely used concept in neuroscience whose neuronal correlates, however, remain elusive. In behavioral conditioning, salience is used to explain various effects, such as stimulus overshadowing, and refers to how fast and strongly a stimulus can be associated with a conditioned event. Here, we identify sounds of equal intensity and perceptual detectability, which due to their spectro-temporal content recruit different levels of population activity in mouse auditory cortex. When using these sounds as cues in a Go/NoGo discrimination task, the degree of cortical recruitment matches the salience parameter of a reinforcement learning model used to analyze learning speed. We test an essential prediction of this model by training mice to discriminate light-sculpted optogenetic activity patterns in auditory cortex, and verify that cortical recruitment causally determines association or overshadowing of the stimulus components. This demonstrates that cortical recruitment underlies major aspects of stimulus salience during reinforcement learning.

## 3.2. Introduction

Sensory stimuli can vary in their efficacy as a conditioned stimulus during behavioral conditioning. In classical conditioning, a well-known example is the so called “overshadowing” effect.When animals are trained to associate two simultaneously presented stimuli (historically a tone and a flash) to a specific unconditioned stimulus (e.g. foot-shock), it is often observed that, after training, the animal is conditioned more strongly to one stimulus than to the other (Kamin, 1967). In their theoretical work originally developed for classical conditioning, but later extended to operant conditioning, Rescorla and Wagner(1972) introduced the notion of salience to explain the overshadowing phenomenon. In their model, salience is a parameter affecting the speed at which a given stimulus is associated with the unconditioned stimulus. Thus, when behavior reaches maximal performance and learning stops, the more salient of the two stimuli has been associated more strongly with the unconditioned stimulus, leading to overshadowing. While this theory captures a number of phenomena and is the basis for important frameworks such as reinforcement learning (Dayan and Balleine, 2002; Sutton and Barto, 1998), the neural underpinnings of the salience parameter remain elusive.

Salience in this context is usually seen as the global amount of neural activity representing the stimulus, like in models of attentional salience (Desimone and Duncan, 1995; Itti and Koch, 2001; Li, 2002; Treue, 2003). This intuitively follows from the idea that if more spikes represent a stimulus, they can produce more synaptic weight changes, as expected from the firing rate sensitivity of typical learning rules(Bienenstock et al., 1982 ; Dayan and Abbott, 2001; Denève et al., 2017; Frémaux and Gerstner, 2016; Martin et al., 2000), and thus modulate more rapidly the relevant connections. However, this idea lacks direct causal experimental verification in a learning task. Moreover, other theories propose that salience could also be encoded in other parameters such as neuronal synchrony levels (Fries, 2015; Shamma et al., 2011; VanRullen, 2003; Womelsdorf and Fries, 2007), which could influence learning via the temporal properties of biological learning rules (Buschman et al., 2012; Cassenaer and Laurent, 2012; Gütig and Sompolinsky, 2006; Kopell et al., 2014; Lee et al., 2009). Thus, the neuronal correlate of stimulus salience is a key question with broad implications for learning theories.

Using auditory discrimination tasks of sounds with different global cortical response strengths, we show that cortical recruitment impacts learning dynamics (Bathellier et al., 2013; Gallistel et al., 2004) similarly to the salience parameter of a reinforcement learning model. To explore this result in more precise experimental settings, we trained mice to discriminate optogenetically-driven response patterns that elicit different levels of cortical activity. Using this paradigm, we directly demonstrate that cortical recruitment determines which part of a compound stimulus drives a learned association while "overshadowing" other parts of the stimulus. This validates a generic prediction of reinforcement learning models and causally establishes the role of cortical recruitment as a neuronal correlate of stimulus salience.

# 3.3. Results

## 3.3.1. Sounds with identical levels can recruit different activity levels

To investigate the relationship between stimulus salience and neuronal recruitment, we first aimed to identify sounds recruiting different amounts of cortical activity. A previous report has shown that complex sounds with different frequency content but equal duration and sound pressure level can recruit population responses of different sizes in cat auditory cortex(Wong and Schreiner, 2003). To test if a similar phenomenon exists in mice, which would then allow us to experimentally decouple recruitment from physical intensity, we chose three short, complex sounds (70ms duration) containing a large range of frequencies and temporal modulations, but normalized at equal mean pressure level (73dB SPL, Figure 3-1A). These sounds displayed different power spectra in the 10-30kHz range (Figure 3-1A) where the mouse ear is most sensitive (Hackett et al., 2011; Kanold et al., 2014; Zheng et al., 1999). We thus wondered if this discrepancy was affecting their detectability. To do so, we trained mice to lick on a water port after presentation of any of the three sounds randomly presented in the same task to obtain a reward (Figure 3-1B). We then measured response probability to decreasing intensity levels. All mice experience the three sounds in the same task. We observed that, for all sounds, response probability steadily decreased down to chance level as measured in the absence of sound (Figure 3-1C). Yet, no significant response difference was observed across the three sounds (Figure 3-1C), indicating

that the chosen 73dB SPL was at a comparable distance from the detection threshold for the three sounds.

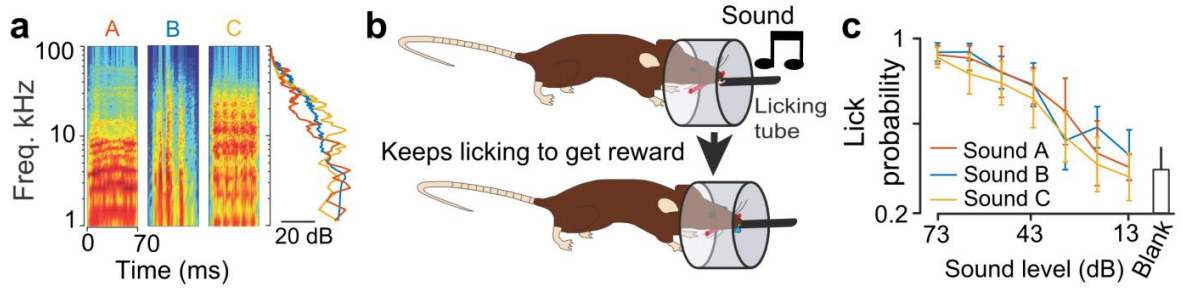


**Figure 3-1. Spectro-temporal differences in complex sounds do not affect near-threshold detectability**

(A) Spectrograms of three 70 ms long complex sounds, with power spectrum on right. (B) Schematics describing the auditory detection task. (C) Mean response probability for 6 mice trained to detect sounds A, B and C at 73 dB to get a reward and probed with lower sound intensities. While the effect of intensity was significant, there was no effect of sound identity (Friedman test, $p_{intensity} = 2.3\times10^{-9}$, $p_{sound} = 0.43$, n=6 mice). Error bars represent standard errors (SEM).

We assessed recruitment of neural activity in the auditory cortex (AC) in response to these three sounds using two-photon calcium imaging in awake, passively listening mice. We imaged 6 mice that were injected with AAV1-GCAMP6s virus in AC (Figure 3-2A). Recordings were followed by an automated image registration and segmentation algorithm(Roland et al., 2017) (Figure 3-2B) that allowed the isolation of 15,511 neurons across 27 imaging sites, from which large fluorescence signals could be observed (Figure 3-2C). The fields-of-view were either 0.5×0.5 or 1×1 mm (Figure 3-2A-B), allowing a rapid tiling of the full extent of primary and secondary auditory cortex (Figure 3-7). Cortical depths were randomly chosen ranging between 100 and 300 µm corresponding to layer II/III. The mouse AC (primary + secondary) contains approximately 200,000 neurons in one hemisphere (Herculano-Houzel et al., 2013) and thus about 50,000 neurons in layer 2/3, so we expect our sample of ~15,000 neurons to be representative for supragranular AC. Because typical learning rules are dependent on pre-synaptic firing rate (Bienenstock et al., 1982; Dayan and Abbott, 2001; Denève et al., 2017; Frémaux and Gerstner, 2016; Martin et al., 2000), we first measured the amplitude of the mean-deconvolved calcium signals, a proxy for neuronal firing rate (Yaksi and Friedrich, 2006), recorded across the entire duration of the response (Figure 3-2D). We observed that at 73 dB intensity, sound A elicited at least two-fold less

cortical activity than sounds B and C (Figure 3-2E). This was consistently observed across mice (Figure 3-7). Sounds producing more firing in the population activated also more neurons (~18% for sound A and ~25% for B and C, Figure 3-2E). But note that the fraction of responsive neurons strongly depends on statistical threshold. Furthermore, the observed differences in neuronal activity recruitment were consistent with previous, independent measurements performed under anesthesia (Figure 3-7). All three sounds elicited distinct response patterns as evaluated by correlation-based population similarity measures and sound identity could be decoded with high accuracy based on single-trial response patterns using linear classifiers (Figure 3-2F), indicating that sound discriminability was not affected by cortical recruitment. Another discrepancy between cortical recruitment and the physical intensity of a stimulus can be observed using sounds with different temporal intensity profiles. Up-ramping sounds elicit larger cortical responses in mice (Deneux et al., 2016) and other animals (Ghazanfar et al., 2002; Wang et al., 2014) than their time-symmetric down–ramps, despite equal physical energies. This effect correlates with asymmetries in subjectively perceived loudness in humans (Neuhoff, 1998). We confirmed this result for 2s white noise sounds ramping between 60 and 85dB, with a clear effect at sound onset despite the lower initial intensity level in up-ramps (Figure 3-2G). Rhythmic amplitude modulations provided another striking example, as we observed that a white noise sound modulated at 1 Hz produces more activity than when modulated at 20Hz, although the two sounds have the same physical energy (Figure 3-2H).

In summary, when different sounds are played above the detection intensity threshold, the amount of recruited cortical activity in mouse AC depends on factors other than intensity and can vary across different sounds. Based on this observation, we asked whether cortical recruitment could be related to stimulus salience in a learning task.

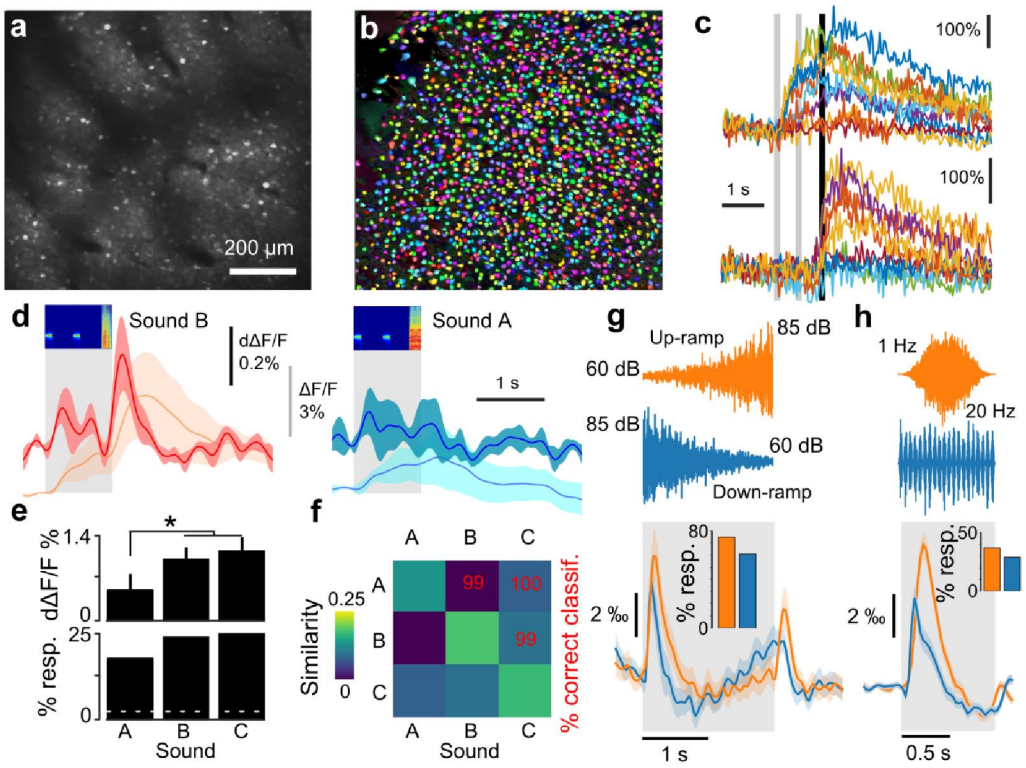


**Figure 3-2. Spectro-temporal differences impact on cortical recruitment.**

a.Example field of view illustrating GCAMP6s labeling of L2/3 auditory cortex neurons. b. Result of automated cell segmentation run on the data acquired in the example shown in a. c. Example single trial responses to sounds (different colors) for two neurons (top and bottom). Gray bars = sound duration. d. Population responses (n = 27 sessions, 15511 neurons in 6 mice) to Sound B (red) and A (blue). Both normalized fluorescence (light colors) and deconvolved (dark colors) calcium signals are shown. e. Mean deconvolved signal and fraction of significantly responding neurons to sounds A, B and C. Mean calcium responses to sound A (0.05 ± 0.03% $\Delta F/F.s^{-1}$, mean ± SEM) were significantly smaller than to B (0.10 ± 0.02% $\Delta F/F.s^{-1}$) and C (0.12 ± 0.02% $\Delta F/F.s^{-1}$ ; sign test, p = 0.0008 and p = 0.026, n = 27 sessions, 15511 neurons in 6 mice). Sound B and C also activated a larger fraction of neurons (24 and 25 % ; two-sided Signed testacross 20 sound repetitions, p<0.05) than A (18% ; $\chi^2$ test, p = $10^{-41}$ and $6\times10^{-31}$, n = 15511). f. Population response reliability (diagonal) and similarity (off-diagonal) matrix for sounds A, B and C. The pair-wise discriminability value, computed with a linear classifier is indicated in red. g. Mean deconvolved calcium signals for 6757 auditory cortex neurons in 12 awake mice during 29 calcium imaging sessions for 2 s long white noise sounds modulated in intensity between 60dB to 85dB upwards and downwards(mean between 0 and 0.5s after sound onset for up: 0.80 ± 0.08 % vs down: 0.62 ± 0.11 %, Signed test p =$3.75\times10^{-4}$, n = 29 sites, in 12 mice; mean between 0 to 2.5 s: 0.166 ± 0.58 % vs down: 0.157 ± 0.57 %, Signed test, p = 0.034). The inset show the significantly different ($\chi^2$ test, p = $10^{-68}$) fraction of responsive cells (75% and 61% ; two-sided Signed test, p<0.05). h. Mean deconvolved calcium signals for 59590 auditory cortex neurons in 7 awake mice during 60 calcium imaging sessions for white noise sounds modulated in intensity at 1

Hz and at 20 Hz (0.357 +- 0. 032 % and 0.15 +- 0.034 % $\Delta F/F.s^{-1}$, signed test, p = 0.0009). The inset show the significantly different ($\chi^2$ test, p = $10^{-189}$) fraction of responsive cells (37% and 29% ; two-sided Signed test, p<0.05). Error bars represent standard errors (SEM).

### 3.3.2. Cortical recruitment influences learning speed

Classically, relative salience measures are performed using an overshadowing paradigm in which two stimuli are conditioned together, as a compound stimulus, to an unconditioned stimulus. Then, salience is derived from the level of the conditioned response elicited by each stimulus component individually. While this approach is valid when the compound is made of stimuli from two different sensory modalities, two simultaneous sounds are likely to fuse perceptually, precluding measurement of their individual saliences with the classical overshadowing design (Brandon et al., 2000). Alternatively, Rescorla and Wagner's model postulates that learning speed follows stimulus salience. We thus decided to test if learning speed relates to cortical recruitment, using an auditory-cued Go/No-Go task. To do so, water-deprived mice were first trained to visit a lick-port and to receive a water reward if they licked after being presented with an S+ sound. The main effect of this pre-training phase was to raise motivation rather than to learn sound-reward association and thus could not be used to measure learning speed. When mice collected rewards in at least 80% of their port visits, the Go/NoGo task was started by introducing a non-rewarded S- sound in half of the trials (Figure 3-3A). After a large number of trials, mice succeeded to both sustain licking to the S+ and withdraw from licking for the S- (Figure 3-3B), demonstrating discrimination of the two sounds. Importantly, as typically observed in such tasks (Bathellier et al., 2013), the S+ sound was rapidly associated with the lick response and the rate limiting factor in task learning was to associate the suppression of licking with the S- sound (Figure 3-3B). Hence, learning speed depends more on the properties of the S- than of the S+ sound in this task. Discrepancies between two stimuli X and Y can thus be measured by comparing the learning speed of the X versus Y Go/NoGo discrimination when X is the S- against the speed observed when Y is the S-. For example, if X is less salient than Y, we expect learning to be slower when X is the S-. We therefore trained eight cohorts of mice to compare learning speed for sounds pairs A-B, A-C, B-C and for the pair of sinusoidaly modulated sounds. We also used learning speed data from an earlier study for discrimination of up and down-ramping sounds (Deneux et al., 2016). Plotting the population learning curves for the sound pairs with maximum cortical recruitment differences (A-B & A-C,), we qualitatively observed that the average

learning speed was faster when cortical recruitment for the S- sound was larger than for the S+ sound (Figure 3-3C), suggesting a link between learning speed and cortical recruitment.

However, looking at learning curves from individual mice, we noticed that the qualitative difference observed at the group level hides a more complex effect. As often observed in animal training (Gallistel et al., 2004) and as we previously reported for our task (Bathellier et al., 2013), most individual learning curves had a sigmoidal rather than exponential time course. Specifically, the curves displayed a delay phase with no increase in performance followed by a learning phase with a steep performance increase. Also, the duration of each phase was highly variable across animals as exemplified in Figure 3-3B. We wondered whether cortical recruitment was affecting one particular phase or both. Using sigmoidal fits (Figure 3-3B), we measured the delay phase duration as the number of trials necessary to reach 20% of maximal performance, and the learning phase duration as the number of trials necessary to go from 20% to 80% maximal performance. We observed across the five sound pairs tested that learning phase duration was systematically longer when the S- sound recruited less activity than the S+ sound (Figure 3-3D) and a non-parametric analysis of variance showed this effect to be highly significant across all mouse populations tested. No systematic effect of cortical recruitment was observed for the delay phase (Figure 3-3D, Figure 3-8). In addition, we noticed that cortical recruitment had also an effect on inter-individual variability. When the S- sound recruited more activity than the S+ sound, learning phase duration was more homogenous than for the opposite sound assignment, especially for the two sound pairs with a large difference of cortical recruitment (mean normalized standard deviation difference: 93% ± 18%, mean ± SEM, n = 5 sound pairs, p = 0.008 Wilcoxon rank-sum test, Figure 3-3D-E andFigure 3-8). Together, these results obtained over a total of 72 mice, indicated clear relationships between cortical recruitment and learning phase duration for the five pairs of sounds tested. It cannot be ruled out a priori that other, non-measured parameters of the sound representations could explain this dependency. Yet, in the hypothesis that these parameters would be randomly assigned to the tested sounds, the probability to obtain by chance a consistent result across five independent experiments would be only about 3% ($2^{-5}$), so we expect this eventuality to be rather unlikely.

### 3.3.3. A reinforcement learning model reproduces recruitment effects

To theoretically evaluate the generality of these results, whether they are predicted in detail by existing reinforcement learning models, we therefore tested a recent model of the discrimination task, extending the Rescorla-Wagner reinforcement learning framework to a simple but more biologically interpretable neuronal model (Figure 3-4A) (Bathellier et al., 2013). The model postulates that associative learning occurs by adjusting the synaptic weights between sensory and decision neural populations described by population firing rate variables. At the input, two populations are specific for the S+ and S- sounds respectively, which we denote as Ŝ+ and Ŝ-, and one population, Ĉ, which represents information common to S+ and S- trials (e.g. overlap between the S+ and S- representations or activity independent of sound, for example, related to visiting the lick port). Population Ĉ is an essential element of the model to reproduce high initial hit-rates during delayed discrimination learning (Bathellier et al., 2013). The decision population has two ensembles: one promoting and one inhibiting licking (Figure 3-4A). Adjustment of synaptic weights happens through a Hebbian learning rule modulated by Rescorla and Wagner's (1972) δ-rule which gates weight updates by the reward expectation error. However, the employed □-rule is asymmetric, meaning that the learning rate is larger by a factor v when an unexpected reward occurs, as compared

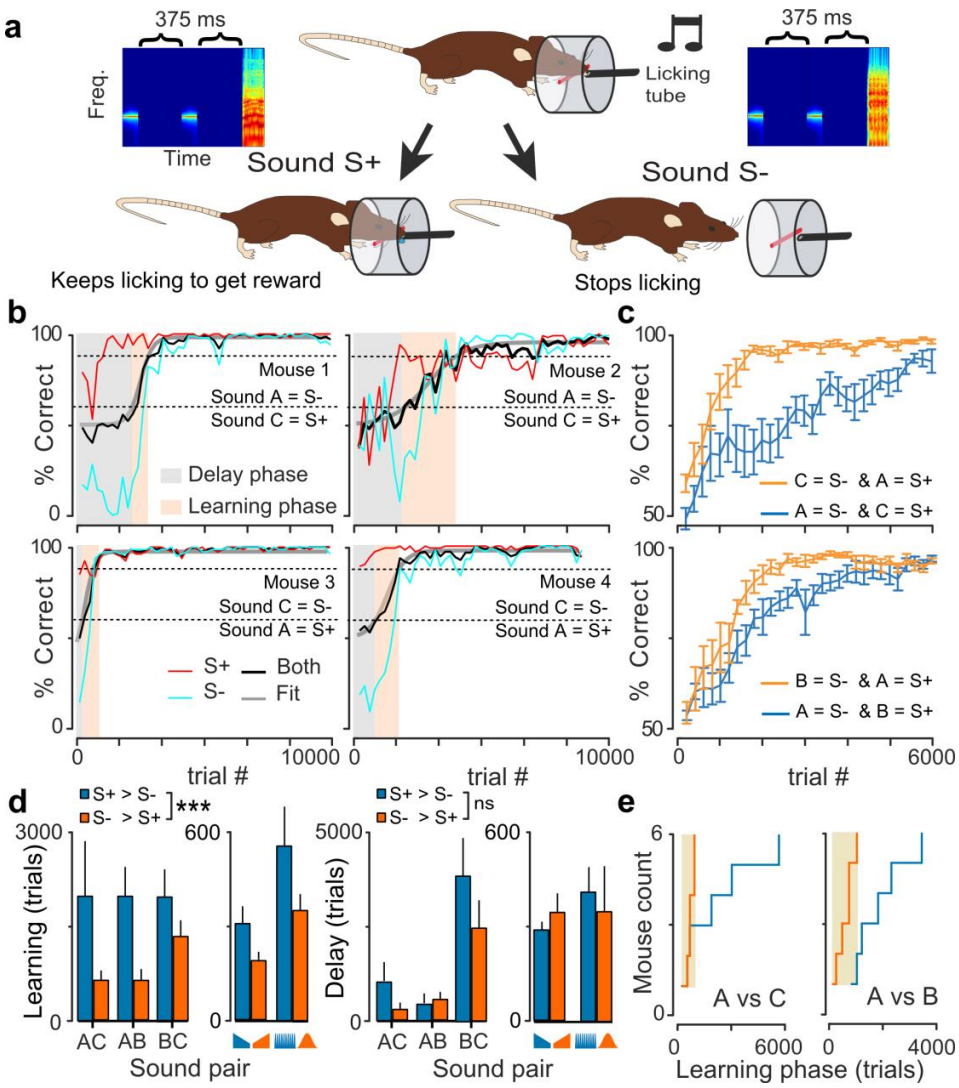


**Figure 3-3. Cortical recruitment differences impacts learning phase duration.**

a. Schematics describing the auditory Go/NoGo discrimination task.b. Individual learning curves for 4 mice discriminating sounds A and C. Performance for S+ (red), S- (light blue) and both (black) sounds are displayed. Mice from the top row have sound A as the S- stimulus while mice from the bottom row have sound C as the S- stimulus. Typical learning curves display a delay and learning phase as shown in light gray and orange colors. c. Mean learning curves for different groups of mice (n = 6 for each curve) discriminating between sounds A and C (top) or A and B (bottom). Slower learning is observed when the S- sound recruits less cortical activity than the S+ sound (blue) as compared to when sound valence is swapped (orange). d. Mean +/- standard error for the learning and delay phase for the five discriminated sound pairs (A vs C, A vs B, B vs C, up- vs down ramp, 20Hz vs 1Hz modulation represented by blue and orange symbols). The conditions “S- recruitment > S+ recruitment” (blue) and “S+ recruitment < S- recruitment” (orange) are significantly different for the

learning phase but not the delay phase (Friedman test, p = 0.0005 indicated as *** and p = 0.72 indicated as ns, n = 6 mice per group except for the up- and down ramps, n = 12). e. Cumulative distributions of learning phase durations for sound pairs A-C, A-B. Error bars represent standard errors (SEM).

to when an expected reward does not occur. This asymmetry is crucial for capturing the fast raise of the hit-rate, and slower adjustment of the correct rejection-rate (Figure 3-3B). Last, synaptic updates are multiplicative, meaning that weight updates are proportional to the current weight value40-43. The key feature of multiplicative learning is that learning speed depends on the current strength of the synapses. Thus, the same model can have very slow learning (low weights) as in the delay phase and faster learning (high weights) as in the learning phase. Furthermore, this feature makes learning dynamics highly sensitive to the initial synaptic weights, which become important parameters that can even account for most of the inter-individual variability (Bathellier et al., 2013). Importantly, the activity level of the $\hat{S}$+ and $\hat{S}$- populations can be varied in the model, allowing to simulate the impact of cortical recruitment for example by setting either $\hat{S}$- or $\hat{S}$+ activity level to 2 while level for the other population is 1 (but note that this value can be widely varied without changing our conclusions, Figure 3-4B, Figure 3-9 & Figure 3-10, Supplementary Note 1).

We therefore wondered whether this model reproduces the observed relationships between cortical recruitment and mean learning speed and its variability. The dynamics of the model depend on the choice of its three core parameters (noise level, learning rate and asymmetry, see Methods) and of its initial synaptic weights, and we showed previously (Bathellier et al., 2013) that individual learning curves can be fitted by adjusting these parameters, even without accounting for recruitment difference. Nevertheless, to test if the model captures the effect of recruitment, one can use a realistic set of parameters and test if asymmetric recruitment produces the effects seen during the behavior. We thus looked at the qualitative behavior of the model using a set of parameters obtained in a previous group of experiments (Bathellier et al., 2013) by fitting the individual learning curves from 15 mice trained in a task identical to the one used in this study. This parameter set included 15 different values of the initial weights, and core parameters were identical for all mice, which we showed is sufficient to account for inter-individual variability (Bathellier et al., 2013). Based on these parameters, and systematically varying the recruitment values in simulations, we observed that recruitment differences were positively correlated to learning phase duration in the model, similar to the experimental results (Figure 3-4B).

Also, as illustrated when neuronal recruitment is doubled for one of the two stimuli, the model reproduced two other experimental observations. First, the delay phase was not significantly influenced by recruitment (Figure 3-4C). Second, the variability of the learning phase duration was much stronger when S- recruited less activity than S+ (Figure 3-4C-D). Thus, without any tuning, the model qualitatively reproduced the complexity of the experimental dynamics, offering an opportunity to explore possible mechanisms for the complex effects of neuronal recruitment on learning behavior in a precise theoretical framework.

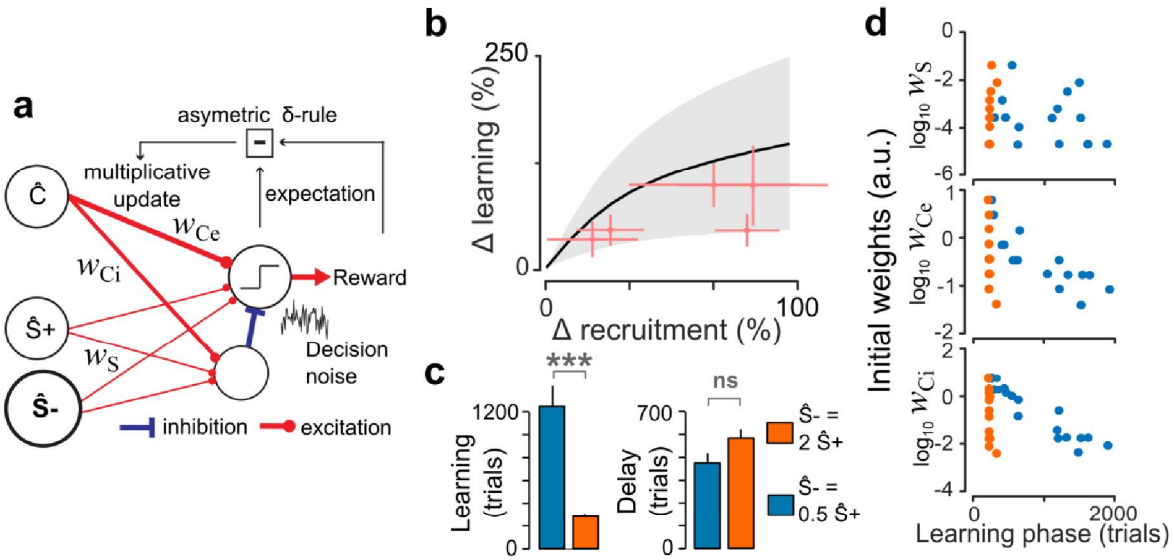


**Figure 3-4. A multiplicative reinforcement learning model reproduces modulations of learning speed by neuronal recruitment**

a. Schematics describing the auditory Go/NoGo discrimination model. b. Mean +/- standard deviation of the difference of learning phase duration against difference in neural recruitment by the stimuli for the model initialized with 15 sets of initial conditions obtained when fitting learning curves from a previous study(Bathellier et al., 2013). The experimental observations of Figure 3-3D are superimposed in red. c. Mean +/- standard errors for the learning and delay phases obtained with the model for a two-fold difference in cortical recruitment between the two stimuli. A longer learning phase (Kolmogorov-Smirnov test, p=8×10-7 indicated as ***, n=15 initial conditions per group) but not delay phase (Kolmogorov-Smirnov test, p=0.13 indicated as ns, n=15 initial conditions per group) is observed when S- recruits less activity (blue) as compared to when S- recruits more activity than S+ (orange). d. Learning phase duration plotted against the value of the modeled initial synaptic weights. Same simulations and color code as in c. Significant correlations were observed only when S- recruits less activity (blue), and for $w_{Ce}$ ($\rho$ = -0.61, p = 0.015, n=15) and $w_{Ci}$ ($\rho$ = -0.70, p = 0.0034, n=15). Error bars represent standard errors (SEM).

### 3.3.4. Learning speed effects depend on initial synaptic strengths

To understand the origin of inter-individual variability in our simulations, we plotted the learning phase duration against the values of the three initial synaptic weight parameters ($\mathbf{w_{Ce}}$ and $\mathbf{w_{Ci}}$ for the Ĉ population, and a single initial value $\mathbf{w_S}$for the four weights of the Ŝ+ and Ŝ- population, as in Figure 3-4A). First, we observed that the initial weight between sound-specific neural populations and the decision populations ($\mathbf{w_S}$) had no correlation with learning speed duration. This was expected as $\mathbf{w_S}$ mostly impact the delay phase because small initial synaptic weights lead to slow initial learning (multiplicative rule). After the delay phase, sufficient learning has occurred for the sound-specific synaptic weights to increase performance at high speed and $\mathbf{w_S}$does not influence learning speed anymore. Our earlier results25 showed that $\mathbf{w_S}$is the main determinant of the delay phase duration and is highly variable across mice. These inter-individual $\mathbf{w_S}$variations induced large variations of delay phase duration masking the smaller impact of neuronal recruitment on delay phase in simulations (Figure 3-4). This suggests that variability in initial connectivity may explain the independence between cortical recruitment and delay phase duration in behavior.A second observation was that the learning phase is long when the initial weights $\mathbf{w_{Ce}}$ and $\mathbf{w_{Ci}}$ (non-specific population Ĉ) are small, but only when S- recruits less activity than S+ (Figure 3-4D). In contrast, for large weights, the recruitment differences between S+ and S- have no effect on learning phase (Figure 3-4D). Hence, variability in initial connectivity from non-specific representation of the task may explain the larger variability in learning phase duration observed in behavior when cortical recruitment for S- is smaller than recruitment for S+ (Figure 3-3E).

To better understand why the initial conditions of $\mathbf{w_{Ce}}$ and $\mathbf{w_{Ci}}$ gate the influence of neuronal recruitment on learning speed, we plotted the time-course of both excitatory and inhibitory connection weights for four combinations of recruitment and initial weights values (Figure 3-5A-D, see also Figure 3-10for the same analysis with a smaller recruitment ratio). These plots show that the large prolongation of the learning phase when neuronal recruitment is lower for S- than for S+ and when $\mathbf{w_{Ce}}$ and $\mathbf{w_{Ci}}$ are small (Figure 3-5D) is due to the maintenance throughout the delay phase of low initial weights from Ŝ- and Ĉ populations to the No-Go population. This impacts the effective speed (multiplicative learning rule) at which correct rejections responses to S- are acquired during the learning phase, flattening the overall learning curve. In contrast, with large initial synaptic weights from the Ĉ population, more rapid S- rejection learning is obtained solely based on the Ĉ common population (Figure 3-5C).

When S- recruits more activity, learning is always fast (Figure 3-5A-B) because, in all cases, the rate limiting process remains the abolition of licking to the NoGo stimulus (due to learning rule asymmetry, see). This process is boosted by strong Ŝ- recruitment. Also, in these conditions, acquisition of the NoGo stimulus is independent of $\mathbf{w_{Ce}}$ and $\mathbf{w_{Ci}}$, because the Ĉ population drives the Go response. Thus, the complex modulation of learning phase duration by neuronal recruitment is due, in the model, to a non-trivial assignment of the three sensory populations to either Go or NoGo responses, based on neuronal recruitment distribution. Specifically, when the Ŝ- population recruits more activity, it is assigned to NoGo, while the Ĉ population drives the Go response. In contrast, when the Ŝ+ population recruits more activity, it is assigned to the Go response, and in this case, the Ĉ population drives the NoGo response. These different solutions of the binary discrimination problem could be seen as different strategies chosen by the model or eventually the animals during the learning process. The existence of multiple solutions to the task provides a testable, general prediction of reinforcement learning models which use population activity as a salience parameter (independent of the magnitude of recruitment differences, see analytical arguments in Supplemental Experimental Procedures). The test would be to isolate and drive the neurons corresponding to Ĉ in the brain. Activation of the Ĉ population alone should drive licking when S- recruits more activity, and should not drive licking when S- recruits less activity (Figure 3-5,Figure 3-10).

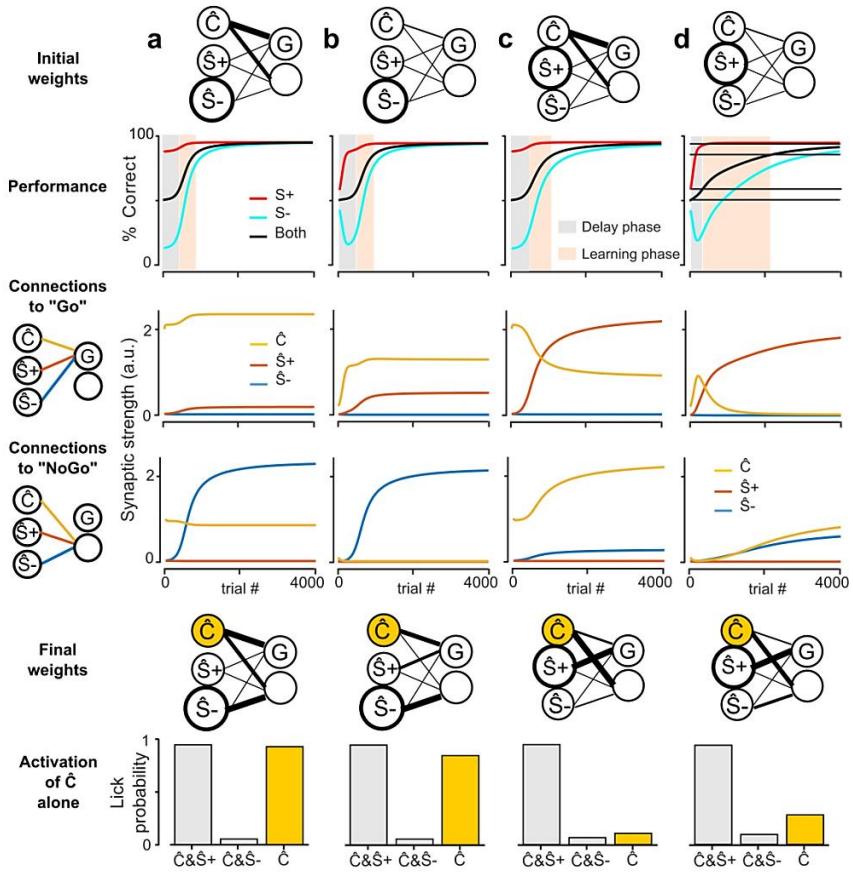


**Figure 3-5. The effects of neuronal recruitment in the model are explained by the differential adjustment of synaptic weights during learning.**

a. (top) Sketch of the initial synaptic weights and simulated model performance for S+ (red), S- (light blue) and both stimuli (black). (middle) Values of the connections to the excitatory (G) and inhibitory decision populations as indicated by the schematics on the left-hand-side. Yellow: connections from the "common" Ĉ population. Red: connections from the Ŝ+ population. Blue: Connections from the Ŝ- population. (bottom) Sketch of the connectivity pattern after and response probability after learning for the S+ (co-activation of Ŝ+ & Ĉ) and S- (co-activation of Ŝ- and Ĉ) reinforced stimuli as well as for the common stimulus component alone (Ĉ, yellow). Simulation parameters: X = [1 ; 1; 2], $\alpha$= 0.01, $\sigma$ = 0.6195, v = 6, $w_{Ci}$ = 1, $w_{Ce}$= 2, and $w_S$= 0.01. b. Same as a, but with $w_{Ci}$ = 0.1, $w_{Ce}$= 0.2. c. Same as a, but with X = [1 ; 2 ; 1]. d. Same as c, but with $w_{Ci}$ = 0.1, $w_{Ce}$= 0.2.

### 3.3.5. Recruitment determines learning strategy

Testing this prediction was impractical with our sound-based Go/NoGo discrimination protocol, because the neurons encoding information common to S+ and S- trials (Ĉ population) likely code for multiple

cues, including (i) the overlap of S+ and S- representations and (ii) all cues related to the decision to visit the lick port, and thus cannot be isolated. Therefore, we decided to test the model predictions in an artificial but better controlled experiment in which head-fixed mice had to discriminate optogenetically-driven cortical ensembles. We used a custom-made video-projector setup (Dhawale et al., 2010) to project precise 2D light patterns through a cranial window placed above the AC in Emx1-Cre x Ai27 mice (Figure 3-6A-B, Figure 3-11). Using intrinsic imaging, we identified the main tonotopic fields of mouse AC (Figure 3-6C) (Bathellier et al., 2012; Moczulska et al., 2013) and thereby reliably positioned optogenetic stimulation spots in homologous regions across mice (Figure 3-6C). We defined three circular optogenetic stimulation spots out of which we constructed two stimuli. One of the three spots, the Ĉ spot, was common to the two S+ and S- stimuli and the two other spots corresponded to the stimulus-specific neuronal populations Ŝ+ and Ŝ- (e.g. Figure 3-6B). Thus, the Go-trial cue consisted of simultaneous activation of Ŝ+ and Ĉ and the NoGo-trial cue consisted of simultaneous activation of Ŝ- and Ĉ. Furthermore, cues common to S+ and S- related to licking port visits in the sound task were eliminated in the head-fixed task design, as mice did not initiate the randomly interleaved trials. Thus the Ĉ spot was the only cue common to Go and NoGo-trials. We doubled the diameter of either the Ŝ+ or the Ŝ- spot to create a difference in cortical recruitment between the two input representations. Electrophysiological measurements of the population firing rate elicited by the small and large spots showed that the recruitment difference between the stronger and weaker stimuli was about 69 % (Figure 3-11), comparable with the population recruitment differences observed for sounds (Figure 3-4B; Figure 3-11). Also, we measured that the large disk activates about 2.5 more neurons than the small disk (Figure 3-11). Given that the Ĉ spot has a small diameter, we could evaluate the fraction of cells commonly activated by the S+ and S- stimuli within the cells activated by S+ and S- as 1 / (1+1+2.5) ≈ 22%, similar to the fraction of cells commonly activated by sounds (e.g. 18%, 18%, 23% for sound pairs A-B, A-C, and B-C, S.E.M = 0.3%, binomial distribution). Thus the artificial stimuli, although not identical to sound responses had comparable characteristics.Mice were then initially trained to obtain a water reward by licking after the coincident activation of the Ŝ+ and Ĉ spot. When 80% performance was reached in this stage, the discrimination training started. Mice kept licking in the presence of the Ŝ+ spot and learned, within hundreds of trials to avoid licking in the presence of the Ŝ- spot (both activated together with Ĉ, Figure 3-6D), reaching a steady state performance of 94.7% ± 4.5% correct trials (hit rate 93.9% ± 3.3%, false alarm rate 4.5% ± 1.3%, n=8 mice, see Figure 3-6E-F). Importantly, in this task setting,

the stringent definition of the common Ĉ population, activated during the initial motivation training, likely resulted in the systematic establishment of strong initial connections for this population at the beginning of the discrimination training, leading to homogenous durations of the learning phase (212 ± 117 trials for the large Ŝ- vs 260 ± 220 for the small Ŝ-, p = 0.26, Wilcoxon rank-sum test, see also Figure 3-6D) independent of recruitment (Figs. 4-5).

However, once mice had learned the behavioral task, we measured their response to Ĉ activation alone in catch trials that were not rewarded (catch trial probability = 0.1; 15 catch trials per mouse). In the group of mice that had a larger Ŝ- spot, we observed that activation of Ĉ elicited strong licking responses (84% ± 6% response probability, n = 6 mice, Figure 3-6E). In contrast, in the group of mice that had a larger Ŝ+ spot, activation of Ĉ elicited no licking response (2% ± 1% response probability, n = 7 mice, Figure 3-6F). Note that these effects are unlikely to be caused by inhibition of Ĉ when paired with the large Ŝ+ or Ŝ- spot, as no inhibition from the larger spot was observed at the location of Ĉ in calibration experiments (Figure 3-11). In addition, behavioral responses to Ŝ+ or Ŝ- alone were compatible with our model (Figure 3-6E, f vs Figure 3-5). By confirming the model's predictions, these results demonstrate, in a causal manner, that cortical recruitment affects the choice of which stimulus is associated to a particular response. Even if simple in essence, this result shows that cortical recruitment is a parameter influencing learning, in a manner compatible with the role of a salience parameter in reinforcement learning models.

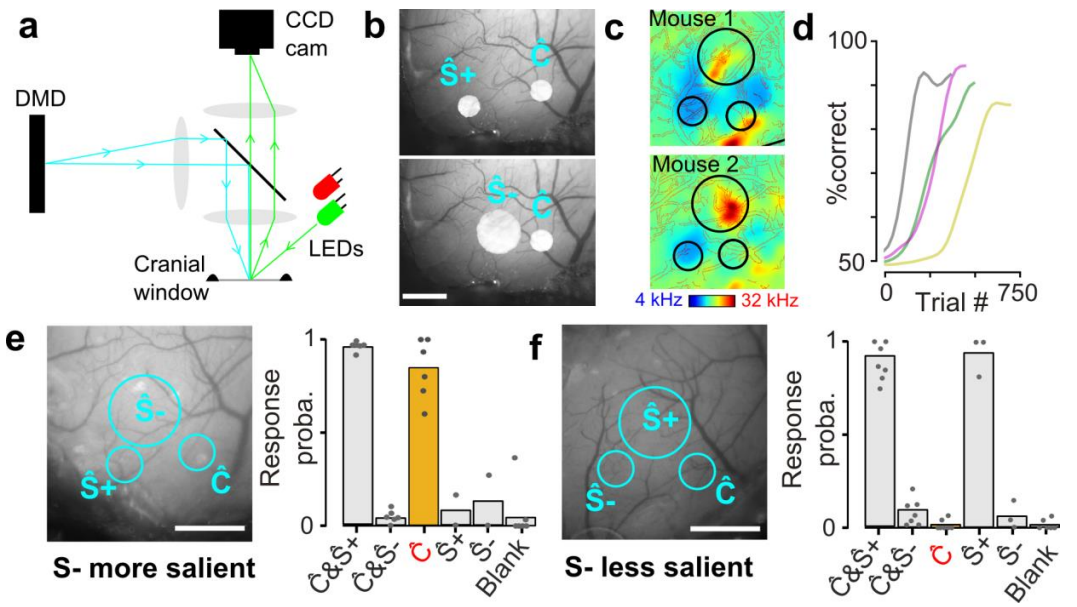


**Figure 3-6. Discrimination training of multi-spot optogenetic patterns reveals a choice of learning strategy depending on the level of cortical recruitment.**

a.Schematics of the optical setup to project arbitrary 2D light patterns onto the surface of auditory cortex. Blue light patterns from a Digital Micromirror Device (DMD) are collimated and deflected through the objective lens by a beam splitter. The surface of the cranial window can be simultaneously imaged by a CCD camera using external LEDs (green for blood vessel, red for intrinsic imaging). b. Examples of light patterns used for the discrimination task. Scale bars: 600 µm. c. Tonotopic maps obtained with intrinsic imaging for two mice, and localization of the three optogenetic stimulation spots in the same high, low and mid frequency fields. d. Four example learning curves for the optogenetic discrimination task. Grey: smaller Ŝ- ; color: larger Ŝ-. e. (left) Light pattern in the task in which the S- stimulus has higher level of cortical recruitment (Ŝ- >Ŝ+). Ĉ = common component of S+ and S- stimuli. (right) Response probability for the two learned target stimuli (Ĉ& Ŝ+ vs Ĉ& Ŝ-), for the presentation of the common part of the stimuli alone (Ĉ, yellow), for the specific parts of the stimuli alone (Ŝ+; Ŝ-) and in absence of stimulation (blank). 10 to 15 catch trials per mouse. Mean and individual data points, n = 6 mice (except Ŝ+ & Ŝ-, n=2 mice). Gray dots: single animals. f. Same as e, but with Ŝ+ larger than Ŝ-. Mean and individual data points, n=7 mice (except Ŝ+ & Ŝ-, n=3 mice). Scale bars: 600 µm.Source data are provided as a Source Data file.

## 3.4. Discussion

Combining behavioral measurements, large scale two-photon imaging, optogenetics and theoretical modeling, we have shown that sounds of different quality but equal mean pressure levels can recruit highly variable levels of neuronal activity in AC, measured as the mean amount of activity in a representative subsample of neurons. We showed that cortical recruitment levels correlate with learning speed effects in a Go/NoGo task as expected if neuronal recruitment corresponds to stimulus salience. Moreover, these effects can be precisely reproduced by a reinforcement learning model of the task. Finally, training mice to discriminate optogenetically evoked cortical patterns, and manipulating these patterns, we showed that neuronal recruitment determines which elements of the cortical representation are selected to drive each conditioned action. This corroborates, in a causal manner, the idea that cortical recruitment is a neuronal correlate of stimulus salience.

Several studies indicate that cortical recruitment can vary across stimuli, even when played at the same sound pressure level (Deneux et al., 2016; Kanold et al., 2014; Wong and Schreiner, 2003). These discrepancies may have multiple origins. First, it is well known that the mouse cochlea is more sensitive in its middle frequency range (Zheng et al., 1999), which could explain the overrepresentations of sounds in this frequency range (10-30 kHz) in cortex (Kanold et al., 2014). In this case, cortical recruitment is expected to reflect recruitment throughout the auditory system, making it a good proxy for sound salience independent of whether the discrimination task requires AC (Kato et al., 2015; Kuchibhotla et al., 2017; Znamenskiy and Zador, 2013)or does not require it (Gimenez et al., 2015; Pai et al., 2011; Rybalko et al., 2006). But a second source of recruitment differences may be the nonlinearities of cortical representations (Atencio et al., 2008; Deneux et al., 2016; Kuchibhotla and Bathellier, 2018; Nelken, 2008). For example, a recent study suggested that cortical response patterns can be invariant to changes in intensity (Sadagopan and Wang, 2008). In this case, cortical recruitment should also depend on the higher level features composing sound representations and on how broadly these features are represented in cortex.

The idea that the amount of neuronal activity recruited by a stimulus influences behavior, has been proposed in different contexts. For example, several studies indicate that attention can boost neuronal

firing associated to behaviorally relevant stimuli (Desimone and Duncan, 1995; Fritz et al., 2007; Goard and Dan, 2009) and thereby make them more discriminable from other stimuli (Zhang et al., 2014). Also, several theoretical studies have proposed that attention impacts learning (Mackintosh, 1975; Pearce and Hall, 1980) and some reinforcement learning models can account for such effects by dynamically weighting stimuli according to their predictive relevance (Niv et al., 2015). It will be an interesting research avenue to analyze the relative contribution of bottom-up sound encoding and attentional top-down mechanisms to the level of cortical recruitment. Earlier reports, using direct micro-stimulation of the cortex, showed that low levels of neuronal recruitment can impact detection probability (Huber et al., 2008; Houweling and Brecht, 2008). Here, we show that neuronal recruitment for stimuli that are well beyond detection threshold still impact the learning process. Even if such effects are predicted by the Rescorla and Wagner's model, capturing their details requires a refinement of the original model (Rescorla and Wagner, 1972). In particular, we had to introduce a more realistic multiplicative learning rule which renders learning speed not only dependent on neuronal recruitment, but also on the current synaptic strength. This property has important consequences. First, it introduces variability in the relationship between recruitment and learning speed, through large inter-individual variations of the initial weights for the synapses involved in the task. Second, the multiplicative rule makes learning speed proportional to the product of neuronal recruitment and connectivity, allowing for more robustness, by compensating weak neuronal recruitment with stronger initial connections (see Supplemental Experimental Procedures). In our experiments, this phenomenon tends to stabilize learning speed, explaining why neuronal recruitment does not always impact the learning phase duration, except for particular initial conditions for which compensation occurs too slowly (Figs. 3-5).

Strong pre-established connections can lead to fast learning for specific stimuli with innate meaning. In this study, we have shown an effect of cortical recruitment on learning speed for five different pairs of sounds which had no particular meaning to the animal. This does not exclude the possibility that some sounds, in particular, sounds with learned or innate meaning would show a different relationship. For example, pup calls are extremely salient to mothers but trigger little activity in cortex (Marlin et al., 2015). This could be due to strong pre-existing wiring between cortical neurons responding to pup calls compensating for limited recruitment. So, even if, as we show, cortical recruitment plays a role in the salience of a sound, general theories of salience should also account for potential a priori meaning of

stimulus, via pre-existing connections, as simple extensions of our model would suggest, or via more complex cognitive processes assigning value to the sounds.

The complex dynamical phenomena described in our study make learning speed measurements a more complicated proxy for stimulus salience than the overshadowing protocol which relies on steady state behavior, after the dynamical phase of the association. However, it allows the comparison of salience for stimuli from the same sensory modality. Because our extended multiplicative model only diverges from the Rescorla-Wagner model for the transient dynamical part of the association process, it reproduces overshadowing effects (Bathellier et al., 2013), and can also predict how elements of sensory representations are assigned to different conditioned responses in a more complex task setting. Here, by conditioning mice to compound stimuli composed of multiple optogenetically activated neuronal ensembles (Figure 3-6), we show, in line with reinforcement learning models, that the brain establishes its stimulus discrimination strategy based on the amount of activity recruited by the different subpopulations representing the stimuli.

# 3.5. Materials and methods

## 3.5.1. Animals

All mice used for imaging and behavior were 8 to 16 weeks old C57Bl6J and GAD2-Cre (Jax #010802) x RCL-TdT (Jax #007909) mice. Mice used for optogenetics were 8 to 16 weeks old males and female obtained by crossing homozygous Emx1$^{IRES\text{-}cre}$ (Jax #005628)mice with Ai27 (Jax # 012567)mice to obtain expression of Td-Tomato-tagged channelrhodopsin (ChR2) in excitatory neurons of the cortex. All animal were group housed. All procedures were approved by the Austrian laboratory animal law guidelines (Approval #: M58 / 02182 / 2007 /11; M58 / 02063 / 2008 /8) and the French Ethical Committee (authorization 00275.01).

## 3.5.2. Two-photon calcium imaging in awake mice

At least three weeks before imaging, mice were anaesthetized under ketamine medetomidine. The right *masseter* was removed and a large craniotomy (~5 mm diameter) was performed above the AC. We then performed three to five injections of 200nL (35-40nL.min$^{-1}$), rAAV1.Syn.GCaMP6s.WPRE virus obtained from U. Penn Vector Core (Philadelphia, PA) and diluted 10 times. The craniotomy was sealed with a glass window and a metal post was implanted using cyanolite glue and dental cement. At least three days before imaging, mice were trained to stand still, head-fixed under the microscope for 20 to 60 min per day. Then mice were imaged one to two hours per day. Imaging was performed using a two-photon microscope (Femtonics, Budapest, Hungary) equipped with an 8kHz resonant scanner combined with a pulsed laser (MaiTai-DS, SpectraPhysics, Santa Clara, CA) tuned at 920 nm or 900nm depending on the experiments. Images were acquired at 31.5Hz. All sounds were delivered at 192 kHz with a NI-PCI-6221 card (National Instrument) driven by Elphy (G. Sadoc, UNIC, France) through an amplifier and high frequency loudspeakers (SAI and MF1-S, Tucker-Davis Technologies, Alachua, FL). Sounds were calibrated in intensity at the location of the mouse ear using a probe microphone (Bruel&Kjaer). In a first experiment, we played three 70 ms complex sounds at 73dB SPL preceded by two 50 ms 4kHz pure tones (inter-tone interval: 375 ms) sounds as in the behavioral task. The three sounds were played in a random order and repeated 30 times. In a second experiment, we played white noise sounds ramping -up or -

down in intensity between 60dB and 85dB SPL during 2s. The ramps were repeated 20 times. In a third experiment, we played 20 repetitions of white noise sounds modulated in intensity at 1 and 20 Hz.

### 3.5.3. Data analysis

Data analysis was performed using Matlab and Python scripts. Motion artifacts were first corrected frame by frame, using a rigid body registration algorithm. Regions Of Interest were selected using a semi-automated hierarchical clustering algorithm based on pixel covariance over time as described in[30](see detailed method below). Neuropil contamination was subtracted[65] by apply the following equation: $F_{true}$ (t*)* = $F_{measured}$ (t) – 0.7 $F_{neuropil}$ (*t*), then the change in fluorescence ($\Delta F/F_0$)was calculated as $(F-F_0) / F_0$, where $F_0$ is estimated as the minimum of the low-pass filtered fluorescence over ~40 s time windows period. To estimate the time course of firing rate, the calcium signal was temporally deconvolved using the following formula*:* $r(t) = f'(t) + f(t) / \tau$ in which $f'$ is the first time derivative of $f$ and $\tau$ the decay constant set to 2 seconds for GCaMP6s. For the complex sounds, the population response was computed as the mean deconvolved signal across all neurons from sound onset to 500ms after sound offset. For the ramps, because the behavioural discrimination response typically occurs within few hundreds of milliseconds after the ramp onset[34], the mean population response was evaluated from 0 to 500ms after sound onset. To estimate the discriminability of two sounds based on cortical population responses, linear Support Vector Machine classifiers were trained to discriminate population activity vectors obtained from 20 presentations of each sound (training set), and were tested on activity vectors obtained for 10 independent presentations of the same sounds (test set).

### 3.5.4. Patterned optogenetics and intrinsic imaging

To flexibly activate different activity patterns in the mouse AC, we used a computer driven (VGA input) video projector (DLP LightCrafter, Texas Instruments) which includes a strong blue LED light source (460 nm) and from which we have removed the objective. To project a two-dimensional image onto the AC surface (Figure 3-6**A-B**), the image of the micromirror chip is collimated through a 150 mm cylindrical lens (Thorlabs, diameter: 2 inches) and focused through a 50 mm objective (NIKKOR, Nikon). Imaging of the cortex at the focal plane is obtained by side illumination with a green (525 nm, blood vessels) or far red (780 nm, intrinsic imaging) LED. The light collected by the objective passes through a dichroic

beamsplitter (long pass, >640nm, FF640-FDi01, Semrock) and is collected by a CCD camera (GC651MP, Smartek Vision) equipped with a 50 mm objective (Fujinon, HF50HA-1B, Fujifilm). Note that the image projected to the cortical surface corresponds to a narrow cone of light extending below the surface and potentially activating ChR2 expressing neurons throughout the cortical depth. Intrinsic imaging was performed in isoflurane anesthetized mice (1.1% delivered through SomnoSuite, Kent Scientific). To compute intrinsic signal maps we divided the red light image of the cortical surface after the onset of a stimulation (average over 2 s) with 2s long pure tones (4, 8, 16 and 32kHz) by the mean image immediately before stimulus onset.

### 3.5.5. Calibration of optogenetic

For calibration of optogenetic stimulation, a small aperture was drilled in the cranial window with a diamond-coated dental drill during isoflurane anesthesia. 30 minutes after surgery, 4x8 silicon probes (Neuronexus) were implanted at a ~35° angle in AC in the awake head-fixed mouse. Recordings were performed at three different depths (400, 600 and 800 µm) using a pre-amplifier and multiplexer coupled to a USB acquisition card (Intan Technologies). Sounds and light stimulations were randomly presented at 2.5 sec and each repeated 10 times. Single unit spikes were detected and sorted from multi-unit spikes using the Phy Suite (https://github.com/kwikteam/phy). Light stimuli consisted of small and large disk (360 µm and 720 µm diameter) presented at different positions of a two-dimensional grid centered on the probe location (Figure 3-11). For small disks, the grid included 5x8 locations with a regular $\Delta x = \Delta y$ = 360 µm spacing. For large disks, the grid included 3x4 locations with a regular spacing of 480 µm. Population firing rate elicited by a single disk was estimated as the integral $\sum_{Locations} r_{x,y} \Delta x \Delta y$ of the responses $r_{x,y}$ to the disk centered at locations that were within in the extent of the smaller of the two grids (large disks: all locations, extent 1440×1920 µm; small disk: 4x5 locations, spanning 1440×1800 µm). The integrals for big and small disks were normalized by $\Delta x_0 \Delta y_0 = 360 \times 360$ µm$^2$. The overall fraction of responsive neurons over the extent of the smaller grid (see firing rate) was computed as $\left( \sum_{x,y} N_{responsive\_cells}(x,y) \right) / \left( N_{locations} \times N_{cells} \right)$, where $N_{responsive\_cells}(x,y)$ is the number responsive cells at each disk location, $N_{locations}$ is the number of locations and $N_{cells}$ the number of recorded cells.

### 3.5.6. Go/NoGo discrimination behavior

Mice were water-deprived and trained daily for 200 to 300 trials. Mice first performed 4 habituation sessions to learn to obtain a water rewards (~5 µl) by licking on a spout over a threshold after the positive stimulus S+. After habituation, the fraction of collected rewards was about 80%. The learning protocol then started in which mice also received a non-rewarded, negative sound S- for which they had to decreasing licking below threshold to avoid an 8 s time-out. For the freely moving complex sound discrimination, S+ and S- sounds consisted of two 4 kHz pips (50 ms) followed by one of the three 70 ms complex click shown in Figure 3-1**A**. The interval between the offset and onset of the pips and click was 375 ms. Licking was assessed 0.58 s after the specific sound cue in a 1 s long window by an infrared beam at the spout. For the intensity ramp discrimination, licking was assessed in a 1.5 s window after sound offset. In both cases, licking was considered above threshold if the infrared beam in front of the licking tube was broken during 75% of the measurement time-window. Positive and negative sounds were played in a pseudorandom order with the constraint that exactly 4 positive and 4 negative sounds must be played every 8 trials. For learning curves, performance was measured as the fraction of correct positive and correct negative trials over bins of 100 trials. For the optogenetically-driven, head-fixed discrimination task, the S+ and S- stimuli were each composed of two disks of blue light (465 nm) flashing at 20 Hz for 1 s. One of the two disks (noted Ĉ) was common to S+ and S- stimuli, the other disk was condition-specific. The three disk locations were chosen in similar tonotopic locations across mice based on intrinsic imaging maps. They were precisely re-positioned for every training session using an automated registration procedure based on blood-vessel patterns. A strong masking light was used to prevent the animal from using visual cues in the task. The common disk was 360 µm in diameter. In one set of mice, the disk specific to S- was 720 µm in diameter, while the S+ specific disk was 360 µm in diameter. In the other set of mice, sizes of the specific disks were swapped. Head-fixed mice performed 200 to 300 trials per day with an inter-trial interval randomized between 3 s and 7 s. Individual licks were detected through an electric circuit connecting the mouse and the lick tube. Then, each trial was started only if the mouse was not spontaneously licking for at least 3 s (in addition to the inter-trial interval). Mice were first trained to respond to the S+ stimulus by producing at least 3 to 5 licks (depending on the mouse) to get the 5 µL water reward. When the mouse could collect more than 80% of the rewards, the S- stimulus was introduced. Licking above threshold after S- was punished with a 7 s timeout.

### 3.5.7. Reinforcement learning model.

The model has been described extensively in a previous publication[25]. In short, it is composed of three sensory units (Ŝ+, Ŝ- and Ĉ, representing populations of neurons) whose activity described by a three-dimensional vector **X**and which are connected to a simple decision circuit (Figure 3-4**A**). Cortical recruitment is modeled by changing the firing value of the sound units. When the S- stimulus recruits less activity than the S+ stimulus, the input vectors are: $\mathbf{X}_{S+}$ = [1 0 2] or $\mathbf{X}_{S-}$ = [1 1 0]. When S- recruits more activity than S+, the input vectors are: $\mathbf{X}_{S+}$ = [1 0 1] or $\mathbf{X}_{S-}$ = [1 2 0].

The decision circuit is composed of all-or-none response unit (*y* = 0 or 1) which linearly sums the three sensory inputs (representing synaptic populations) under the form of three direct excitatory connections and of a graded feed-forward inhibition from a virtual inhibitory unit in fact equivalent to three direct inhibitory connections. The output of model is described by a single equation for the decision unit:

$$y = \theta(\mathbf{W}_{\mathrm{E}}.\mathbf{X} - \mathbf{W}_{\mathrm{I}}.\mathbf{X} - \xi) \quad (1)$$

in which $\theta$ is the Heaviside step function. $\mathbf{W}_{\mathrm{E}}$ and $\mathbf{W}_{\mathrm{I}}$are three-dimensional positive vectors describing the excitatory synaptic weights from the sensory units to the decision and inhibitory units respectively. The variable $\xi$ is a Gaussian random noise process of unit variance which models the stochasticity of behavioral choices.

Based on the action outcome (*R* = 1 for a reward, *R* = -1 for no reward), the learning rule for the synaptic weights is implemented as:

$$\delta\mathbf{W}_{\mathrm{E}} = \alpha\mathbf{W}_{\mathrm{E}} \otimes f[R - \sigma(\mathbf{W}_{\mathrm{E}} - \mathbf{W}_{\mathrm{I}}).\mathbf{X}]y\mathbf{X} \quad (2)$$

$$\delta\mathbf{W}_{\mathrm{I}} = -\alpha\mathbf{W}_{\mathrm{I}} \otimes f[R - \sigma(\mathbf{W}_{\mathrm{E}} - \mathbf{W}_{\mathrm{I}}).\mathbf{X}]y\mathbf{X} \quad (3)$$

in which $\otimes$ is the Hadamard (element-wise) product implementing the multiplicative rule, $y\vec{x}$ is a Hebbian term, $\alpha$ is the learning rate and $\sigma$ is a parameter related to the noisiness of the model and setting its asymptotic performance. To account for the faster improvement of performance for rewarded as compared to non-rewarded trials, positive expectation errors are more strongly weighted than negative ones, thanks to the asymmetric function $f[u] = u$ if $u \leq 0$ and $f[u] = \nu u$ if $u > 0$. The

parameter $\nu$ is typically larger than 1, consistent with the activity of basal ganglia dopaminergic neurons in mice(Cohen et al., 2012)and monkeys(Schultz et al., 1997) coding for reward expectation error.

As described above, the equations of the model are stochastic due to the Gaussian random noise process $\xi$ . To compute the response probability estimates plotted throughout the study, we used a previously established probability equation (Bathellier et al., 2013), valid for learning dynamics much slower than fluctuations (ergodic approximation). The probability to make a lick response given the input vector $\mathbf{X}_{S+}$ or $\mathbf{X}_{S-}$ is:

$$p_{S+|S-} = p(y=1|\,\mathbf{X}=\mathbf{X}_{S+|S-}) = \frac{1}{2}\left(1+\mathrm{erf}\left(\frac{\Delta\mathbf{W}.\mathbf{X}_{S+|S-}}{\sqrt{2}}\right)\right) \quad (4)$$

where $\Delta\vec{w} = \vec{w}_E - \vec{w}_I$ represents now the average observed values of difference between the excitatory and inhibitory connections. In addition, the plasticity equations become:

$$\delta\mathbf{W}_{\mathrm{E}} = \frac{\alpha}{2}\mathbf{W}_{\mathrm{E}} \square \left( f[1-\sigma\Delta\mathbf{W}.\mathbf{X}_{S+}]p_{S+}\mathbf{X}_{S+} + f[-1-\sigma\Delta\mathbf{W}.\mathbf{X}_{S-}]p_{S-}\mathbf{X}_{S-}\right) \quad (5)$$

$$\delta\mathbf{W}_{\mathrm{I}} = -\frac{\alpha}{2}\mathbf{W}_{\mathrm{I}} \square \left( f[1-\sigma\Delta\mathbf{W}.\mathbf{X}_{S+}]p_{S+}\mathbf{X}_{S+} + f[-1-\sigma\Delta\mathbf{W}.\mathbf{X}_{S-}]p_{S-}\mathbf{X}_{S-}\right) \quad (6)$$

### 3.5.8. Statistical tests

Unless otherwise specified, all quantifications are given as mean ± standard error (SEM). To statistically assess the differences between paired measurements (e.g. activity for two different sounds elicited in the same neuronal populations) we used the non-parametric Signed test. To compare two sets of measurements (e.g. delay and learning phase duration for two groups of mice) we used the non-parametric Wilcoxon rank sum test. Assessment of the differences in the fraction of responsive neurons for different sounds was done with the $\chi^2$ test which evaluates differences in the distributions of two binary variables. All tests are two-sided. No data was excluded from the analysis sample.

### 3.5.9. Data and software availability

All datasets, analysis software and codes for running the simulations of our model are freely available on the Dryad Digital Repository (http://datadryad.org/) doi:10.5061/dryad.47h8t87 or on https://www.bathellier-lab.org/downloads.

## 3.6. Acknowledgements

We thank K. Kuchibhotla, E. Harrell and M. Stüttgen for comments on the manuscript, P. Pindi, S. Sikirić and L. François for help with behavioral and imaging experiments. We thank the GENIE Project, Janelia Farm Research Campus, Howard Hughes Medical Institute, for GCAMP6s constructs. This work was supported by the Agence Nationale pour la Recherche (ANR "SENSEMAKER"), the Fyssen foundation, the DIM "Region Ile de France", the Marie Curie Program (CIG 334581), the International Human Frontier Science Program Organization (CDA-0064-2015), by the Fondation pour l'Audition (Laboratory grant), the École Doctorale Frontières du Vivant (FdV) – Programme Bettencourt (support to AK), the DIM Cerveau et Pensée and Ecole des Neurosciences de Paris Ile-de-France (ENP, support to SC) and the Deutsche Forschungsgemeinschaft (DFG CRC1080/2).

## 3.7. Author contributions

BB and SR designed the study. AK, **SC**, and BB performed and analyzed the imaging experiments. BB and JB performed the modeling. AD and BB performed and analyzed behavioral experiments. ZP designed the patterned optogenetic setup, **SC** and PP performed the optogenetic experiments. TD designed software for data analysis and behavior. BB and SR wrote the manuscript with comments from all authors.

## 3.8. Supplementary figures

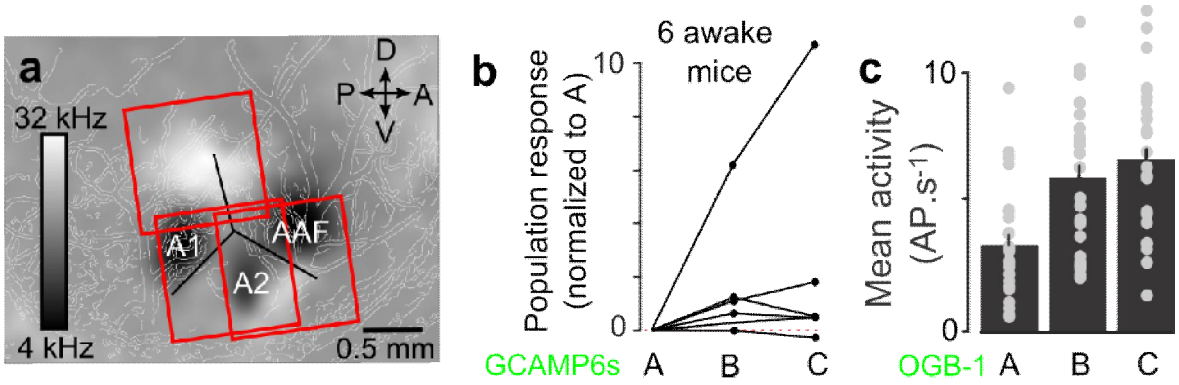


**Figure 3-7. Cortical recruitment differences are robust across mice and experiments**

a.Localization and horizontal extent of the imaging fields-of-view (red squares) in one of the imaged mouse. The 1x1 mm fields-of-view were localized with blood vessels patterns (white lines). The auditory cortex is identified by subtracting intrinsic imaging responses to 4kHz (black colors) and 32 kHz (white colors) tones revealing the main tonotopic gradients. b.Responses of neural population recorded in each of the 6 awake mice included in the averages shown in presented in Figure 1 (activity is measured with GCAMP6s). Responses are measured as mean deconvolved calcium signals during the entire duration of the response (sound duration +0.5s). Normalization in obtained by subtracting and dividing with response to sound A. The distribution of responses to B and C are significantly above zero (n=6 mice, Wilcoxon signed rank test, p=0.031 for B and C) c. Average population activity in OGB1 labelled neurons imaged with two-photon microscopy in 7 isoflurane anesthetized mice (28 population, 1994 neurons) for sounds A, B and C. Mean ± SEM, for A: 3.1176 ± 0.3726 $AP.s^{-1}$, B: 5.4527  0.4982 $AP.s^{-1}$, C:  6.3453 ±  0.4978 $AP.s^{-1}$. Responses to sound B and C are significantly different from A, but not from each other Wilcoxon rank sum test, p=0.0012, $p=1.5\times10^{-5}$,  p=0.31. Error bars represent standard errors (SEM).

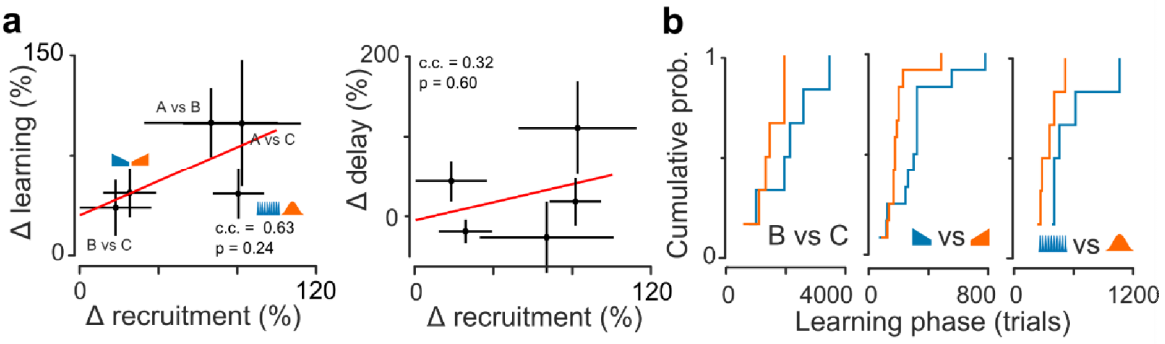


**Figure 3-8. Impact of cortical recruitment on learning and delay phase durations.**

a. Mean +/- standard error of the difference of learning (left) and delay (right) phase durations plotted against the difference in neural recruitment by the stimuli. Correlation coefficients: 0.63 (p=0.24, n=5) for the learning phase, 0.32 for the delay phase (p=0.60, n=5). Note that high correlations are expected to occur by chance for low sample size. b. Cumulative distributions of learning phase durations for sound pairs B-C, for the up- (orange symbol) and down-ramp (blue symbol) and for the 1 Hz(orange symbol) and 20Hz (blue symbol) modulated sounds.

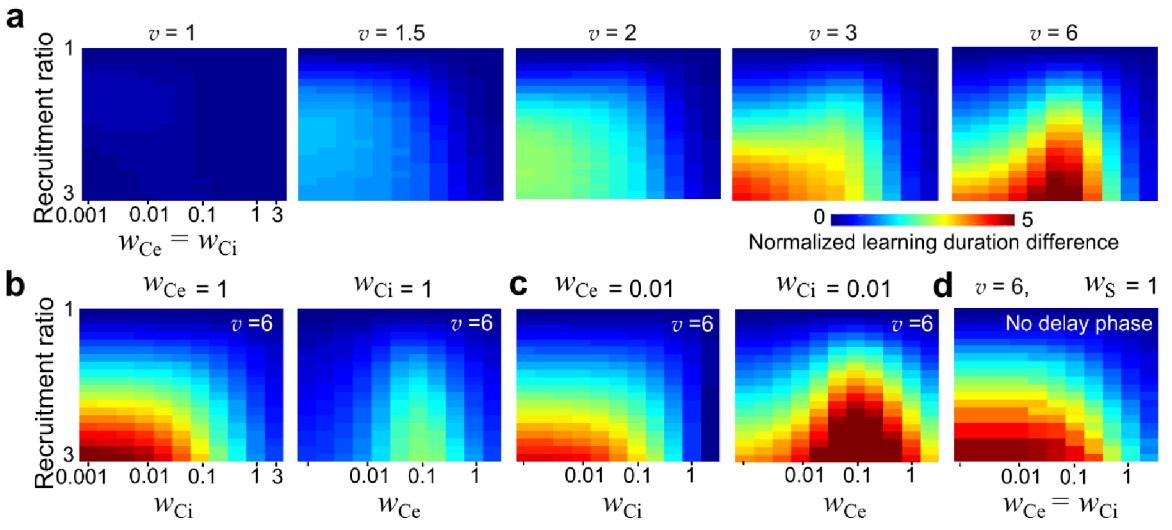


**Figure 3-9.The impact of neuronal recruitment on learning speed depends on the initial strengths of synaptic connections in the model**

a. Normalized learning phase duration difference (duration S- with more recruitment - duration S- with more recruitment)/(duration S- with more recruitment) is color-coded and plotted against the cortical recruitment ratio of the discriminated stimuli and the strength of the initial inhibitory and excitatory connection to unspecific cues ($w_{Ci}$ and $w_{Ce}$, same value for both). From left to right the value of the asymmetric learning rate parameter $\upsilon$ is increased. Simulation parameters: $w_S$ = 0.01, $\alpha$= 0.01, $\sigma$ = 0.6195. b. Same as a, but varying only the initial inhibitory (left) or excitatory connection (right) while the other connection is kept constant at value 1. c. Same as b, but with the non-varied initial connection kept at a constant value of 0.01. d. Same as a, but now with initial connectivity from sound stimuli $w_S$ = 1 such that there is no delay phase. In all plots, the recruitment ratio is equal to the larger of the two saliency values.

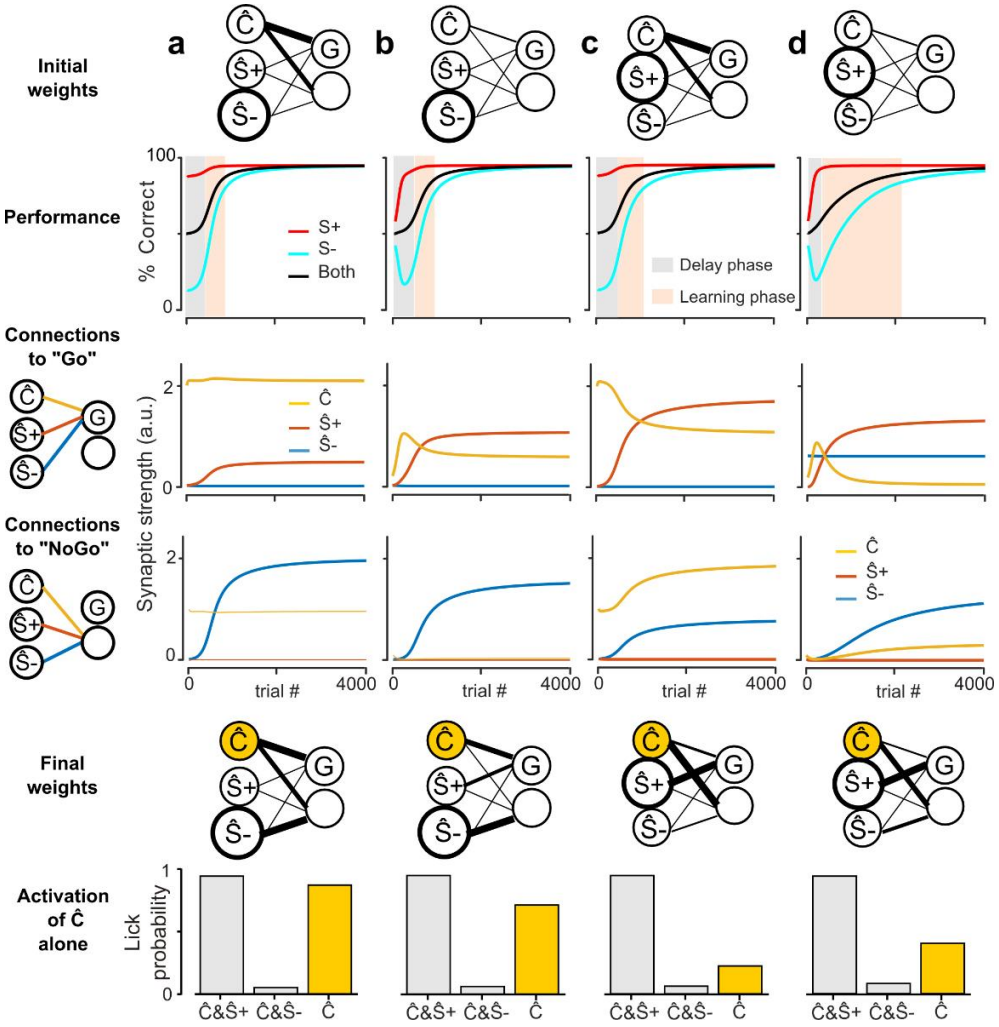


**Figure 3-10. The effects of neuronal recruitment in the model do not crucially depend on the magnitude of recruitment differences.**

Same simulations asinFigure 3-5, butwith a ratio of recruitment between the least and the most active stimulus equal to 1.4 (corresponding to the ratio of numbers of recruited neurons by sounds C and A) instead of 2 (chosen according to the ratio of population firing rates for sounds C and A). Simulation parameters: X= [1 ; 1; 1.4], $\alpha$= 0.01, $\sigma$ = 0.6195, $v$= 6, $w_{Ci}$ = 1, $w_{Ce}$= 2, and $w_S$= 0.01. b. Same as a, but with $w_{Ci}$ = 0.1, $w_{Ce}$= 0.2. c. Same as a, but with X = [1 ; 1.4 ; 1]. d. Same as c, but with $w_{Ci}$ = 0.1, $w_{Ce}$ = 0.2.

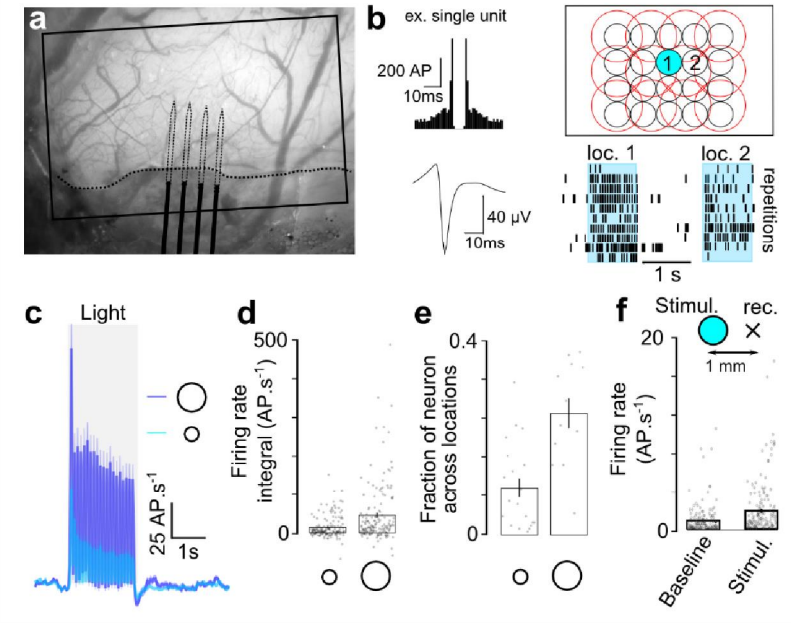


**Figure 3-11. Cortical responses to patterned optogenetic stimulations.**

a. Picture of the electrophysiolocal experiment setting. A 4-shanks silicon probe (sketched) is inserted with a shallow angle through a hole under the glass window (curved dashed line). The rectangle indicates the area covered by the videoprojector. b. Example waveform (bottom left) and spike train autocorrelogram (top left) of a single unit. An array of 3 x 4 stimulus locations (spacing 480 µm) was probed to reconstruct the spread of activity for the large disk (red, top right), and 4 x 5 locations (out of 5 x 8) were selected for the small disk in order to cover a similar extent as the grid of large disk centers. Example raster plots for two locations are shown at the bottom right. c. Mean response time course for all selected locations and single units (160 single units, 2 mice, 5 recording locations), for the small (light blue) and large (dark blue) disk. d. Integral of population (bars) and single units (gray dots) firing rate computed by summing over the grids of stimulus location for the small and large disk, in order to estimate the total response elicited by one disk across auditory cortex. The small disk elicits about 3 times less activity than the large disk (small 13.7 ± 2.0 $AP.s^{-1}$; large: 42.3 ± 5.7 $AP.s^{-1}$, n = 160 cells, in 2 mice). Thus, the recruitment difference (as measured for sounds in Figure 3-4B andFigure 3-8A) between the strong (1 small + 1 large disk) and weaker (2 small disks) stimuli is equal to $2*(S_{strong}-S_{weak})/(S_{strong}+S_{weak})$ = 69%. e. Average fraction of responsive neurons over the 160 neurons recorded across the same range of grid location centers for the small and large disks. Grey dots indicate the fraction of responsive neurons for individual locations. The small disk activated about 2.5 times less neurons than the large disk (small 10% ± 2%, n = 20 locations; large: 25 ± 3 %, n = 12 locations). Thus, the recruitment difference between the stronger and weaker stimuli is equal to 55%. f. Average activity recorded at the relative position of the Ĉ spot (1 mm away, Figure 3-6) with respect to the center of the large disk (estimated as the stimulus location that elicits the best response) before large disk stimulation (baseline) and during stimulation (stimul.). A residual

positive response is observed at the Ĉ spot location (baseline 0.87 ± 0.12 AP.s$^{-1}$, stimul. 1.89± 0.22 AP.s$^{-1}$, n = 160 cells). Error bars represent standard errors (SEM).

# 4. General discussion

Throughout this thesis, I have treated the role of later stages of the auditory system in sensory based decisions and learning processes in parallel. One of the aims of this section is to better link the concepts emerging from our two studies and propose new perspectives to feed future avenues of research.

## 4.1. Learning and remodeling of auditory cortex

Learning involves the correct extraction of behaviorally relevant stimulus features to generate the appropriate action and maximize reward. Here we use a simple associative learning paradigm to study different learning principles employed in auditory sensory processing. Learning and perceptual sensory decisions involve and generate structural changes in sensory cortices. These changes are thought to be an essential substrate for learning and for the expression of amemory trace. Different electrophysiological studies as well as more recent targeted two photon calcium imaging experiments, have highlighted that these individual neuronal changes through learning increase a neuron's ability to discriminate between sensory stimuli (*e.g.* Chu et al., 2016; Polley, 2006; Poort et al., 2015). These learning related changes at the single neuronal level, theoretically improve an animal's performance during a perceptual decision task (Makino et al., 2016). Particularly for audition, a vast literature exists showing the remapping of cortical features representations induced by learning, even for a simple pure tone detection task. Cortical remapping or features reorganization has also been observed during a sustained increment of neuromodulatory inputs (*e.g.* Bakin and Weinberger, 1996) as well as via targeted cortical micro-stimulations directly into AC (*e.g.* Maldonado and Gerstein, 1996). In some way, these observations are counterintuitive with one of our first and compelling results about the dispensable role of AC for simple pure tones discriminations (*see page* 60 and Figure 2-2).

In more detail, studies in non-human primates, as also in rodents, have shown the existence of a strong correlation between learning and an expansion in the cortical representation for the sound used to trained the subjects, even for a simple frequency detection task (Polley, 2006; Recanzone et al., 1993; Weinberger, 2007). These results have also been observed in other sensory systems for their corresponding sensory features (Poort et al., 2015; Wiest et al., 2010). These non-transient changes in

coding of a single sensory dimension after learning, are usually referred to as like ‘representational plasticity’ (RP) (Weinberger, 2015). In the auditory system, substantial gain in the tonotopic representations for frequency detection thresholds and tuning bandwidth sharpening has been observed. These changes would confer an increase detectability and acuity towards the trained frequency. Also others sound parameters have been tested and given similar results,examples being repetition rate(Bao et al., 2004),preferred stimulus intensity (Polley, 2006) or direction of frequency modulation(Ohl et al., 2001). In another line of experiments,Bieszczad and Weinberger (2010) observed that RP is dependent on the strategy that the animals use to solve a sounddetection combined withthe determination of sound duration.In their task, thirsty rats had to bar press (BP) to collect a water reward during the presentation of a pure tone. Animals could adopt two strategies to obtain the maximal amount of rewards, (i) BP until the end of the sound or (ii) bar press until the presentation of an alarm light indicating the end of the trialwhich gives a ‘grace period’ after sound offset. BPs during the Inter-Trial-Interval (ITI) were punished with a long time out period. Consequently, animals that used the first strategy, paid more attention to the onset and offset of the sound, while the other group paid attention to the onset of the sound but they keptpressing after sound offset until the appearance of the warning light(Bieszczad and Weinberger, 2010b). This change in strategy lead to different results were only the animals with the ‘grace period’ and alarm light, developed RP for the frequency of the pure tone used to trained the animals (Bieszczad and Weinberger, 2010a). Theseresults suggest that the change or reorganization of the tonotopic field in AC does not only depend on the pairing of a sound with a reward but also on the learning strategy used by the animalstogether with contextual factors, which suggests limitations about the scope of those observations. Artificial manipulations of brain circuitshave tackled this issue and tried to induced RPoutside of a behavioral setup-up in orderto show that tonotopic remappingis not only related to learning. Intra-cortical micro-stimulations (ICMS) experiments performed directly into the AC,which have been shown to affect the cortical organization by modulating nearby neuron’s receptive fields towards the center of the micro-stimulated area, producingsimilar reorganizations thanthe learning-induced changes in the tonotopic field, corroborating the multidimensionality and scope of this kind of results (Maldonado and Gerstein, 1996; Talwar and Gerstein, 2001).

Learning and memory formation cannot be accessed directly but only inferred from behavioral changes. From the coding stand point it is not because a change in the tuning curve of a particular neuron are

observed that these effects are causal to learning and that animals really used that sensory 'upgrade' to perform a sensory- based decision. Also contrary to the previously described experiments and results, several observations of an auditory memory formation without AC remapping or a sounds-related area expansion have been reported (Galindo-Leon et al., 2009; Gdalyahu et al., 2012; Shepard et al., 2016). When the actual behavioral effect of artificially induced AC remapping has been precisely tested, no improvement in frequency discrimination or detectability has been observed suggesting that these changes are insufficient to drive better perceptual capabilities (Talwar and Gerstein, 2001). As well as artificial manipulations, like the large tonotopic reorganizations observed due to paired electrical activations of the nucleus basalis and pure tone presentations (Bakin and Weinberger, 1996; Kilgard and Merzenich, 1998; Ma and Suga, 2003; Suga et al., 2002; Weinberger, 2007), has also been shown to not be behaviorally relevant in an already trained animal or required for good behavioral performance (Reed et al., 2011). Altogether these results have shown that tonotopic map expansion or the increase of some sensory feature representation in primary auditory cortex (AI) is not necessary for the expression of an auditory memory trace or the performance of an animal in a classical instrumental sound discrimination task. These conclusions are in close agreement with the results shown in our study, where AC proved to be dispensable in a pure tone vs pure tone discrimination task.Previous studies where dependency of AC for similar decision tasks was shown, have used the Ɣ-aminobutyric acid $(GABA)_A$ receptor agonist, muscimol, to inactivate transiently the AC during ongoing behavior (Jaramillo and Zador, 2011; Kuchibhotla et al., 2017; Smith et al. 2004; Talwar et al. 2001). It has been suggested that this compound can alter thalamocortical connectivity (Intskirveli et al., 2016), and could also diffuse to different brain structures necessary for any sound-driven behavior (*see below*). These possible caveats limit the interpretation of muscimol-based results and leave the possibility that secondary effects might explain the changes in performance observed.

## 4.2. Frequency discrimination without AC

During learning several parallel streams of information should adjust their connections based on reward and predictions errors. As described before,improved cortical discrimination of sensory stimuli acquired through learning and experience canbetter 'inform' than drive, downstream or association areasprecisely when this information is needed and available (Znamenskiy and Zador, 2013). We propose

with our work that during simple discrimination tasks, the cortical flow of activity towards decision and action centers in the brain can be easily bypassed by faster circuits. It has been described that projections from midbrain auditory stations or thalamus towards different decision centers in the brain can drive innate or conditioned behaviors (Xiong et al., 2015). Supporting this idea is the well-known and largely accepted observations that for the expression of conditioned fear to a specific pure tone, the AC is not necessary (Letzkus et al., 2011; Romanski and LeDoux, 1992). However, the medial part of the medial geniculate nucleus in the thalamus (MGm), which has projections to the amygdaloid complex, is sufficient to generate fear under those simple circumstances (Antunes and Moita, 2010; LeDoux et al., 1990; Maren, 2003; Quirk et al., 1997 ; Romanski and LeDoux, 1992). Also, defensive unconditioned innate behaviors can be drive by direct activations of the connections between inferior colliculus (IC) and the periaqueductal gray (PAG) (Xiong et al., 2015; Tovote et al., 2016). Moreover, in lower auditory centers, transient learning-based neuronal changes have been observed but their role is still poorly understood. Very few studies have shown this type of modulations, which has mostly been artificially induced through activations of corticofugal projections from AC (Kong et al., 2014; Ma and Suga, 2003; Yan and Ehret, 2001; Zhang et al., 1997; Zhang and Suga, 2005), leaving open the question of the relevance of these learning related changes undermore natural conditions.

In an appetitive associative conditioningparadigm, it is less clear whatis the minimumset of brain areas that is necessary and sufficient to sustain a simple discrimination behavior. Here we show that at least the information need to be routed from the inferior colliculus (IC) to the following downstream processing stations, as an optogenetic perturbation at this stage is detrimental for any type of sound discrimination (Figure 2-2). New evidence suggests that the thalamus has an important role during behavioral discriminations by conducting and orchestrating several cognitive faculties suchas attentional allocation and contextual shift (Nakajima and Halassa, 2017; Schmitt et al., 2017). Projections from lower stages of sensory processing could arrive to the same regions as corticofugal AC projectionsin decision centersand could trigger reward-associated actions. Recently, projections from the dorsal division of the MGB (MGd) to the dorsal striatum (Beckstead, 1984; Hunnicutt et al., 2016) haven been revisited showing their contribution in an overall frequency discrimination task using a cloud of tones (Chen et al., 2019). Silencing specifically MGd projections to the dorsal striatum or the ‘auditory striatum’ has an impact in the overall judgment of the frequency content of a cloud of short pure tones (100 ms) without having an impact on motivation or motor control (Chen et al., 2019). Despite the low number of MGd

projecting neurons that have a significant response to sounds (206/1178) showed in that study, they were still able to perturb part of the task. Those results in parallel brought some questions about what type of information these connections carry on (if it is not auditory as the majority of neurons do no respond to simple sounds) and what is their specific role in sensory-based decision tasks. This will be an interesting avenue for future research as now it is possible to label specifically different subpopulations of projecting neurons together with their specific targets (Nassi et al., 2015; Oyibo et al., 2014; Sjulson et al., 2016; Zingg et al., 2017) and image them withdeep-brain fluorescence microscopy in freely moving animals (Flusberg et al., 2008; Klaus et al., 2017; Ozbay et al., 2018; Ziv et al., 2013).

## 4.3. Frequency modulated sound vs pure tone

Frequency modulated sounds (FMs) are common in natural sounds and an important signature of vocalizations in most mammals (Kuchibhotla and Bathellier, 2018). Human speech as well, comprises several types of FMs, where certain aspects such as their frequency change modulation rate or the direction of the frequency modulation are crucial to distinguish between similar syllables and therefore different words. As mentioned before, there is a lot of ongoing work aimed at understanding theemergence, processing and integration of FMs responses in the auditory system. It is well known that the number of neurons tuned to certain FMs properties, increase from the brainstem to central stations of the auditory pathway (e.g., Whitfield 1969; Kelly and Whitfield 1971; Phillips et al. 1991), where AC processing is fundamental for their proper perception. Although the discrimination of FMs has been tested and proven to be cortically dependent, in recent works (*see page* 60: Role of auditory cortex in the discriminations of sounds), FMs discrimination tasks have used symmetrical sweeps where animals can use primary and solely spectral clues to solve the task, disregarding entirely the frequency modulation of the sounds (Rybalko et al., 2006). As introduced in previous chapters, It has been proposed that reinforcement learning can be achieved by focusing and paying attention to only a few stimulus features more than the overall or whole stimuli (Niv et al., 2015). In this way, testing auditory processing of precise sound features using symmetric FMs can lead to misleading conclusions, as the spectral content of FMs and its contribution to the proper discrimination of this type of sounds is often overlooked. Following with this idea, early observations in cats where AC lesions have an important effect in the correct discrimination of pure tone sequences (Diamond and Neff 1957; Kelly 1973),

indicates that cortical dependency can be due more to the temporal order of simple spectral features embedded in more 'complex' sounds than the overall discriminability of sound envelopes. Only one experiment of my knowledge has tested if animals could generate broad categorization of different FMs regarding the direction of the frequency modulation (Wetzel et al., 1998). The results showed good categorical performance when untrained FMs were presented, suggesting that animals have the cognitive capability, but only after several months of training (Wetzel et al., 1998). It is not entirely possible to rule outthe possibility that animals use simple spectral information in that task, as very similar sweeps were used in that study. Sounds varied in the rate of the modulation more than in the frequency content at sound onset allowing the animals to use that information and again disregardthe entire envelope or the overall frequency modulation of the sound. Others experiments, have tackled this issue by the use of 'cloud' or fast self-repeated FMs which in turn creates a more complex perceptual sound, where the processing power of AC to solve this type of discriminations is undoubtedly necessary for both, appetitive (Kelly and Whitfield, 1971) and aversive associative conditioning (Letzkus et al., 2011).

In our study we use the previous knowledge about the dependency of AC to treat and process FMs, in order to study the perceptual and causal contribution of the tonotopic organization for the discriminations of sounds in the mouse AC. We used a Go/noGo discrimination task of a frequency modulated sound against a pure tone (FMvsPT), with the particularity that both sounds started at the same frequency, forcing the animal to discriminate the sound identity by using more complex comparisons (Figure 2-1). The surprisingly large number of trials that the animals needed to achieve a good discriminative performance was the first indication that for the animalsthis was not a simple discrimination task, even though perceptually the two sounds are very different (Figure 2-1). The results obtained when the necessity of AC was tested, supported the previous observations, as in the presence of bilateral silencing of AC all subjects presented low discrimination performance back to chance levels (Figure 2-2). In order to explain the cortical dependency of this type of task and others using FMs, only few studies have looked into the details and tried to uncover the role of AC. In this respect, it has been suggested that the cortical necessity to perform a sound discrimination task can be related, either to animal's deficits for sound selectivity or sound sensitivity. For example in cats (Kelly and Whitfield, 1971) and gerbils (Ohl et al., 1999), a clear decrease in performance has been observed associated to an increased rate of False Alarms (FA), suggesting a potential cortical role of 'inhibitor' for the conditioned

behavior during the presentation of the CS- (Jarrell et al., 1987). The results obtained in this work, using the multiplicative reinforcement learning model can lean favor of this hypothesis (*see page* 124; Recruitment determines learning strategy). The model strongly indicates that animals trained under this type of Go/noGo discrimination task, the action of licking in the behavioral context by itself (Port unit) can be strongly reinforced and even overshadow the CS+ when this stimulus is not salient enough (Figure 3-5). In fact animals can solve a Go/noGo discrimination task by using the strategy of licking at every trial onset and only pay attention to the CS- sound to inhibit their conditioned behavior. In our study, even using random inter-trial-intervals and a 'wait' for no lick period, a clear strategy was not fully evident as close to the half of the animals presented selectivity and the other half sensitivity deficits. In 3/7 mice, discrimination went down due to a high rate of FA, contrary to the 4/7 of mice, where there was a clear effect in detection, as the discrimination performance went down due to the decreased rate of Hits and maintained correct rejection (CR) responses, meaning that the animals did not lick at all during the optogenetics trials (Figure 4-1). It needs to be clarified that both effects were observed only in trials with the optogenetic inactivation of AC, as regular trials were unaffected during the same sessions (Figure 2-2). It is unlikelythat the light by itself would have perturbed the animals during behavior as they were well habituated to the random presence of light inside the behavioral box.

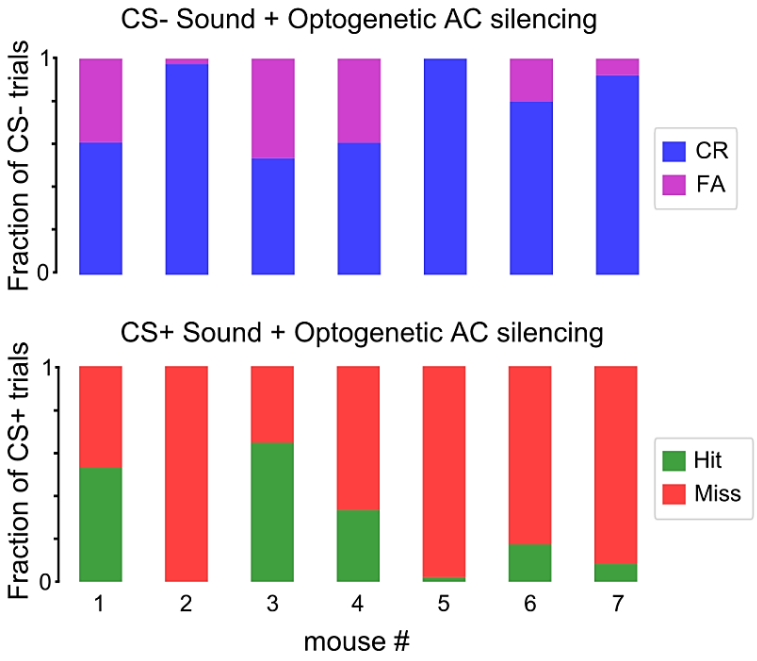


**Figure 4-1. Error type for mice during AC silencing.**

Fraction of trials that correspond to the different behavioral outputs in response to CS+ and CS- during optogenetic AC silencing. Colors correspond to hits, misses, correct rejections (CR) and false alarms (FA).

To better understand our results, we studied the licking profile of the animals during this task revealing that all subjects presented an early licking behavior for both sounds (Figure 2-4). This pattern indicates that in fact the subjects indeed did not discriminate the sound identity at the beginning, starting to respond at every trial precisely at sound onset. Only later subjects could use the deviant frequencies between the two sounds to continue or to stop licking. Using two photon calcium imaging in awake naïve mice, we could observe that indeed both sounds activate the same population of neurons by the strong correlation of cortical activity at sound onset (Figure 4-2A). Cortical activity elicited by the sounds diverge as time continues and only after ~100 ms the activity should be deviant enough to generate or report the decision as observed with the carefully measured decision time of about ~ 350 ms for this task (Figure 2-4 and Figure 4-2B).

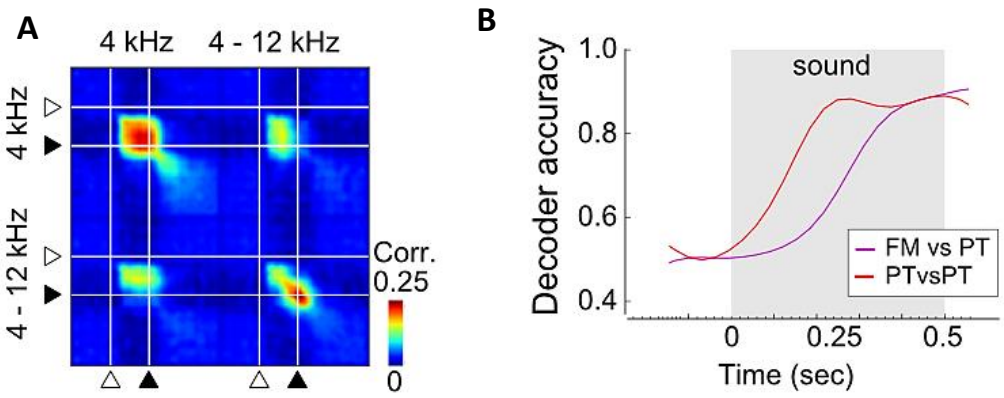


**Figure 4-2.AC cortical activity is correlated at the onset of sounds.**
(A) Activity correlation matrix of the sounds used in the hard task. White filled triangle indicates sound onset and black filled triangle indicates sound offset. (B) SVM trained with cortical activity of different sounds and tested discrimination accuracy in time for the different sound discriminations labeled. Lines were smoothed applying a Gaussian filter.

These observations strongly suggest that animals faced withthis 'difficult' discrimination task adopted a strategy to maximize the amount of reward and in this case, using an early and probably subcortical mechanism,they initiatethe conditioned behavior irrespective of the stimulus identity.Only after the involvement of AC to temporally discriminate spectral deviantsound features, the ongoing behavior can

be maintained or 'corrected' to avoid unwanted delays (as false alarms leads to 'long' and also variable time outs) (Figure 2-7). This strategy in a certain way can be imposed due to our learning contingencies, as for example by the use of a first phase where a certain number of rewards are given irrespective of the behavior and only the CS+ is regularly presented (*see page* 131; Material and Methods). This behavioral training paradigm is thought to rapidly train the animals to lick and maintain high levels of motivation. When a good and reliable level of conditioning in this starting phase of training is observed, the CS- is introduced, making the animals to pay more attention to the stimuli and learn to discriminate between them, in order to obtain the best amount of rewards in the least amount of time. In summary, the difference in cortical dependency for the complex discrimination compared to the easy PTvsPT task, may be that animals cannot solve it using spectral cues at the beginning and they need to track the sound in the temporal domain in the decision circuit. This additional processing power is provided by cortical areas, as AC silencing disrupts the correct performance of the taskindependent of the strategy used by the animal (Figure 2-2). This type of selectivity has been observed in the context of fear conditioning using a sound (CS) paired with mild foot shock (US) (Guimarãis et al., 2011). The correct acquisition and expression of a classic fear conditioning, requires the amygdala and medial prefrontal cortex (mPFC) but not the hippocampus. Guimarãis and colleages (2011) shown that using different time intervals between the CS and US has a direct influence in the brain areas involved in this task. Increasing the time gap between the two events the dorsal-hippocampus becomes involved and necessary for the acquisition of the fear conditioning (Guimarãis et al., 2011). In summary with these observations and our results, it becomes clear that the temporal relationship between events and their integration in the brain to solve a sensory-based decision task requires the activity of multiple and distinctive areas of the brain.

## 4.4. Optogenetics to study sensory perception

The use of optogenetics has become the state of the art to dissect the role of different brain circuit components. Even though, only a few groups have shown that it is possible to train an animal to detect an artificial optogenetically-induced activity pattern (Choi et al., 2011; Huber et al., 2008; Nomura et al., 2015).Still fewer studies have enhance sensory thresholds or stimulus detectability using precise optogenetic manipulations (Musall et al., 2014; Aizenberg et al., 2015) or transiently biased perceptual-based decisions with optogenetics perturbations during ongoing behavior (O'Connor et al., 2013; Peng et

al., 2015; Znamenskiy and Zador, 2013). Here we have shown for the first time that animals can discriminate two different light-sculpted optogenetic activations in the same hemisphere and cortical domain (Figure 2-4 and Figure 3-6). More interestingly, it was also possible to train the animals using more complex light stimuli, as the use of three independent circles of different sizes and different combination patterns (Figure 3-6). These novel, artificially created stimulus combinations helped to elucidate the causal role of neuronal recruitment to determine learning strategy and establish the relationship between cortical recruitment as the saliency parameter in regular learning models (Figure 3-6). The use of patterned optogenetic stimulation in awake animals makes it also possible to combine targeted cortical activations within a sound discrimination task. Using this approach, we tested if a pure tonotopically-targeted artificial activation could be used to trigger the conditioned behavior in a cortex dependent sound-driven discrimination task (FMvsPT) and determine the precise information that animals used to solve this 'hard' task. In this way and in parallel, we could test if the subjects learned to recognize different 'classes' of sounds (one modulated and the other static) or if they use simple spectral features to differentiate between the two sounds to solve the task. Directed optogenetics stimulations in AC during the FMvsPT task, indeed helped to elucidate the role of AC and the strategy that the animals used to solve the task, showing that in the presence of the 4 kHz pure tone an artificial activation of middle frequency coding neurons was sufficient to bias the perceptual decision of the mousefor few trials in most animals tested (Figure 2-5). Some studies have found special areas that respond to FMs in AC using different techniques and there is evidence for a topographic map of FMs in AC observed across several species (*see page* 23; Other stimulus representations in auditory cortex). For example, Honma and colleagues (2013) showed specific responses to a series of continuous FMs using flavoprotein fluorescence responses in UF and DP in mice. Going further and more recently, they observed different projection patterns towards these areas in the mouse AC, showing that their inputs are coming preferentially from a distinct area of the ventral division of the auditory thalamus (MGv) than the ones arriving to AI (Honma et al., 2013; Tsukano et al., 2015; Tsukano et al., 2017b). Our results are also in agreement with recent suggestions about the cortical organization of AC in mice and its subdivisions, emerging from the previous studies just described (Tsukano et al., 2017a). The optogenetic 'HotSpot' will probably be located in the new delineated tonotopic gradient, the dorsomedial area (DM) (Figure 1-11 and Figure 2-6), but a more detail study is needed. Issa and colleagues (2014) using widefield transcranial imaging of calcium responses together with single-cell two-photon calcium imaging in mice, showed an unspecific intermediate zone responsive almost exclusively to vocalizations and FMs, close to the tail of

our delignated 'HotSpot' (Figure 2-6). Even though our results in general indicate that the activation of middle frequency neurons is crucial and sufficient to solve this task, we cannot rule out the contribution of neurons specialized in the processing of FMs. Targeting this specific set of neurons and studying their rolein a discrimination task of this type can be a promising venue for future research. A robust approximation towards this framework has already been done by Tasaka and collegues (2018). In their study, they use the expression of immediate early genes (IEG) for targeting an specific set of neurons responsive only to pup wriggling calls and ultrasonic vocalizations (USVs) in AC of mice (Tasaka et al., 2018). Finally, targeted expression of ChR2 can be achieved using these types of techniques, as it has been done to stimulate engram neurons in the hippocampus and express a fear memory (Liu et al., 2012). The combination of auditory stimulation and precise neuronal targeting then can be the next way to study precisely the role of different type of neuronal responses and their direct and specific role in behavioral paradigms.

## 4.5. General observations

The results attained within this thesis, are different in several aspects from previous studies that have used direct optogenetic stimulations on cortical surfaces to study sensory perception. Here, we have used complete cortical mapping before doing any cortical manipulation in order to target precisely the same sub-regions of AC across different animals. It has been observed that the blood vessel pattern as well as the position and size of AC can vary between animals (Issa et al., 2014; Stiebler et al., 1997; Tsukano et al., 2016), therefore electrode or optical fiber insertions without a functional mapping of AC for each individual can lead to misleading results and conclusions.In our experiments we have used optical imaging of intrinsic signals using a red shifted LED (780 nm) in anesthetize animals with isoflurane (Figure 2-10; Figure 2-12 and Figure 3-6). This wavelength was used because of mismatches observed between electrode mapping experiments and optical spatial responses obtained with the regular green LEDs used in most previous studies (540 nm). These mismatches can be due to local and more superficial blood volume changes independent of neuronal activity (Spitzer et al., 2001). It is well known that intrinsic imaging depends on deoxyhemoglobin changes which can be registered better with red light than green light. Therefore, by using a red-shifted lightin our experiments, it is conceivable that deeper and more reliable intrinsic signals were obtained.Together with the coarse mapping of the AC, here we

used light-sculpted optogenetics (Dhawale et al., 2010; Sakai et al., 2013) to scan and test the contribution of different tonotopic locations of the entire AC in the same animal during ongoing behavior. This had a great advantage compared to other studies that have used tetrodes combined with optical fibers to deliver the light (Znamenskiy and Zador, 2013). Is it well-know that electrophysiological measurements can be biased towards the most active cells hiding maybe the real averaged best frequency of a certain area. Probably that is the reason why Znamenskiy and Zador (2013) failed to bias the decision of the animals using non-targeted optogenetics stimulations in AC and only succeededlater when a small portion of cortical neurons was targeted. Also, in our study all optogenetics perturbations were done in the right AC. Several studies have suggested that an hemispheric division in control and processing of certain auditory features (Rauschecker and Scott, 2009), such as vocalizations and/or frequency modulations responses are more localized in the right (Abrams et al., 2008; Petersen et al., 1978; Poeppel et al., 2004; Poremba et al., 2004; Rybalko et al., 2006; Wetzel et al., 1998) and amplitude modulations in the left hemisphere (Rybalko et al., 2010; Schulze et al., 2014). Contrary to the study of Guo and colleagues (2014) where they scan the entire neocortex in search of regions that can perturb a whisker-based decision task in mice, we scan the tonotopic organization of AC in search of areas that trigger the opposite behavior (Go response) of the one orchestrated by the presence of the noGo sound or CS- (Figure 2-5). This search led to the finding of a particular 'HotSpot' where optogenetics perturbations had a significant behavioraloutput with a clear interpretation (Figure 2-5). Also the framework used here of a cortically dependent Go/NoGo sound discrimination task was really important. Cortexindependent tasks could make use of faster and shorter circuits (Antunes and Moita, 2010;Xiong et al., 2015). One drawback of our manipulations was the lability of catch trial responses over a large number of repeats, observed for our optogenetic manipulations (Figure 2-5). We think that the total absence of reward and the big number of these test trials could have been the explanation for these transient responses plus the non-specificity of our ChR2 targeting (see below). Highly trained animals try to maximize the reward with the minimal effortas they show very stereotypical behavior. This could make them stop fast to non-rewarded trials as they were not encouraged to keep responding to them in any sense. CS+ that leads to highly predictable rewards can also be detrimental for this kind of protocols as described in earlier chapters (*see page*40; Learning from predictions). The use of a variable percentage of CS+ rewarded can maintain the animal's motivation to explore, having on average more trials to study perceptual manipulations in behaving animals. On the other hand, the used of non-rewarded trials allowed us to cleanly address the perceptual contribution of ouroptogenetic perturbations, contrary to

previous studies were test conditions were rewarded in the same way as the CS+ (O'Connor et al., 2013; Peng et al., 2015; Znamenskiy and Zador, 2013). As we also showed here, animals can easily learn to detect an optogenetic stimulation and trigger the same behavioral output of any conditioned stimulus paired with a reward (Figure 2-4). A solution can also be to reward only a percentage of these test trials to keep animals motivated to explore and generalized in a greater degree and not so restrictively. Lastly, another drawback of our work is that we have used broad expression of ChR2 in all layers of AC, contrary to previous works (O'Connor et al., 2013; Znamenskiy and Zador, 2013), where ChR2 expression was restricted to either one particular layer of the cortex or subpopulations of projecting neurons. Targeting a vast number of cortical neurons could also have been detrimental for our results due to the obvious non-specific interactions of neuronal tuning features, incrementing the dissimilarity of the artificially generated 'sound' perception. This is one 'easy' aspect that can be studied in the future in more detail to improve the reproducibility and scope of our results.

## 4.6. Considerations about the auditory neural code

Whether animals base their sensory decisions on the population average activity or a sparse but precise spike sequences has been a long standing question in neuroscience (Brette, 2015; Panzeri et al., 2017; Parker and Newsome, 1998). O'Connor and colleagues (2010) studying the somatosensory cortex of mice during a vibrissa-based pole localization, have suggested that neuronal discriminability of stimulus identity is highly correlated with the neuronal firing rate. Neurons with intrinsically high firing rates, as for example neurons located in layer IV and V,have more discriminative power about pole position than others (Daniel H. O'Connor et al., 2010). Despite this observation, they also found a sparse group of neurons in superficial layers of S1 that were highly discriminative, suggesting that their precise activation could drive behavior. Other results at that time obtained by Huber and colleagues (2008) certainly showed that the optogenetic activation of only few hundreds of superficially located neuronscan generate a behaviorally detectable neuronal activity (Huber et al., 2008). O'Connor and colleagues(2013) expanded their previous observations and described that precise genetically targeted optogenetic perturbations in layer IV of S1, can indeed generate 'illusory' sensation of a virtual pole. Going further they observed that precise spike timing perturbations did not have an enhanced effect for thedevelopment of the virtual touch compared tocoarse firing rate modifications (O'Connor et al., 2013).

Similar 'illusory' sensory perception was achieved by the coarse activation of 'taste' neurons in the insular cortex of mice trained to discriminate different tastes in water(Peng et al., 2015). Contrary to this, Poort and colleagues (2015) observed in animals performing a grating discrimination task in a virtual reality environment, atransient and more restricted increase in the discriminability ofneurons in superficial layers of V1. This effect was highly reduced when animals were not engaged in the visual discrimination task (Poort et al., 2015). This important observation suggested that the improved decoding of stimulus identity can be due to top-down neuromodulatory signals directly impacting superficial cortical circuits, as it has also been shown recently for mouse AC (Kuchibhotla et al., 2017; Bagur et al., 2018). Summarizing these previous observations in awake animals, it looks like an acute reduction of non-specific population responses and increased discriminability by only a portion of neurons in primary sensory areas, is a common feature of learned sensory-based decisions (Chen et al., 2013; Chu et al., 2016; Makino and Komiyama, 2015; Makino et al., 2016; Peron et al., 2015; Tsunada et al., 2016). In fact, recent evidence support these observations but suggests that these learning induced changes rely on the behavioral state of the animal (Bagur et al., 2018; Kuchibhotla et al., 2017; Makino and Komiyama, 2015; Poort et al., 2015). Finally, independent of previous observations, it is apparent that coarse activations of many non-discriminative and a few highly discriminative cells in superficial cortical layers, is sufficient to inform downstream areas and drive the proper behavioral decision (Figure 2-5). In the auditory system especially of mice, this is the matter of a strong debate as there is no ground proof of basic organizational features or the final scope and contribution of cortical processing for sound discrimination and perception (*see page* 60; Role of auditory cortex in the discriminations of sounds). Some studies suggest that even though tonotopy is a well-known canonical organization, stimulus features beyond frequency emerge through the auditory system. For example, precise temporal details are transformed and coded only into firing rates (Guo et al., 2015). Putting together previous observations with our results, it seems possible to implement coarse perturbations of sound perception at the level of the AC, based on the tonotopic map, but certainly, finer spatial resolution will be necessary to study precise sensory features.

Coming back to the transient effects observed in primary sensory areas regarding the behavioral state of the animal. In our experiments, we addressed this issue by measuring the cortical representation of the task sounds across different behavioral states of the animals (Figure 2-12 and Figure 2-13). Intrinsic imaging was performed during anesthesia and the possible variation of sensory representations between

different attentive states was studied in awake animals using two photon calcium imaging in both, passive listening and active ongoing behavior. Overall we observed a good correspondence between the different techniques (Figure 2-12). We also showed that animals who have learned to discriminate our FMvsPT task presented a surprising behavioral categorization for pure tones (Figure 2-7). Recording sound responses with two photon calcium imaging in naïve animals and training a classifier with these responses resulted in similar classifier categorization boundaries as the observed in trained animals (Figure 2-7). Similar results have been obtained in AC and other sensory modalities, where the cortical activity can be used to predict the categorization of trained animals (*see page* 58; Linking two disciplines). These results, together with our optogenetics manipulations elucidated causally the strategy that the animals were using to solve this cortically dependent task (Figure 2-7).

Different types of cortical manipulations have shown that coarse manipulations of the neural activity have profound perceptual consequences. Here, we show that coarse activity patterns imposed in cortical circuits can trigger the same behavioral outputs trained and learned by the animals in appetitive conditioning paradigms. Several routes can be taken to improve and better control the results obtained as some of them have been already mentioned but also, the increasing optical power and targeting technology can be now combined to achieve single cell recording and optogenetics activations/silencing (Chen et al., 2018; Chen et al., 2019; Packer et al., 2015; Pégard et al., 2017; Quan et al., 2018; Ronzitti et al., 2017; Ronzitti et al., 2018; Yang et al., 2018). These precise manipulations can have plausible behavioral readouts as the striking results o fHouweling and Brecht (2008), where they have shown that perturbations in the activity of only one single neuron can be already behaviorally detectable.

## 4.7. Therapeutic strategies using optogenetics

Several alternative therapeutic strategies for partial or complete deaf people have been under investigation during the last years in order to improve speech understanding and music appreciation (Kohlberg et al., 2014). Usually, it is noted that cochlear implant users have lower frequency or pitch resolution together with poor sound intensity perception and reduced temporal acuity (Jeschke and Moser, 2015). The idea of optogenetic prostheses for the amelioration of acoustic disorders has been gathering a lot of attention in the last years, as the first attempts and prototypes have shown impressive

temporal and spectral sound encoding capabilities compared to regular electric cochlear implants (Guo et al., 2015; Keppeler et al., 2018). Several mutations and diseases can affect sound transduction from the cochlea to midbrain auditory stations (Starr et al., 2008). Also, It is well-known that certain sound properties and sound perception in general is not only encoded in the cochlea, as for example the phase locked responses to the periodicity of sound by spiral ganglion neurons of the auditory nerve (Nayagam et al., 2011). Sound level or intensity is also mediated by asymmetrical recruitment of out-of-frequency spiral ganglion neurons. Under these constrains together with direct lesion on the auditory nerve, alternative approaches are needed to directly translate sounds into the midbrain auditory stations (Darrow et al., 2015) and, directly into the cortical surface, as it has been shown recently for V1 of non-human primates (Chernov et al., 2018). There is a lot of room to improve ChR2 delivery systems into human tissues, besides the ongoing targeted genetic therapy approaches which are exponentially growing every year. Until now, there are more than 2000 clinical trials that have occurred and/or are in progress, related to restoring vision in blind people, eradication of blood cancer, correction of hemoglobinopathies and immune system deficiencies (Kumar et al., 2016), which makesit likely to soon solve gene delivery issues into human cells at any developmental stage. In summary, the growing fields of research on the generation of new and/or upgraded optogenetic tools combined with prosthetics engineering will soon converge into the implementation of optogenetic prostheses into human hosts.

## 4.8. Towards a complete and inclusive learning model

Modern neuroscience has a strong bias towards reverse-engineering the brain. This approach combined with powerful computational tools can engender different type of models which could help to explain observed neurophysiological data and propose novel predictions. Several approaches have been already implemented at different scales and complexity levels, as today we can find models from single neurons to complex neuronal networks or even entire brain structures (Erö et al., 2018). Reductionism approaches have tried to model more simple organism but it is still an ongoing multidisciplinary effort, being able today to only account for only few thousands of neurons and run in resting state-like behavior (Epelde et al., 2018; Huang et al., 2018; Sarma et al., 2018; Szigeti et al., 2014). Taking this into account, for the mammalian brain a more realistic and minimalistic approach is necessary as modeling only one sensory modality (with vision winning the race) and all possible *ad-hoc* sensory feature interactions. A

complete detailed model of the auditory systems does not exist yet but many efforts have been made to model accurately some auditory responses at different levels (Deneux et al., 2016). Auditory models have expanded their scope from simple linear spectro-temporal receptive fields models (STRFs) (Aertsen and Johannesma, 1981), towards the use of several non-linearities and deep neuronal networks to explain, the appearance of direction of frequency modulation and other sound interactions (Patil et al., 2012). In parallel, the modeling of neuronal processes such as associative learning and sensory discrimination have gained an enormous complexity (*see page* 33; Learning from predictions), reaching several different fields of research. The final aim is to be able to combine these different types of models into one integrative framework that could account for the coding of different sensory features and their integration in the brain through sensory experience.

Here we described that saliency, an important and so far unexplained experimentally sensory feature, in fact has a neurophysiological correlate that can be now introduced in future learning models as the degree of neuronal recruitment. It is obvious that more work needs to be done to completely model animal learning, even under simple learning paradigms such as the one that we described in this work. Go/no-Go discriminations tasks are simple in essence but complicated to disassemble as several components have not yet been considered by any learning model, such as the animal motivation and impulsive behaviors. More in detail, it has been observed that animals in this type of behavioral paradigm, show differential behavioral states during the course of one training session (Berditchevskaia et al., 2016). High levels of impulsivity can be observed at the beginning of each session, decreasing as trials proceed and the level of deprivation decreases, to reach a middle point where the instrumental conditioning strategy and motivation of the animal is crucial to keep responding robustly. In a final stage, satiety or tiredness determines when the animal stops responding and the behavioral session ends. These important parameters have to be implemented in future models as they govern finally the measurable sensory readouts. The used of self-initiated trials in freely moving animals or during two-alternative forcedchoice tasks (2AFC) can help to dissociate these variables, but animals under these different learning paradigms take significantly longer to reach good performance levels (Schmitt et al., 2017).

Simply in principle, rewarded actions can impact several brain structures. As described by Bathellier and colleagues (2013), their reinforcement learning model (RLM) learns by using a multiplicative rule and a

biologically plausible prediction-error term. Based on the literature, there are several intermediary steps in between the sensory domain (modeled in the RLM as independent sensory units) and the decision center (modeled in the RLM as one single sensory unit). An important hub of sensory information in the brain is the striatum, as it corresponds to the main input center of the basal ganglia and the anatomically preferential site where sensory inputs can encounter prediction-error signals from dopaminergic neurons (Xiong et al., 2015). Learning then can be seen in this region as the weighting of corticostriatal connections through the gating of dopaminergic feedback under the rules of long term potentiation (LTP) and depression (LTD), as in most spike-timing dependent plasticity mechanisms (Markram et al., 1997). Through LTP and LTD of the different output pathways of the striatum (direct and indirect), which provide GABAergic inputs to motor centers in the brain (Ficalora and Mize, 1989; Klaus et al., 2017), motor actions can be selected and controlled as activations of the direct pathway potentiate movement and activations of the indirect pathway inhibit it (Barbera et al., 2016; Kravitz et al., 2010). Certainly these two subpopulations of neurons do not have totally orthogonal behavioral readouts and their orchestrated activation lead to the proper control of the learned motor actions (Cui et al., 2013; Tecuapetla et al., 2014; Tecuapetla et al., 2016).

## 4.9. Concluding remarks

Optogenetic manipulations combined with recent technological advances and new genetic targeting strategiesis the best currentstrategy to achieve a better understanding and control of sensory perception in behaving animals. Moving towards a broader and more biologically precise learning model, all sensory feature interactions and non-linearities defined so far could be integrated in the ‘sensory units’ of the RLM described here. Intermediate steps between the ‘sensation’ and ‘decision’ parts could be included as new motor-skill selection layers inspired by the brain’s hierarchical connectivity patterns. Through dopaminergic-like prediction-error signals, these intermediate steps could also be implemented with the ability to learn and weigh the proper behavioral repertoire. To account for the different learning strategies, experimenters should consider the more instinctive behaviors observed at the beginning of any behavioral training. In this way, associative learning and its governing rules could be precisely modeled and finally unraveled.

# References


Abeles, M., Bredberg, Gö., Butler, R.A., Casseday, J.H., Desmedt, J.E., Diamond, I.T., Erulkar, S.D., Evans, E.F., Goldberg, J.M., Goldstein, M.H., Green, D.M., Hunter-Duvar, I.M., Jeffress, L.A., Neff, W.D., Yost, W.A., Zwicker, E., Keidel, W.D., 1975. Auditory System: Physiology (CNS)· Behavioral Studies Psychoacoustics. Springer Berlin Heidelberg, Berlin, Heidelberg.

Abeles, M., Goldstein, M.H., 1970. Functional architecture in cat primary auditory cortex: columnar organization and organization according to depth. J. Neurophysiol. 33, 172–187. https://doi.org/10.1152/jn.1970.33.1.172

Abrams, D.A., Nicol, T., Zecker, S., Kraus, N., 2008. Right-hemisphere auditory cortex is dominant for coding syllable patterns in speech. J. Neurosci. Off. J. Soc. Neurosci. 28, 3958–3965. https://doi.org/10.1523/JNEUROSCI.0187-08.2008

Aertsen, A.M., Johannesma, P.I., 1981. The spectro-temporal receptive field. A functional characteristic of auditory neurons. Biol. Cybern. 42, 133–143.

Aizenberg, M., Mwilambwe-Tshilobo, L., Briguglio, J.J., Natan, R.G., Geffen, M.N., 2015. Bidirectional Regulation of Innate and Learned Behaviors That Rely on Frequency Discrimination by Cortical Inhibitory Neurons. PLoS Biol. 13, e1002308. https://doi.org/10.1371/journal.pbio.1002308

Andermann, M.L., Moore, C.I., 2006. A somatotopic map of vibrissa motion direction within a barrel column. Nat. Neurosci. 9, 543–551. https://doi.org/10.1038/nn1671

Angeloni, C., Geffen, M.N., 2018. Contextual modulation of sound processing in the auditory cortex. Curr. Opin. Neurobiol. 49, 8–15. https://doi.org/10.1016/j.conb.2017.10.012

Antunes, R., Moita, M.A., 2010. Discriminative Auditory Fear Learning Requires Both Tuned and Nontuned Auditory Pathways to the Amygdala. J. Neurosci. 30, 9782–9787. https://doi.org/10.1523/JNEUROSCI.1037-10.2010

Arcediano, F., Matute, H., Miller, R.R., 1997. Blocking of Pavlovian Conditioning in Humans. Learn. Motiv. 28, 188–199. https://doi.org/10.1006/lmot.1996.0957

Arenkiel, B.R., Peca, J., Davison, I.G., Feliciano, C., Deisseroth, K., Augustine, G.J., Ehlers, M.D., Feng, G., 2007. In vivo light-induced activation of neural circuitry in transgenic mice expressing channelrhodopsin-2. Neuron 54, 205–218. https://doi.org/10.1016/j.neuron.2007.03.005

Asaba, A., Hattori, T., Mogi, K., Kikusui, T., 2014. Sexual attractiveness of male chemicals and vocalizations in mice. Front. Neurosci. 8, 231. https://doi.org/10.3389/fnins.2014.00231

Assael, Y.M., Shillingford, B., Whiteson, S., de Freitas, N., 2016. LipNet: End-to-End Sentence-level Lipreading. ArXiv161101599 Cs.

Atencio, C.A., Schreiner, C.E., 2010. Laminar Diversity of Dynamic Sound Processing in Cat Primary Auditory Cortex. J. Neurophysiol. 103, 192–205. https://doi.org/10.1152/jn.00624.2009

Atencio, C.A., Sharpee, T.O., Schreiner, C.E., 2008. Cooperative nonlinearities in auditory cortical neurons. Neuron 58, 956–966. https://doi.org/10.1016/j.neuron.2008.04.026

Bachatene, L., Bharmauria, V., Cattan, S., Chanauria, N., Etindele-Sosso, F.A., Molotchnikoff, S., 2016. Functional synchrony and stimulus selectivity of visual cortical units: Comparison between cats and mice. Neuroscience 337, 331–338. https://doi.org/10.1016/j.neuroscience.2016.09.030

Baetu, I., Baker, A.G., 2010. Extinction and blocking of conditioned inhibition in human causal learning. Learn. Behav. 38, 394–407. https://doi.org/10.3758/LB.38.4.394

Bagur, S., Averseng, M., Elgueda, D., David, S., Fritz, J., Yin, P., Shamma, S., Boubenec, Y., Ostojic, S., 2018. Go/No-Go task engagement enhances population representation of target stimuli in primary auditory cortex. Nat. Commun. 9, 2529. https://doi.org/10.1038/s41467-018-04839-9

Bajo, V.M., Nodal, F.R., Bizley, J.K., Moore, D.R., King, A.J., 2007. The ferret auditory cortex: descending projections to the inferior colliculus. Cereb. Cortex N. Y. N 1991 17, 475–491. https://doi.org/10.1093/cercor/bhj164

Bajo, V.M., Nodal, F.R., Moore, D.R., King, A.J., 2010. The descending corticocollicular pathway mediates learning-induced auditory plasticity. Nat. Neurosci. 13, 253–260. https://doi.org/10.1038/nn.2466

Bakin, J.S., Kwon, M.C., Masino, S.A., Weinberger, N.M., Frostig, R.D., 1996. Suprathreshold auditory cortex activation visualized by intrinsic signal optical imaging. Cereb. Cortex N. Y. N 1991 6, 120–130.

Bakin, J.S., Weinberger, N.M., 1996. Induction of a physiological memory in the cerebral cortex by stimulation of the nucleus basalis. Proc. Natl. Acad. Sci. U. S. A. 93, 11219–11224.

Bandyopadhyay, S., Shamma, S.A., Kanold, P.O., 2010. Dichotomy of functional organization in the mouse auditory cortex. Nat. Neurosci. 13, 361–368. https://doi.org/10.1038/nn.2490

Bao, S., Chan, V.T., Merzenich, M.M., 2001. Cortical remodelling induced by activity of ventral tegmental dopamine neurons. Nature 412, 79–83. https://doi.org/10.1038/35083586

Bao, S., Chang, E.F., Woods, J., Merzenich, M.M., 2004. Temporal plasticity in the primary auditory cortex induced by operant perceptual learning. Nat. Neurosci. 7, 974–981. https://doi.org/10.1038/nn1293

Barbera, G., Liang, B., Zhang, L., Gerfen, C.R., Culurciello, E., Chen, R., Li, Y., Lin, D.-T., 2016. Spatially Compact Neural Clusters in the Dorsal Striatum Encode Locomotion Relevant Information. Neuron 92, 202–213. https://doi.org/10.1016/j.neuron.2016.08.037

Barkat, T.R., Polley, D.B., Hensch, T.K., 2011. A critical period for auditory thalamocortical connectivity. Nat. Neurosci. 14, 1189–1194. https://doi.org/10.1038/nn.2882

Barnstedt, O., Keating, P., Weissenberger, Y., King, A.J., Dahmen, J.C., 2015. Functional Microarchitecture of the Mouse Dorsal Inferior Colliculus Revealed through In Vivo Two-Photon Calcium Imaging. J. Neurosci. Off. J. Soc. Neurosci. 35, 10927–10939. https://doi.org/10.1523/JNEUROSCI.0103-15.2015

Bartlett, E.L., Wang, X., 2005. Long-lasting modulation by stimulus context in primate auditory cortex. J. Neurophysiol. 94, 83–104. https://doi.org/10.1152/jn.01124.2004

Basch, M.L., Brown, R.M., Jen, H.-I., Groves, A.K., 2016. Where hearing starts: the development of the mammalian cochlea. J. Anat. 228, 233–254. https://doi.org/10.1111/joa.12314

Bathellier, B., Tee, S.P., Hrovat, C., Rumpel, S., 2013. A multiplicative reinforcement learning model capturing learning dynamics and interindividual variability in mice. Proc. Natl. Acad. Sci. U. S. A. 110, 19950–19955. https://doi.org/10.1073/pnas.1312125110

Bathellier, B., Ushakova, L., Rumpel, S., 2012. Discrete Neocortical Dynamics Predict Behavioral Categorization of Sounds. Neuron 76, 435–449. https://doi.org/10.1016/j.neuron.2012.07.008

Beckstead, R.M., 1984. The thalamostriatal projection in the cat. J. Comp. Neurol. 223, 313–346. https://doi.org/10.1002/cne.902230302

Benison, A.M., Rector, D.M., Barth, D.S., 2007. Hemispheric mapping of secondary somatosensory cortex in the rat. J. Neurophysiol. 97, 200–207. https://doi.org/10.1152/jn.00673.2006

Berditchevskaia, A., Cazé, R.D., Schultz, S.R., 2016. Performance in a GO/NOGO perceptual task reflects a balance between impulsive and instrumental components of behaviour. Sci. Rep. 6. https://doi.org/10.1038/srep27389

Berg, C.A., Sternberg, R.J., 1985. Response to novelty: continuity versus discontinuity in the developmental course of intelligence. Adv. Child Dev. Behav. 19, 1–47.

Bienenstock, E.L., Cooper, L.N., Munro, P.W., 1982. Theory for the development of neuron selectivity: orientation specificity and binocular interaction in visual cortex. J. Neurosci. Off. J. Soc. Neurosci. 2, 32–48.

Bieszczad, K.M., Weinberger, N.M., 2010a. Learning strategy trumps motivational level in determining learning-induced auditory cortical plasticity. Neurobiol. Learn. Mem. 93, 229–239. https://doi.org/10.1016/j.nlm.2009.10.003

Bieszczad, K.M., Weinberger, N.M., 2010b. Remodeling the cortex in memory: Increased use of a learning strategy increases the representational area of relevant acoustic cues. Neurobiol. Learn. Mem. 94, 127–144. https://doi.org/10.1016/j.nlm.2010.04.009

Bimbard, C., Demene, C., Girard, C., Radtke-Schuller, S., Shamma, S., Tanter, M., Boubenec, Y., 2018. Multi-scale mapping along the auditory hierarchy using high-resolution functional UltraSound in the awake ferret. eLife 7. https://doi.org/10.7554/eLife.35028

Boyden, E.S., Zhang, F., Bamberg, E., Nagel, G., Deisseroth, K., 2005. Millisecond-timescale, genetically targeted optical control of neural activity. Nat. Neurosci. 8, 1263–1268. https://doi.org/10.1038/nn1525

Brandon, S.E., Vogel, E.H., Wagner, A.R., 2000. A componential view of configural cues in generalization and discrimination in Pavlovian conditioning. Behav. Brain Res. 110, 67–72. https://doi.org/10.1016/S0166-4328(99)00185-0

Brette, R., 2015. Philosophy of the Spike: Rate-Based vs. Spike-Based Theories of the Brain. Front. Syst. Neurosci. 9. https://doi.org/10.3389/fnsys.2015.00151

Briguglio, J.J., Aizenberg, M., Balasubramanian, V., Geffen, M.N., 2018. Cortical Neural Activity Predicts Sensory Acuity Under Optogenetic Manipulation. J. Neurosci. Off. J. Soc. Neurosci. 38, 2094–2105. https://doi.org/10.1523/JNEUROSCI.2457-17.2017

Britten, K.H., Newsome, W.T., Shadlen, M.N., Celebrini, S., Movshon, J.A., 1996. A relationship between behavioral choice and the visual responses of neurons in macaque MT. Vis. Neurosci. 13, 87–100.

Brown, S., Heathcote, A., 2003. Averaging learning curves across and within participants. Behav. Res. Methods Instrum. Comput. J. Psychon. Soc. Inc 35, 11–21.

Bruce, D., 2001. Fifty years since Lashley's In search of the Engram: refutations and conjectures. J. Hist. Neurosci. 10, 308–318. https://doi.org/10.1076/jhin.10.3.308.9086

Burns, R.S., Chiueh, C.C., Markey, S.P., Ebert, M.H., Jacobowitz, D.M., Kopin, I.J., 1983. A primate model of parkinsonism: selective destruction of dopaminergic neurons in the pars compacta of the

substantia nigra by N-methyl-4-phenyl-1,2,3,6-tetrahydropyridine. Proc. Natl. Acad. Sci. U. S. A. 80, 4546–4550.

Buschman, T.J., Denovellis, E.L., Diogo, C., Bullock, D., Miller, E.K., 2012. Synchronous Oscillatory Neural Ensembles for Rules in the Prefrontal Cortex. Neuron 76, 838–846. https://doi.org/10.1016/j.neuron.2012.09.029

Bush, R.R., Mosteller, F., 1951. A model for stimulus generalization and discrimination. Psychol. Rev. 58, 413–423.

Butler, R.A., Diamond, I.T., Neff, W.D., 1957. Role of auditory cortex in discrimination of changes in frequency. J. Neurophysiol. 20, 108–120. https://doi.org/10.1152/jn.1957.20.1.108

Cardin, J.A., Carlén, M., Meletis, K., Knoblich, U., Zhang, F., Deisseroth, K., Tsai, L.-H., Moore, C.I., 2009. Driving fast-spiking cells induces gamma rhythm and controls sensory responses. Nature 459, 663–667. https://doi.org/10.1038/nature08002

Carruthers, I.M., Laplagne, D.A., Jaegle, A., Briguglio, J.J., Mwilambwe-Tshilobo, L., Natan, R.G., Geffen, M.N., 2015. Emergence of invariant representation of vocalizations in the auditory cortex. J. Neurophysiol. 114, 2726–2740. https://doi.org/10.1152/jn.00095.2015

Casanova, M.F., Buxhoeveden, D., Gomez, J., 2003. Disruption in the inhibitory architecture of the cell minicolumn: implications for autism. Neurosci. Rev. J. Bringing Neurobiol. Neurol. Psychiatry 9, 496–507. https://doi.org/10.1177/1073858403253552

Casseday, J.H., Covey, E., 1996. A neuroethological theory of the operation of the inferior colliculus. Brain. Behav. Evol. 47, 311–336. https://doi.org/10.1159/000113249

Cassenaer, S., Laurent, G., 2012. Conditional modulation of spike-timing-dependent plasticity for olfactory learning. Nature 482, 47–52. https://doi.org/10.1038/nature10776

Castro, J.B., Kandler, K., 2010. Changing tune in auditory cortex. Nat. Neurosci. 13, 271–273. https://doi.org/10.1038/nn0310-271

Centanni, T.M., Sloan, A.M., Reed, A.C., Engineer, C.T., Rennaker, R.L., Kilgard, M.P., 2014. Detection and identification of speech sounds using cortical activity patterns. Neuroscience 258, 292–306. https://doi.org/10.1016/j.neuroscience.2013.11.030

Cerella, J., 1980. The pigeon's analysis of pictures. Pattern Recognit. 12, 1–6. https://doi.org/10.1016/0031-3203(80)90048-5

Cheatham, M.A., 1993. Cochlear function reflected in mammalian hair cell responses. Prog. Brain Res. 97, 13–19.

Chen, C., Cheng, M., Ito, T., Song, S., 2018. Neuronal Organization in the Inferior Colliculus Revisited with Cell-Type-Dependent Monosynaptic Tracing. J. Neurosci. Off. J. Soc. Neurosci. 38, 3318–3332. https://doi.org/10.1523/JNEUROSCI.2173-17.2018

Chen, I.-W., Papagiakoumou, E., Emiliani, V., 2018. Towards circuit optogenetics. Curr. Opin. Neurobiol. 50, 179–189. https://doi.org/10.1016/j.conb.2018.03.008

Chen, I.-W., Ronzitti, E., Lee, B.R., Daigle, T.L., Dalkara, D., Zeng, H., Emiliani, V., Papagiakoumou, E., 2019. In vivo sub-millisecond two-photon optogenetics with temporally focused patterned light. J. Neurosci. Off. J. Soc. Neurosci. https://doi.org/10.1523/JNEUROSCI.1785-18.2018

Chen, J.L., Carta, S., Soldado-Magraner, J., Schneider, B.L., Helmchen, F., 2013. Behaviour-dependent recruitment of long-range projection neurons in somatosensory cortex. Nature 499, 336–340. https://doi.org/10.1038/nature12236

Chen, L., Wang, X., Ge, S., Xiong, Q., 2019. Medial geniculate body and primary auditory cortex differentially contribute to striatal sound representations. Nat. Commun. 10. https://doi.org/10.1038/s41467-019-08350-7

Chen, S.X., Kim, A.N., Peters, A.J., Komiyama, T., 2015. Subtype-specific plasticity of inhibitory circuits in motor cortex during motor learning. Nat. Neurosci. 18, 1109–1115. https://doi.org/10.1038/nn.4049

Chen, X., Gabitto, M., Peng, Y., Ryba, N.J.P., Zuker, C.S., 2011. A gustotopic map of taste qualities in the mammalian brain. Science 333, 1262–1266. https://doi.org/10.1126/science.1204076

Chernov, M.M., Friedman, R.M., Chen, G., Stoner, G.R., Roe, A.W., 2018. Functionally specific optogenetic modulation in primate visual cortex. Proc. Natl. Acad. Sci. 115, 10505–10510. https://doi.org/10.1073/pnas.1802018115

Chittka, L., Shmida, A., Troje, N., Menzel, R., 1994. Ultraviolet as a component of flower reflections, and the colour perception of Hymenoptera. Vision Res. 34, 1489–1508.

Choi, G.B., Stettler, D.D., Kallman, B.R., Bhaskar, S.T., Fleischmann, A., Axel, R., 2011. Driving opposing behaviors with ensembles of piriform neurons. Cell 146, 1004–1015. https://doi.org/10.1016/j.cell.2011.07.041

Chu, M.W., Li, W.L., Komiyama, T., 2016. Balancing the Robustness and Efficiency of Odor Representations during Learning. Neuron 92, 174–186. https://doi.org/10.1016/j.neuron.2016.09.004

Clarey, J.C., Barone, P., Imig, T.J., 1994. Functional organization of sound direction and sound pressure level in primary auditory cortex of the cat. J. Neurophysiol. 72, 2383–2405. https://doi.org/10.1152/jn.1994.72.5.2383

Clopton, B.M., Winfield, J.A., 1974. Unit responses in the inferior colliculus of rat to temporal auditory patterns of tone sweeps and noise bursts. Exp. Neurol. 42, 532–540.

Cohen, J.Y., Haesler, S., Vong, L., Lowell, B.B., Uchida, N., 2012. Neuron-type-specific signals for reward and punishment in the ventral tegmental area. Nature 482, 85–88. https://doi.org/10.1038/nature10754

Colgin, L.L., Denninger, T., Fyhn, M., Hafting, T., Bonnevie, T., Jensen, O., Moser, M.-B., Moser, E.I., 2009. Frequency of gamma oscillations routes flow of information in the hippocampus. Nature 462, 353–357. https://doi.org/10.1038/nature08573

Cooke, J.E., Zhang, H., Kelly, J.B., 2007. Detection of sinusoidal amplitude modulated sounds: deficits after bilateral lesions of auditory cortex in the rat. Hear. Res. 231, 90–99. https://doi.org/10.1016/j.heares.2007.06.002

Cowey, A., 2010. Visual system: how does blindsight arise? Curr. Biol. CB 20, R702-704. https://doi.org/10.1016/j.cub.2010.07.014

Crair, M.C., Ruthazer, E.S., Gillespie, D.C., Stryker, M.P., 1997. Relationship between the Ocular Dominance and Orientation Maps in Visual Cortex of Monocularly Deprived Cats. Neuron 19, 307–318. https://doi.org/10.1016/S0896-6273(00)80941-1

Crick, F.H.C., 1979. Thinking about the Brain. Sci. Am. 241, 219–233.

Cui, G., Jun, S.B., Jin, X., Pham, M.D., Vogel, S.S., Lovinger, D.M., Costa, R.M., 2013. Concurrent activation of striatal direct and indirect pathways during action initiation. Nature 494, 238–242. https://doi.org/10.1038/nature11846

Damasio, A.R., Geschwind, N., 1984. The neural basis of language. Annu. Rev. Neurosci. 7, 127–147. https://doi.org/10.1146/annurev.ne.07.030184.001015

Darrow, K.N., Slama, M.C.C., Owoc, M., Kozin, E., Hancock, K., Kempfle, J., Edge, A., Lacour, S., Boyden, E., Polley, D., Brown, M.C., Lee, D.J., 2015. Optogenetic stimulation of the cochlear nucleus using channelrhodopsin-2 evokes activity in the central auditory pathway. Brain Res. 1599, 44–56. https://doi.org/10.1016/j.brainres.2014.11.044

Davey, G.C., 1988. Pavlovian conditioning in humans: UCS revaluation and the self-observation of conditioned responding. Med. Sci. Res. 16, 957–961.

Davies, P.W., Erulkar, S.D., Rose, J.E., 1956. Single unit activity in the auditory cortex of the cat. Bull. Johns Hopkins Hosp. 99, 55–86.

Dayan, P., Abbott, L.F., 2001. Theoretical neuroscience: computational and mathematical modeling of neural systems, Computational neuroscience. Massachusetts Institute of Technology Press, Cambridge, Mass.

Dayan, P., Balleine, B.W., 2002. Reward, Motivation, and Reinforcement Learning. Neuron 36, 285–298. https://doi.org/10.1016/S0896-6273(02)00963-7

de Castro, F., Merchán, M.A. (Eds.), 2017. The Major Discoveries of Cajal and His Disciples: Consolidated Milestones for the Neuroscience of the XXIst Century, Frontiers Research Topics. Frontiers Media SA. https://doi.org/10.3389/978-2-88945-066-4

Dehaene-Lambertz, G., Spelke, E.S., 2015. The Infancy of the Human Brain. Neuron 88, 93–109. https://doi.org/10.1016/j.neuron.2015.09.026

Deisseroth, K., 2015. Optogenetics: 10 years of microbial opsins in neuroscience. Nat. Neurosci. 18, 1213–1225. https://doi.org/10.1038/nn.4091

Deisseroth, K., Feng, G., Majewska, A.K., Miesenböck, G., Ting, A., Schnitzer, M.J., 2006. Next-generation optical technologies for illuminating genetically targeted brain circuits. J. Neurosci. Off. J. Soc. Neurosci. 26, 10380–10386. https://doi.org/10.1523/JNEUROSCI.3863-06.2006

Deliano, M., Tabelow, K., König, R., Polzehl, J., 2016. Improving Accuracy and Temporal Resolution of Learning Curve Estimation for within- and across-Session Analysis. PloS One 11, e0157355. https://doi.org/10.1371/journal.pone.0157355

Deneux, T., Kempf, A., Daret, A., Ponsot, E., Bathellier, B., 2016. Temporal asymmetries in auditory coding and perception reflect multi-layered nonlinearities. Nat. Commun. 7, 12682. https://doi.org/10.1038/ncomms12682

Denève, S., Alemi, A., Bourdoukan, R., 2017. The Brain as an Efficient and Robust Adaptive Learner. Neuron 94, 969–977. https://doi.org/10.1016/j.neuron.2017.05.016

Denk, W., Strickler, J.H., Webb, W.W., 1990. Two-photon laser scanning fluorescence microscopy. Science 248, 73–76.

Desimone, R., Duncan, J., 1995. Neural mechanisms of selective visual attention. Annu. Rev. Neurosci. 18, 193–222. https://doi.org/10.1146/annurev.ne.18.030195.001205

Dewson, J.H., 1964. Speech Sound Discrimination By Cats. Science 144, 555–556.

Dhawale, A.K., Hagiwara, A., Bhalla, U.S., Murthy, V.N., Albeanu, D.F., 2010. Non-redundant odor coding by sister mitral cells revealed by light addressable glomeruli in the mouse. Nat. Neurosci. 13, 1404–1412. https://doi.org/10.1038/nn.2673

Diamond, I.T., Fisher, J.F., Neff, W.D., Yela, M., 1956. Role of auditory cortex in discrimination requiring localization of sound in space. J. Neurophysiol. 19, 500–512. https://doi.org/10.1152/jn.1956.19.6.500

Diamond, I.T., Goldberg, J.M., Neff, W.D., 1962. Tonal discrimination after ablation of auditory cortex. J. Neurophysiol. 25, 223–235. https://doi.org/10.1152/jn.1962.25.2.223

Dias, R., Robbins, T.W., Roberts, A.C., 1996. Dissociation in prefrontal cortex of affective and attentional shifts. Nature 380, 69–72. https://doi.org/10.1038/380069a0

Dickinson, A., 1981. Conditioning and associative learning. Br. Med. Bull. 37, 165–168.

Dickinson, A., Hall, G., Mackintosh, N.J., 1976. Surprise and the Attenuation of Blocking.

Domjan, M., Grau, J.W., 2015. Principles of learning and behavior, 7th ed. ed. Cengage Learning, Stamford, CT.

Douglas, R.J., Martin, K.A.C., 2007. Mapping the Matrix: The Ways of Neocortex. Neuron 56, 226–238. https://doi.org/10.1016/j.neuron.2007.10.017

Eggermont, J.J., 1998. Representation of spectral and temporal sound features in three cortical fields of the cat. Similarities outweigh differences. J. Neurophysiol. 80, 2743–2764. https://doi.org/10.1152/jn.1998.80.5.2743

Engineer, C.T., Perez, C.A., Carraway, R.S., Chang, K.Q., Roland, J.L., Sloan, A.M., Kilgard, M.P., 2013. Similarity of cortical activity patterns predicts generalization behavior. PloS One 8, e78607. https://doi.org/10.1371/journal.pone.0078607

Engineer, C.T., Perez, C.A., Chen, Y.H., Carraway, R.S., Reed, A.C., Shetake, J.A., Jakkamsetti, V., Chang, K.Q., Kilgard, M.P., 2008. Cortical activity patterns predict speech discrimination ability. Nat. Neurosci. 11, 603–608. https://doi.org/10.1038/nn.2109

Epelde, G., Morgan, F., Mujika, A., Callaly, F., Leškovský, P., McGinley, B., Álvarez, R., Blau, A., Krewer, F., 2018. Web-Based Interfaces for Virtual C. elegans Neuron Model Definition, Network Configuration, Behavioral Experiment Definition and Experiment Results Visualization. Front. Neuroinformatics 12, 80. https://doi.org/10.3389/fninf.2018.00080

Erö, C., Gewaltig, M.-O., Keller, D., Markram, H., 2018. A Cell Atlas for the Mouse Brain. Front. Neuroinformatics 12. https://doi.org/10.3389/fninf.2018.00084

Evans, B.M., 2003. Sleep, consciousness and the spontaneous and evoked electrical activity of the brain. Is there a cortical integrating mechanism? Neurophysiol. Clin. Clin. Neurophysiol. 33, 1–10.

Evans, E.F., Ross, H.F., Whitfield, I.C., 1965. The spatial distribution of unit characteristic frequency in the primary auditory cortex of the cat. J. Physiol. 179, 238–247.

Evans, E.F., Whitfield, I.C., 1964a. CLASSIFICATION OF UNIT RESPONSES IN THE AUDITORY CORTEX OF THE UNANAESTHETIZED AND UNRESTRAINED CAT. J. Physiol. 171, 476–493.

Evans, E.F., Whitfield, I.C., 1964b. Classification of unit responses in the auditory cortex of the unanaesthetized and unrestrained cat. J. Physiol. 171, 476–493.

Fay, R.R., Popper, A.N., 1994. Comparative Hearing: Mammals. Springer New York, New York, NY.

Felsheim, C., Ostwald, J., 1996. Responses to exponential frequency modulations in the rat inferior colliculus. Hear. Res. 98, 137–151.

Fenno, L., Yizhar, O., Deisseroth, K., 2011. The development and application of optogenetics. Annu. Rev. Neurosci. 34, 389–412. https://doi.org/10.1146/annurev-neuro-061010-113817

Ferrier on the Functions of the Brain, 1877. . Br. Foreign Medico-Chir. Rev. 60, 99–114.

Ficalora, A.S., Mize, R.R., 1989. The neurons of the substantia nigra and zona incerta which project to the cat superior colliculus are GABA immunoreactive: a double-label study using GABA immunocytochemistry and lectin retrograde transport. Neuroscience 29, 567–581.

Flusberg, B.A., Nimmerjahn, A., Cocker, E.D., Mukamel, E.A., Barretto, R.P.J., Ko, T.H., Burns, L.D., Jung, J.C., Schnitzer, M.J., 2008. High-speed, miniaturized fluorescence microscopy in freely moving mice. Nat. Methods 5, 935–938. https://doi.org/10.1038/nmeth.1256

Formisano, E., Kim, D.-S., Di Salle, F., van de Moortele, P.-F., Ugurbil, K., Goebel, R., 2003. Mirror-Symmetric Tonotopic Maps in Human Primary Auditory Cortex. Neuron 40, 859–869. https://doi.org/10.1016/S0896-6273(03)00669-X

Frémaux, N., Gerstner, W., 2016. Neuromodulated Spike-Timing-Dependent Plasticity, and Theory of Three-Factor Learning Rules. Front. Neural Circuits 9. https://doi.org/10.3389/fncir.2015.00085

Fries, P., 2015. Rhythms for Cognition: Communication through Coherence. Neuron 88, 220–235. https://doi.org/10.1016/j.neuron.2015.09.034

Fritz, J., Shamma, S., Elhilali, M., Klein, D., 2003. Rapid task-related plasticity of spectrotemporal receptive fields in primary auditory cortex. Nat. Neurosci. 6, 1216–1223. https://doi.org/10.1038/nn1141

Fritz, J.B., David, S.V., Radtke-Schuller, S., Yin, P., Shamma, S.A., 2010. Adaptive, behaviorally gated, persistent encoding of task-relevant auditory information in ferret frontal cortex. Nat. Neurosci. 13, 1011–1019. https://doi.org/10.1038/nn.2598

Fritz, J.B., Elhilali, M., David, S.V., Shamma, S.A., 2007. Auditory attention—focusing the searchlight on sound. Curr. Opin. Neurobiol. 17, 437–455. https://doi.org/10.1016/j.conb.2007.07.011

Fu, Y., Tucciarone, J.M., Espinosa, J.S., Sheng, N., Darcy, D.P., Nicoll, R.A., Huang, Z.J., Stryker, M.P., 2014. A cortical circuit for gain control by behavioral state. Cell 156, 1139–1152. https://doi.org/10.1016/j.cell.2014.01.050

Galindo-Leon, E.E., Lin, F.G., Liu, R.C., 2009. Inhibitory plasticity in a lateral band improves cortical detection of natural vocalizations. Neuron 62, 705–716. https://doi.org/10.1016/j.neuron.2009.05.001

Gallistel, C.R., Fairhurst, S., Balsam, P., 2004. The learning curve: implications of a quantitative analysis. Proc. Natl. Acad. Sci. U. S. A. 101, 13124–13131. https://doi.org/10.1073/pnas.0404965101

Gao, P., Sultan, K.T., Zhang, X.-J., Shi, S.-H., 2013. Lineage-dependent circuit assembly in the neocortex. Dev. Camb. Engl. 140, 2645–2655. https://doi.org/10.1242/dev.087668

Garcia, J., Koelling, R.A., 1966. Relation of cue to consequence in avoidance learning. Psychon. Sci. 4, 123–124. https://doi.org/10.3758/BF03342209

Gdalyahu, A., Tring, E., Polack, P.-O., Gruver, R., Golshani, P., Fanselow, M.S., Silva, A.J., Trachtenberg, J.T., 2012. Associative fear learning enhances sparse network coding in primary sensory cortex. Neuron 75, 121–132. https://doi.org/10.1016/j.neuron.2012.04.035

Gemberling, G.A., Domjan, M., 1982. Selective associations in one-day-old rats: taste-toxicosis and texture-shock aversion learning. J. Comp. Physiol. Psychol. 96, 105–113.

George, D.N., Pearce, J.M., 2003. Discrimination of structure: II. Feature binding. J. Exp. Psychol. Anim. Behav. Process. 29, 107–117. https://doi.org/10.1037/0097-7403.29.2.107

George, D.N., Pearce, J.M., 1999. Acquired Distinctiveness Is Controlled by Stimulus Relevance Not Correlation With Reward 11.

George, D.N., Ward-Robinson, J., Pearce, J.M., 2001. Discrimination of structure: I. Implications for connectionist theories of discrimination learning. J. Exp. Psychol. Anim. Behav. Process. 27, 206–218. https://doi.org/10.1037//0097-7403.27.3.206

Gerstein, G.L., Kiang, N.Y., 1964. Responses of single units in the auditory cortex. Exp. Neurol. 10, 1–18. https://doi.org/10.1016/0014-4886(64)90083-4

Gervain, J., Geffen, M.N., 2019. Efficient Neural Coding in Auditory and Speech Perception. Trends Neurosci. 42, 56–65. https://doi.org/10.1016/j.tins.2018.09.004

Ghazanfar, A.A., Neuhoff, J.G., Logothetis, N.K., 2002. Auditory looming perception in rhesus monkeys. Proc. Natl. Acad. Sci. U. S. A. 99, 15755–15757. https://doi.org/10.1073/pnas.242469699

Gil, V., Nocentini, S., Del Río, J.A., 2014. Historical first descriptions of Cajal-Retzius cells: from pioneer studies to current knowledge. Front. Neuroanat. 8, 32. https://doi.org/10.3389/fnana.2014.00032

Gimenez, T.L., Lorenc, M., Jaramillo, S., 2015. Adaptive categorization of sound frequency does not require the auditory cortex in rats. J. Neurophysiol. 114, 1137–1145. https://doi.org/10.1152/jn.00124.2015

Glickfeld, L.L., Histed, M.H., Maunsell, J.H.R., 2013. Mouse primary visual cortex is used to detect both orientation and contrast changes. J. Neurosci. Off. J. Soc. Neurosci. 33, 19416–19422. https://doi.org/10.1523/JNEUROSCI.3560-13.2013

Gluck, M.A., Bower, G.H., 1988. From conditioning to category learning: an adaptive network model. J. Exp. Psychol. Gen. 117, 227–247.

Goard, M., Dan, Y., 2009. Basal forebrain activation enhances cortical coding of natural scenes. Nat. Neurosci. 12, 1444–1449. https://doi.org/10.1038/nn.2402

Godey, B., Atencio, C.A., Bonham, B.H., Schreiner, C.E., Cheung, S.W., 2005. Functional organization of squirrel monkey primary auditory cortex: responses to frequency-modulation sweeps. J. Neurophysiol. 94, 1299–1311. https://doi.org/10.1152/jn.00950.2004

Goldberg, J.M., Neff, W.D., 1961. Frequency discrimination after bilateral ablation of cortical auditory areas. J. Neurophysiol. 24, 119–128. https://doi.org/10.1152/jn.1961.24.2.119

Goldstein, M.H., Abeles, M., 1975. Note on tonotopic organization of primary auditory cortex in the cat. Brain Res. 100, 188–191.

Goldstein, M.H., Abeles, M., Daly, R.L., McIntosh, J., 1970. Functional architecture in cat primary auditory cortex: tonotopic organization. J. Neurophysiol. 33, 188–197. https://doi.org/10.1152/jn.1970.33.1.188

Gradinaru, V., Thompson, K.R., Deisseroth, K., 2008. eNpHR: a Natronomonas halorhodopsin enhanced for optogenetic applications. Brain Cell Biol. 36, 129–139. https://doi.org/10.1007/s11068-008-9027-6

Grinvald, A., Lieke, E., Frostig, R.D., Gilbert, C.D., Wiesel, T.N., 1986. Functional architecture of cortex revealed by optical imaging of intrinsic signals. Nature 324, 361. https://doi.org/10.1038/324361a0

Grothe, B., 2018. How the Barn Owl Computes Auditory Space. Trends Neurosci. 41, 115–117. https://doi.org/10.1016/j.tins.2018.01.004

Grothe, B., Pecka, M., McAlpine, D., 2010. Mechanisms of Sound Localization in Mammals. Physiol. Rev. 90, 983–1012. https://doi.org/10.1152/physrev.00026.2009

Guimarãis, M., Gregório, A., Cruz, A., Guyon, N., Moita, M.A., 2011. Time determines the neural circuit underlying associative fear learning. Front. Behav. Neurosci. 5, 89. https://doi.org/10.3389/fnbeh.2011.00089

Gunaydin, L.A., Yizhar, O., Berndt, A., Sohal, V.S., Deisseroth, K., Hegemann, P., 2010. Ultrafast optogenetic control. Nat. Neurosci. 13, 387–392. https://doi.org/10.1038/nn.2495

Guo, L., Ponvert, N.D., Jaramillo, S., 2017. The role of sensory cortex in behavioral flexibility. Neuroscience 345, 3–11. https://doi.org/10.1016/j.neuroscience.2016.03.067

Guo, L., Walker, W.I., Ponvert, N.D., Penix, P.L., Jaramillo, S., 2018. Stable representation of sounds in the posterior striatum during flexible auditory decisions. Nat. Commun. 9, 1534. https://doi.org/10.1038/s41467-018-03994-3

Guo, W., Chambers, A.R., Darrow, K.N., Hancock, K.E., Shinn-Cunningham, B.G., Polley, D.B., 2012. Robustness of Cortical Topography across Fields, Laminae, Anesthetic States, and Neurophysiological Signal Types. J. Neurosci. 32, 9159–9172. https://doi.org/10.1523/JNEUROSCI.0065-12.2012

Guo, W., Hight, A.E., Chen, J.X., Klapoetke, N.C., Hancock, K.E., Shinn-Cunningham, B.G., Boyden, E.S., Lee, D.J., Polley, D.B., 2015. Hearing the light: neural and perceptual encoding of optogenetic stimulation in the central auditory pathway. Sci. Rep. 5, 10319. https://doi.org/10.1038/srep10319

Guo, Z.V., Li, N., Huber, D., Ophir, E., Gutnisky, D., Ting, J.T., Feng, G., Svoboda, K., 2014. Flow of Cortical Activity Underlying a Tactile Decision in Mice. Neuron 81, 179–194. https://doi.org/10.1016/j.neuron.2013.10.020

Guskjolen, A., Kenney, J.W., de la Parra, J., Yeung, B.-R.A., Josselyn, S.A., Frankland, P.W., 2018. Recovery of “Lost” Infant Memories in Mice. Curr. Biol. CB 28, 2283-2290.e3. https://doi.org/10.1016/j.cub.2018.05.059

Gütig, R., Sompolinsky, H., 2006. The tempotron: a neuron that learns spike timing–based decisions. Nat. Neurosci. 9, 420–428. https://doi.org/10.1038/nn1643

Hackett, T.A., 2011. Information flow in the auditory cortical network. Hear. Res. 271, 133–146. https://doi.org/10.1016/j.heares.2010.01.011

Hackett, T.A., Barkat, T.R., O'Brien, B.M.J., Hensch, T.K., Polley, D.B., 2011. Linking Topography to Tonotopy in the Mouse Auditory Thalamocortical Circuit. J. Neurosci. 31, 2983–2995. https://doi.org/10.1523/JNEUROSCI.5333-10.2011

Hackett, T.A., Preuss, T.M., Kaas, J.H., 2001. Architectonic identification of the core region in auditory cortex of macaques, chimpanzees, and humans. J. Comp. Neurol. 441, 197–222.

Hage, S.R., Ehret, G., 2003. Mapping responses to frequency sweeps and tones in the inferior colliculus of house mice. Eur. J. Neurosci. 18, 2301–2312.

Haider, B., Häusser, M., Carandini, M., 2013. Inhibition dominates sensory responses in the awake cortex. Nature 493, 97–100. https://doi.org/10.1038/nature11665

Harel, N., Mori, N., Sawada, S., Mount, R.J., Harrison, R.V., 2000. Three distinct auditory areas of cortex (AI, AII, and AAF) defined by optical imaging of intrinsic signals. NeuroImage 11, 302–312. https://doi.org/10.1006/nimg.1999.0537

Harrington, I.A., Heffner, R.S., Heffner, H.E., 2001. An investigation of sensory deficits underlying the aphasia-like behavior of macaques with auditory cortex lesions. Neuroreport 12, 1217–1221.

Harrison, R.V., Harel, N., Kakigi, A., Raveh, E., Mount, R.J., 1998. Optical imaging of intrinsic signals in chinchilla auditory cortex. Audiol. Neurootol. 3, 214–223. https://doi.org/10.1159/000013791

Harvey, M.A., Saal, H.P., Dammann, J.F., Bensmaia, S.J., 2013. Multiplexing stimulus information through rate and temporal codes in primate somatosensory cortex. PLoS Biol. 11, e1001558. https://doi.org/10.1371/journal.pbio.1001558

Hayashi, A., Yoshida, T., Ohki, K., 2018. Cell Type Specific Representation of Vibro-tactile Stimuli in the Mouse Primary Somatosensory Cortex. Front. Neural Circuits 12, 109. https://doi.org/10.3389/fncir.2018.00109

Heffner, H., 1978. Effect of auditory cortex ablation on localization and discrimination of brief sounds. J. Neurophysiol. 41, 963–976. https://doi.org/10.1152/jn.1978.41.4.963

Heffner, H.E., Heffner, R.S., 1990. Effect of bilateral auditory cortex lesions on sound localization in Japanese macaques. J. Neurophysiol. 64, 915–931. https://doi.org/10.1152/jn.1990.64.3.915

Heffner, H.E., Heffner, R.S., 1986. Hearing loss in Japanese macaques following bilateral auditory cortex lesions. J. Neurophysiol. 55, 256–271. https://doi.org/10.1152/jn.1986.55.2.256

Heil, P., Rajan, R., Irvine, D.R., 1994. Topographic representation of tone intensity along the isofrequency axis of cat primary auditory cortex. Hear. Res. 76, 188–202.

Hennessey, T.M., Rucker, W.B., McDiarmid, C.G., 1979. Classical conditioning in paramecia. Anim. Learn. Behav. 7, 417–423. https://doi.org/10.3758/BF03209695

Herculano-Houzel, S., Watson, C., Paxinos, G., 2013. Distribution of neurons in functional areas of the mouse cerebral cortex reveals quantitatively different cortical zones. Front. Neuroanat. 7. https://doi.org/10.3389/fnana.2013.00035

Hernstein, R.J., Loveland, D.H., Cable, C., 1976. Natural concepts in pigeons. J. Exp. Psychol. Anim. Behav. Process. 2, 285–302.

Hikosaka, O., Wurtz, R.H., 1985. Modification of saccadic eye movements by GABA-related substances. II. Effects of muscimol in monkey substantia nigra pars reticulata. J. Neurophysiol. 53, 292–308. https://doi.org/10.1152/jn.1985.53.1.292

Hinchy, J., Lovibond, P.F., Ter-Horst, K.M., 1995. Blocking in human electrodermal conditioning. Q. J. Exp. Psychol. B 48, 2–12.

Holland, P.C., Schiffino, F.L., 2016. Mini-review: Prediction errors, attention and associative learning. Neurobiol. Learn. Mem. 131, 207–215. https://doi.org/10.1016/j.nlm.2016.02.014

Hollis, K.L., Pharr, V.L., Dumas, M.J., Britton, G.B., Field, J., 1997. Classical conditioning provides paternity advantage for territorial male blue gouramis (Trichogaster trichopterus). J. Comp. Psychol. 111, 219–225. https://doi.org/10.1037/0735-7036.111.3.219

Holy, T.E., Guo, Z., 2005. Ultrasonic songs of male mice. PLoS Biol. 3, e386. https://doi.org/10.1371/journal.pbio.0030386

Honey, R.C., Hall, G., 1991. Acquired equivalence and distinctiveness of cues using a sensory-preconditioning procedure. Q. J. Exp. Psychol. B 43, 121–135.

Hong, Y.K., Lacefield, C.O., Rodgers, C.C., Bruno, R.M., 2018. Sensation, movement and learning in the absence of barrel cortex. Nature 561, 542–546. https://doi.org/10.1038/s41586-018-0527-y

Honma, Y., Tsukano, H., Horie, M., Ohshima, S., Tohmi, M., Kubota, Y., Takahashi, K., Hishida, R., Takahashi, S., Shibuki, K., 2013. Auditory Cortical Areas Activated by Slow Frequency-Modulated Sounds in Mice. PLoS ONE 8, e68113. https://doi.org/10.1371/journal.pone.0068113

Horie, M., Tsukano, H., Hishida, R., Takebayashi, H., Shibuki, K., 2013. Dual compartments of the ventral division of the medial geniculate body projecting to the core region of the auditory cortex in C57BL/6 mice. Neurosci. Res. 76, 207–212. https://doi.org/10.1016/j.neures.2013.05.004

Houweling, A.R., Brecht, M., 2008. Behavioural report of single neuron stimulation in somatosensory cortex. Nature 451, 65–68. https://doi.org/10.1038/nature06447

Howard, R.J., Brammer, M., Wright, I., Woodruff, P.W., Bullmore, E.T., Zeki, S., 1996. A direct demonstration of functional specialization within motion-related visual and auditory cortex of the human brain. Curr. Biol. CB 6, 1015–1019.

Huang, Y.-C., Wang, C.-T., Su, T.-S., Kao, K.-W., Lin, Y.-J., Chuang, C.-C., Chiang, A.-S., Lo, C.-C., 2018. A Single-Cell Level and Connectome-Derived Computational Model of the Drosophila Brain. Front. Neuroinformatics 12, 99. https://doi.org/10.3389/fninf.2018.00099

Hubel, D.H., Wiesel, T.N., 1962. Receptive fields, binocular interaction and functional architecture in the cat's visual cortex. J. Physiol. 160, 106–154.

Hubel, D.H., Wiesel, T.N., 1959. Receptive fields of single neurones in the cat's striate cortex. J. Physiol. 148, 574–591. https://doi.org/10.1113/jphysiol.1959.sp006308

Huber, D., Petreanu, L., Ghitani, N., Ranade, S., Hromádka, T., Mainen, Z., Svoboda, K., 2008. Sparse optical microstimulation in barrel cortex drives learned behaviour in freely moving mice. Nature 451, 61–64. https://doi.org/10.1038/nature06445

Hunnicutt, B.J., Jongbloets, B.C., Birdsong, W.T., Gertz, K.J., Zhong, H., Mao, T., 2016. A comprehensive excitatory input map of the striatum reveals novel functional organization. eLife 5. https://doi.org/10.7554/eLife.19103

Intskirveli, I., Joshi, A., Vizcarra-Chacón, B.J., Metherate, R., 2016. Spectral breadth and laminar distribution of thalamocortical inputs to A1. J. Neurophysiol. 115, 2083–2094. https://doi.org/10.1152/jn.00887.2015

Issa, J.B., Haeffele, B.D., Agarwal, A., Bergles, D.E., Young, E.D., Yue, D.T., 2014. Multiscale Optical Ca2+ Imaging of Tonal Organization in Mouse Auditory Cortex. Neuron 83, 944–959. https://doi.org/10.1016/j.neuron.2014.07.009

Issa, J.B., Haeffele, B.D., Young, E.D., Yue, D.T., 2017. Multiscale mapping of frequency sweep rate in mouse auditory cortex. Hear. Res. 344, 207–222. https://doi.org/10.1016/j.heares.2016.11.018

Itti, L., Koch, C., 2001. Computational modelling of visual attention. Nat. Rev. Neurosci. 2, 194–203. https://doi.org/10.1038/35058500

Jaramillo, S., Zador, A.M., 2011. The auditory cortex mediates the perceptual effects of acoustic temporal expectation. Nat. Neurosci. 14, 246–251. https://doi.org/10.1038/nn.2688

Jarvers, C., Brosch, T., Brechmann, A., Woldeit, M.L., Schulz, A.L., Ohl, F.W., Lommerzheim, M., Neumann, H., 2016. Reversal Learning in Humans and Gerbils: Dynamic Control Network Facilitates Learning. Front. Neurosci. 10, 535. https://doi.org/10.3389/fnins.2016.00535

Jenkins, W.M., Masterton, R.B., 1982. Sound localization: effects of unilateral lesions in central auditory system. J. Neurophysiol. 47, 987–1016. https://doi.org/10.1152/jn.1982.47.6.987

Jenkins, W.M., Merzenich, M.M., 1984. Role of cat primary auditory cortex for sound-localization behavior. J. Neurophysiol. 52, 819–847. https://doi.org/10.1152/jn.1984.52.5.819

Jeschke, M., Moser, T., 2015. Considering optogenetic stimulation for cochlear implants. Hear. Res. 322, 224–234. https://doi.org/10.1016/j.heares.2015.01.005

Joachimsthaler, B., Uhlmann, M., Miller, F., Ehret, G., Kurt, S., 2014. Quantitative analysis of neuronal response properties in primary and higher-order auditory cortical fields of awake house mice (Mus musculus). Eur. J. Neurosci. 39, 904–918. https://doi.org/10.1111/ejn.12478

Johnson, B.A., Leon, M., 2000. Modular representations of odorants in the glomerular layer of the rat olfactory bulb and the effects of stimulus concentration. J. Comp. Neurol. 422, 496–509.

Johnston, T.D., 1982. Selective Costs and Benefits in the Evolution of Learning, in: Rosenblatt, J.S., Hinde, R.A., Beer, C., Busnel, M.-C. (Eds.), Advances in the Study of Behavior. Academic Press, pp. 65–106. https://doi.org/10.1016/S0065-3454(08)60046-7

Kalatsky, V.A., Polley, D.B., Merzenich, M.M., Schreiner, C.E., Stryker, M.P., 2005. Fine functional organization of auditory cortex revealed by Fourier optical imaging. Proc. Natl. Acad. Sci. 102, 13325–13330. https://doi.org/10.1073/pnas.0505592102

Kamin, L.J., 1967. Predictability, surprise, attention, and conditioning.

Kandler, K., Clause, A., Noh, J., 2009. Tonotopic reorganization of developing auditory brainstem circuits. Nat. Neurosci. 12, 711–717. https://doi.org/10.1038/nn.2332

Kanold, P.O., Nelken, I., Polley, D.B., 2014. Local versus global scales of organization in auditory cortex. Trends Neurosci. 37, 502–510. https://doi.org/10.1016/j.tins.2014.06.003

Kapuria, S., Steele, C.R., Puria, S., 2017. Unraveling the mystery of hearing in gerbil and other rodents with an arch-beam model of the basilar membrane. Sci. Rep. 7, 228. https://doi.org/10.1038/s41598-017-00114-x

Kato, H.K., Gillet, S.N., Isaacson, J.S., 2015. Flexible Sensory Representations in Auditory Cortex Driven by Behavioral Relevance. Neuron 88, 1027–1039. https://doi.org/10.1016/j.neuron.2015.10.024

Katsuki, Y., Murata, K., Suga, N., Takenaka, T., 1959. Electrical Activity of Cortical Auditory Neurons of Unanaesthetized and Unrestrained Cat. Proc. Jpn. Acad. 35, 571–574. https://doi.org/10.2183/pjab1945.35.571

Kaufman, M.A., Bolles, R.C., 1981. A nonassociative aspect of overshadowing. Bull. Psychon. Soc. 18, 318–320. https://doi.org/10.3758/BF03333639

Kavanagh, G.L., Kelly, J.B., 1987. Contribution of auditory cortex to sound localization by the ferret (Mustela putorius). J. Neurophysiol. 57, 1746–1766. https://doi.org/10.1152/jn.1987.57.6.1746

Kelly, J.B., 1980. Effects of auditory cortical lesions on sound localization by the rat. J. Neurophysiol. 44, 1161–1174. https://doi.org/10.1152/jn.1980.44.6.1161

Kelly, J.B., Glazier, S.J., 1978. Auditory cortex lesions and discrimination of spatial location by the rat. Brain Res. 145, 315–321.

Kelly, J.B., Whitfield, I.C., 1971. Effects of auditory cortical lesions on discriminations of rising and falling frequency-modulated tones. J. Neurophysiol. 34, 802–816. https://doi.org/10.1152/jn.1971.34.5.802

Keppeler, D., Merino, R.M., Morena, D.L. de la, Bali, B., Huet, A.T., Gehrt, A., Wrobel, C., Subramanian, S., Dombrowski, T., Wolf, F., Rankovic, V., Neef, A., Moser, T., 2018. Ultrafast optogenetic stimulation of the auditory pathway by targeting-optimized Chronos. EMBO J. e99649. https://doi.org/10.15252/embj.201899649

Kilgard, M.P., Merzenich, M.M., 1998. Plasticity of temporal information processing in the primary auditory cortex. Nat. Neurosci. 1, 727–731. https://doi.org/10.1038/3729

Kim, C.K., Adhikari, A., Deisseroth, K., 2017. Integration of optogenetics with complementary methodologies in systems neuroscience. Nat. Rev. Neurosci. 18, 222–235. https://doi.org/10.1038/nrn.2017.15

Kim, H., Ährlund-Richter, S., Wang, X., Deisseroth, K., Carlén, M., 2016. Prefrontal Parvalbumin Neurons in Control of Attention. Cell 164, 208–218. https://doi.org/10.1016/j.cell.2015.11.038

Kimura, A., Donishi, T., Okamoto, K., Tamai, Y., 2005. Topography of projections from the primary and non-primary auditory cortical areas to the medial geniculate body and thalamic reticular nucleus in the rat. Neuroscience 135, 1325–1342. https://doi.org/10.1016/j.neuroscience.2005.06.089

King, A.J., Jiang, Z.D., Moore, D.R., 1998. Auditory brainstem projections to the ferret superior colliculus: anatomical contribution to the neural coding of sound azimuth. J. Comp. Neurol. 390, 342–365.

King, A.J., Teki, S., Willmore, B.D.B., 2018. Recent advances in understanding the auditory cortex. F1000Research 7. https://doi.org/10.12688/f1000research.15580.1

Klaus, A., Martins, G.J., Paixao, V.B., Zhou, P., Paninski, L., Costa, R.M., 2017. The Spatiotemporal Organization of the Striatum Encodes Action Space. Neuron 95, 1171-1180.e7. https://doi.org/10.1016/j.neuron.2017.08.015

Knudsen, E.I., 1984. Auditory properties of space-tuned units in owl's optic tectum. J. Neurophysiol. 52, 709–723. https://doi.org/10.1152/jn.1984.52.4.709

Ko, H., Hofer, S.B., Pichler, B., Buchanan, K.A., Sjöström, P.J., Mrsic-Flogel, T.D., 2011. Functional specificity of local synaptic connections in neocortical networks. Nature 473, 87–91. https://doi.org/10.1038/nature09880

Kohlberg, G., Spitzer, J.B., Mancuso, D., Lalwani, A.K., 2014. Does cochlear implantation restore music appreciation? The Laryngoscope 124, 587–588. https://doi.org/10.1002/lary.24171

Kong, L., Xiong, C., Li, L., Yan, J., 2014. Frequency-specific corticofugal modulation of the dorsal cochlear nucleus in mice. Front. Syst. Neurosci. 8, 125. https://doi.org/10.3389/fnsys.2014.00125

Kopell, N.J., Gritton, H.J., Whittington, M.A., Kramer, M.A., 2014. Beyond the Connectome: The Dynome. Neuron 83, 1319–1328. https://doi.org/10.1016/j.neuron.2014.08.016

Kornack, D.R., 2000. Neurogenesis and the evolution of cortical diversity: mode, tempo, and partitioning during development and persistence in adulthood. Brain. Behav. Evol. 55, 336–344. https://doi.org/10.1159/000006668

Kosten, T.A., Kim, J.J., Lee, H.J., 2012. Early life manipulations alter learning and memory in rats. Neurosci. Biobehav. Rev. 36, 1985–2006. https://doi.org/10.1016/j.neubiorev.2012.07.003

Kravitz, A.V., Freeze, B.S., Parker, P.R.L., Kay, K., Thwin, M.T., Deisseroth, K., Kreitzer, A.C., 2010. Regulation of parkinsonian motor behaviours by optogenetic control of basal ganglia circuitry. Nature 466, 622–626. https://doi.org/10.1038/nature09159

Krubitzer, L., 1995. The organization of neocortex in mammals: are species differences really so different? Trends Neurosci. 18, 408–417.

Kubota, Y., Kamatani, D., Tsukano, H., Ohshima, S., Takahashi, K., Hishida, R., Kudoh, M., Takahashi, S., Shibuki, K., 2008. Transcranial photo-inactivation of neural activities in the mouse auditory cortex. Neurosci. Res. 60, 422–430. https://doi.org/10.1016/j.neures.2007.12.013

Kuchibhotla, K., Bathellier, B., 2018. Neural encoding of sensory and behavioral complexity in the auditory cortex. Curr. Opin. Neurobiol. 52, 65–71. https://doi.org/10.1016/j.conb.2018.04.002

Kuchibhotla, K.V., Gill, J.V., Lindsay, G.W., Papadoyannis, E.S., Field, R.E., Sten, T.A.H., Miller, K.D., Froemke, R.C., 2017. Parallel processing by cortical inhibition enables context-dependent behavior. Nat. Neurosci. 20, 62–71. https://doi.org/10.1038/nn.4436

Kudoh, M., Nakayama, Y., Hishida, R., Shibuki, K., 2006. Requirement of the auditory association cortex for discrimination of vowel-like sounds in rats. Neuroreport 17, 1761–1766. https://doi.org/10.1097/WNR.0b013e32800fef9d

Kühn, T., Helias, M., 2017. Locking of correlated neural activity to ongoing oscillations. PLoS Comput. Biol. 13, e1005534. https://doi.org/10.1371/journal.pcbi.1005534

Kumar, S.R., Markusic, D.M., Biswas, M., High, K.A., Herzog, R.W., 2016. Clinical development of gene therapy: results and lessons from recent successes. Mol. Ther. - Methods Clin. Dev. 3. https://doi.org/10.1038/mtm.2016.34

Kuśmierek, P., Rauschecker, J.P., 2009. Functional Specialization of Medial Auditory Belt Cortex in the Alert Rhesus Monkey. J. Neurophysiol. 102, 1606–1622. https://doi.org/10.1152/jn.00167.2009

Langner, G., Dinse, H.R., Godde, B., 2009. A map of periodicity orthogonal to frequency representation in the cat auditory cortex. Front. Integr. Neurosci. 3. https://doi.org/10.3389/neuro.07.027.2009

Larriva-Sahd, J.A., 2014. Some predictions of Rafael Lorente de Nó 80 years later. Front. Neuroanat. 8. https://doi.org/10.3389/fnana.2014.00147

Le Pelley, M.E., 2004. The Role of Associative History in Models of Associative Learning: A Selective Review and a Hybrid Model. Q. J. Exp. Psychol. Sect. B 57, 193–243. https://doi.org/10.1080/02724990344000141

LeCun, Y., Bengio, Y., Hinton, G., 2015. Deep learning. Nature 521, 436–444. https://doi.org/10.1038/nature14539

LeDoux, J.E., Cicchetti, P., Xagoraris, A., Romanski, L.M., 1990. The lateral amygdaloid nucleus: sensory interface of the amygdala in fear conditioning. J. Neurosci. Off. J. Soc. Neurosci. 10, 1062–1069.

LeDoux, J.E., Farb, C.R., Romanski, L.M., 1991. Overlapping projections to the amygdala and striatum from auditory processing areas of the thalamus and cortex. Neurosci. Lett. 134, 139–144.

LeDoux, J.E., Sakaguchi, A., Reis, D.J., 1984. Subcortical efferent projections of the medial geniculate nucleus mediate emotional responses conditioned to acoustic stimuli. J. Neurosci. Off. J. Soc. Neurosci. 4, 683–698.

Lee, C.C., 2015. Exploring functions for the non-lemniscal auditory thalamus. Front. Neural Circuits 9. https://doi.org/10.3389/fncir.2015.00069

Lee, C.C., Winer, J.A., 2008. Connections of cat auditory cortex: I. Thalamocortical system. J. Comp. Neurol. 507, 1879–1900. https://doi.org/10.1002/cne.21611

Lee, S., Sen, K., Kopell, N., 2009. Cortical gamma rhythms modulate NMDAR-mediated spike timing dependent plasticity in a biophysical model. PLoS Comput. Biol. 5, e1000602. https://doi.org/10.1371/journal.pcbi.1000602

Lefort, S., Tomm, C., Floyd Sarria, J.-C., Petersen, C.C.H., 2009. The excitatory neuronal network of the C2 barrel column in mouse primary somatosensory cortex. Neuron 61, 301–316. https://doi.org/10.1016/j.neuron.2008.12.020

Letzkus, J.J., Wolff, S.B.E., Lüthi, A., 2015. Disinhibition, a Circuit Mechanism for Associative Learning and Memory. Neuron 88, 264–276. https://doi.org/10.1016/j.neuron.2015.09.024

Letzkus, J.J., Wolff, S.B.E., Meyer, E.M.M., Tovote, P., Courtin, J., Herry, C., Lüthi, A., 2011. A disinhibitory microcircuit for associative fear learning in the auditory cortex. Nature 480, 331–335. https://doi.org/10.1038/nature10674

Leverton, T., 2019. Depression in older adults: hearing loss is an important factor. BMJ 364, l160. https://doi.org/10.1136/bmj.l160

Li, C.-M., Zhang, X., Hoffman, H.J., Cotch, M.F., Themann, C.L., Wilson, M.R., 2014. Hearing impairment associated with depression in US adults, National Health and Nutrition Examination Survey 2005-2010. JAMA Otolaryngol.-- Head Neck Surg. 140, 293–302. https://doi.org/10.1001/jamaoto.2014.42

Li, L.-Y., Xiong, X.R., Ibrahim, L.A., Yuan, W., Tao, H.W., Zhang, L.I., 2015. Differential Receptive Field Properties of Parvalbumin and Somatostatin Inhibitory Neurons in Mouse Auditory Cortex. Cereb. Cortex N. Y. N 1991 25, 1782–1791. https://doi.org/10.1093/cercor/bht417

Li, M., Xie, K., Kuang, H., Liu, J., Wang, D., Fox, G.E., Shi, Z., Chen, L., Zhao, F., Mao, Y., Tsien, J.Z., 2018. Neural Coding of Cell Assemblies via Spike-Timing Self-Information. Cereb. Cortex N. Y. N 1991 28, 2563–2576. https://doi.org/10.1093/cercor/bhy081

Li, Z., 2002. A saliency map in primary visual cortex. Trends Cogn. Sci. 6, 9–16.

Lin, J.Y., Knutsen, P.M., Muller, A., Kleinfeld, D., Tsien, R.Y., 2013. ReaChR: a red-shifted variant of channelrhodopsin enables deep transcranial optogenetic excitation. Nat. Neurosci. 16, 1499–1508. https://doi.org/10.1038/nn.3502

Linster, C., Johnson, B.A., Yue, E., Morse, A., Xu, Z., Hingco, E.E., Choi, Y., Choi, M., Messiha, A., Leon, M., 2001. Perceptual correlates of neural representations evoked by odorant enantiomers. J. Neurosci. Off. J. Soc. Neurosci. 21, 9837–9843.

Liu, X., Ramirez, S., Pang, P.T., Puryear, C.B., Govindarajan, A., Deisseroth, K., Tonegawa, S., 2012. Optogenetic stimulation of a hippocampal engram activates fear memory recall. Nature 484, 381–385. https://doi.org/10.1038/nature11028

Long, M.A., Fee, M.S., 2008. Using temperature to analyse temporal dynamics in the songbird motor pathway. Nature 456, 189–194. https://doi.org/10.1038/nature07448

Lubow, R.E., 1989. Latent inhibition and conditioned attention theory, Problems in the behavioural sciences. Cambridge University Press, Cambridge [England] ; New York.

Lubow, R.E., Moore, A.U., 1959. Latent inhibition: The effect of nonreinforced pre-exposure to the conditional stimulus. J. Comp. Physiol. Psychol. 52, 415–419. https://doi.org/10.1037/h0046700

Lütkenhöner, B., Steinsträter, O., 1998. High-precision neuromagnetic study of the functional organization of the human auditory cortex. Audiol. Neurootol. 3, 191–213. https://doi.org/10.1159/000013790

Lyzwa, D., Herrmann, J.M., Wörgötter, F., 2015. Natural Vocalizations in the Mammalian Inferior Colliculus are Broadly Encoded by a Small Number of Independent Multi-Units. Front. Neural Circuits 9, 91. https://doi.org/10.3389/fncir.2015.00091

Ma, X., Suga, N., 2003. Augmentation of plasticity of the central auditory system by the basal forebrain and/or somatosensory cortex. J. Neurophysiol. 89, 90–103. https://doi.org/10.1152/jn.00968.2001

Mackintosh, N.J., 1975. A theory of attention: Variations in the associability of stimuli with reinforcement. Psychol. Rev. 82, 276–298. https://doi.org/10.1037/h0076778

Mackintosh, N.J., 1971. An Analysis of Overshadowing and Blocking. Q. J. Exp. Psychol. 23, 118–125. https://doi.org/10.1080/00335557143000121

Mackintosh, N.J., Little, L., 1969. Intradimensional and extradimensional shift learning by pigeons. Psychon. Sci. 14, 5–6. https://doi.org/10.3758/BF03336395

Madisen, L., Mao, T., Koch, H., Zhuo, J., Berenyi, A., Fujisawa, S., Hsu, Y.-W.A., Garcia, A.J., Gu, X., Zanella, S., Kidney, J., Gu, H., Mao, Y., Hooks, B.M., Boyden, E.S., Buzsáki, G., Ramirez, J.M., Jones, A.R., Svoboda, K., Han, X., Turner, E.E., Zeng, H., 2012. A toolbox of Cre-dependent optogenetic

transgenic mice for light-induced activation and silencing. Nat. Neurosci. 15, 793–802. https://doi.org/10.1038/nn.3078

Mahoney, W.J., Ayres, J.J.B., 1976. One-trial simultaneous and backward fear conditioning as reflected in conditioned suppression of licking in rats. Anim. Learn. Behav. 4, 357–362. https://doi.org/10.3758/BF03214421

Makino, H., Hwang, E.J., Hedrick, N.G., Komiyama, T., 2016. Circuit Mechanisms of Sensorimotor Learning. Neuron 92, 705–721. https://doi.org/10.1016/j.neuron.2016.10.029

Makino, H., Komiyama, T., 2015. Learning enhances the relative impact of top-down processing in the visual cortex. Nat. Neurosci. 18, 1116–1122. https://doi.org/10.1038/nn.4061

Maldonado, P.E., Gerstein, G.L., 1996. Reorganization in the auditory cortex of the rat induced by intracortical microstimulation: a multiple single-unit study. Exp. Brain Res. 112, 420–430.

Malmierca, M.S., Anderson, L.A., Antunes, F.M., 2015. The cortical modulation of stimulus-specific adaptation in the auditory midbrain and thalamus: a potential neuronal correlate for predictive coding. Front. Syst. Neurosci. 9. https://doi.org/10.3389/fnsys.2015.00019

Mann, Z.F., Kelley, M.W., 2011. Development of tonotopy in the auditory periphery. Hear. Res. 276, 2–15. https://doi.org/10.1016/j.heares.2011.01.011

Maor, I., Shalev, A., Mizrahi, A., 2016. Distinct Spatiotemporal Response Properties of Excitatory Versus Inhibitory Neurons in the Mouse Auditory Cortex. Cereb. Cortex N. Y. N 1991 26, 4242–4252. https://doi.org/10.1093/cercor/bhw266

Maren, S., 2003. The amygdala, synaptic plasticity, and fear memory. Ann. N. Y. Acad. Sci. 985, 106–113.

Markram, H., Lübke, J., Frotscher, M., Sakmann, B., 1997. Regulation of synaptic efficacy by coincidence of postsynaptic APs and EPSPs. Science 275, 213–215.

Markram, H., Muller, E., Ramaswamy, S., Reimann, M.W., Abdellah, M., Sanchez, C.A., Ailamaki, A., Alonso-Nanclares, L., Antille, N., Arsever, S., Kahou, G.A.A., Berger, T.K., Bilgili, A., Buncic, N., Chalimourda, A., Chindemi, G., Courcol, J.-D., Delalondre, F., Delattre, V., Druckmann, S., Dumusc, R., Dynes, J., Eilemann, S., Gal, E., Gevaert, M.E., Ghobril, J.-P., Gidon, A., Graham, J.W., Gupta, A., Haenel, V., Hay, E., Heinis, T., Hernando, J.B., Hines, M., Kanari, L., Keller, D., Kenyon, J., Khazen, G., Kim, Y., King, J.G., Kisvarday, Z., Kumbhar, P., Lasserre, S., Le Bé, J.-V., Magalhães, B.R.C., Merchán-Pérez, A., Meystre, J., Morrice, B.R., Muller, J., Muñoz-Céspedes, A., Muralidhar, S., Muthurasa, K., Nachbaur, D., Newton, T.H., Nolte, M., Ovcharenko, A., Palacios, J., Pastor, L., Perin, R., Ranjan, R., Riachi, I., Rodríguez, J.-R., Riquelme, J.L., Rössert, C., Sfyrakis, K., Shi, Y.,

Shillcock, J.C., Silberberg, G., Silva, R., Tauheed, F., Telefont, M., Toledo-Rodriguez, M., Tränkler, T., Van Geit, W., Díaz, J.V., Walker, R., Wang, Y., Zaninetta, S.M., DeFelipe, J., Hill, S.L., Segev, I., Schürmann, F., 2015. Reconstruction and Simulation of Neocortical Microcircuitry. Cell 163, 456–492. https://doi.org/10.1016/j.cell.2015.09.029

Markram, H., Toledo-Rodriguez, M., Wang, Y., Gupta, A., Silberberg, G., Wu, C., 2004. Interneurons of the neocortical inhibitory system. Nat. Rev. Neurosci. 5, 793–807. https://doi.org/10.1038/nrn1519

Marlin, B.J., Mitre, M., D'amour, J.A., Chao, M.V., Froemke, R.C., 2015. Oxytocin enables maternal behaviour by balancing cortical inhibition. Nature 520, 499–504. https://doi.org/10.1038/nature14402

Martin, S.J., Grimwood, P.D., Morris, R.G.M., 2000. Synaptic Plasticity and Memory: An Evaluation of the Hypothesis. Annu. Rev. Neurosci. 23, 649–711. https://doi.org/10.1146/annurev.neuro.23.1.649

Matzel, L.D., Han, Y.R., Grossman, H., Karnik, M.S., Patel, D., Scott, N., Specht, S.M., Gandhi, C.C., 2003. Individual Differences in the Expression of a "General" Learning Ability in Mice. J. Neurosci. 23, 6423–6433. https://doi.org/10.1523/JNEUROSCI.23-16-06423.2003

Matzel, L.D., Schachtman, T.R., Miller, R.R., 1985. Recovery of an overshadowed association achieved by extinction of the overshadowing stimulus. Learn. Motiv. 16, 398–412. https://doi.org/10.1016/0023-9690(85)90023-2

McCormick, D.A., Connors, B.W., Lighthall, J.W., Prince, D.A., 1985. Comparative electrophysiology of pyramidal and sparsely spiny stellate neurons of the neocortex. J. Neurophysiol. 54, 782–806. https://doi.org/10.1152/jn.1985.54.4.782

Mendelson, J.R., Schreiner, C.E., Sutter, M.L., 1997. Functional topography of cat primary auditory cortex: response latencies. J. Comp. Physiol. [A] 181, 615–633.

Mendelson, J.R., Schreiner, C.E., Sutter, M.L., Grasse, K.L., 1993. Functional topography of cat primary auditory cortex: responses to frequency-modulated sweeps. Exp. Brain Res. 94, 65–87.

Mendez, M.F., Geehan, G.R., 1988. Cortical auditory disorders: clinical and psychoacoustic features. J. Neurol. Neurosurg. Psychiatry 51, 1–9.

Mery, F., Kawecki, T.J., 2003. A fitness cost of learning ability in Drosophila melanogaster. Proc. Biol. Sci. 270, 2465–2469. https://doi.org/10.1098/rspb.2003.2548

Meyer, D.R., Woolsey, C.N., 1952. Effects of localized cortical destruction on auditory discriminative conditioning in cat. J. Neurophysiol. 15, 149–162. https://doi.org/10.1152/jn.1952.15.2.149

Meyer, H.S., Schwarz, D., Wimmer, V.C., Schmitt, A.C., Kerr, J.N.D., Sakmann, B., Helmstaedter, M., 2011. Inhibitory interneurons in a cortical column form hot zones of inhibition in layers 2 and 5A. Proc. Natl. Acad. Sci. U. S. A. 108, 16807–16812. https://doi.org/10.1073/pnas.1113648108

Miller, R.R., Barnet, R.C., Grahame, N.J., 1995. Assessment of the Rescorla-Wagner model. Psychol. Bull. 117, 363–386.

Moczulska, K.E., Tinter-Thiede, J., Peter, M., Ushakova, L., Wernle, T., Bathellier, B., Rumpel, S., 2013. Dynamics of dendritic spines in the mouse auditory cortex during memory formation and memory recall. Proc. Natl. Acad. Sci. 110, 18315–18320. https://doi.org/10.1073/pnas.1312508110

Moffat, J.J., Ka, M., Jung, E.-M., Kim, W.-Y., 2015. Genes and brain malformations associated with abnormal neuron positioning. Mol. Brain 8. https://doi.org/10.1186/s13041-015-0164-4

Mountcastle, V.B., 1957. Modality and topographic properties of single neurons of cat's somatic sensory cortex. J. Neurophysiol. 20, 408–434. https://doi.org/10.1152/jn.1957.20.4.408

Mountcastle, V.B., Powell, T.P., 1959. Central nervous mechanisms subserving position sense and kinesthesis. Bull. Johns Hopkins Hosp. 105, 173–200.

Muralidhar, S., Wang, Y., Markram, H., 2013. Synaptic and cellular organization of layer 1 of the developing rat somatosensory cortex. Front. Neuroanat. 7, 52. https://doi.org/10.3389/fnana.2013.00052

Musall, S., von der Behrens, W., Mayrhofer, J.M., Weber, B., Helmchen, F., Haiss, F., 2014. Tactile frequency discrimination is enhanced by circumventing neocortical adaptation. Nat. Neurosci. 17, 1567–1573. https://doi.org/10.1038/nn.3821

Nagel, G., Brauner, M., Liewald, J.F., Adeishvili, N., Bamberg, E., Gottschalk, A., 2005. Light activation of channelrhodopsin-2 in excitable cells of Caenorhabditis elegans triggers rapid behavioral responses. Curr. Biol. CB 15, 2279–2284. https://doi.org/10.1016/j.cub.2005.11.032

Nagel, G., Ollig, D., Fuhrmann, M., Kateriya, S., Musti, A.M., Bamberg, E., Hegemann, P., 2002. Channelrhodopsin-1: a light-gated proton channel in green algae. Science 296, 2395–2398. https://doi.org/10.1126/science.1072068

Nakajima, M., Halassa, M.M., 2017. Thalamic control of functional cortical connectivity. Curr. Opin. Neurobiol. 44, 127–131. https://doi.org/10.1016/j.conb.2017.04.001

Narayanan, R.T., Egger, R., Johnson, A.S., Mansvelder, H.D., Sakmann, B., de Kock, C.P.J., Oberlaender, M., 2015. Beyond Columnar Organization: Cell Type- and Target Layer-Specific Principles of

Horizontal Axon Projection Patterns in Rat Vibrissal Cortex. Cereb. Cortex N. Y. N 1991 25, 4450–4468. https://doi.org/10.1093/cercor/bhv053

Nassi, J.J., Cepko, C.L., Born, R.T., Beier, K.T., 2015. Neuroanatomy goes viral! Front. Neuroanat. 9, 80. https://doi.org/10.3389/fnana.2015.00080

Natan, R.G., Rao, W., Geffen, M.N., 2017. Cortical Interneurons Differentially Shape Frequency Tuning following Adaptation. Cell Rep. 21, 878–890. https://doi.org/10.1016/j.celrep.2017.10.012

Nayagam, B.A., Muniak, M.A., Ryugo, D.K., 2011. The spiral ganglion: connecting the peripheral and central auditory systems. Hear. Res. 278, 2–20. https://doi.org/10.1016/j.heares.2011.04.003

Neff, W.D., Diamond, I.T., Casseday, J.H., 1975. Behavioral Studies of Auditory Discrimination: Central Nervous System, in: Abeles, M., Bredberg, Gö., Butler, R.A., Casseday, J.H., Desmedt, J.E., Diamond, I.T., Erulkar, S.D., Evans, E.F., Goldberg, J.M., Goldstein, M.H., Green, D.M., Hunter-Duvar, I.M., Jeffress, L.A., Neff, W.D., Yost, W.A., Zwicker, E., Keidel, W.D., Neff, W.D. (Eds.), Auditory System: Physiology (CNS)· Behavioral Studies Psychoacoustics, Handbook of Sensory Physiology. Springer Berlin Heidelberg, Berlin, Heidelberg, pp. 307–400. https://doi.org/10.1007/978-3-642-65995-9_8

Nelken, I., 2008. Processing of complex sounds in the auditory system. Curr. Opin. Neurobiol. 18, 413–417. https://doi.org/10.1016/j.conb.2008.08.014

Nelken, I., Bizley, J.K., Nodal, F.R., Ahmed, B., Schnupp, J.W.H., King, A.J., 2004. Large-scale organization of ferret auditory cortex revealed using continuous acquisition of intrinsic optical signals. J. Neurophysiol. 92, 2574–2588. https://doi.org/10.1152/jn.00276.2004

Neuhoff, J.G., 1998. Perceptual bias for rising tones. Nature 395, 123–124. https://doi.org/10.1038/25862

Nevin, J., 1999. Analyzing Thorndike's Law Of Effect: The Question Of Stimulus–response Bonds. J. Exp. Anal. Behav. 72, 447–450. https://doi.org/10.1901/jeab.1999.72-447

Newsome, W.T., Britten, K.H., Movshon, J.A., 1989. Neuronal correlates of a perceptual decision. Nature 341, 52–54. https://doi.org/10.1038/341052a0

Newsome, W.T., Mikami, A., Wurtz, R.H., 1986. Motion selectivity in macaque visual cortex. III. Psychophysics and physiology of apparent motion. J. Neurophysiol. 55, 1340–1351. https://doi.org/10.1152/jn.1986.55.6.1340

Nishiyama, M., Matsui, T., Murakami, T., Hagihara, K.M., Ohki, K., 2019. Cell-Type-Specific Thalamocortical Inputs Constrain Direction Map Formation in Visual Cortex. Cell Rep. 26, 1082-1088.e3. https://doi.org/10.1016/j.celrep.2019.01.008

Niv, Y., Daniel, R., Geana, A., Gershman, S.J., Leong, Y.C., Radulescu, A., Wilson, R.C., 2015. Reinforcement Learning in Multidimensional Environments Relies on Attention Mechanisms. J. Neurosci. 35, 8145–8157. https://doi.org/10.1523/JNEUROSCI.2978-14.2015

Nomura, H., Hara, K., Abe, R., Hitora-Imamura, N., Nakayama, R., Sasaki, T., Matsuki, N., Ikegaya, Y., 2015. Memory formation and retrieval of neuronal silencing in the auditory cortex. Proc. Natl. Acad. Sci. 112, 9740–9744. https://doi.org/10.1073/pnas.1500869112

Nyberg, S., Abbott, N.J., Shi, X., Steyger, P.S., Dabdoub, A., 2019. Delivery of therapeutics to the inner ear: The challenge of the blood-labyrinth barrier. Sci. Transl. Med. 11. https://doi.org/10.1126/scitranslmed.aao0935

O'Connor, D. H., Clack, N.G., Huber, D., Komiyama, T., Myers, E.W., Svoboda, K., 2010. Vibrissa-Based Object Localization in Head-Fixed Mice. J. Neurosci. 30, 1947–1967. https://doi.org/10.1523/JNEUROSCI.3762-09.2010

O'Connor, D.H., Hires, S.A., Guo, Z.V., Li, N., Yu, J., Sun, Q.-Q., Huber, D., Svoboda, K., 2013. Neural coding during active somatosensation revealed using illusory touch. Nat. Neurosci. 16, 958–965. https://doi.org/10.1038/nn.3419

O'Connor, Daniel H., Peron, S.P., Huber, D., Svoboda, K., 2010. Neural activity in barrel cortex underlying vibrissa-based object localization in mice. Neuron 67, 1048–1061. https://doi.org/10.1016/j.neuron.2010.08.026

Ohki, K., Chung, S., Ch'ng, Y.H., Kara, P., Reid, R.C., 2005. Functional imaging with cellular resolution reveals precise micro-architecture in visual cortex. Nature 433, 597–603. https://doi.org/10.1038/nature03274

Ohki, K., Chung, S., Kara, P., Hübener, M., Bonhoeffer, T., Reid, R.C., 2006. Highly ordered arrangement of single neurons in orientation pinwheels. Nature 442, 925–928. https://doi.org/10.1038/nature05019

Ohl, F.W., Scheich, H., Freeman, W.J., 2001. Change in pattern of ongoing cortical activity with auditory category learning. Nature 412, 733–736. https://doi.org/10.1038/35089076

Ohl, F.W., Wetzel, W., Wagner, T., Rech, A., Scheich, H., 1999. Bilateral ablation of auditory cortex in Mongolian gerbil affects discrimination of frequency modulated tones but not of pure tones. Learn. Mem. Cold Spring Harb. N 6, 347–362.

O'Neill, W.E., Frisina, R.D., Gooler, D.M., 1989. Functional organization of mustached bat inferior colliculus: I. Representation of FM frequency bands important for target ranging revealed by 14C-2-deoxyglucose autoradiography and single unit mapping. J. Comp. Neurol. 284, 60–84. https://doi.org/10.1002/cne.902840106

Orduña, I., Mercado, E., Gluck, M.A., Merzenich, M.M., 2005. Cortical responses in rats predict perceptual sensitivities to complex sounds. Behav. Neurosci. 119, 256–264. https://doi.org/10.1037/0735-7044.119.1.256

Otchy, T.M., Wolff, S.B.E., Rhee, J.Y., Pehlevan, C., Kawai, R., Kempf, A., Gobes, S.M.H., Ölveczky, B.P., 2015. Acute off-target effects of neural circuit manipulations. Nature 528, 358–363. https://doi.org/10.1038/nature16442

Oviedo, H.V., Bureau, I., Svoboda, K., Zador, A.M., 2010. The functional asymmetry of auditory cortex is reflected in the organization of local cortical circuits. Nat. Neurosci. 13, 1413–1420. https://doi.org/10.1038/nn.2659

Oyibo, H.K., Znamenskiy, P., Oviedo, H.V., Enquist, L.W., Zador, A.M., 2014. Long-term Cre-mediated retrograde tagging of neurons using a novel recombinant pseudorabies virus. Front. Neuroanat. 8, 86. https://doi.org/10.3389/fnana.2014.00086

Ozbay, B.N., Futia, G.L., Ma, M., Bright, V.M., Gopinath, J.T., Hughes, E.G., Restrepo, D., Gibson, E.A., 2018. Three dimensional two-photon brain imaging in freely moving mice using a miniature fiber coupled microscope with active axial-scanning. Sci. Rep. 8, 8108. https://doi.org/10.1038/s41598-018-26326-3

Pachitariu, M., Lyamzin, D.R., Sahani, M., Lesica, N.A., 2015. State-dependent population coding in primary auditory cortex. J. Neurosci. Off. J. Soc. Neurosci. 35, 2058–2073. https://doi.org/10.1523/JNEUROSCI.3318-14.2015

Packer, A.M., Russell, L.E., Dalgleish, H.W.P., Häusser, M., 2015. Simultaneous all-optical manipulation and recording of neural circuit activity with cellular resolution in vivo. Nat. Methods 12, 140–146. https://doi.org/10.1038/nmeth.3217

Pai, S., Erlich, J.C., Kopec, C., Brody, C.D., 2011. Minimal Impairment in a Rat Model of Duration Discrimination Following Excitotoxic Lesions of Primary Auditory and Prefrontal Cortices. Front. Syst. Neurosci. 5. https://doi.org/10.3389/fnsys.2011.00074

Panniello, M., King, A.J., Dahmen, J.C., Walker, K.M.M., 2018. Local and Global Spatial Organization of Interaural Level Difference and Frequency Preferences in Auditory Cortex. Cereb. Cortex N. Y. N 1991 28, 350–369. https://doi.org/10.1093/cercor/bhx295

Panzeri, S., Harvey, C.D., Piasini, E., Latham, P.E., Fellin, T., 2017. Cracking the Neural Code for Sensory Perception by Combining Statistics, Intervention, and Behavior. Neuron 93, 491–507. https://doi.org/10.1016/j.neuron.2016.12.036

Parker, A.J., Newsome, W.T., 1998. Sense and the single neuron: probing the physiology of perception. Annu. Rev. Neurosci. 21, 227–277. https://doi.org/10.1146/annurev.neuro.21.1.227

Patil, K., Pressnitzer, D., Shamma, S., Elhilali, M., 2012. Music in Our Ears: The Biological Bases of Musical Timbre Perception. PLOS Comput. Biol. 8, e1002759. https://doi.org/10.1371/journal.pcbi.1002759

Patriarchi, T., Cho, J.R., Merten, K., Howe, M.W., Marley, A., Xiong, W.-H., Folk, R.W., Broussard, G.J., Liang, R., Jang, M.J., Zhong, H., Dombeck, D., von Zastrow, M., Nimmerjahn, A., Gradinaru, V., Williams, J.T., Tian, L., 2018. Ultrafast neuronal imaging of dopamine dynamics with designed genetically encoded sensors. Science 360. https://doi.org/10.1126/science.aat4422

Pearce, J.M., Bouton, M.E., 2001. Theories of Associative Learning in Animals. Annu. Rev. Psychol. 52, 111–139. https://doi.org/10.1146/annurev.psych.52.1.111

Pearce, J.M., Hall, G., 1980. A Model for Pavlovian Learning: Variations in the Effectiveness of Conditioned But Not of Unconditioned Stimuli. Psychol. Rev. 87, 21.

Pégard, N.C., Mardinly, A.R., Oldenburg, I.A., Sridharan, S., Waller, L., Adesnik, H., 2017. Three-dimensional scanless holographic optogenetics with temporal focusing (3D-SHOT). Nat. Commun. 8, 1228. https://doi.org/10.1038/s41467-017-01031-3

Peinado, A., Yuste, R., Katz, L.C., 1993. Gap junctional communication and the development of local circuits in neocortex. Cereb. Cortex N. Y. N 1991 3, 488–498.

Peng, Y., Gillis-Smith, S., Jin, H., Tränkner, D., Ryba, N.J.P., Zuker, C.S., 2015. Sweet and bitter taste in the brain of awake behaving animals. Nature 527, 512–515. https://doi.org/10.1038/nature15763

Perez, M., Giurfa, M., d'Ettorre, P., 2015. The scent of mixtures: rules of odour processing in ants. Sci. Rep. 5, 8659. https://doi.org/10.1038/srep08659

Peron, S.P., Freeman, J., Iyer, V., Guo, C., Svoboda, K., 2015. A Cellular Resolution Map of Barrel Cortex Activity during Tactile Behavior. Neuron 86, 783–799. https://doi.org/10.1016/j.neuron.2015.03.027

Petersen, C.C.H., Hahn, T.T.G., Mehta, M., Grinvald, A., Sakmann, B., 2003. Interaction of sensory responses with spontaneous depolarization in layer 2/3 barrel cortex. Proc. Natl. Acad. Sci. U. S. A. 100, 13638–13643. https://doi.org/10.1073/pnas.2235811100

Petersen, M.R., Beecher, M.D., Zoloth, S.R., Moody, D.B., Stebbins, W.C., 1978. Neural lateralization of species-specific vocalizations by Japanese macaques (Macaca fuscata). Science 202, 324–327.

Poeppel, D., Guillemin, A., Thompson, J., Fritz, J., Bavelier, D., Braun, A.R., 2004. Auditory lexical decision, categorical perception, and FM direction discrimination differentially engage left and right auditory cortex. Neuropsychologia 42, 183–200.

Polley, D.B., 2006. Perceptual Learning Directs Auditory Cortical Map Reorganization through Top-Down Influences. J. Neurosci. 26, 4970–4982. https://doi.org/10.1523/JNEUROSCI.3771-05.2006

Polley, D.B., Read, H.L., Storace, D.A., Merzenich, M.M., 2007. Multiparametric auditory receptive field organization across five cortical fields in the albino rat. J. Neurophysiol. 97, 3621–3638. https://doi.org/10.1152/jn.01298.2006

Poort, J., Khan, A.G., Pachitariu, M., Nemri, A., Orsolic, I., Krupic, J., Bauza, M., Sahani, M., Keller, G.B., Mrsic-Flogel, T.D., Hofer, S.B., 2015. Learning Enhances Sensory and Multiple Non-sensory Representations in Primary Visual Cortex. Neuron 86, 1478–1490. https://doi.org/10.1016/j.neuron.2015.05.037

Poremba, A., Malloy, M., Saunders, R.C., Carson, R.E., Herscovitch, P., Mishkin, M., 2004. Species-specific calls evoke asymmetric activity in the monkey's temporal poles. Nature 427, 448–451. https://doi.org/10.1038/nature02268

Porter, B.A., Rosenthal, T.R., Ranasinghe, K.G., Kilgard, M.P., 2011. Discrimination of brief speech sounds is impaired in rats with auditory cortex lesions. Behav. Brain Res. 219, 68–74. https://doi.org/10.1016/j.bbr.2010.12.015

Poulet, J.F.A., Crochet, S., 2018. The Cortical States of Wakefulness. Front. Syst. Neurosci. 12, 64. https://doi.org/10.3389/fnsys.2018.00064

Prinster, A., Cantone, E., Verlezza, V., Magliulo, M., Sarnelli, G., Iengo, M., Cuomo, R., Salle, F.D., Esposito, F., 2017. Cortical representation of different taste modalities on the gustatory cortex: A pilot study. PLOS ONE 12, e0190164. https://doi.org/10.1371/journal.pone.0190164

Pritchard, T.C., Nedderman, E.N., Edwards, E.M., Petticoffer, A.C., Schwartz, G.J., Scott, T.R., 2008. Satiety-responsive neurons in the medial orbitofrontal cortex of the macaque. Behav. Neurosci. 122, 174–182. https://doi.org/10.1037/0735-7044.122.1.174

Purves, D. (Ed.), 2004. Neuroscience, 3rd ed. ed. Sinauer Associates, Publishers, Sunderland, Mass.

Quan, X., Kumar, M., Matoba, O., Awatsuji, Y., Hayasaki, Y., Hasegawa, S., Wake, H., 2018. Three-dimensional stimulation and imaging-based functional optical microscopy of biological cells. Opt. Lett. 43, 5447–5450. https://doi.org/10.1364/OL.43.005447

Quirk, G.J., Armony, J.L., LeDoux, J.E., 1997. Fear Conditioning Enhances Different Temporal Components of Tone-Evoked Spike Trains in Auditory Cortex and Lateral Amygdala. Neuron 19, 613–624. https://doi.org/10.1016/S0896-6273(00)80375-X

Raab, D.H., Ades, H.W., 1946. Cortical and midbrain mediation of a conditioned discrimination of acoustic intensities. Am. J. Psychol. 59, 59–83.

Radnikow, G., Feldmeyer, D., 2018. Layer- and Cell Type-Specific Modulation of Excitatory Neuronal Activity in the Neocortex. Front. Neuroanat. 12. https://doi.org/10.3389/fnana.2018.00001

Ramirez, S., Liu, X., MacDonald, C.J., Moffa, A., Zhou, J., Redondo, R.L., Tonegawa, S., 2015. Activating positive memory engrams suppresses depression-like behavior. Nature 522, 335–339. https://doi.org/10.1038/nature14514

Rauschecker, J.P., Scott, S.K., 2009. Maps and streams in the auditory cortex: nonhuman primates illuminate human speech processing. Nat. Neurosci. 12, 718–724. https://doi.org/10.1038/nn.2331

Recanzone, G.H., Schreiner, C.E., Merzenich, M.M., 1993. Plasticity in the frequency representation of primary auditory cortex following discrimination training in adult owl monkeys. J. Neurosci. Off. J. Soc. Neurosci. 13, 87–103.

Redhead, E.S., Prados, J., Pearce, J.M., 2001. The effects of pre-exposure on escape from a Morris pool. Q. J. Exp. Psychol. B 54, 353–367. https://doi.org/10.1080/713932764

Reed, A., Riley, J., Carraway, R., Carrasco, A., Perez, C., Jakkamsetti, V., Kilgard, M.P., 2011. Cortical map plasticity improves learning but is not necessary for improved performance. Neuron 70, 121–131. https://doi.org/10.1016/j.neuron.2011.02.038

Rees, A., Møller, A.R., 1983. Responses of neurons in the inferior colliculus of the rat to AM and FM tones. Hear. Res. 10, 301–330.

Reich, D.S., Mechler, F., Victor, J.D., 2001. Independent and redundant information in nearby cortical neurons. Science 294, 2566–2568. https://doi.org/10.1126/science.1065839

Rescorla, R.A., Wagner, A.R., 1972. A Theory of Pavlovian Conditioning: Variations in the Effectiveness of Reinforcement and Nonreinforcement 18.

Robertson, D., Irvine, D.R., 1989. Plasticity of frequency organization in auditory cortex of guinea pigs with partial unilateral deafness. J. Comp. Neurol. 282, 456–471. https://doi.org/10.1002/cne.902820311

Roland, B., Deneux, T., Franks, K.M., Bathellier, B., Fleischmann, A., 2017. Odor identity coding by distributed ensembles of neurons in the mouse olfactory cortex. eLife 6. https://doi.org/10.7554/eLife.26337

Romanski, L.M., LeDoux, J.E., 1992. Bilateral destruction of neocortical and perirhinal projection targets of the acoustic thalamus does not disrupt auditory fear conditioning. Neurosci. Lett. 142, 228–232. https://doi.org/10.1016/0304-3940(92)90379-L

Ronzitti, E., Conti, R., Zampini, V., Tanese, D., Foust, A.J., Klapoetke, N., Boyden, E.S., Papagiakoumou, E., Emiliani, V., 2017. Submillisecond Optogenetic Control of Neuronal Firing with Two-Photon Holographic Photoactivation of Chronos. J. Neurosci. Off. J. Soc. Neurosci. 37, 10679–10689. https://doi.org/10.1523/JNEUROSCI.1246-17.2017

Ronzitti, E., Emiliani, V., Papagiakoumou, E., 2018. Methods for Three-Dimensional All-Optical Manipulation of Neural Circuits. Front. Cell. Neurosci. 12, 469. https://doi.org/10.3389/fncel.2018.00469

Rose, J.E., Woolsey, C.N., 1949. The relations of thalamic connections, cellular structure and evocable electrical activity in the auditory region of the cat. J. Comp. Neurol. 91, 441–466.

Rost, B.R., Schneider-Warme, F., Schmitz, D., Hegemann, P., 2017. Optogenetic Tools for Subcellular Applications in Neuroscience. Neuron 96, 572–603. https://doi.org/10.1016/j.neuron.2017.09.047

Rothschild, G., Nelken, I., Mizrahi, A., 2010. Functional organization and population dynamics in the mouse primary auditory cortex. Nat. Neurosci. 13, 353–360. https://doi.org/10.1038/nn.2484

Rubin, B.D., Katz, L.C., 1999. Optical Imaging of Odorant Representations in the Mammalian Olfactory Bulb. Neuron 23, 499–511. https://doi.org/10.1016/S0896-6273(00)80803-X

Rumelhart, D.E., Hinton, G.E., Williams, R.J., 1986. Learning representations by back-propagating errors. Nature 323, 533. https://doi.org/10.1038/323533a0

Runyan, C.A., Piasini, E., Panzeri, S., Harvey, C.D., 2017. Distinct timescales of population coding across cortex. Nature 548, 92–96. https://doi.org/10.1038/nature23020

Rybalko, N., Šuta, D., Nwabueze-Ogbo, F., Syka, J., 2006. Effect of auditory cortex lesions on the discrimination of frequency-modulated tones in rats: Discrimination of FM tones after cortical lesioning. Eur. J. Neurosci. 23, 1614–1622. https://doi.org/10.1111/j.1460-9568.2006.04688.x

Rybalko, N., Šuta, D., Popelář, J., Syka, J., 2010. Inactivation of the left auditory cortex impairs temporal discrimination in the rat. Behav. Brain Res. 209, 123–130. https://doi.org/10.1016/j.bbr.2010.01.028

Sachidhanandam, S., Sreenivasan, V., Kyriakatos, A., Kremer, Y., Petersen, C.C.H., 2013. Membrane potential correlates of sensory perception in mouse barrel cortex. Nat. Neurosci. 16, 1671–1677. https://doi.org/10.1038/nn.3532

Sacks, O., 1933-2015, 1985. The man who mistook his wife for a hat and other clinical tales. New York : Summit Books, [1985] ©1985.

Sadagopan, S., Wang, X., 2008. Level invariant representation of sounds by populations of neurons in primary auditory cortex. J. Neurosci. Off. J. Soc. Neurosci. 28, 3415–3426. https://doi.org/10.1523/JNEUROSCI.2743-07.2008

Saenz, M., Langers, D.R.M., 2014. Tonotopic mapping of human auditory cortex. Hear. Res., Human Auditory NeuroImaging 307, 42–52. https://doi.org/10.1016/j.heares.2013.07.016

Sakai, S., Ueno, K., Ishizuka, T., Yawo, H., 2013. Parallel and patterned optogenetic manipulation of neurons in the brain slice using a DMD-based projector. Neurosci. Res. 75, 59–64. https://doi.org/10.1016/j.neures.2012.03.009

Salzman, C.D., Britten, K.H., Newsome, W.T., 1990. Cortical microstimulation influences perceptual judgements of motion direction. Nature 346, 174. https://doi.org/10.1038/346174a0

Salzman, C.D., Murasugi, C.M., Britten, K.H., Newsome, W.T., 1992. Microstimulation in visual area MT: effects on direction discrimination performance. J. Neurosci. Off. J. Soc. Neurosci. 12, 2331–2355.

Salzman, C.D., Newsome, W.T., 1994. Neural mechanisms for forming a perceptual decision. Science 264, 231–237.

Sanders, M.D., Warrington, E.K., Marshall, J., Wieskrantz, L., 1974. “Blindsight”: Vision in a field defect. Lancet Lond. Engl. 1, 707–708.

Sarma, G.P., Lee, C.W., Portegys, T., Ghayoomie, V., Jacobs, T., Alicea, B., Cantarelli, M., Currie, M., Gerkin, R.C., Gingell, S., Gleeson, P., Gordon, R., Hasani, R.M., Idili, G., Khayrulin, S., Lung, D., Palyanov, A., Watts, M., Larson, S.D., 2018. OpenWorm: overview and recent advances in integrative biological simulation of Caenorhabditis elegans. Philos. Trans. R. Soc. Lond. B. Biol. Sci. 373. https://doi.org/10.1098/rstb.2017.0382

Sawatari, H., Tanaka, Y., Takemoto, M., Nishimura, M., Hasegawa, K., Saitoh, K., Song, W.-J., 2011. Identification and characterization of an insular auditory field in mice. Eur. J. Neurosci. 34, 1944–1952. https://doi.org/10.1111/j.1460-9568.2011.07926.x

Scharlock, D.P., Tucker, T.J., Strominger, N.L., 1963. Auditory Discrimination by the Cat after Neonatal Ablation of Temporal Cortex. Science 141, 1197–1198. https://doi.org/10.1126/science.141.3586.1197

Scheich, H., Brechmann, A., Brosch, M., Budinger, E., Ohl, F.W., 2007. The cognitive auditory cortex: task-specificity of stimulus representations. Hear. Res. 229, 213–224. https://doi.org/10.1016/j.heares.2007.01.025

Schmid, M.C., Mrowka, S.W., Turchi, J., Saunders, R.C., Wilke, M., Peters, A.J., Ye, F.Q., Leopold, D.A., 2010. Blindsight depends on the lateral geniculate nucleus. Nature 466, 373–377. https://doi.org/10.1038/nature09179

Schmitt, L.I., Wimmer, R.D., Nakajima, M., Happ, M., Mofakham, S., Halassa, M.M., 2017. Thalamic amplification of cortical connectivity sustains attentional control. Nature 545, 219–223. https://doi.org/10.1038/nature22073

Schnitzler, H.U., Kalko, E., Miller, L., Surlykke, A., 1987. The echolocation and hunting behavior of the bat, Pipistrellus kuhli. J. Comp. Physiol. [A] 161, 267–274.

Schnupp, J., Nelken, I., King, A., 2011. Auditory neuroscience: making sense of sound. MIT Press, Cambridge, Mass.

Schnupp, J.W.H., Hall, T.M., Kokelaar, R.F., Ahmed, B., 2006. Plasticity of temporal pattern codes for vocalization stimuli in primary auditory cortex. J. Neurosci. Off. J. Soc. Neurosci. 26, 4785–4795. https://doi.org/10.1523/JNEUROSCI.4330-05.2006

Schreiner, C.E., Read, H.L., Sutter, M.L., 2000. Modular Organization of Frequency Integration in Primary Auditory Cortex. Annu. Rev. Neurosci. 23, 501–529. https://doi.org/10.1146/annurev.neuro.23.1.501

Schreiner, C.E., Winer, J.A., 2007. Auditory Cortex Mapmaking: Principles, Projections, and Plasticity. Neuron 56, 356–365. https://doi.org/10.1016/j.neuron.2007.10.013

Schubert, D., Kötter, R., Staiger, J.F., 2007. Mapping functional connectivity in barrel-related columns reveals layer- and cell type-specific microcircuits. Brain Struct. Funct. 212, 107–119. https://doi.org/10.1007/s00429-007-0147-z

Schubert, D., Kötter, R., Zilles, K., Luhmann, H.J., Staiger, J.F., 2003. Cell type-specific circuits of cortical layer IV spiny neurons. J. Neurosci. Off. J. Soc. Neurosci. 23, 2961–2970.

Schultz, W., 2007. Multiple dopamine functions at different time courses. Annu. Rev. Neurosci. 30, 259–288. https://doi.org/10.1146/annurev.neuro.28.061604.135722

Schultz, W., 1998. Predictive reward signal of dopamine neurons. J. Neurophysiol. 80, 1–27. https://doi.org/10.1152/jn.1998.80.1.1

Schultz, W., Dayan, P., Montague, P.R., 1997. A neural substrate of prediction and reward. Science 275, 1593–1599.

Schultz, W., Dickinson, A., 2000. Neuronal coding of prediction errors. Annu. Rev. Neurosci. 23, 473–500. https://doi.org/10.1146/annurev.neuro.23.1.473

Schulze, H., Deutscher, A., Tziridis, K., Scheich, H., 2014. Unilateral Auditory Cortex Lesions Impair or Improve Discrimination Learning of Amplitude Modulated Sounds, Depending on Lesion Side. PLoS ONE 9, e87159. https://doi.org/10.1371/journal.pone.0087159

Schulze, H., Hess, A., Ohl, F.W., Scheich, H., 2002. Superposition of horseshoe-like periodicity and linear tonotopic maps in auditory cortex of the Mongolian gerbil. Eur. J. Neurosci. 15, 1077–1084.

See, J.Z., Atencio, C.A., Sohal, V.S., Schreiner, C.E., 2018. Coordinated neuronal ensembles in primary auditory cortical columns. eLife 7. https://doi.org/10.7554/eLife.35587

Shadlen, M.N., Newsome, W.T., 1994. Noise, neural codes and cortical organization. Curr. Opin. Neurobiol. 4, 569–579.

Shamma, S.A., Elhilali, M., Micheyl, C., 2011. Temporal coherence and attention in auditory scene analysis. Trends Neurosci. 34, 114–123. https://doi.org/10.1016/j.tins.2010.11.002

Shanks, D.R., Lopez, F.J., 1996. Causal order does not affect cue selection in human associative learning. Mem. Cognit. 24, 511–522.

Shapiro, K.L., Jacobs, W.J., LoLordo, V.M., 1980. Stimulus-reinforcer interactions in Pavlovian conditioning of pigeons: Implications for selective associations. Anim. Learn. Behav. 8, 586–594. https://doi.org/10.3758/BF03197773

Shepard, K.N., Chong, K.K., Liu, R.C., 2016. Contrast Enhancement without Transient Map Expansion for Species-Specific Vocalizations in Core Auditory Cortex during Learning. eNeuro 3. https://doi.org/10.1523/ENEURO.0318-16.2016

Shetake, J.A., Wolf, J.T., Cheung, R.J., Engineer, C.T., Ram, S.K., Kilgard, M.P., 2011. Cortical activity patterns predict robust speech discrimination ability in noise. Eur. J. Neurosci. 34, 1823–1838. https://doi.org/10.1111/j.1460-9568.2011.07887.x

Siegel, S., Allan, L.G., 1985. Overshadowing and blocking of the orientation-contingent color aftereffect: Evidence for a conditioning mechanism. Learn. Motiv. 16, 125–138. https://doi.org/10.1016/0023-9690(85)90008-6

Simons, D.J., Woolsey, T.A., 1984. Morphology of Golgi-Cox-impregnated barrel neurons in rat SmI cortex. J. Comp. Neurol. 230, 119–132. https://doi.org/10.1002/cne.902300111

Sineshchekov, O.A., Jung, K.-H., Spudich, J.L., 2002. Two rhodopsins mediate phototaxis to low- and high-intensity light in Chlamydomonas reinhardtii. Proc. Natl. Acad. Sci. U. S. A. 99, 8689–8694. https://doi.org/10.1073/pnas.122243399

Sissons, H.T., Urcelay, G.P., Miller, R.R., 2009. Overshadowing and CS Duration: Counteraction and a Reexamination of the Role of Within-Compound Associations in Cue Competition. Learn. Behav. 37, 254–268. https://doi.org/10.3758/LB.37.3.254

Sjulson, L., Cassataro, D., DasGupta, S., Miesenböck, G., 2016. Cell-Specific Targeting of Genetically Encoded Tools for Neuroscience. Annu. Rev. Genet. 50, 571–594. https://doi.org/10.1146/annurev-genet-120215-035011

Skinner, B.F., 1932. On the Rate of Formation of a Conditioned Reflex. J. Gen. Psychol. 7, 274–286. https://doi.org/10.1080/00221309.1932.9918467

Smith, A.L., Parsons, C.H., Lanyon, R.G., Bizley, J.K., Akerman, C.J., Baker, G.E., Dempster, A.C., Thompson, I.D., King, A.J., 2004. An investigation of the role of auditory cortex in sound localization using muscimol-releasing Elvax. Eur. J. Neurosci. 19, 3059–3072. https://doi.org/10.1111/j.0953-816X.2004.03379.x

Smith, J.C., Roll, D.L., 1967. Trace conditioning with X-rays as an aversive stimulus. Psychon. Sci. 9, 11–12. https://doi.org/10.3758/BF03330734

Sohal, V.S., Zhang, F., Yizhar, O., Deisseroth, K., 2009. Parvalbumin neurons and gamma rhythms enhance cortical circuit performance. Nature 459, 698–702. https://doi.org/10.1038/nature07991

Spitzer, M.W., Calford, M.B., Clarey, J.C., Pettigrew, J.D., Roe, A.W., 2001. Spontaneous and Stimulus-Evoked Intrinsic Optical Signals in Primary Auditory Cortex of the Cat. J. Neurophysiol. 85, 1283–1298. https://doi.org/10.1152/jn.2001.85.3.1283

Starr, A., Zeng, F.G., Michalewski, H.J., Moser, T., 2008. 3.23 - Perspectives on Auditory Neuropathy: Disorders of Inner Hair Cell, Auditory Nerve, and Their Synapse, in: Masland, R.H., Albright, T.D., Albright, T.D., Masland, R.H., Dallos, P., Oertel, D., Firestein, S., Beauchamp, G.K., Catherine Bushnell, M., Basbaum, A.I., Kaas, J.H., Gardner, E.P. (Eds.), The Senses: A Comprehensive Reference. Academic Press, New York, pp. 397–412. https://doi.org/10.1016/B978-012370880-9.00033-5

Stein, B.E., Stanford, T.R., 2008. Multisensory integration: current issues from the perspective of the single neuron. Nat. Rev. Neurosci. 9, 255–266. https://doi.org/10.1038/nrn2331

Stewart, W.B., Kauer, J.S., Shepherd, G.M., 1979. Functional organization of rat olfactory bulb analysed by the 2-deoxyglucose method. J. Comp. Neurol. 185, 715–734. https://doi.org/10.1002/cne.901850407

Stiebler, I., 1987. A distinct ultrasound-processing area in the auditory cortex of the mouse. Naturwissenschaften 74, 96–97.

Stiebler, I., Neulist, R., Fichtel, I., Ehret, G., 1997. The auditory cortex of the house mouse: left-right differences, tonotopic organization and quantitative analysis of frequency representation. J. Comp. Physiol. A 181, 559–571. https://doi.org/10.1007/s003590050140

Strominger, N.L., 1969. Localization of sound in space after unilateral and bilateral ablation of auditory cortex. Exp. Neurol. 25, 521–533.

Suga, N., Xiao, Z., Ma, X., Ji, W., 2002. Plasticity and corticofugal modulation for hearing in adult animals. Neuron 36, 9–18.

Sutton, R.S., Barto, A.G., 1998. Reinforcement Learning: An Introduction 551.

Svoboda, K., Denk, W., Kleinfeld, D., Tank, D.W., 1997. In vivo dendritic calcium dynamics in neocortical pyramidal neurons. Nature 385, 161–165. https://doi.org/10.1038/385161a0

Syka, J., 1997. Acoustical Signal Processing in the Central Auditory System. Springer US, Boston, MA.

Szigeti, B., Gleeson, P., Vella, M., Khayrulin, S., Palyanov, A., Hokanson, J., Currie, M., Cantarelli, M., Idili, G., Larson, S., 2014. OpenWorm: an open-science approach to modeling Caenorhabditis elegans. Front. Comput. Neurosci. 8. https://doi.org/10.3389/fncom.2014.00137

Takahashi, K., Hishida, R., Kubota, Y., Kudoh, M., Takahashi, S., Shibuki, K., 2006. Transcranial fluorescence imaging of auditory cortical plasticity regulated by acoustic environments in mice. Eur. J. Neurosci. 23, 1365–1376. https://doi.org/10.1111/j.1460-9568.2006.04662.x

Talavage, T.M., Ledden, P.J., Benson, R.R., Rosen, B.R., Melcher, J.R., 2000. Frequency-dependent responses exhibited by multiple regions in human auditory cortex. Hear. Res. 150, 225–244.

Talwar, S.K., Gerstein, G.L., 2001. Reorganization in awake rat auditory cortex by local microstimulation and its effect on frequency-discrimination behavior. J. Neurophysiol. 86, 1555–1572. https://doi.org/10.1152/jn.2001.86.4.1555

Talwar, S.K., Musial, P.G., Gerstein, G.L., 2001. Role of mammalian auditory cortex in the perception of elementary sound properties. J. Neurophysiol. 85, 2350–2358. https://doi.org/10.1152/jn.2001.85.6.2350

Tasaka, G.-I., Guenthner, C.J., Shalev, A., Gilday, O., Luo, L., Mizrahi, A., 2018. Genetic tagging of active neurons in auditory cortex reveals maternal plasticity of coding ultrasonic vocalizations. Nat. Commun. 9, 871. https://doi.org/10.1038/s41467-018-03183-2

Tecuapetla, F., Jin, X., Lima, S.Q., Costa, R.M., 2016. Complementary Contributions of Striatal Projection Pathways to Action Initiation and Execution. Cell 166, 703–715. https://doi.org/10.1016/j.cell.2016.06.032

Tecuapetla, F., Matias, S., Dugue, G.P., Mainen, Z.F., Costa, R.M., 2014. Balanced activity in basal ganglia projection pathways is critical for contraversive movements. Nat. Commun. 5, 4315. https://doi.org/10.1038/ncomms5315

Thompson, R.F., 1960. Function of auditory cortex of cat in frequency discrimination. J. Neurophysiol. 23, 321–334. https://doi.org/10.1152/jn.1960.23.3.321

Thompson, R.F., 1959. The effect of training procedure upon auditory frequency discrimination in the cat. J. Comp. Physiol. Psychol. 52, 186–190.

Thorndike, E.L., 1898. Animal intelligence: An experimental study of the associative processes in animals. Psychol. Rev. Monogr. Suppl. 2, i–109. https://doi.org/10.1037/h0092987

Tian, L., Hires, S.A., Mao, T., Huber, D., Chiappe, M.E., Chalasani, S.H., Petreanu, L., Akerboom, J., McKinney, S.A., Schreiter, E.R., Bargmann, C.I., Jayaraman, V., Svoboda, K., Looger, L.L., 2009. Imaging neural activity in worms, flies and mice with improved GCaMP calcium indicators. Nat. Methods 6, 875–881. https://doi.org/10.1038/nmeth.1398

Tonneau, F., González, C., 2004. Function transfer in human operant experiments: the role of stimulus pairings. J. Exp. Anal. Behav. 81, 239–255. https://doi.org/10.1901/jeab.2004.81-239

Tovote, P., Esposito, M.S., Botta, P., Chaudun, F., Fadok, J.P., Markovic, M., Wolff, S.B.E., Ramakrishnan, C., Fenno, L., Deisseroth, K., Herry, C., Arber, S., Lüthi, A., 2016. Midbrain circuits for defensive behaviour. Nature 534, 206–212. https://doi.org/10.1038/nature17996

Town, S.M., Wood, K.C., Bizley, J.K., 2018. Sound identity is represented robustly in auditory cortex during perceptual constancy. Nat. Commun. 9, 4786. https://doi.org/10.1038/s41467-018-07237-3

Tremblay, R., Lee, S., Rudy, B., 2016. GABAergic interneurons in the neocortex: From cellular properties to circuits. Neuron 91, 260–292. https://doi.org/10.1016/j.neuron.2016.06.033

Treue, S., 2003. Visual attention: the where, what, how and why of saliency. Curr. Opin. Neurobiol. 13, 428–432. https://doi.org/10.1016/S0959-4388(03)00105-3

Trobalon, J.B., Miguelez, D., McLaren, I.P.L., Mackintosh, N.J., 2003. Intradimensional and extradimensional shifts in spatial learning. J. Exp. Psychol. Anim. Behav. Process. 29, 143–152.

Tsukano, H., Horie, M., Bo, T., Uchimura, A., Hishida, R., Kudoh, M., Takahashi, K., Takebayashi, H., Shibuki, K., 2015. Delineation of a frequency-organized region isolated from the mouse primary auditory cortex. J. Neurophysiol. 113, 2900–2920. https://doi.org/10.1152/jn.00932.2014

Tsukano, H., Horie, M., Hishida, R., Takahashi, K., Takebayashi, H., Shibuki, K., 2016. Quantitative map of multiple auditory cortical regions with a stereotaxic fine-scale atlas of the mouse brain. Sci. Rep. 6, 22315. https://doi.org/10.1038/srep22315

Tsukano, H., Horie, M., Ohga, S., Takahashi, K., Kubota, Y., Hishida, R., Takebayashi, H., Shibuki, K., 2017a. Reconsidering Tonotopic Maps in the Auditory Cortex and Lemniscal Auditory Thalamus in Mice. Front. Neural Circuits 11. https://doi.org/10.3389/fncir.2017.00014

Tsukano, H., Horie, M., Takahashi, K., Hishida, R., Takebayashi, H., Shibuki, K., 2017b. Independent tonotopy and thalamocortical projection patterns in two adjacent parts of the classical primary auditory cortex in mice. Neurosci. Lett. 637, 26–30. https://doi.org/10.1016/j.neulet.2016.11.062

Tsunada, J., Liu, A.S.K., Gold, J.I., Cohen, Y.E., 2016. Causal contribution of primate auditory cortex to auditory perceptual decision-making. Nat. Neurosci. 19, 135–142. https://doi.org/10.1038/nn.4195

Uzquiano, A., Gladwyn-Ng, I., Nguyen, L., Reiner, O., Götz, M., Matsuzaki, F., Francis, F., 2018. Cortical progenitor biology: key features mediating proliferation versus differentiation. J. Neurochem. 146, 500–525. https://doi.org/10.1111/jnc.14338

Vandorpe, S., De Houwer, J., 2005. A comparison of forward blocking and reduced overshadowing in human causal learning. Psychon. Bull. Rev. 12, 945–949.

VanRullen, R., 2003. Visual saliency and spike timing in the ventral visual pathway. J. Physiol.-Paris 97, 365–377. https://doi.org/10.1016/j.jphysparis.2003.09.010

Vasquez-Lopez, S.A., Weissenberger, Y., Lohse, M., Keating, P., King, A.J., Dahmen, J.C., 2017. Thalamic input to auditory cortex is locally heterogeneous but globally tonotopic. eLife 6. https://doi.org/10.7554/eLife.25141

Vater, M., Kössl, M., 2011. Comparative aspects of cochlear functional organization in mammals. Hear. Res. 273, 89–99. https://doi.org/10.1016/j.heares.2010.05.018

Vaughan, W., Greene, S.L., 1984. Pigeon visual memory capacity. J. Exp. Psychol. Anim. Behav. Process. 10, 256–271. https://doi.org/10.1037/0097-7403.10.2.256

Versnel, H., Mossop, J.E., Mrsic-Flogel, T.D., Ahmed, B., Moore, D.R., 2002. Optical Imaging of Intrinsic Signals in Ferret Auditory Cortex: Responses to Narrowband Sound Stimuli. J. Neurophysiol. 88, 1545–1558. https://doi.org/10.1152/jn.2002.88.3.1545

Wakita, M., 1996. Recovery of function after neonatal ablation of the auditory cortex in rats (Rattus norvegicus). Behav. Brain Res. 78, 201–209.

Wallace, M.N., Kitzes, L.M., Jones, E.G., 1991. Chemoarchitectonic organization of the cat primary auditory cortex. Exp. Brain Res. 86, 518–526.

Wang, J., Qin, L., Chimoto, S., Tazunoki, S., Sato, Y., 2014. Response characteristics of primary auditory cortex neurons underlying perceptual asymmetry of ramped and damped sounds. Neuroscience 256, 309–321. https://doi.org/10.1016/j.neuroscience.2013.10.042

Warren, J., 2005. The Auditory Cortex, A Synthesis of Human and Animal Research. J. Neurol. Neurosurg. Psychiatry 76, 1746. https://doi.org/10.1136/jnnp.2005.071746

Weinberger, N.M., 2015. New perspectives on the auditory cortex, in: Handbook of Clinical Neurology. Elsevier, pp. 117–147. https://doi.org/10.1016/B978-0-444-62630-1.00007-X

Weinberger, N.M., 2007. Associative representational plasticity in the auditory cortex: a synthesis of two disciplines. Learn. Mem. Cold Spring Harb. N 14, 1–16. https://doi.org/10.1101/lm.421807

Wetzel, W, Ohl, F.., Wagner, T., Scheich, H., 1998. Right auditory cortex lesion in Mongolian gerbils impairs discrimination of rising and falling frequency-modulated tones. Neurosci. Lett. 252, 115–118. https://doi.org/10.1016/S0304-3940(98)00561-8

Wetzel, W., Wagner, T., Ohl, F.W., Scheich, H., 1998. Categorical discrimination of direction in frequency-modulated tones by Mongolian gerbils. Behav. Brain Res. 91, 29–39.

Wiest, M.C., Thomson, E., Pantoja, J., Nicolelis, M.A.L., 2010. Changes in S1 neural responses during tactile discrimination learning. J. Neurophysiol. 104, 300–312. https://doi.org/10.1152/jn.00194.2010

Wietek, J., Prigge, M., 2016. Enhancing Channelrhodopsins: An Overview. Methods Mol. Biol. Clifton NJ 1408, 141–165. https://doi.org/10.1007/978-1-4939-3512-3_10

Wilson, N.R., Runyan, C.A., Wang, F.L., Sur, M., 2012. Division and subtraction by distinct cortical inhibitory networks in vivo. Nature 488, 343–348. https://doi.org/10.1038/nature11347

Winer, J.A. (Ed.), 2011. The auditory cortex. Springer, New York.

Winer, J.A., Diehl, J.J., Larue, D.T., 2001. Projections of auditory cortex to the medial geniculate body of the cat. J. Comp. Neurol. 430, 27–55.

Winer, J.A., Larue, D.T., Diehl, J.J., Hefti, B.J., 1998. Auditory cortical projections to the cat inferior colliculus. J. Comp. Neurol. 400, 147–174.

Winer, J.A., Lee, C.C., 2007. The distributed auditory cortex. Hear. Res. 229, 3–13. https://doi.org/10.1016/j.heares.2007.01.017

Winkowski, D.E., Kanold, P.O., 2013. Laminar transformation of frequency organization in auditory cortex. J. Neurosci. Off. J. Soc. Neurosci. 33, 1498–1508. https://doi.org/10.1523/JNEUROSCI.3101-12.2013

Witnauer, J.E., Hutchings, R., Miller, R.R., 2017. Methods of comparing associative models and an application to retrospective revaluation. Behav. Processes 144, 20–32. https://doi.org/10.1016/j.beproc.2017.08.004

Witnauer, J.E., Urcelay, G.P., Miller, R.R., 2014. The error in total error reduction. Neurobiol. Learn. Mem. 108, 119–135. https://doi.org/10.1016/j.nlm.2013.07.018

Womelsdorf, T., Fries, P., 2007. The role of neuronal synchronization in selective attention. Curr. Opin. Neurobiol. 17, 154–160. https://doi.org/10.1016/j.conb.2007.02.002

Wong, S.W., Schreiner, C.E., 2003. Representation of CV-sounds in cat primary auditory cortex: intensity dependence. Speech Commun., The Nature of Speech Perception 41, 93–106. https://doi.org/10.1016/S0167-6393(02)00096-1

Woolsey, C., Walzl, E., 1942. Topical Projection of Nerve Fibres from Local Regions of the Cochlea to the Cerebral Cortex of the Cat.

Wright, B.A., Zhang, Y., 2009. A review of the generalization of auditory learning. Philos. Trans. R. Soc. B Biol. Sci. 364, 301–311. https://doi.org/10.1098/rstb.2008.0262

Xiong, Q., Znamenskiy, P., Zador, A.M., 2015. Selective corticostriatal plasticity during acquisition of an auditory discrimination task. Nature 521, 348–351. https://doi.org/10.1038/nature14225

Xiong, X.R., Liang, F., Zingg, B., Ji, X., Ibrahim, L.A., Tao, H.W., Zhang, L.I., 2015. Auditory cortex controls sound-driven innate defense behaviour through corticofugal projections to inferior colliculus. Nat. Commun. 6. https://doi.org/10.1038/ncomms8224

Yaksi, E., Friedrich, R.W., 2006. Reconstruction of firing rate changes across neuronal populations by temporally deconvolved Ca2+ imaging. Nat. Methods 3, 377–383. https://doi.org/10.1038/nmeth874

Yamasaki, D.S., Wurtz, R.H., 1991. Recovery of function after lesions in the superior temporal sulcus in the monkey. J. Neurophysiol. 66, 651–673. https://doi.org/10.1152/jn.1991.66.3.651

Yan, J., Ehret, G., 2001. Corticofugal reorganization of the midbrain tonotopic map in mice. Neuroreport 12, 3313–3316.

Yang, S., Zhang, L.S., Gibboni, R., Weiner, B., Bao, S., 2014. Impaired development and competitive refinement of the cortical frequency map in tumor necrosis factor-α-deficient mice. Cereb. Cortex N. Y. N 1991 24, 1956–1965. https://doi.org/10.1093/cercor/bht053

Yang, W., Carrillo-Reid, L., Bando, Y., Peterka, D.S., Yuste, R., 2018. Simultaneous two-photon imaging and two-photon optogenetics of cortical circuits in three dimensions. eLife 7. https://doi.org/10.7554/eLife.32671

Yang, Y., DeWeese, M.R., Otazu, G.H., Zador, A.M., 2008. Millisecond-scale differences in neural activity in auditory cortex can drive decisions. Nat. Neurosci. 11, 1262–1263. https://doi.org/10.1038/nn.2211

Yang, Y., Zador, A.M., 2012. Differences in sensitivity to neural timing among cortical areas. J. Neurosci. Off. J. Soc. Neurosci. 32, 15142–15147. https://doi.org/10.1523/JNEUROSCI.1411-12.2012

Zeng, F.-G., Tang, Q., Lu, T., 2014. Abnormal pitch perception produced by cochlear implant stimulation. PloS One 9, e88662. https://doi.org/10.1371/journal.pone.0088662

Zeng, H.-H., Huang, J.-F., Chen, M., Wen, Y.-Q., Shen, Z.-M., Poo, M.-M., 2019. Local homogeneity of tonotopic organization in the primary auditory cortex of marmosets. Proc. Natl. Acad. Sci. U. S. A. 116, 3239–3244. https://doi.org/10.1073/pnas.1816653116

Zhang, F., Gradinaru, V., Adamantidis, A.R., Durand, R., Airan, R.D., de Lecea, L., Deisseroth, K., 2010. Optogenetic interrogation of neural circuits: technology for probing mammalian brain structures. Nat. Protoc. 5, 439–456. https://doi.org/10.1038/nprot.2009.226

Zhang, F., Wang, L.-P., Brauner, M., Liewald, J.F., Kay, K., Watzke, N., Wood, P.G., Bamberg, E., Nagel, G., Gottschalk, A., Deisseroth, K., 2007. Multimodal fast optical interrogation of neural circuitry. Nature 446, 633–639. https://doi.org/10.1038/nature05744

Zhang, L.I., Tan, A.Y.Y., Schreiner, C.E., Merzenich, M.M., 2003. Topography and synaptic shaping of direction selectivity in primary auditory cortex. Nature 424, 201–205. https://doi.org/10.1038/nature01796

Zhang, S., Xu, M., Kamigaki, T., Hoang Do, J.P., Chang, W.-C., Jenvay, S., Miyamichi, K., Luo, L., Dan, Y., 2014. Long-range and local circuits for top-down modulation of visual cortex processing. Science 345, 660–665. https://doi.org/10.1126/science.1254126

Zhang, Y., Dyck, R.H., Hamilton, S.E., Nathanson, N.M., Yan, J., 2005. Disrupted tonotopy of the auditory cortex in mice lacking M1 muscarinic acetylcholine receptor. Hear. Res. 201, 145–155. https://doi.org/10.1016/j.heares.2004.10.003

Zhang, Y., Suga, N., 2005. Corticofugal feedback for collicular plasticity evoked by electric stimulation of the inferior colliculus. J. Neurophysiol. 94, 2676–2682. https://doi.org/10.1152/jn.00549.2005

Zhang, Y., Suga, N., Yan, J., 1997. Corticofugal modulation of frequency processing in bat auditory system. Nature 387, 900–903. https://doi.org/10.1038/43180

Zheng, Q.Y., Johnson, K.R., Erway, L.C., 1999. Assessment of hearing in 80 inbred strains of mice by ABR threshold analyses. Hear. Res. 130, 94–107. https://doi.org/10.1016/S0378-5955(99)00003-9

Zhu, P., Fajardo, O., Shum, J., Zhang Schärer, Y.-P., Friedrich, R.W., 2012. High-resolution optical control of spatiotemporal neuronal activity patterns in zebrafish using a digital micromirror device. Nat. Protoc. 7, 1410–1425. https://doi.org/10.1038/nprot.2012.072

Zingg, B., Chou, X.-L., Zhang, Z.-G., Mesik, L., Liang, F., Tao, H.W., Zhang, L.I., 2017. AAV-Mediated Anterograde Transsynaptic Tagging: Mapping Corticocollicular Input-Defined Neural Pathways for Defense Behaviors. Neuron 93, 33–47. https://doi.org/10.1016/j.neuron.2016.11.045

Ziv, Y., Burns, L.D., Cocker, E.D., Hamel, E.O., Ghosh, K.K., Kitch, L.J., El Gamal, A., Schnitzer, M.J., 2013. Long-term dynamics of CA1 hippocampal place codes. Nat. Neurosci. 16, 264–266. https://doi.org/10.1038/nn.3329

Znamenskiy, P., Zador, A.M., 2013. Corticostriatal neurons in auditory cortex drive decisions during auditory discrimination. Nature 497, 482–485. https://doi.org/10.1038/nature12077